# ISM Dynamics and Star Formation

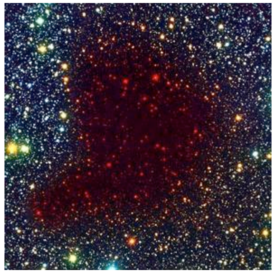
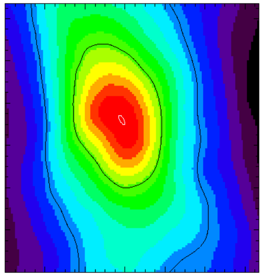

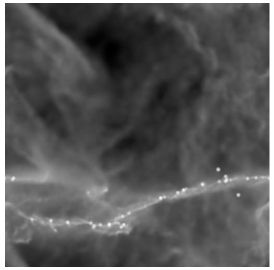

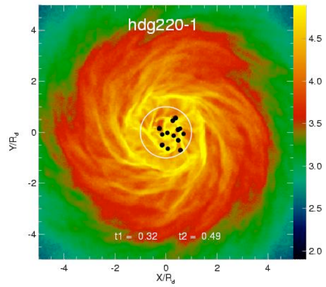


**Ralf Klessen**

Zentrum für Astronomie der Universität Heidelberg
Institut für Theoretische Astrophysik

# thanks to ...

- many thanks to
  - Robi Banerjee (ITA)
  - Paul Clark (ITA)
  - Clare Dobbs (Munich)
  - Christoph Federrath (ITA)
  - Simon Glover (ITA)
  - Thomas Greif (MPA)
  - Patrick Hennebelle (ENS)
  - Mordecai Mac Low (AMNH)
  - Dominik Schleicher (ESO)
  - Enrique Vazquez-Semadeni (UNAM)

# Agenda

- phenomenology
  - what we need to explain
- dynamic star formation theory
  - gravity vs. turbulence (and all the rest)
- examples and predictions
  - formation of molecular clouds in galactic disks ($H_2$ & CO chemistry)
  - universal IMF: importance of turbulence and thermodynamics

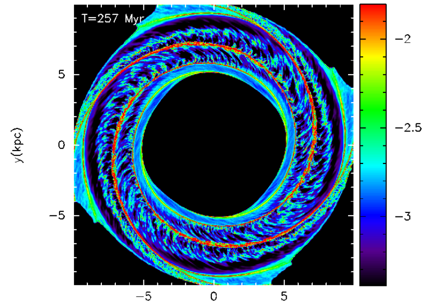


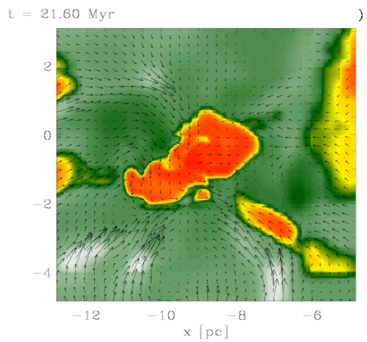


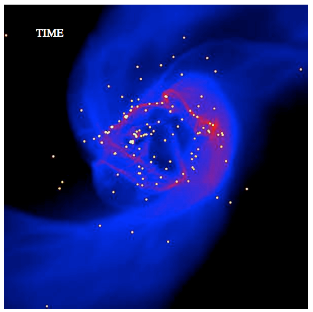

# phenomenology

# correlation between $H_2$ and HI

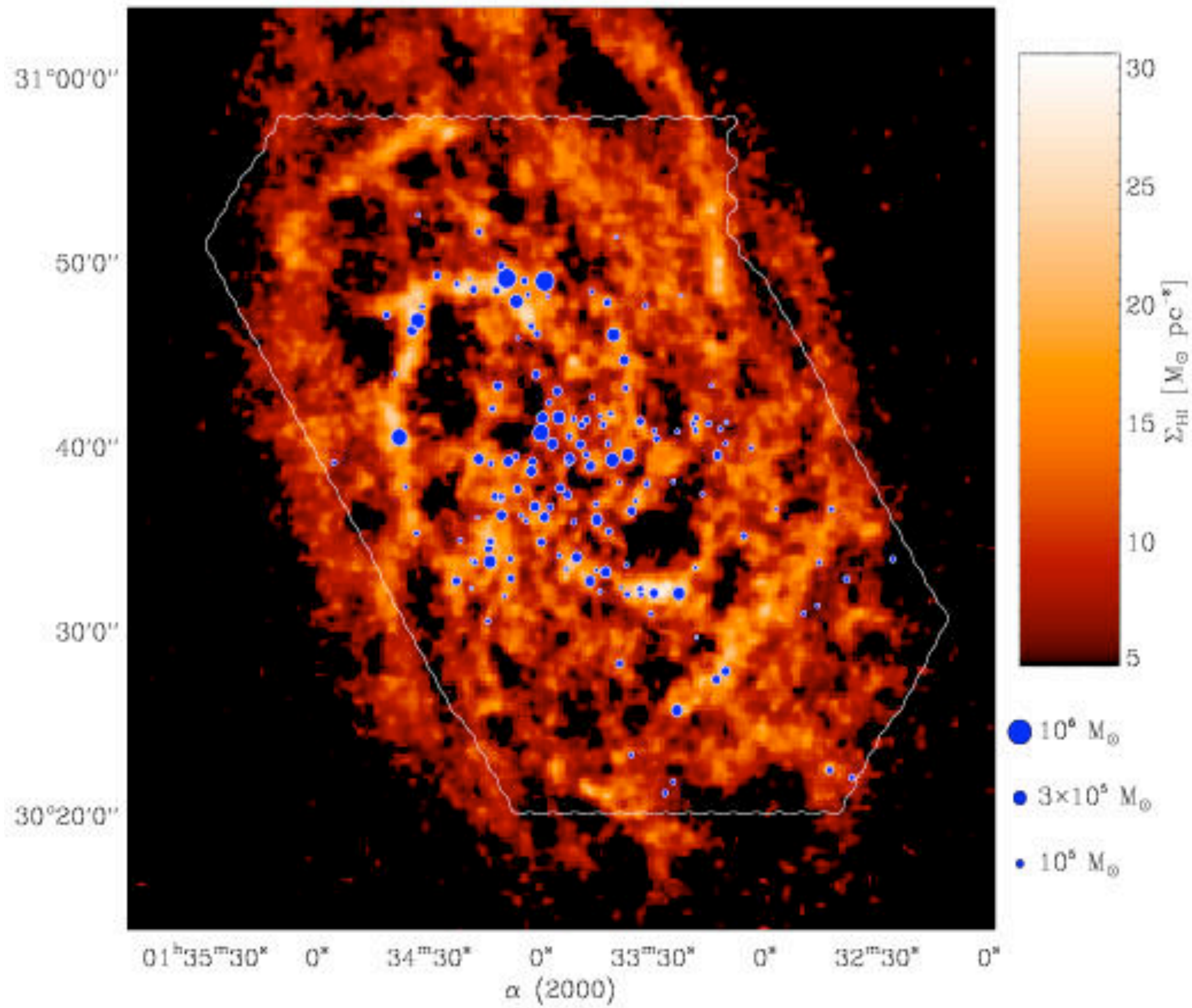


(Deul & van der Hulst 1987, Blitz et al. 2004)

Compare $H_2$ - HI in M33:

- $H_2$: BIMA-SONG Survey, see Blitz et al.
- HI: Observations with Westerbork Radio T.

$H_2$ clouds are seen in regions of high HI density
(in spiral arms and filaments)

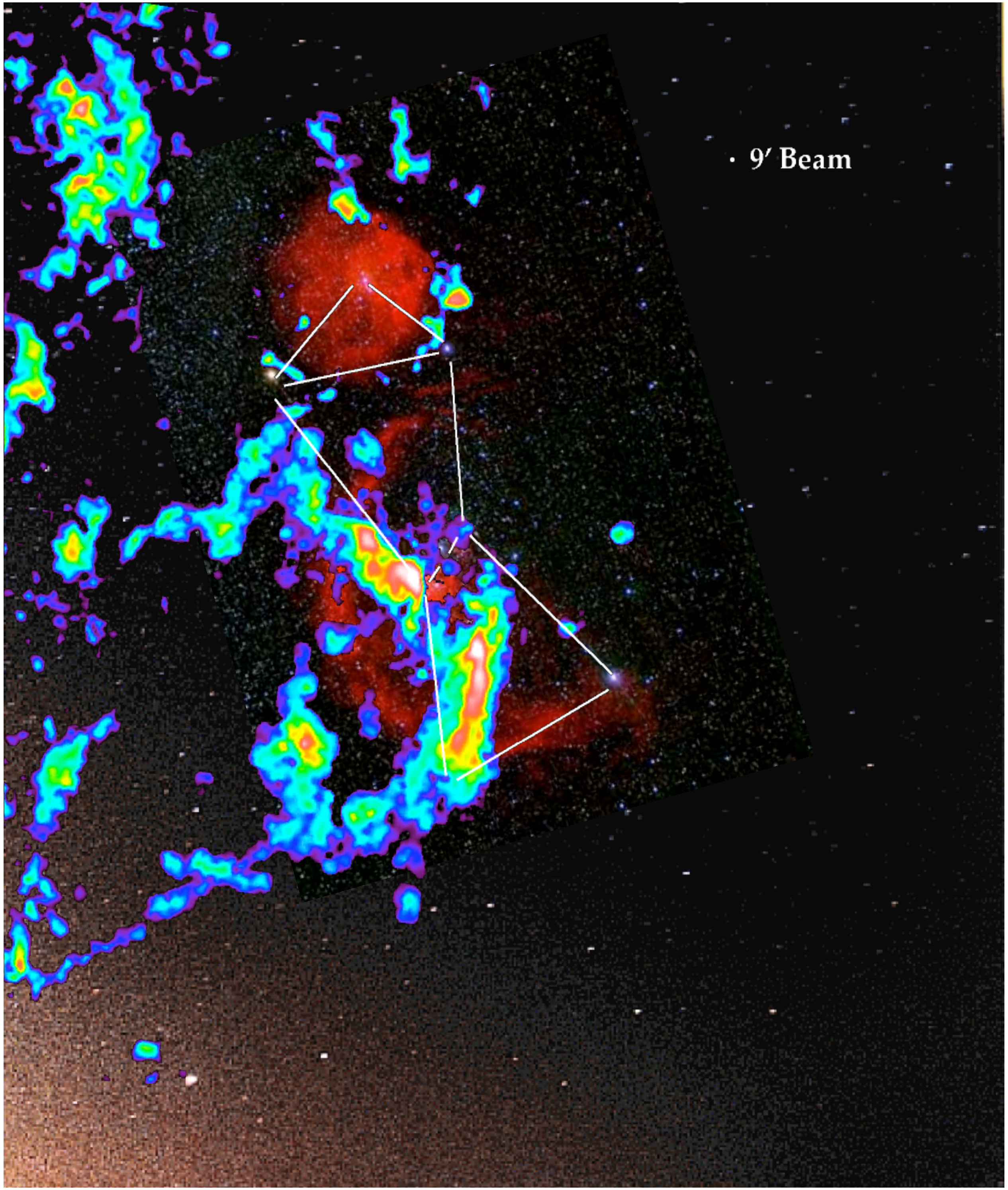


# Star formation in Orion

We see

- *Stars* (in visible light)
- Atomic hydrogen (in Hα -- red)
- Molecular hydrogen $H_2$ (radio emission -- color coded)

# Local star forming region: The Trapezium Cluster in Orion

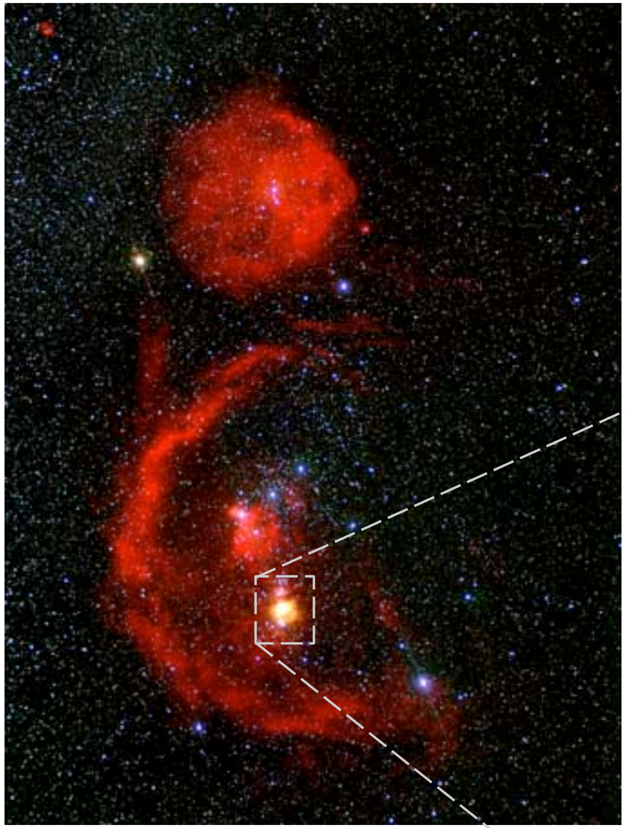

Orion molecular cloud

The Orion molecular cloud is the birth- place of several young embedded star clusters.

The Trapezium cluster is only visible in the IR and contains about 2000 newly born stars.

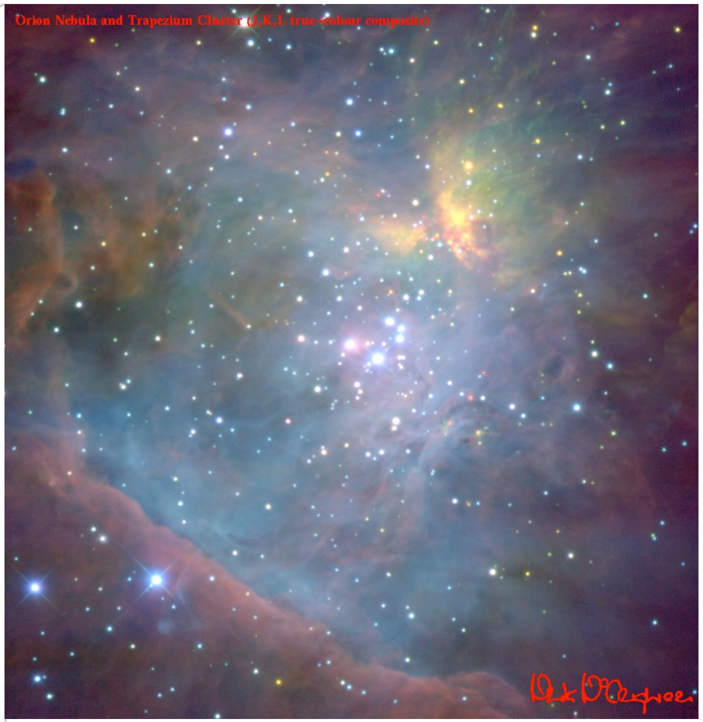


Trapezium cluster

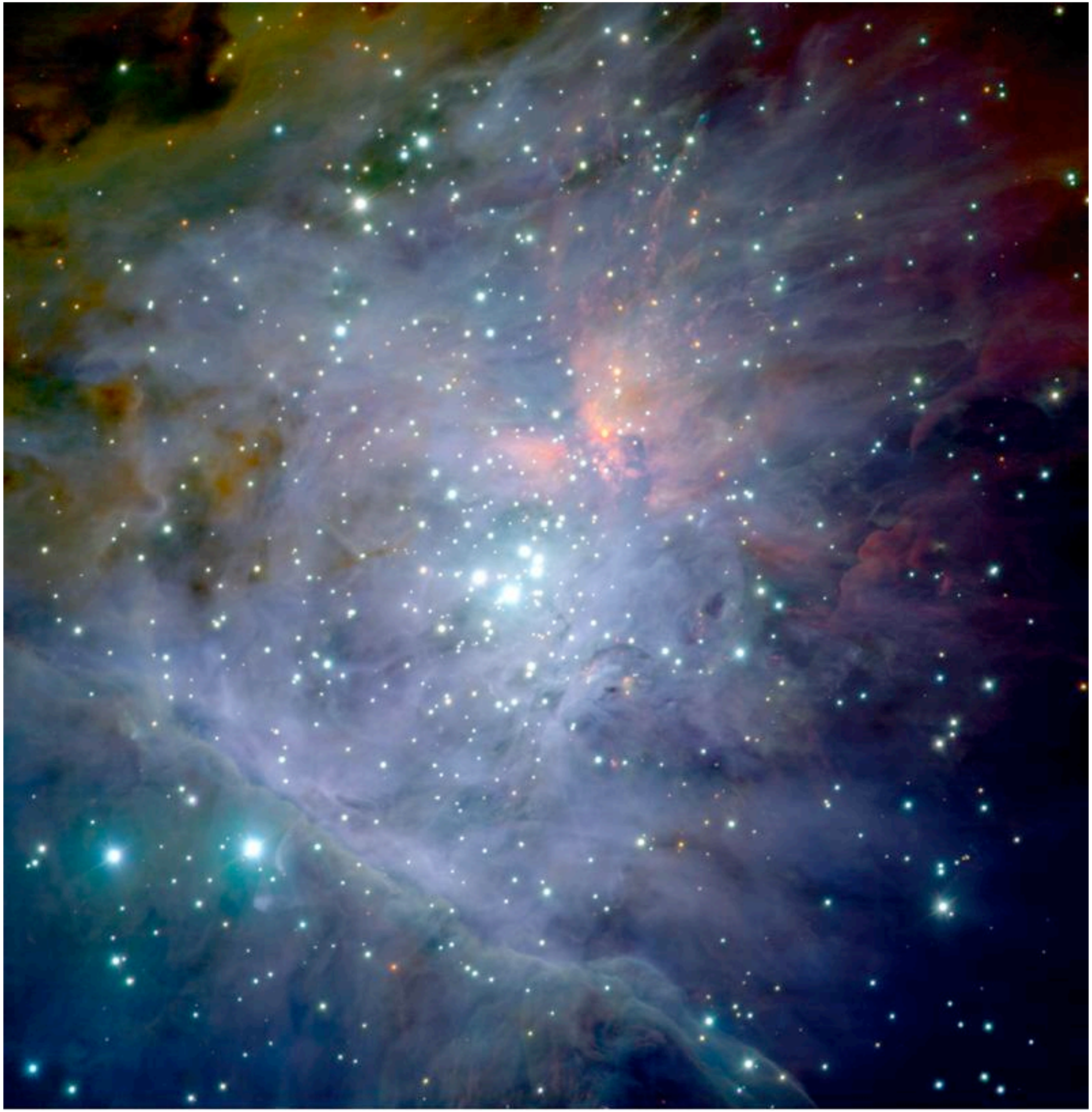

# Trapezium Cluster

(detail)

- stars form in clusters
- stars form in molecular clouds
- (proto)stellar feedback is important

(color composite J,H,K by M. McCaughrean, VLT, Paranal, Chile)

# Trapezium Cluster: Central Region

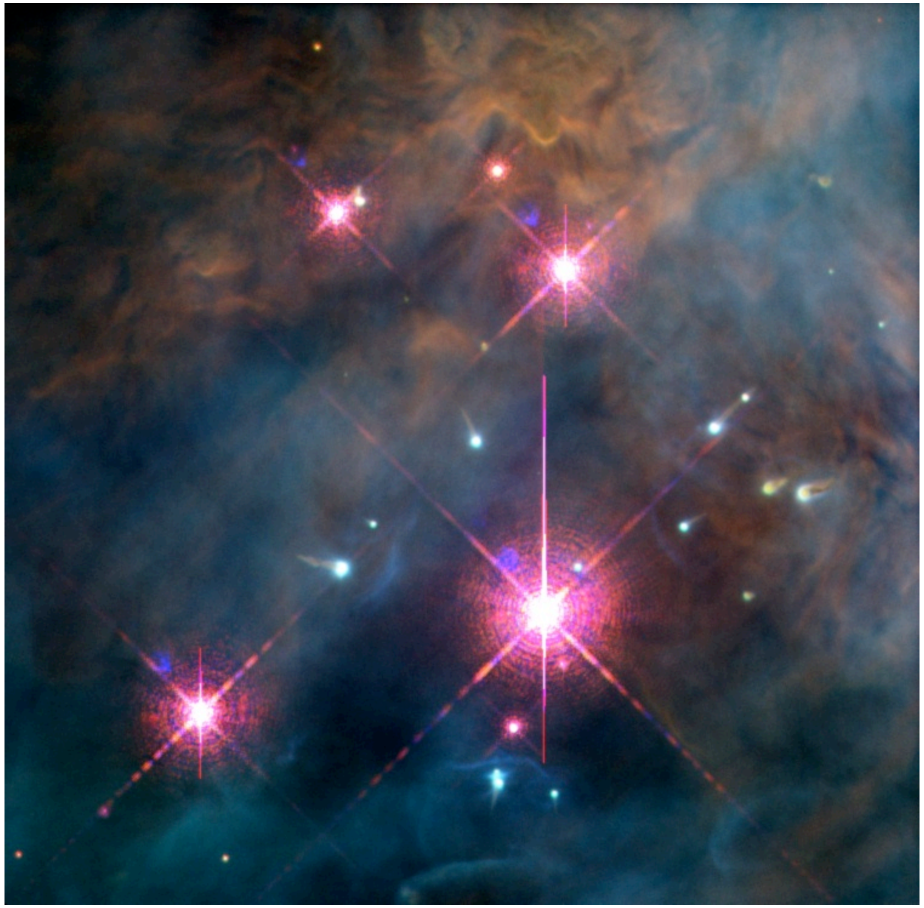

Ionizing radiation from central star
**Θ1C Orionis**

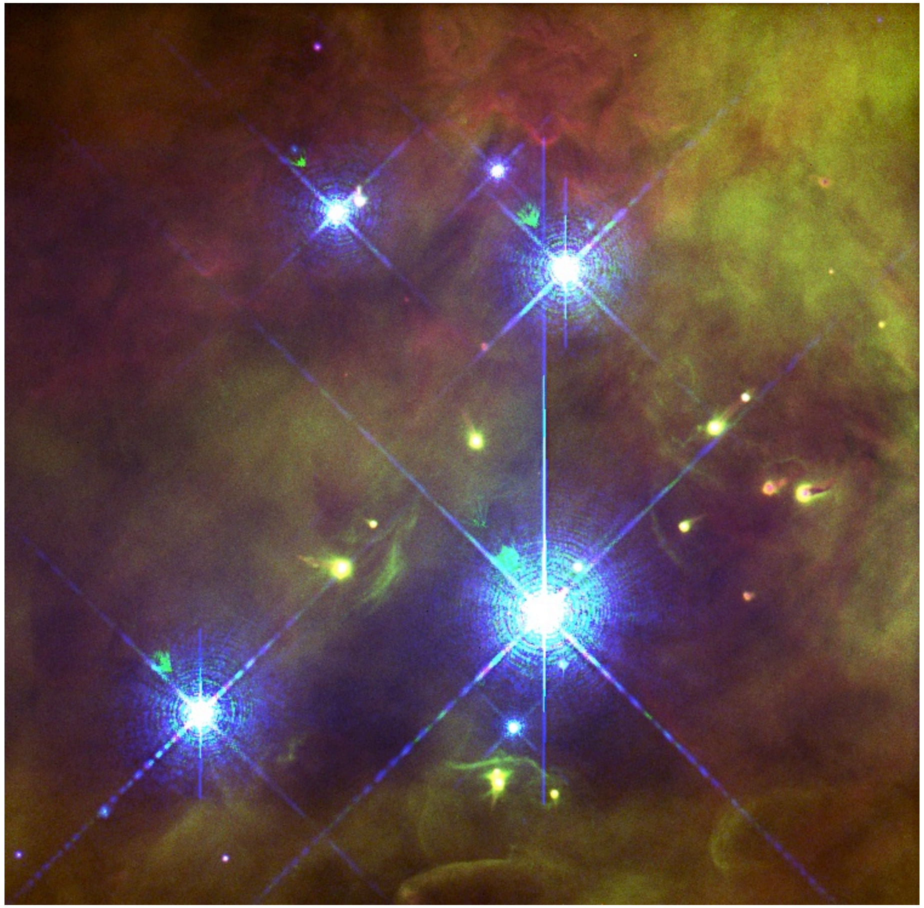

**Proplyds:** Evaporating ``protoplanetary´´ disks around young low-mass protostars

(images: Doug Johnstone et al.)

# stellar mass fuction

- stars seem to follow a universal mass function at birth --> IMF

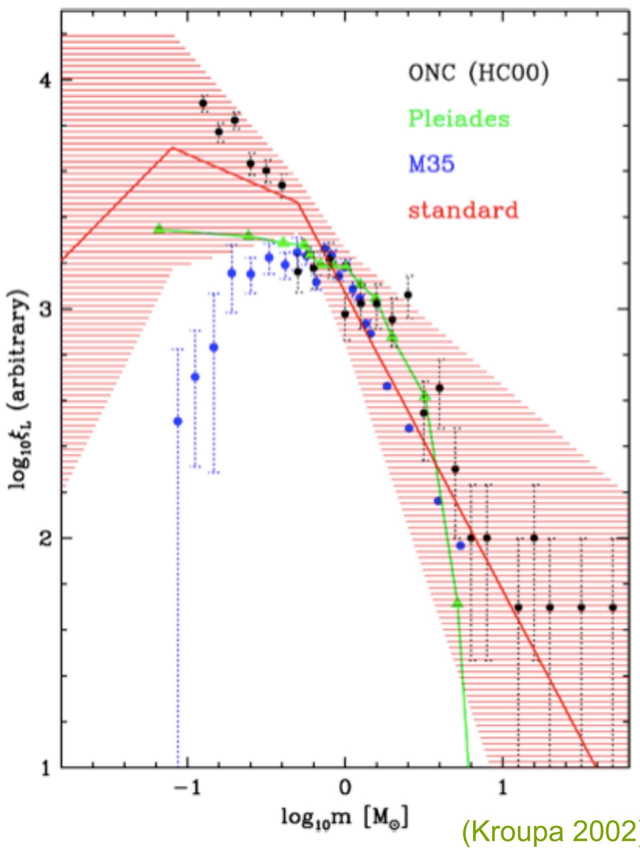


(Kroupa 2002)

Orion, NGC 3603, 30 Doradus
(Zinnecker & Yorke 2007)

# nearby molecular clouds

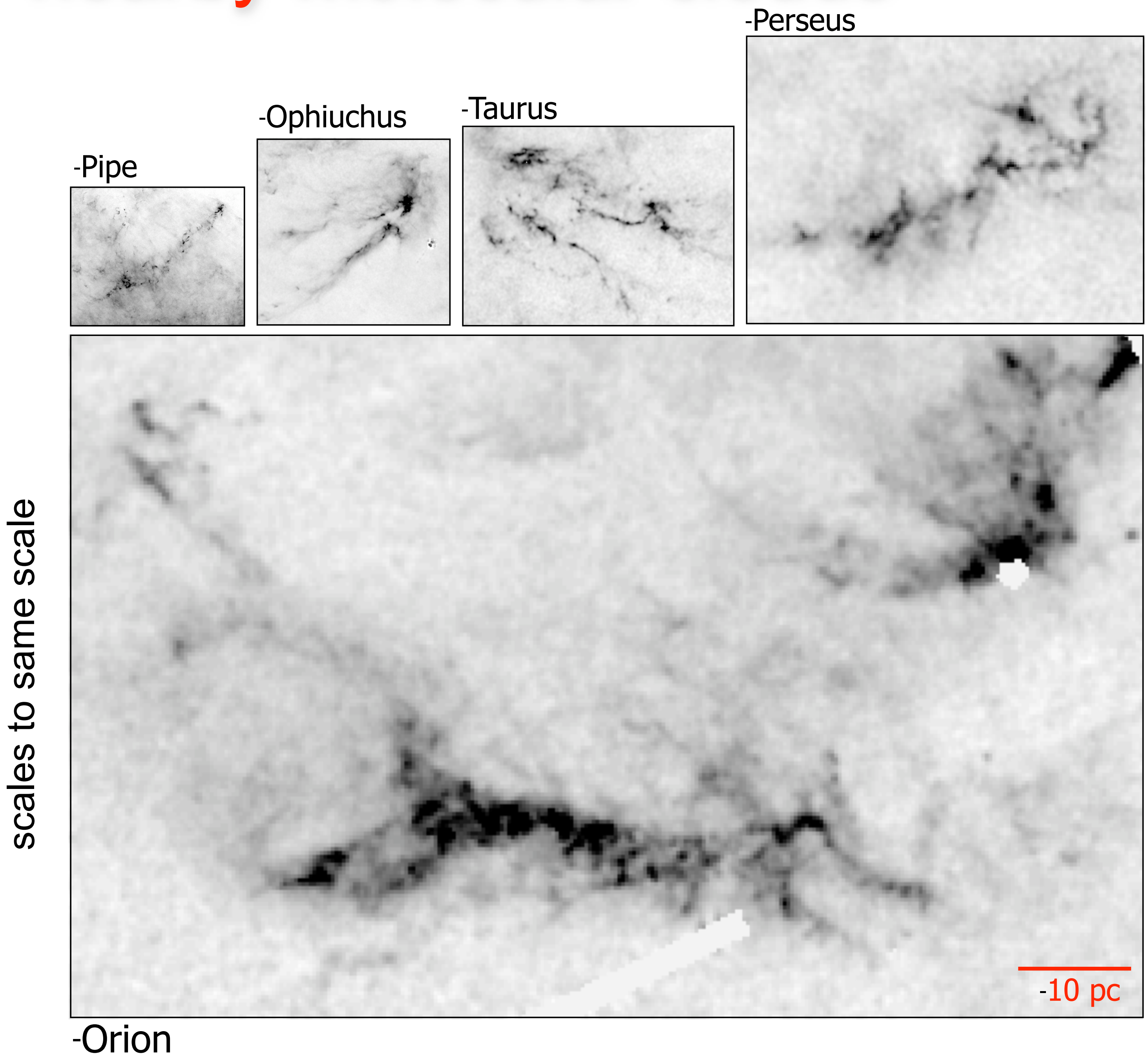


(from A. Goodman)

# nearby molecular clouds

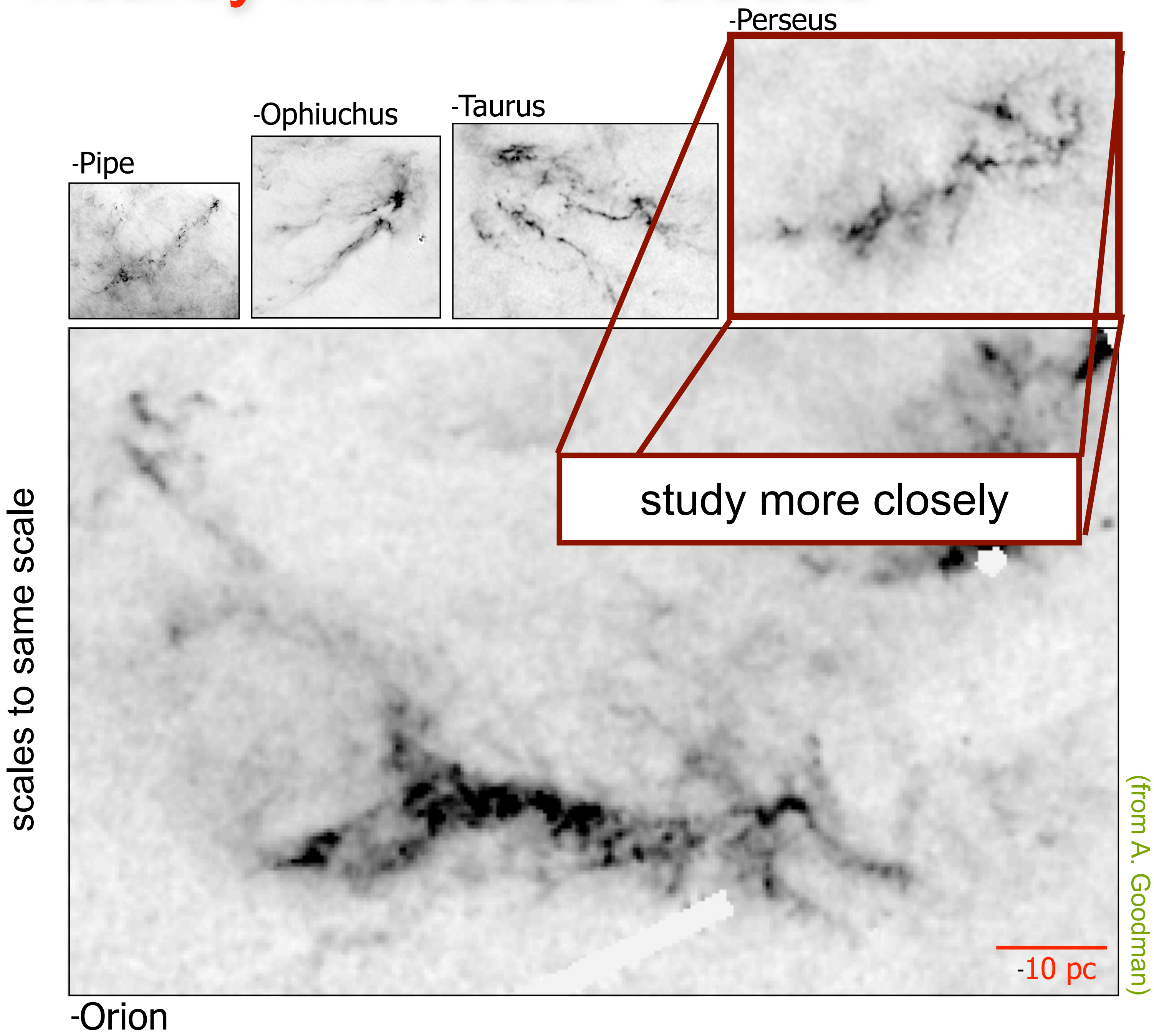

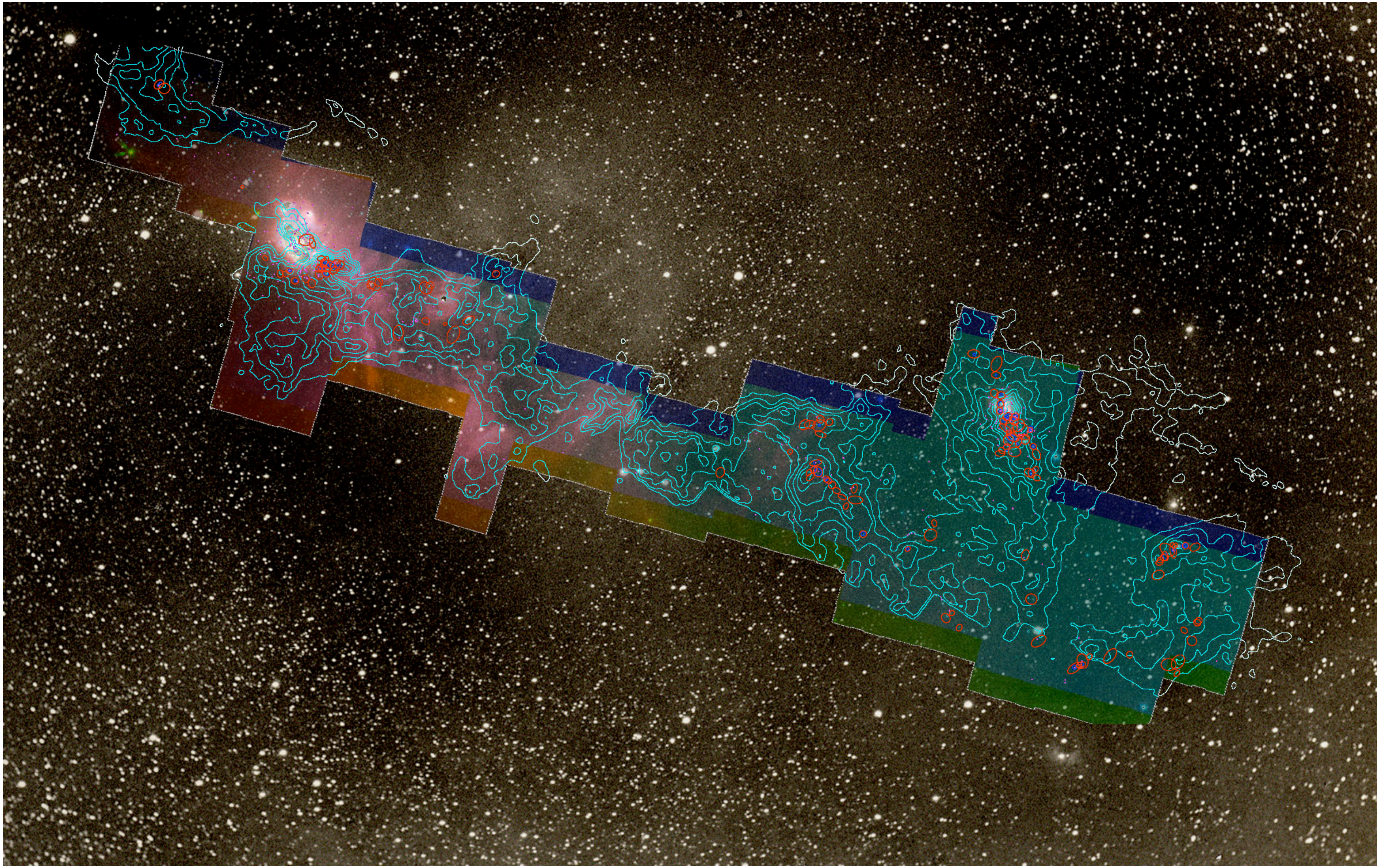

image from Alyssa Goodman: COMPLETE survey

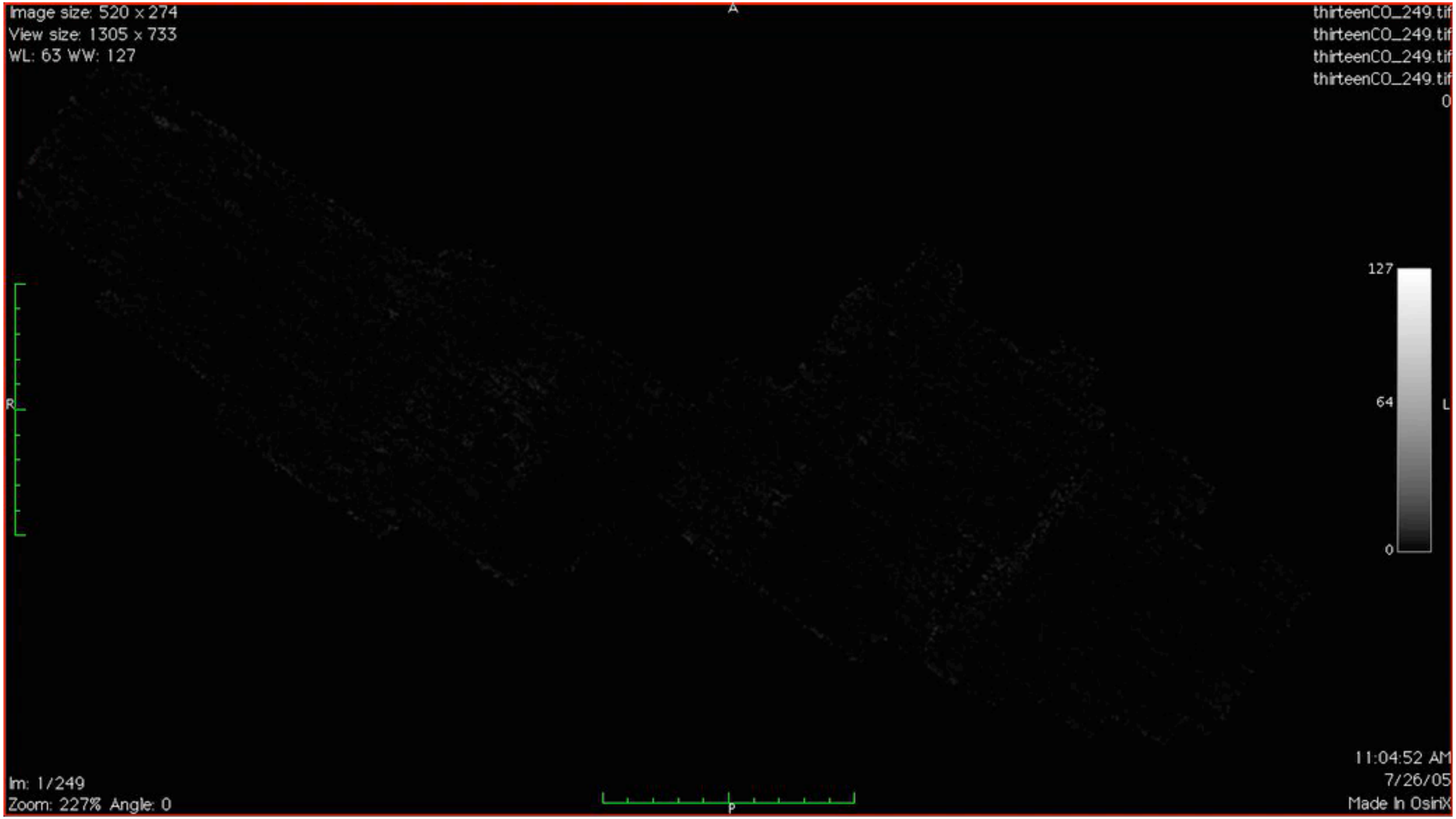


LOS Geschwindigkeitsverteilung in Perseus

velocity cube from Alyssa Goodman: COMPLETE survey

# what we need to consider ...

- *correlation* between large and small scales in galaxy (stars “know” where to form and when)
- all stars form in *molecular cloud* complexes (star formation linked to molecular cloud formation)
- molecular clouds are *turbulent* (understand turbulence to understand star formation)
- stars form in *clusters* (importance of dynamical interactions during formation)
- star formation has *universal* characteristics (e.g. initial mass fuction)

# basic idea

# dynamical SF in a nutshell

- interstellar gas is highly *inhomogeneous*

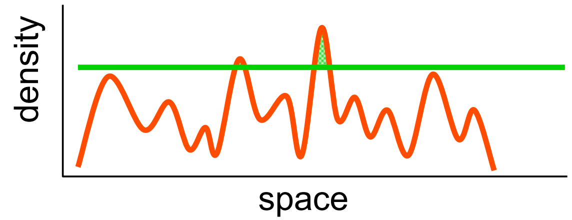


  - *gravitational instability*
  - *thermal instability*
  - *turbulent compression* (in shocks $\delta\rho/\rho \propto \mathcal{M}^2$; in atomic gas: $\mathcal{M} \approx 1...3$)

- cold *molecular clouds* can form rapidly in high-density regions at *stagnation points* of *convergent large-scale flows*
  - chemical *phase transition*: atomic → molecular
  - process is *modulated* by large-scale *dynamics* in the galaxy

- inside *cold clouds:* turbulence is highly supersonic ($\mathcal{M} \approx 1...20$)
  → *turbulence* creates large density contrast,
  *gravity* selects for collapse

  ⟶ ***GRAVOTUBULENT FRAGMENTATION***

- *turbulent cascade:* local compression *within* a cloud provokes collapse
  → formation of individual *stars* and *star clusters*

(e.g. Mac Low & Klessen, 2004, Rev. Mod. Phys., 76, 125-194)

# Turbulent cascade

Kolmogorov (1941) theory
incompressible turbulence

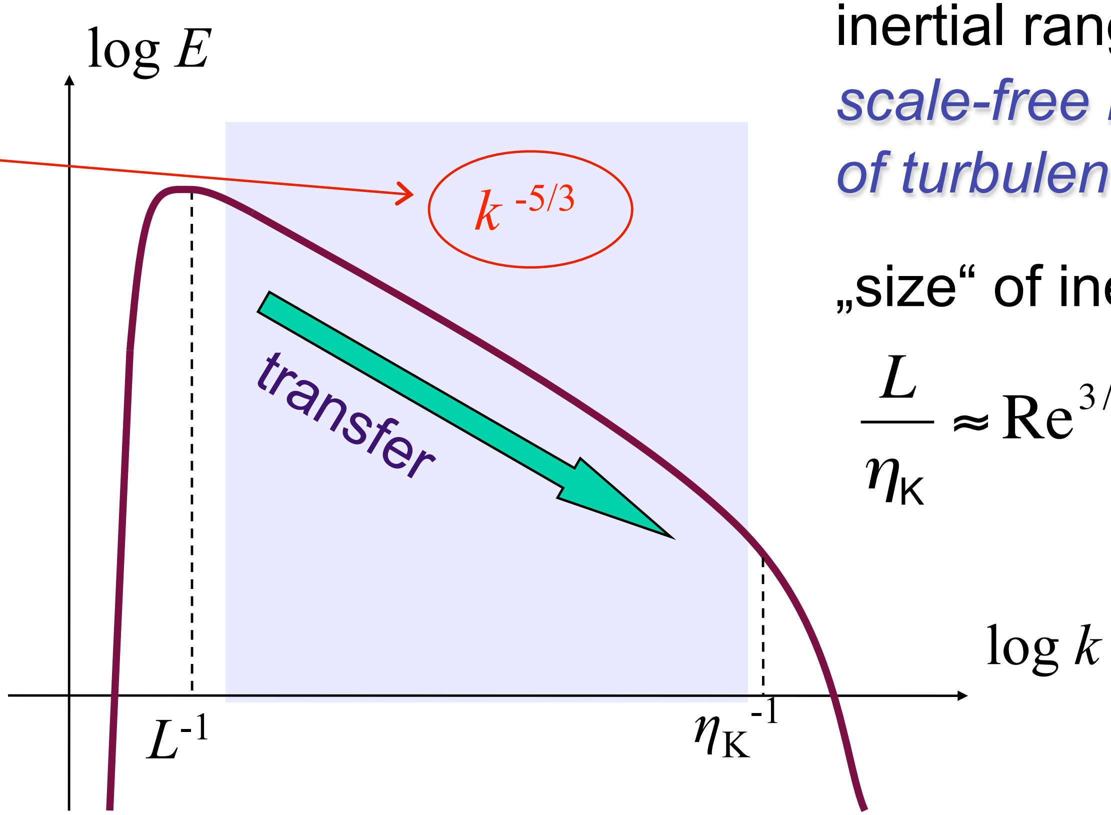


energy
input
scale

energy
dissipation
scale

inertial range:

*scale-free behavior of turbulence*

„size" of inertial range:

$$\frac{L}{\eta_K} \approx \mathrm{Re}^{3/4}$$

# Turbulent cascade

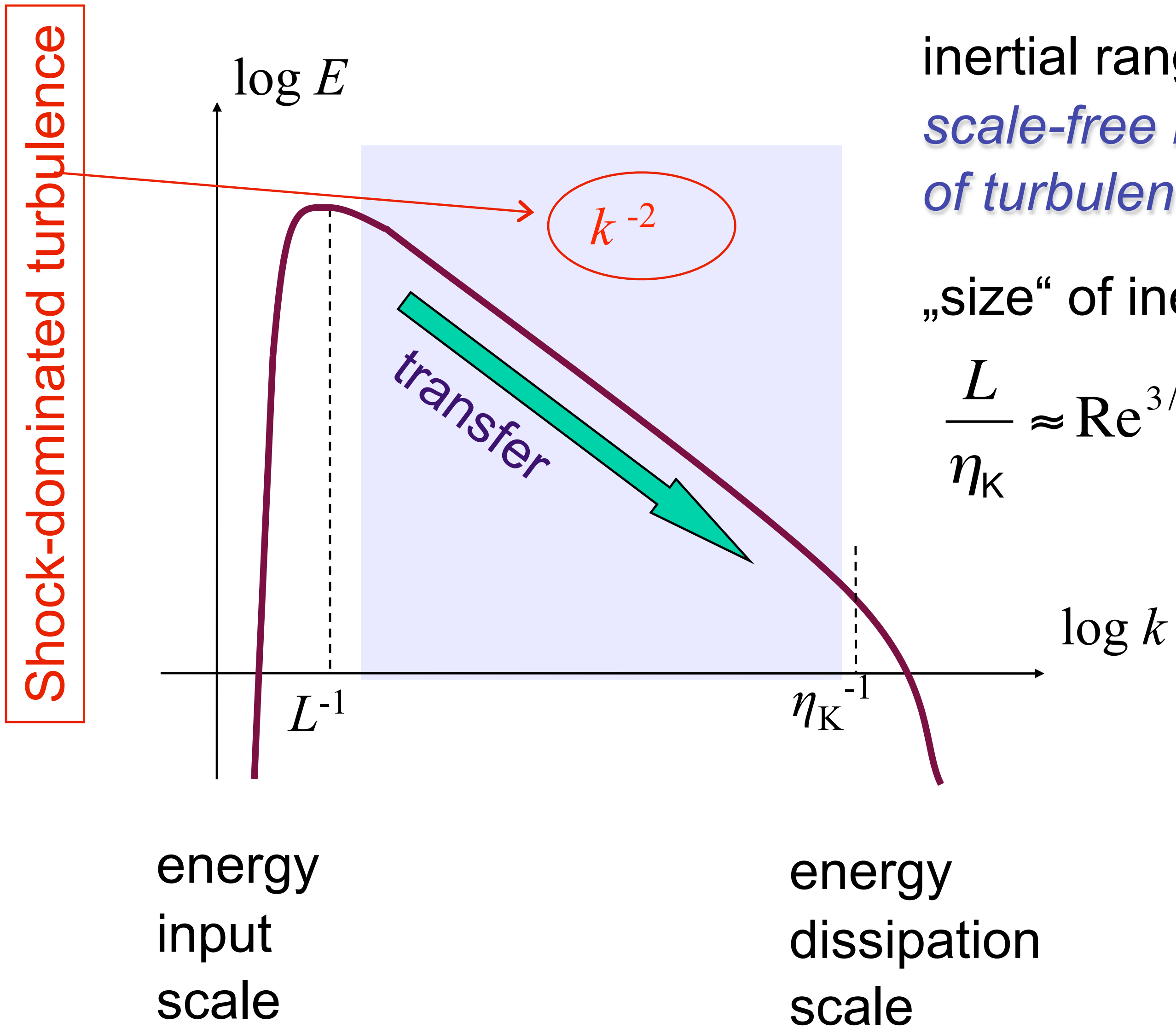


inertial range:

*scale-free behavior of turbulence*

„size" of inertial range:

$$\frac{L}{\eta_K} \approx \mathrm{Re}^{3/4}$$

# Turbulent cascade in ISM

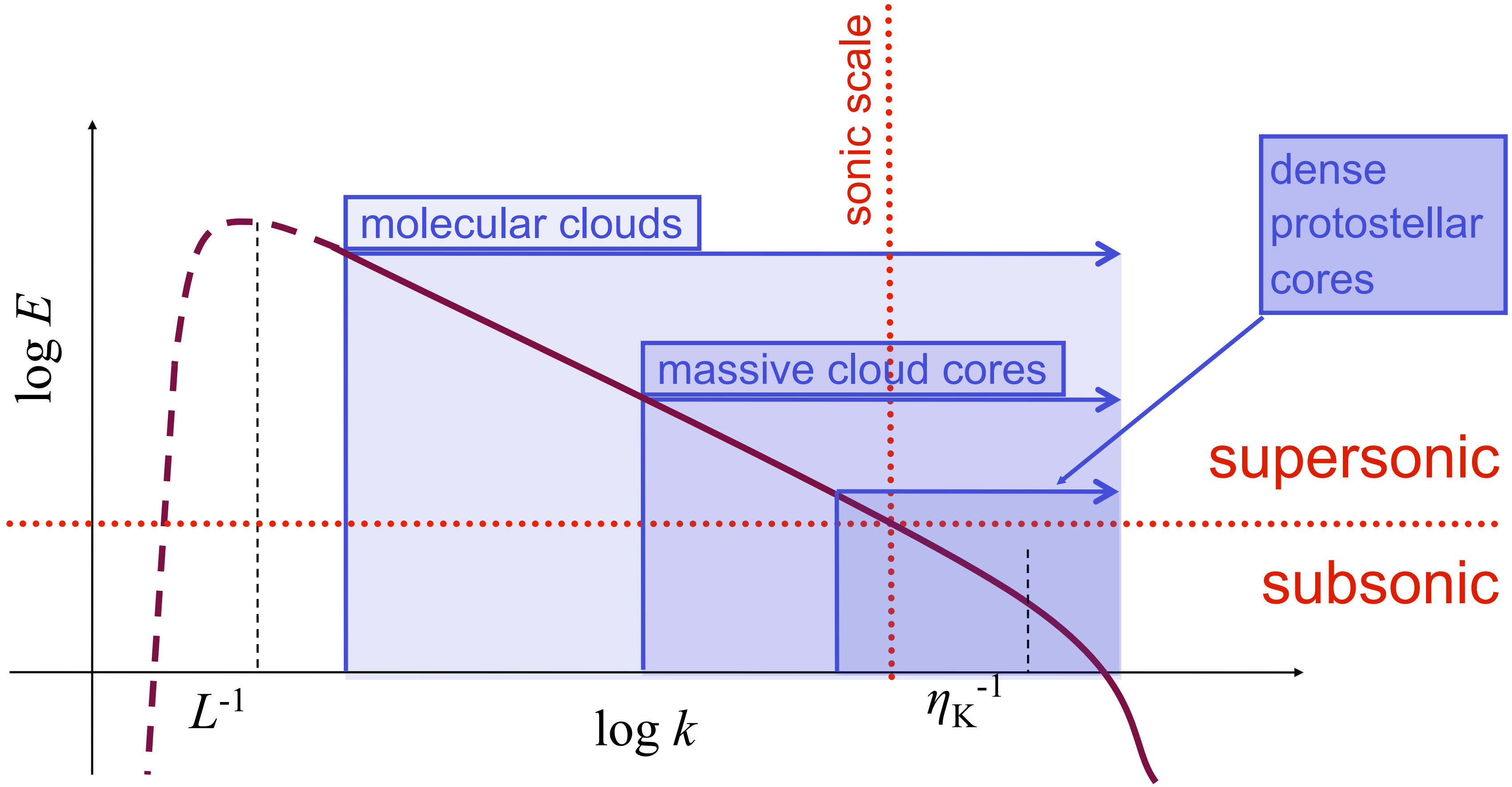


energy source & scale *NOT known* (supernovae, winds, spiral density waves?)

$\sigma_{rms}$ << 1 km/s
$M_{rms} \leq 1$
L ≈ 0.1 pc

dissipation scale not known (ambipolar diffusion, molecular diffusion?)

# Density structure of MC's

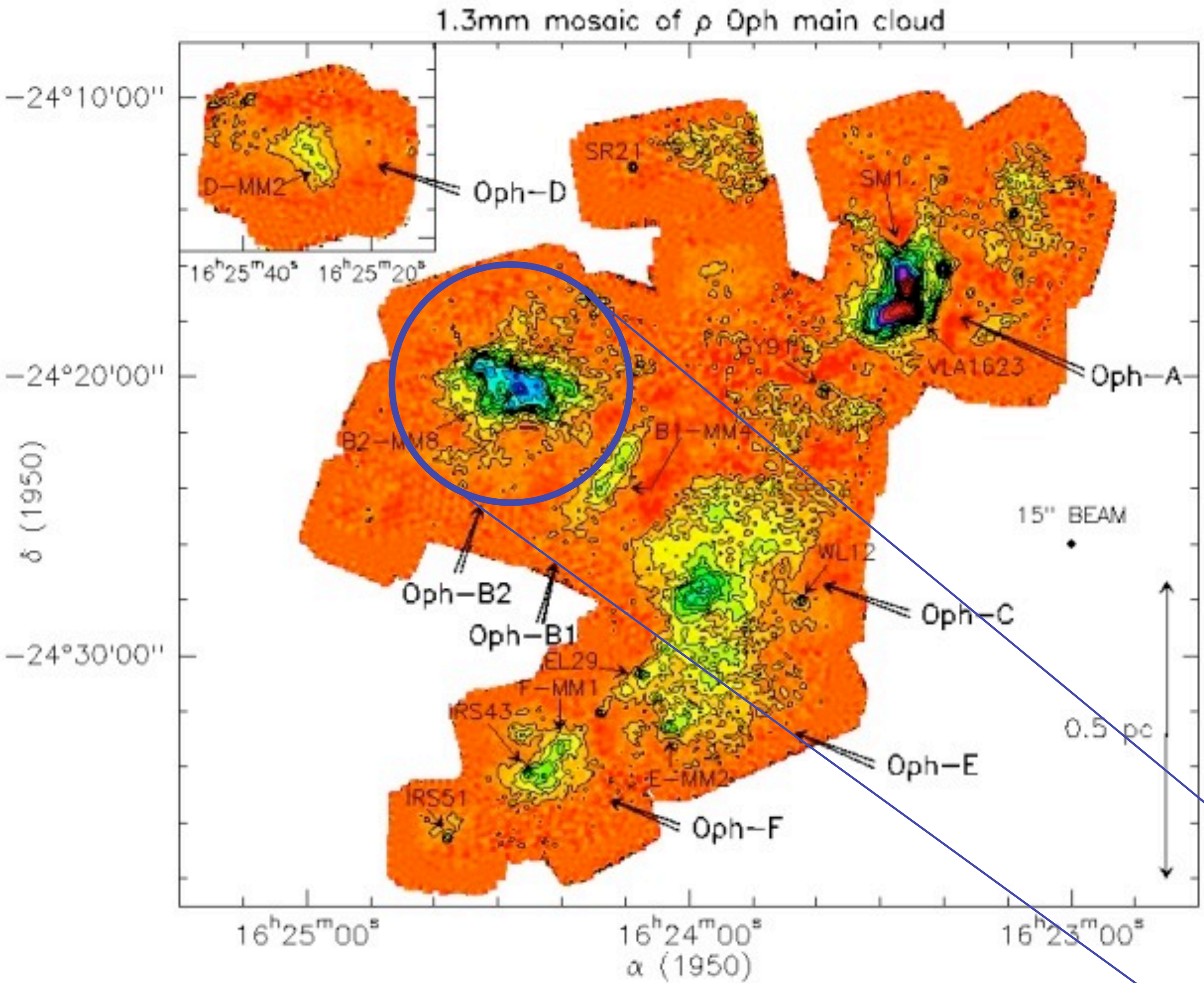


(Motte, André, & Neri 1998)

molecular clouds are highly inhomogeneous

stars form in the densest and coldest parts of the cloud

ρ-Ophiuchus cloud seen in dust emission

let's focus on a cloud core like this one

# Evolution of cloud cores

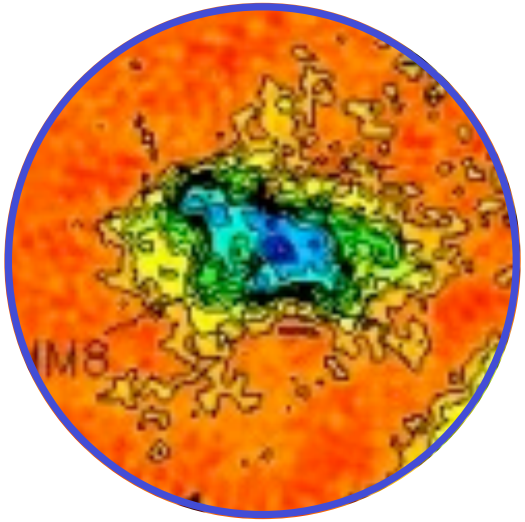


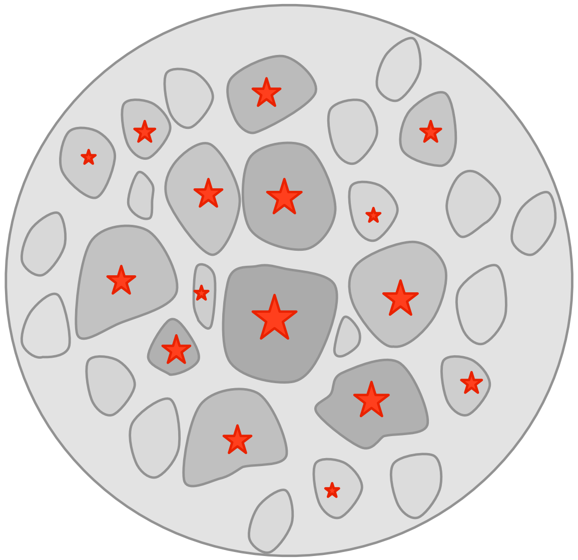

- How does this core evolve?
  Does it form one single massive star
  or cluster with mass distribution?

- Turbulent cascade „goes through“ cloud core
  --> NO *scale separation* possible
  --> NO *effective sound speed*
- Turbulence is supersonic!
  --> produces strong density contrasts:
  $\delta\rho/\rho \approx M^2$
  --> with typical $M \approx 10$ --> $\delta\rho/\rho \approx 100$!
- many of the shock-generated fluctuations are Jeans unstable and go into collapse
- --> expectation: *core breaks up and forms a cluster of stars*

# Evolution of cloud cores

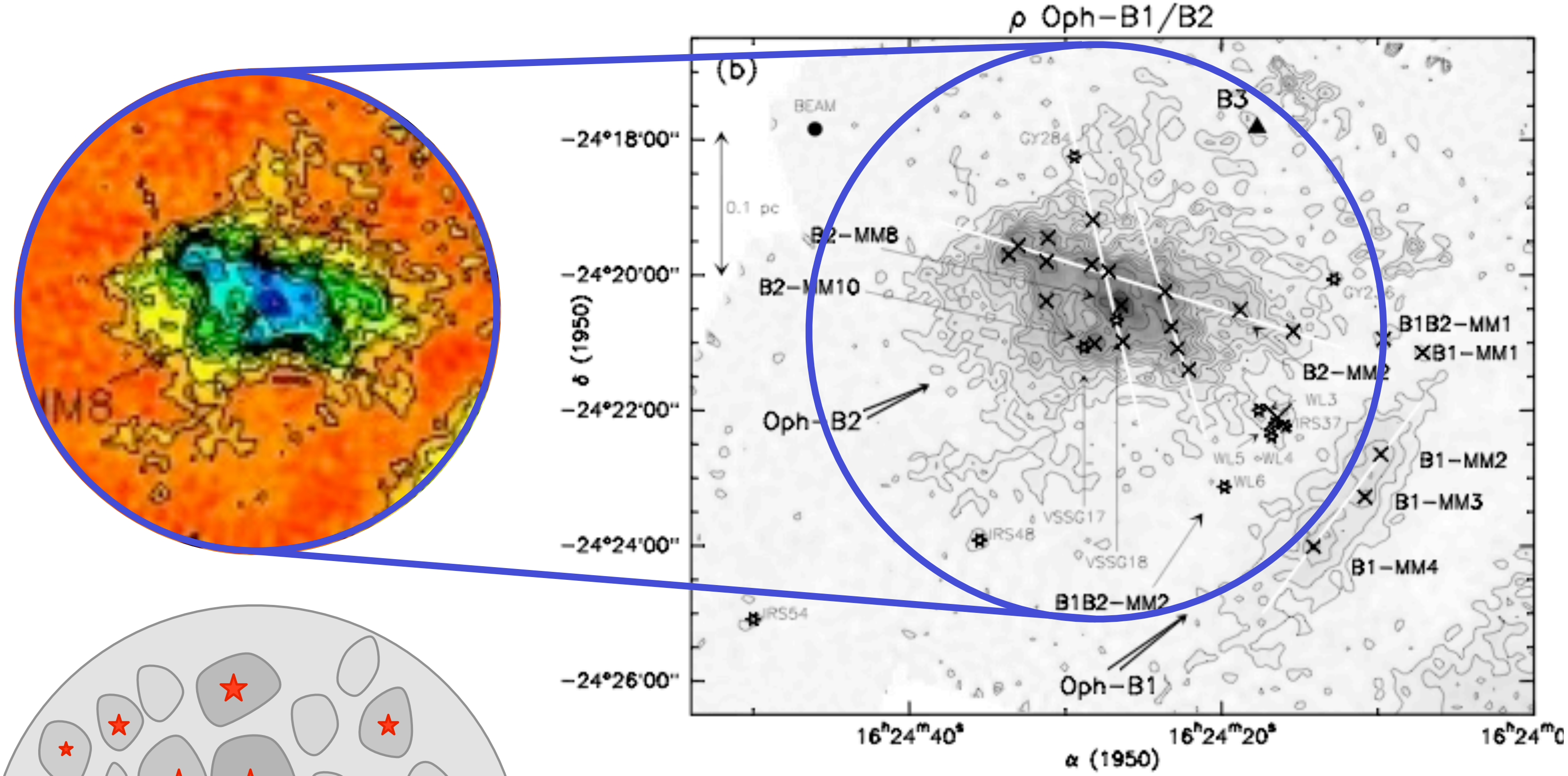


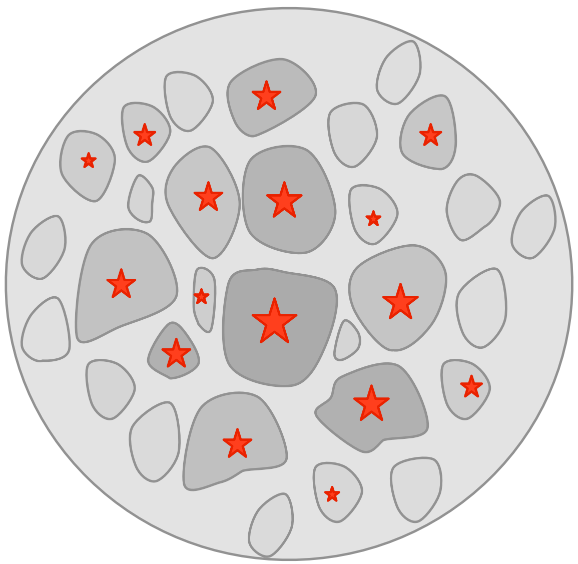

indeed ρ-Oph B1/2 contains several cores ("starless" cores are denoted by ×, cores with embedded protostars by ☆)

(Motte, André, & Neri 1998)

# Formation and evolution of cores

What happens to distribution of cloud cores?

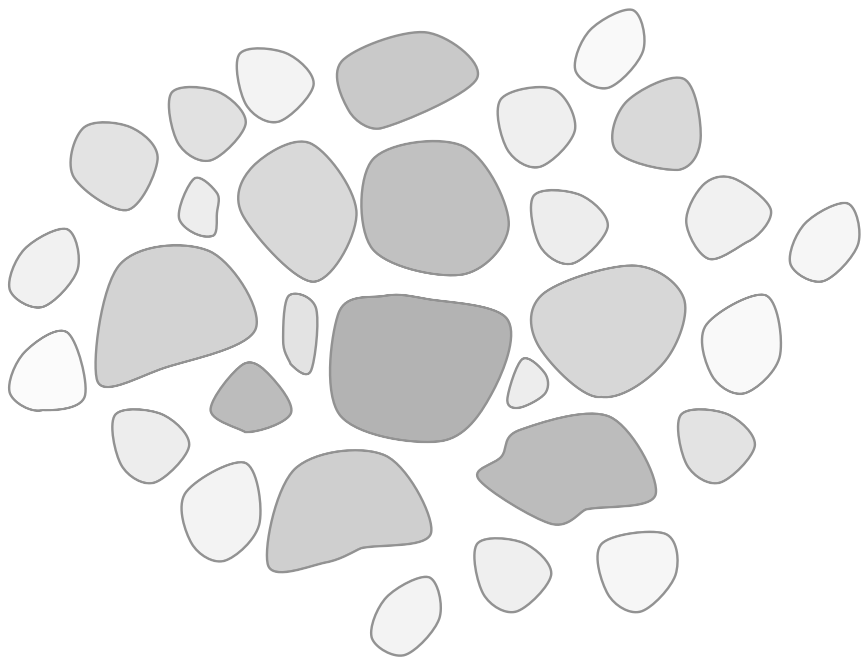

Two exteme cases:

(1) turbulence dominates energy budget:

$\alpha = E_{kin}/|E_{pot}| > 1$

--> individual cores do *not* interact

--> *collapse* of *individual* cores dominates *stellar mass growth*

--> *loose cluster of low-mass stars*

(2) turbulence decays, i.e. gravity dominates: $\alpha = E_{kin}/|E_{pot}| < 1$

--> *global contraction*

--> core do *interact* while collapsing

--> *competition* influences *mass growth*

--> *dense cluster with high-mass stars*

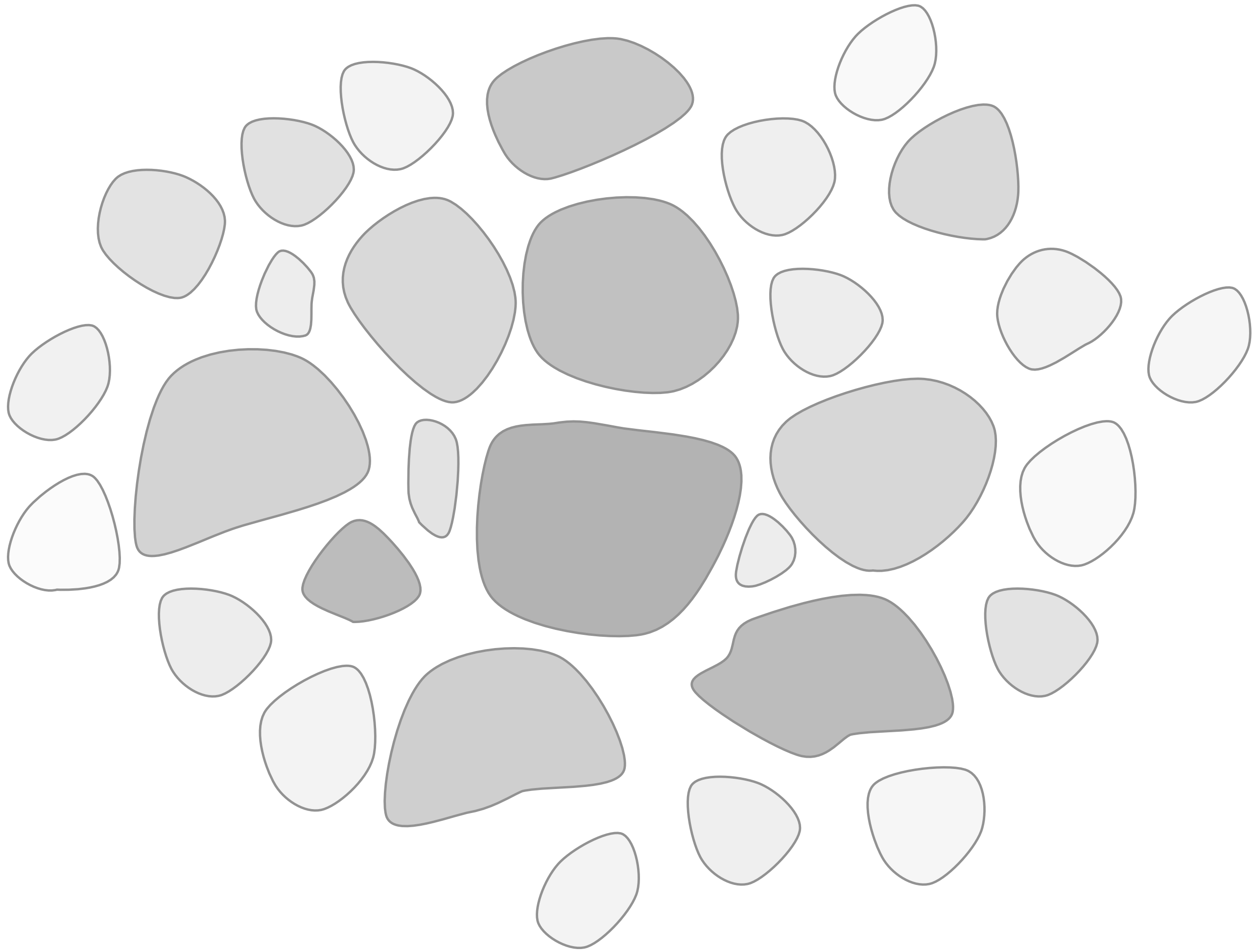

turbulence creates a hierarchy of clumps

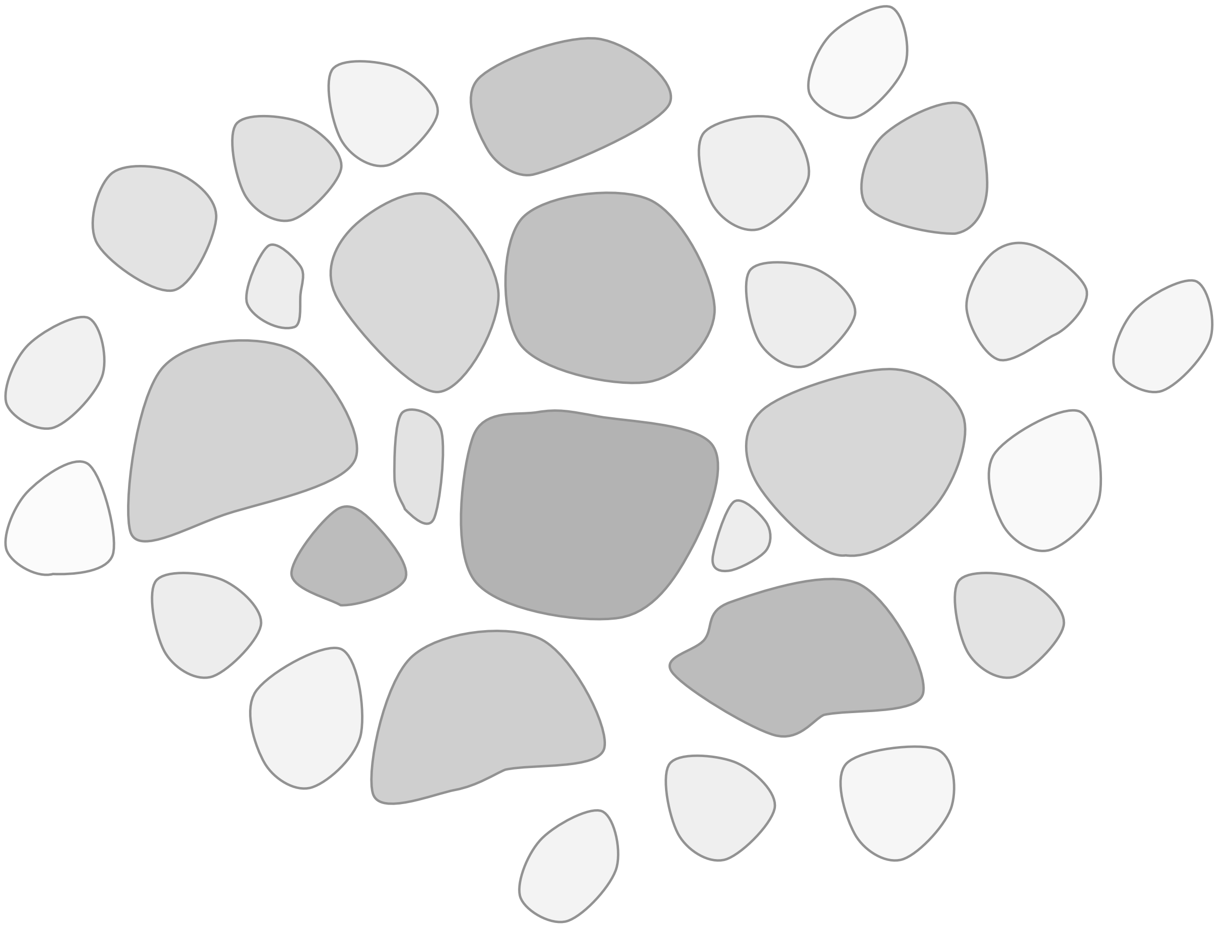

as turbulence decays locally, contraction sets in

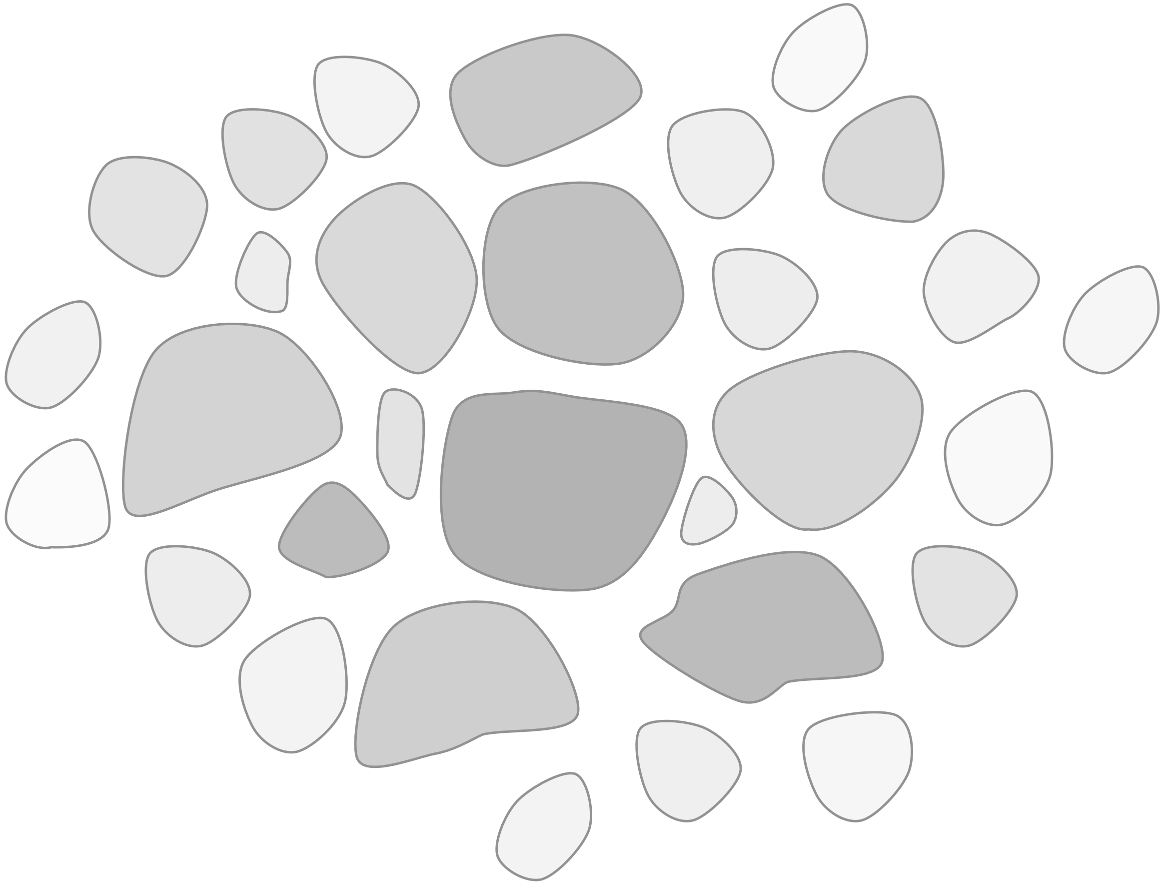

as turbulence decays locally, contraction sets in

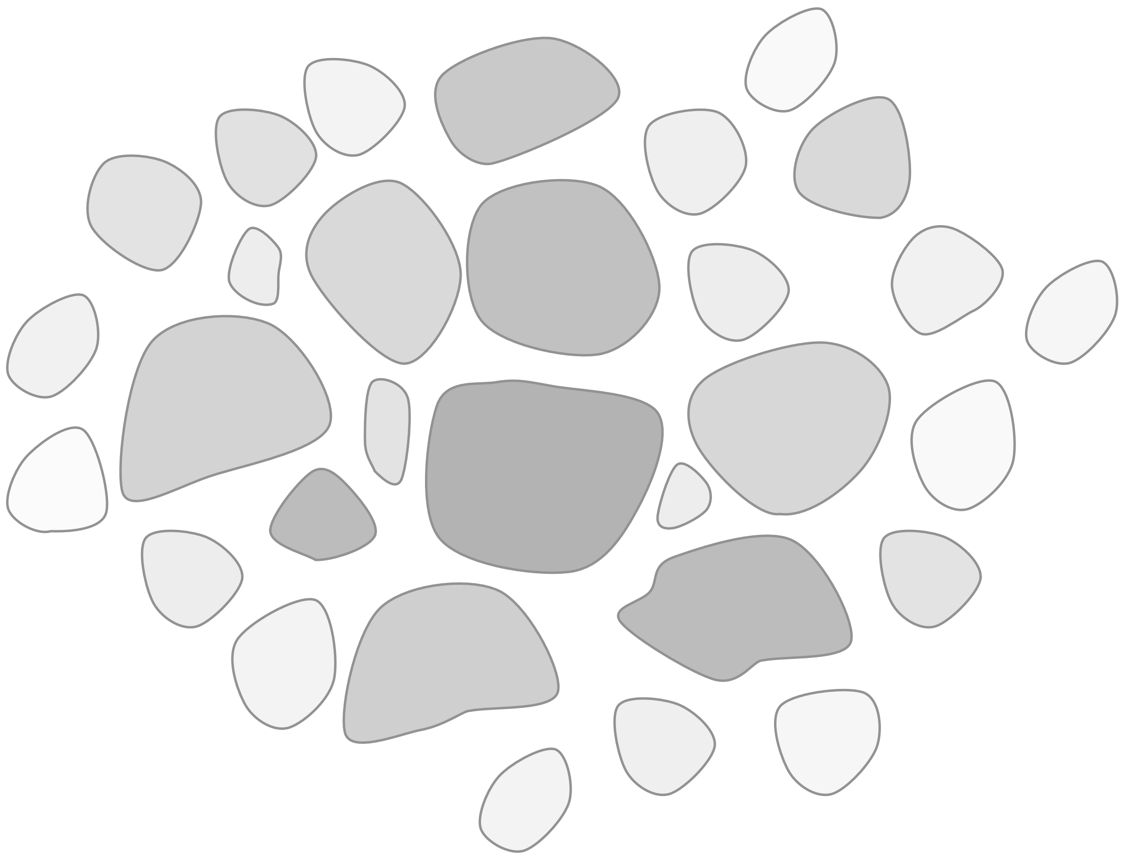

while region contracts, individual clumps collapse to form stars

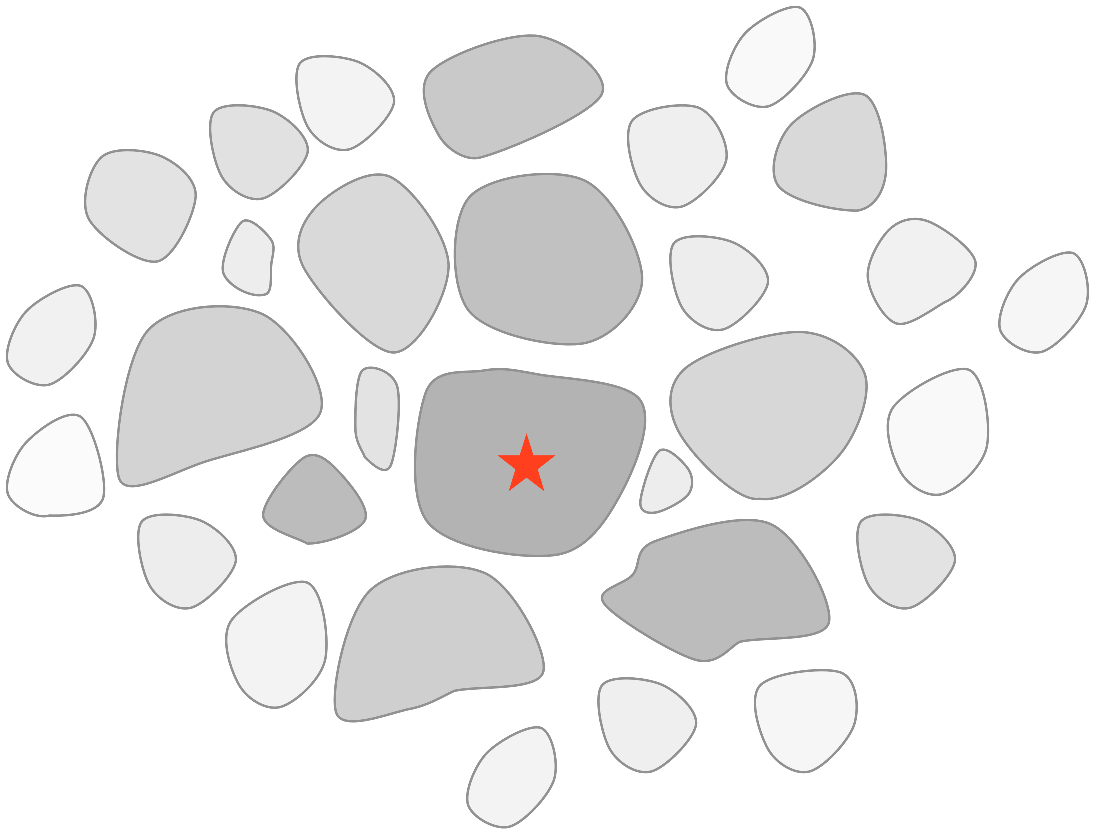

while region contracts, individual clumps collapse to form stars

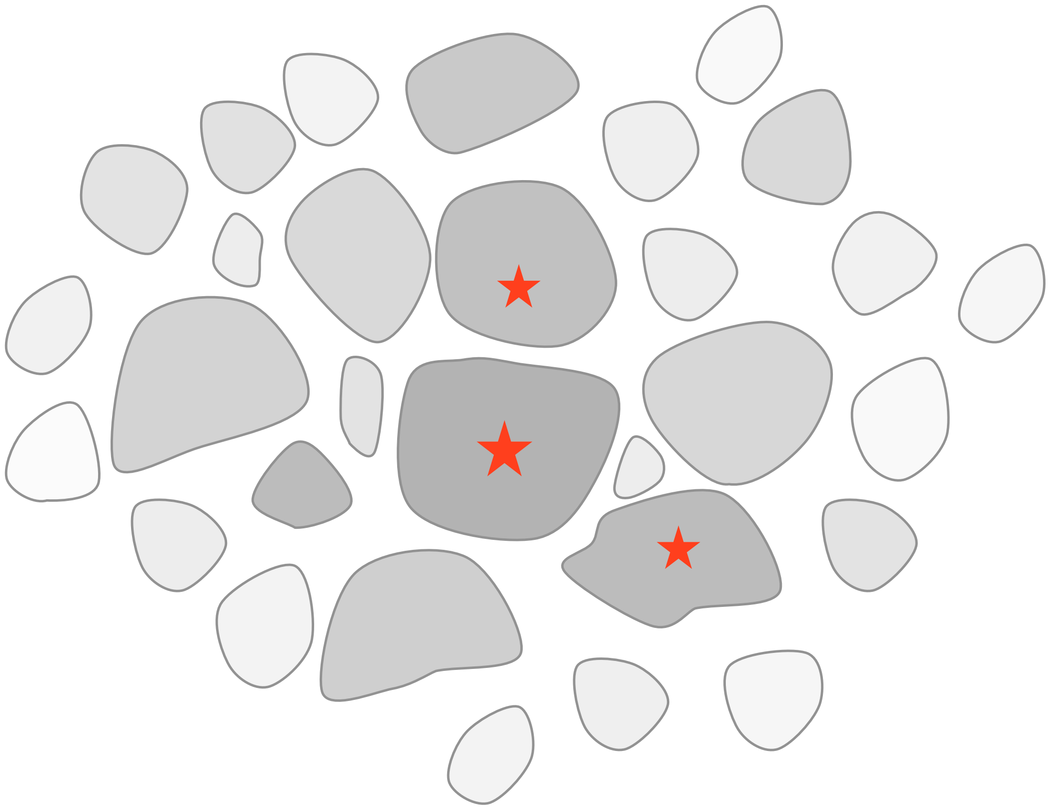

individual clumps collapse to form stars

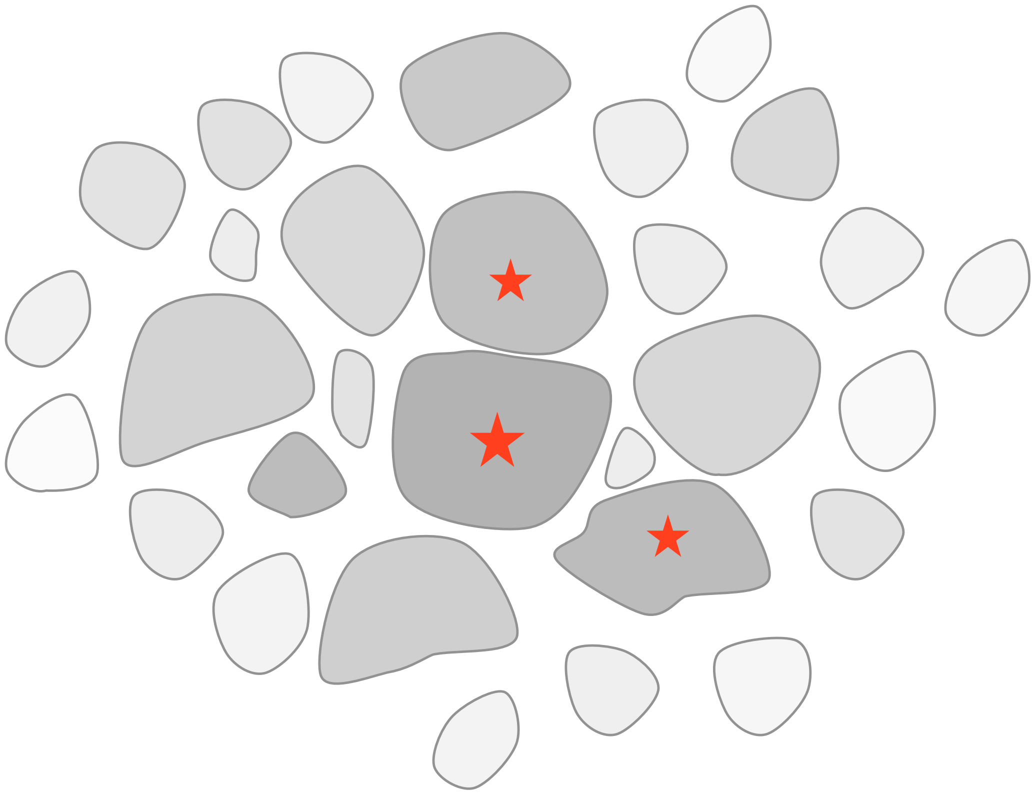

individual clumps collapse to form stars

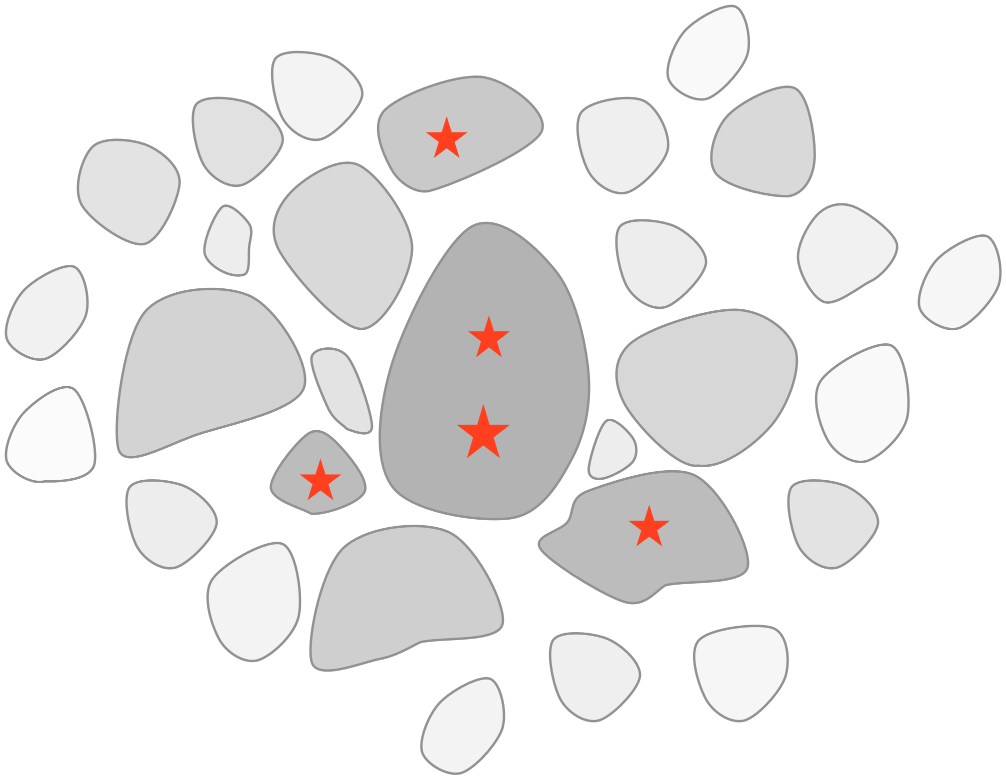

$\alpha = E_{kin}/|E_{pot}| < 1$

in *dense clusters*, clumps may merge while collapsing
--> then contain multiple protostars

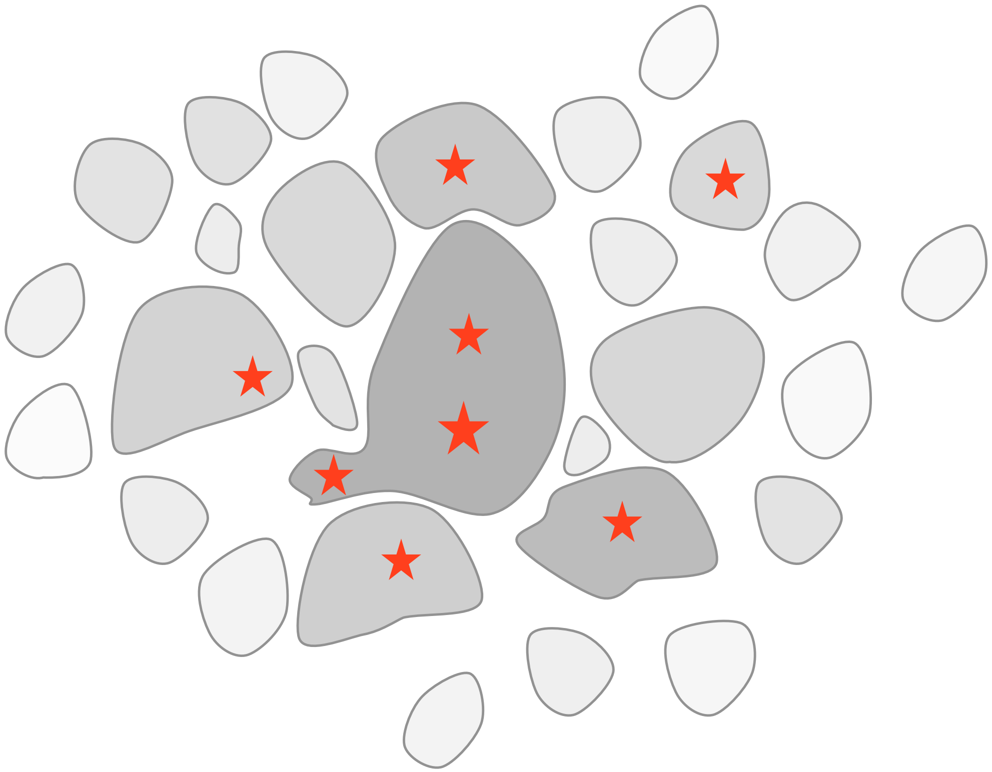

in *dense clusters*, clumps may merge while collapsing
--> then contain multiple protostars

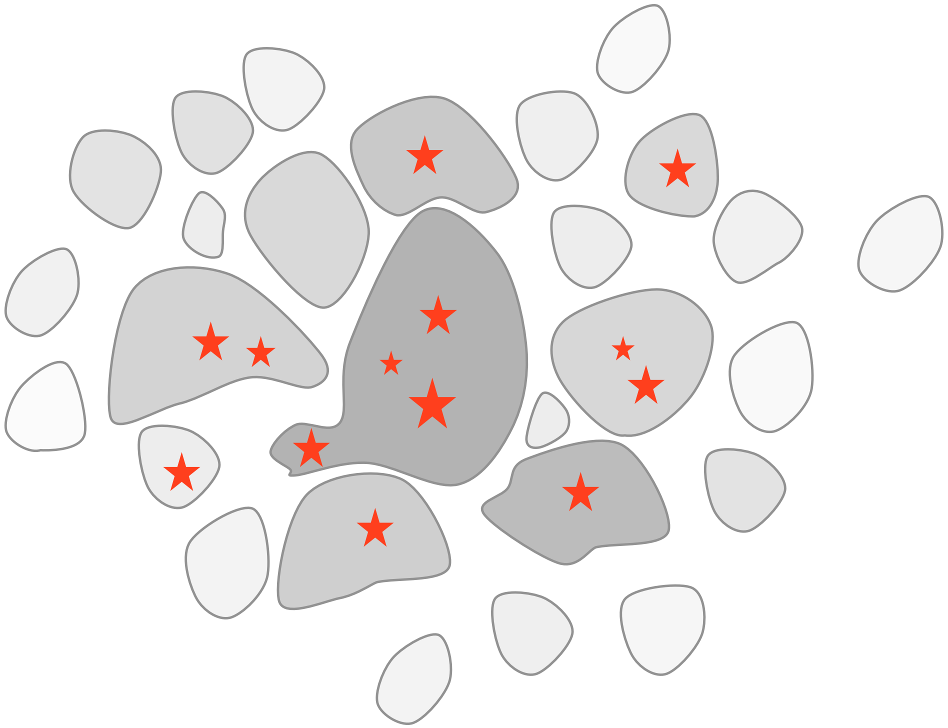

in *dense clusters*, clumps may merge while collapsing
--> then contain multiple protostars

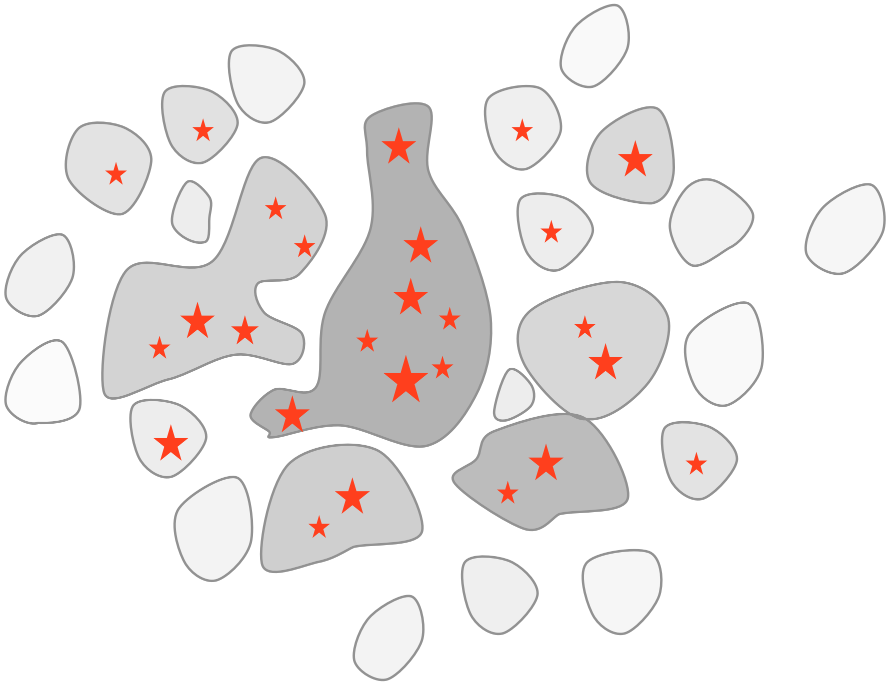

in *dense clusters*, competitive mass growth becomes important

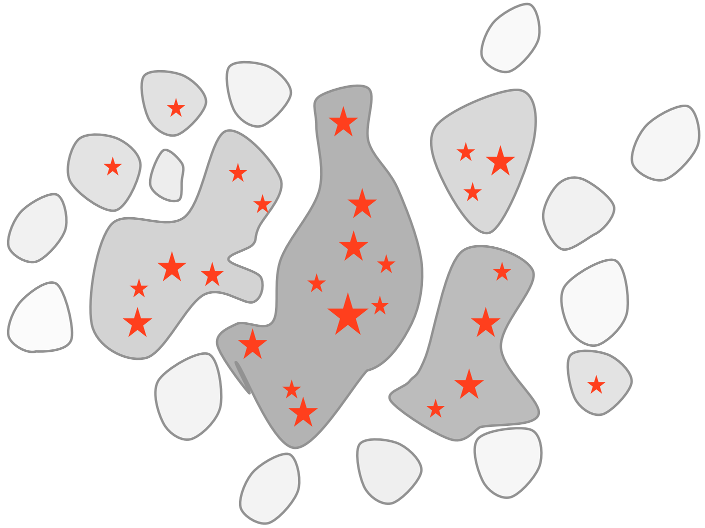

in *dense clusters*, competitive mass growth
becomes important

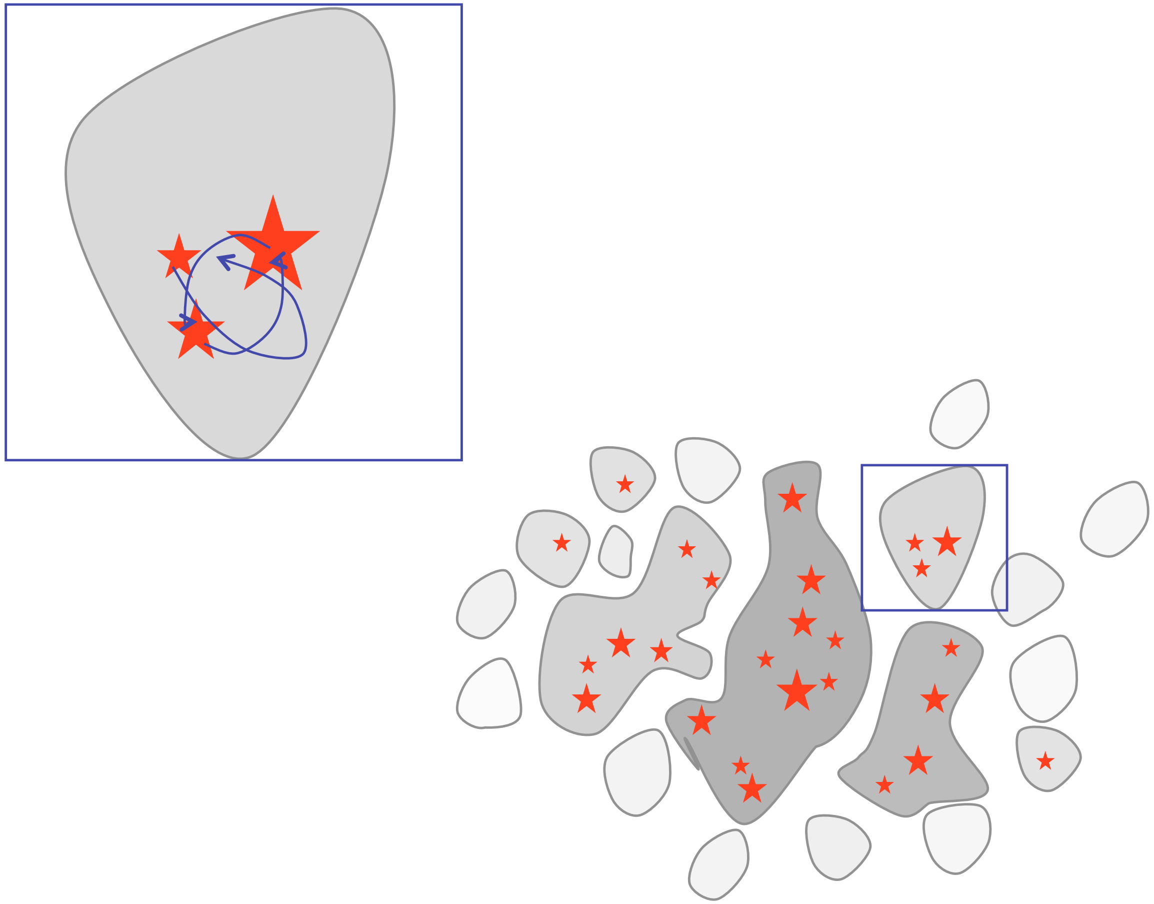

in *dense clusters*, *N*-body effects influence mass growth

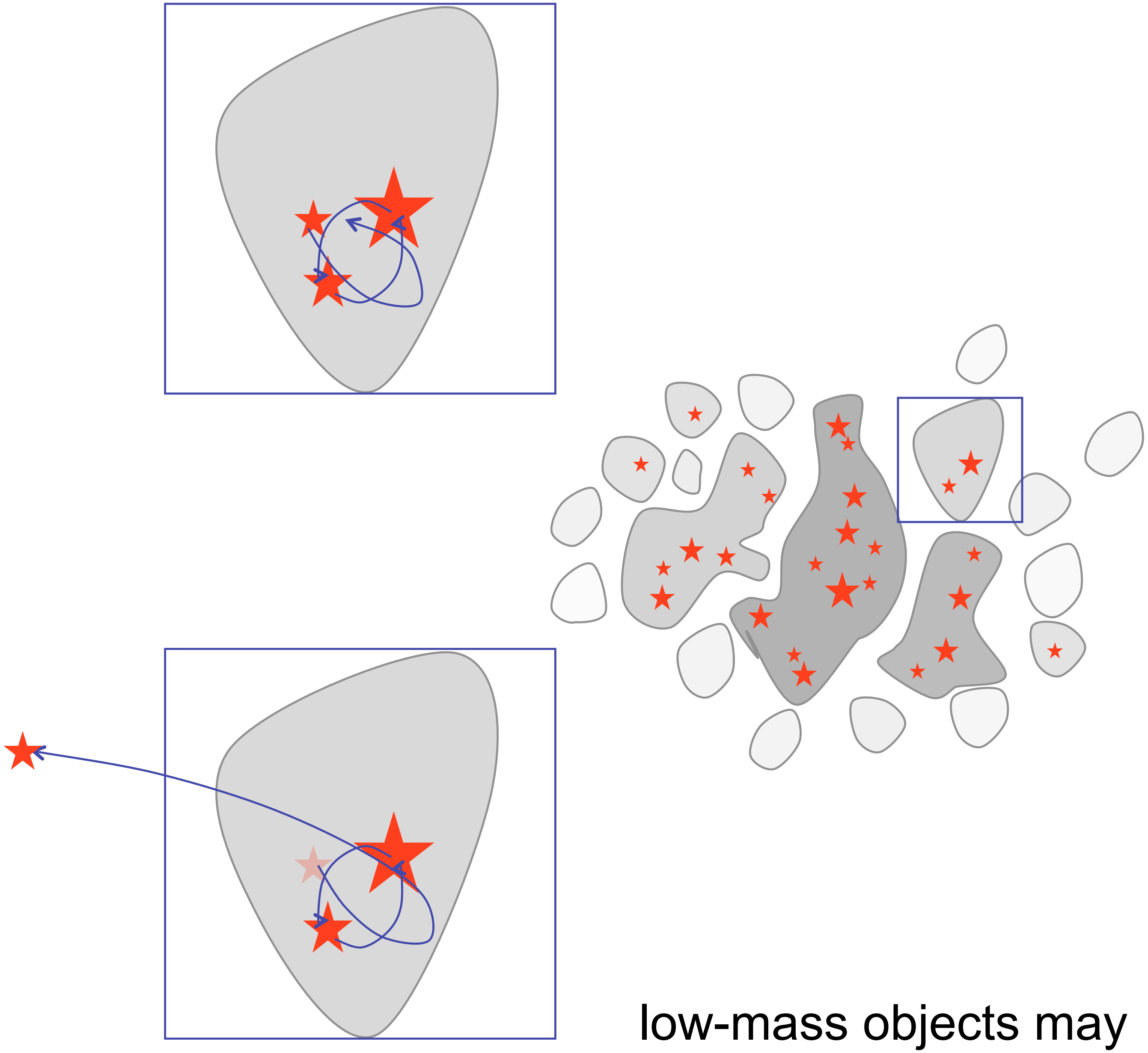

low-mass objects may
become ejected --> accretion stops

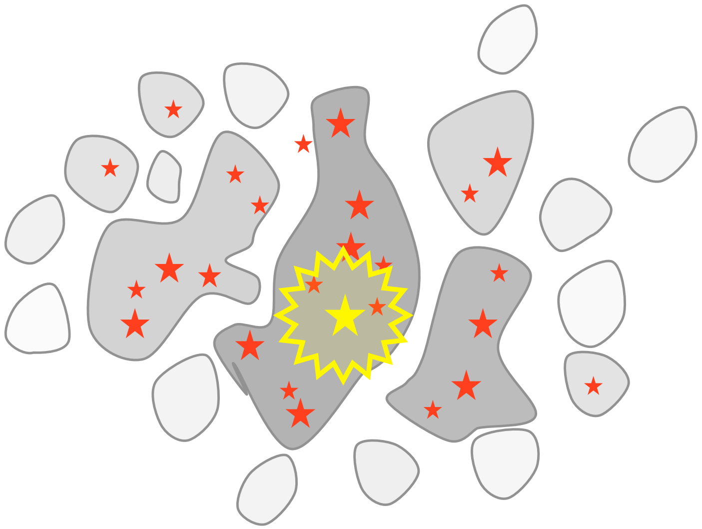

feedback terminates star formation

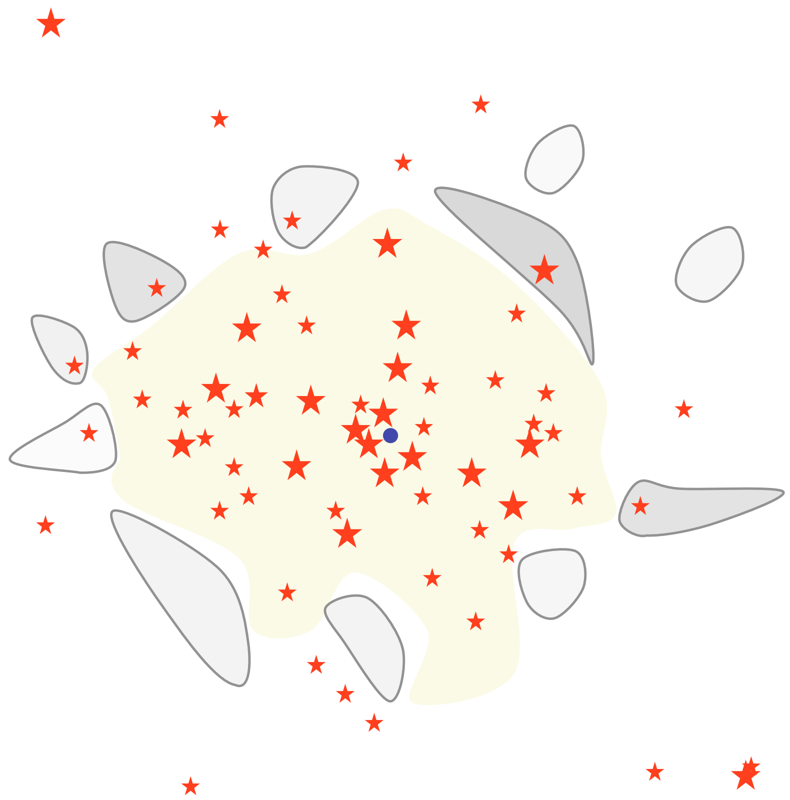

result: *star cluster*, possibly with HII region

NGC 602 in the LMC: Hubble Heritage Image

result: *star cluster* with HII region

applications

# two examples

- formation of molecular clouds in the disk of the Milky Way
  - timescales
  - dynamic properties
  - x-factor
- formation of star clusters inside these clouds
  - IMF

# molecular cloud formation

# molecular cloud formation

- star formation on galactic scales
  → missing link so far:
  *formation of molecular clouds*
- questions
  - *where* and *when* do molecular clouds form?
  - *what* are their properties?
  - *how* does that correlation to star formation?
  - global correlations? → *Schmidt law*

# molecular cloud formation

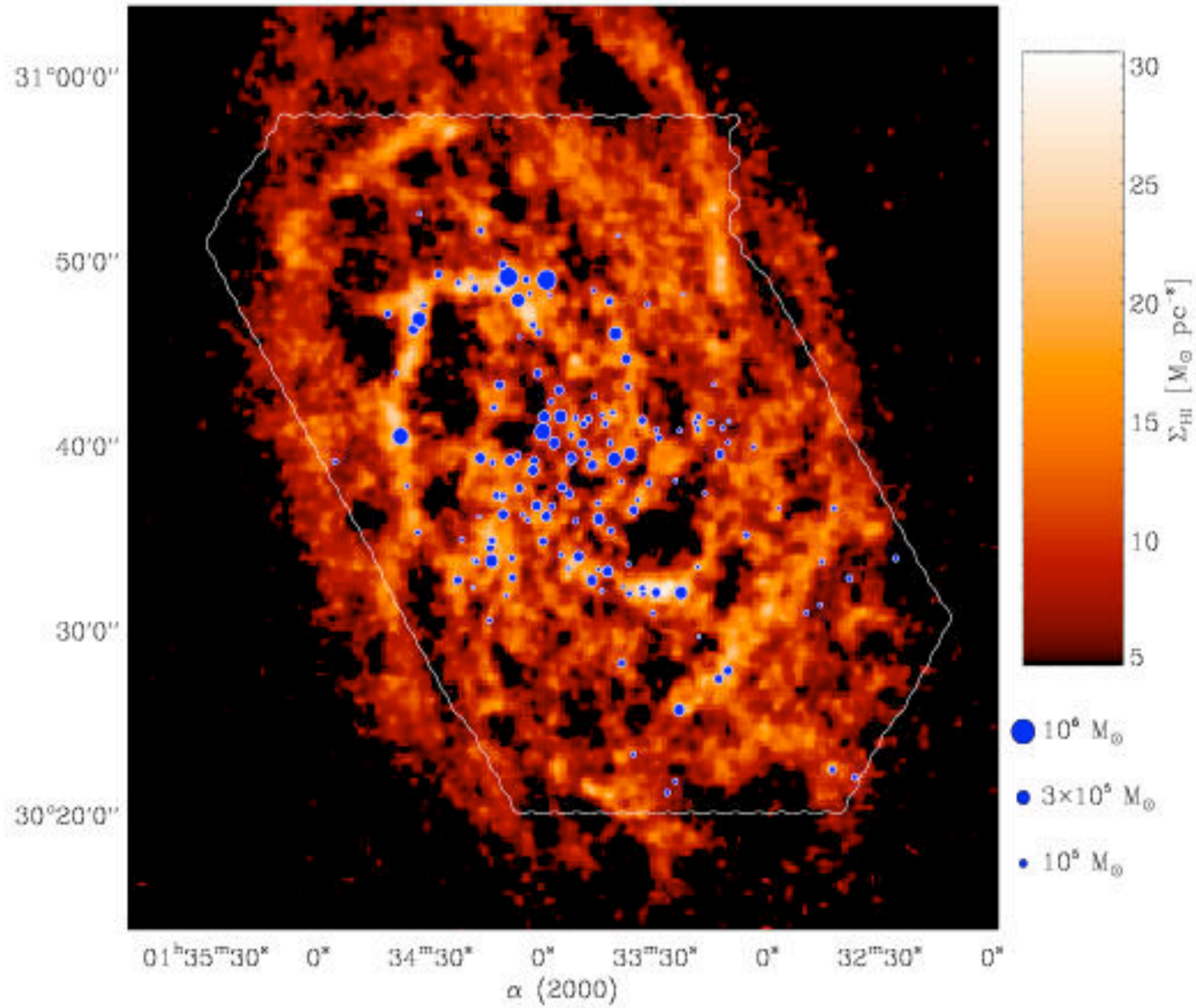


Thesis:

Molecular clouds form at *stagnation points* of large-scale convergent flows, mostly triggered by global (or external) perturbations.

(Deul & van der Hulst 1987, Blitz et al. 2004)

# modeling galactic SF

SPH calculations of self-gravitating disks of stars and (isothermal) gas in dark-matter potential, sink particles measure local collapse --> star formation

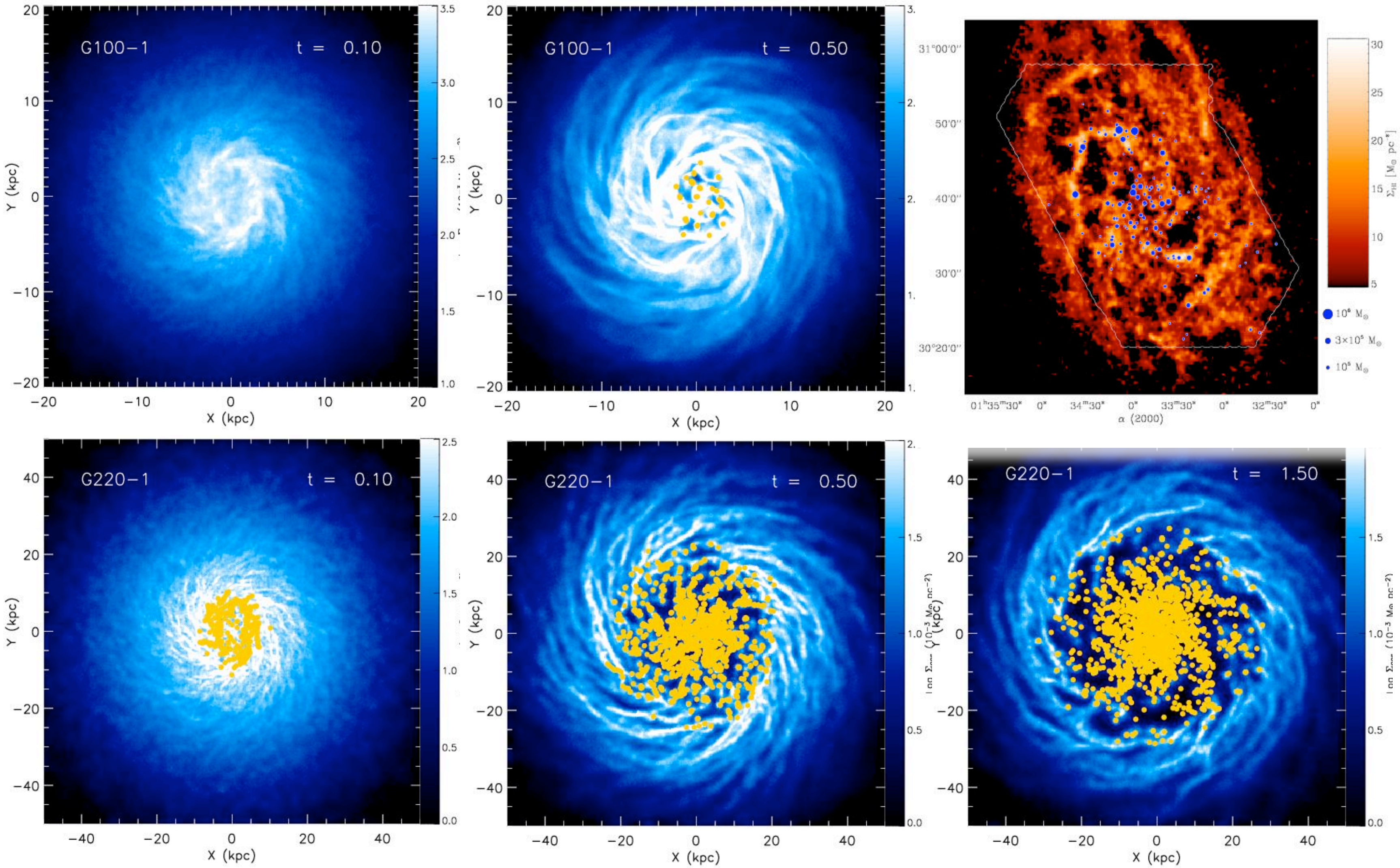


(Li, Mac Low, & Klessen, 2005, ApJ, 620,L19 - L22)

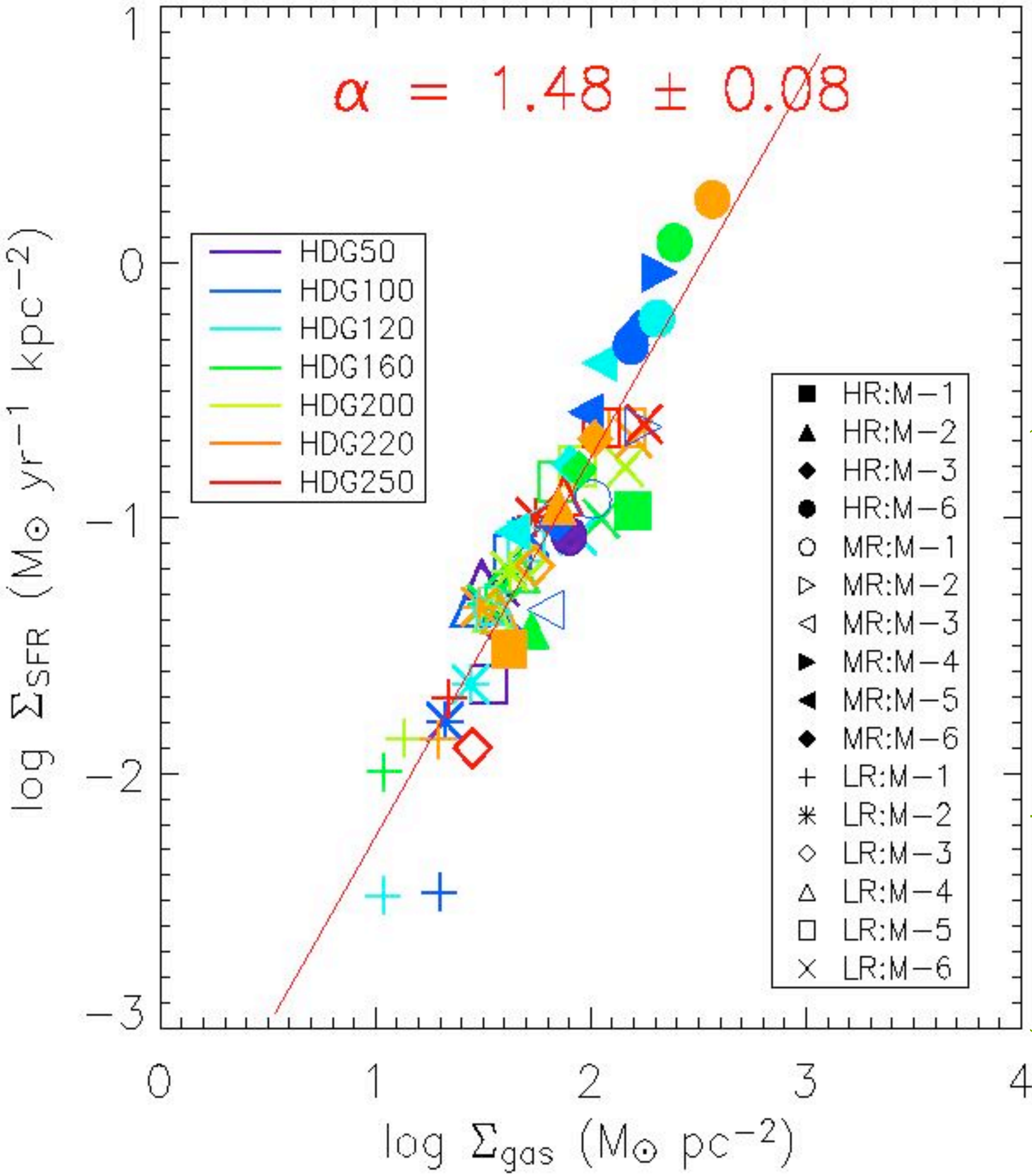


(Li, Mac Low, & Klessen, 2005, ApJ, 620, L19 - L22)

We find correlation between *star formation rate* and *gas surface density:*

$$\boxed{\Sigma_{SFR} \propto \Sigma_{gas}^{1.5}}$$

*global Schmidt law*

# observed Schmidt law

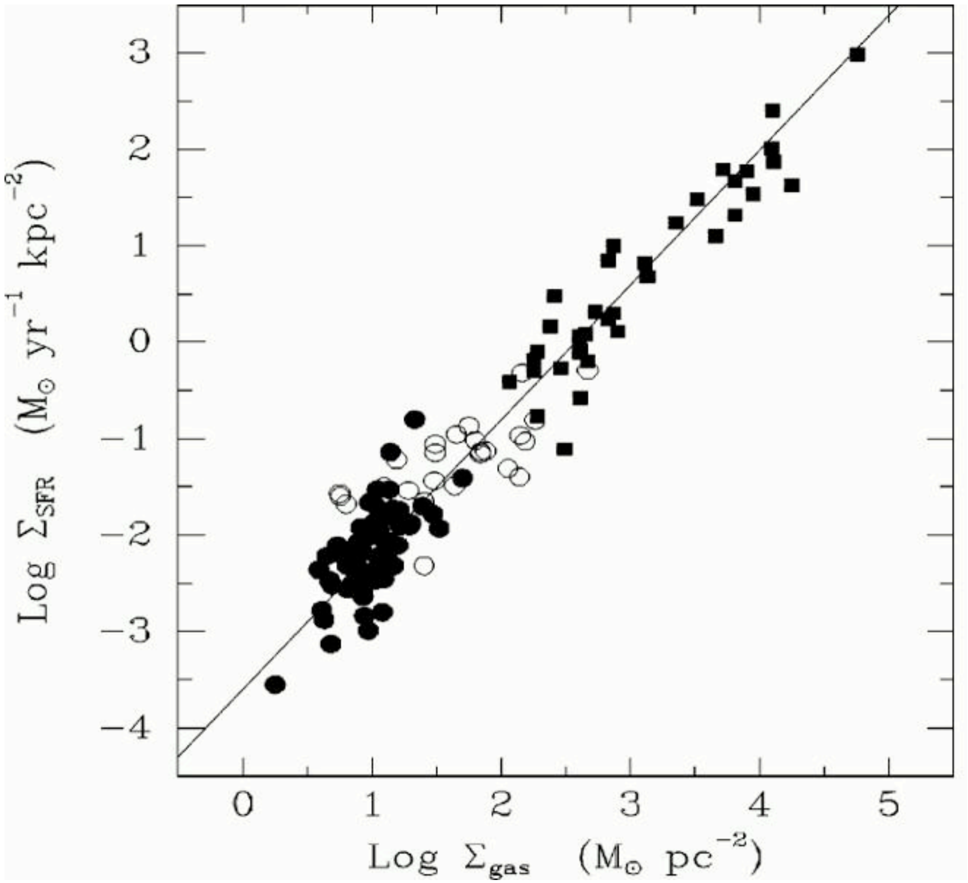


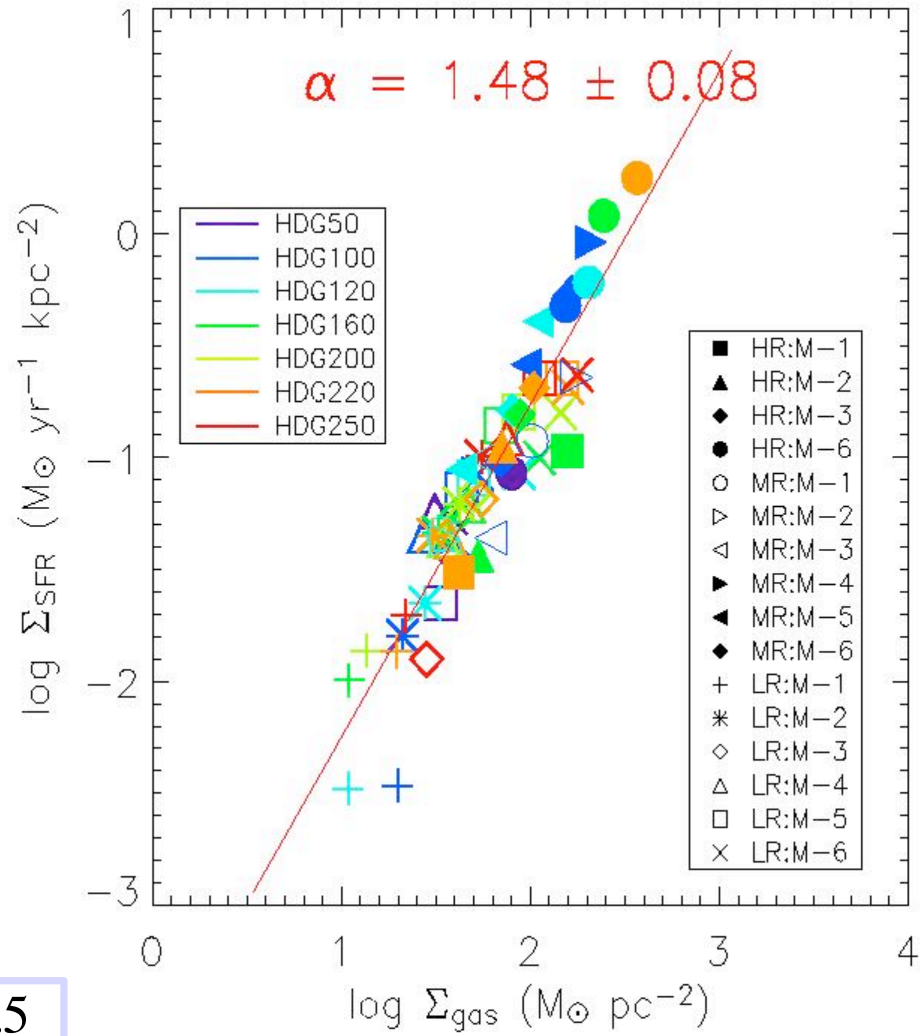


in both cases: $\boxed{\Sigma_{SFR} \propto \Sigma_{gas}^{1.5}}$

(from Kennicutt 1998)

# correlation with large-scale perturbations

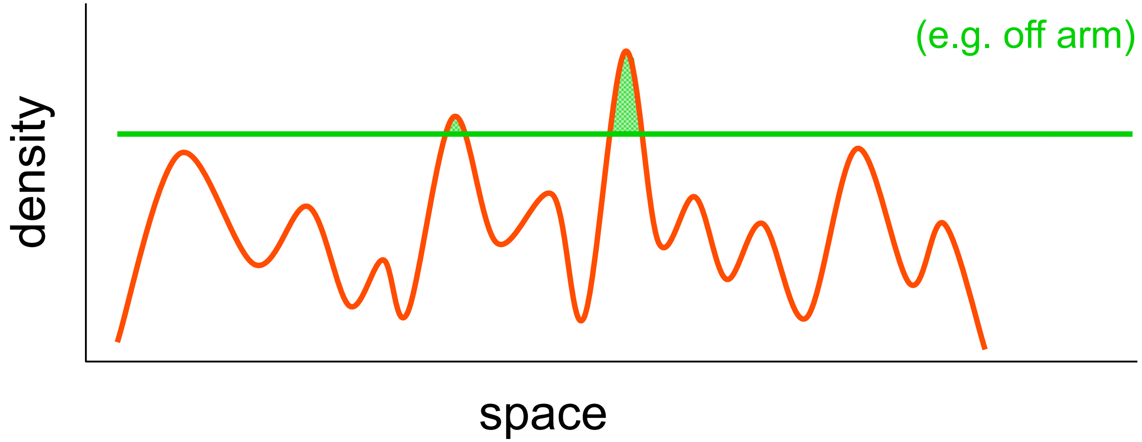


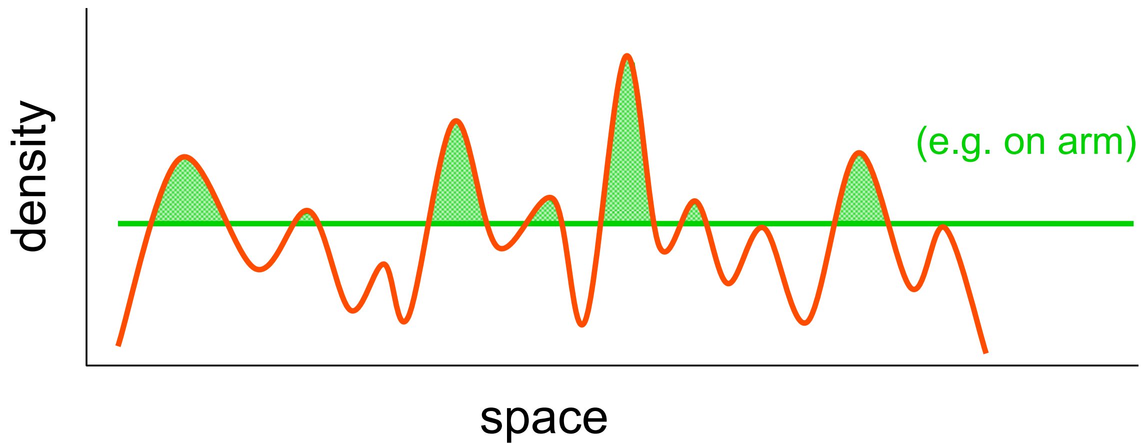


*density/temperature fluctuations* in warm atomar ISM are caused by *thermal/gravitational instability* and/or *supersonic turbulence*

some fluctuations are *dense* enough to *form* $H_2$ within "*reasonable time*"
→ *molecular cloud*

(Glover & Mac Low 2007a,b)

*external perturbations* (i.e. potential changes) *increase* likelihood

# molecular cloud formation

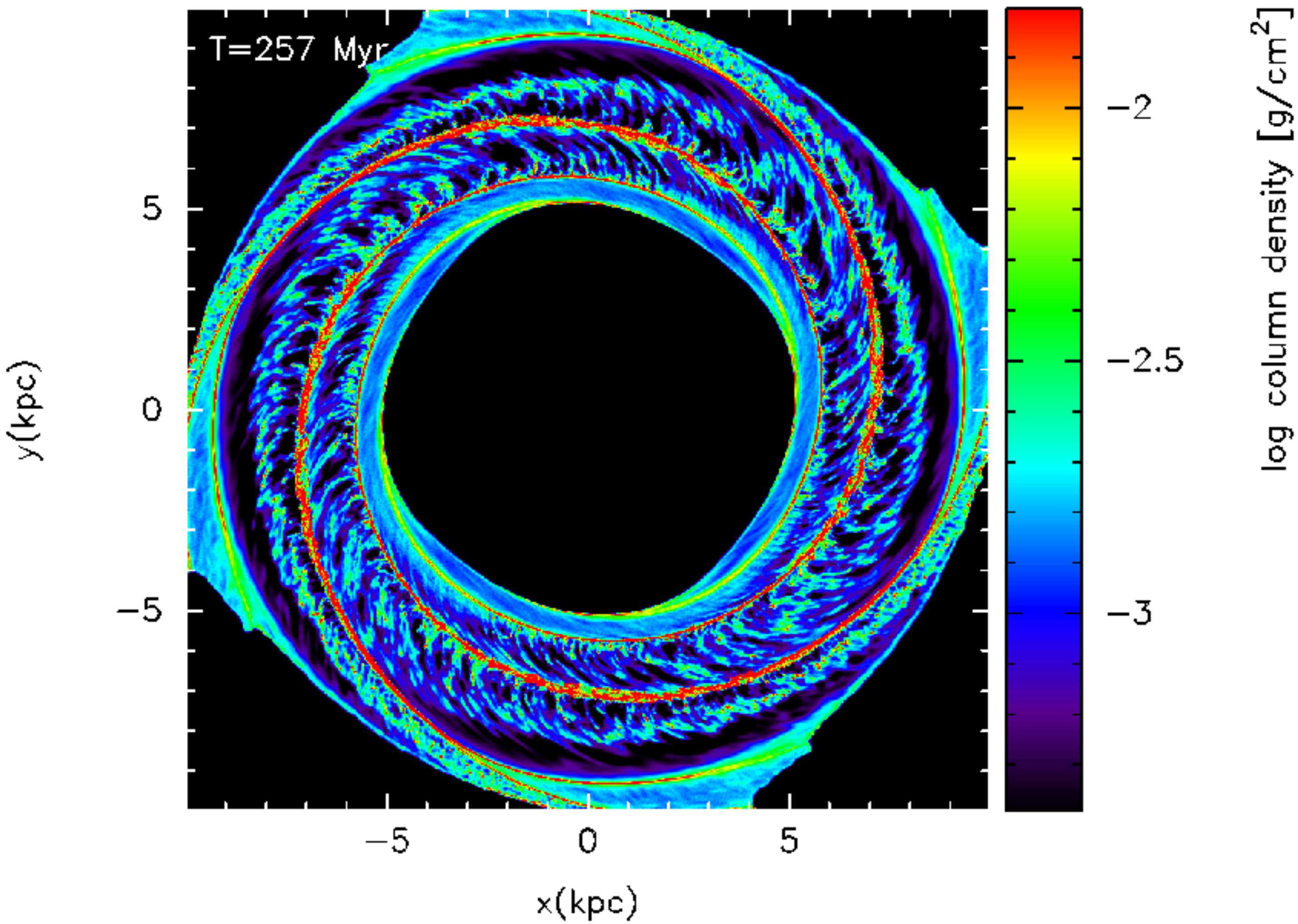


(from Dobbs, Glover, Clark, Klessen 2008)

# molecular cloud formation

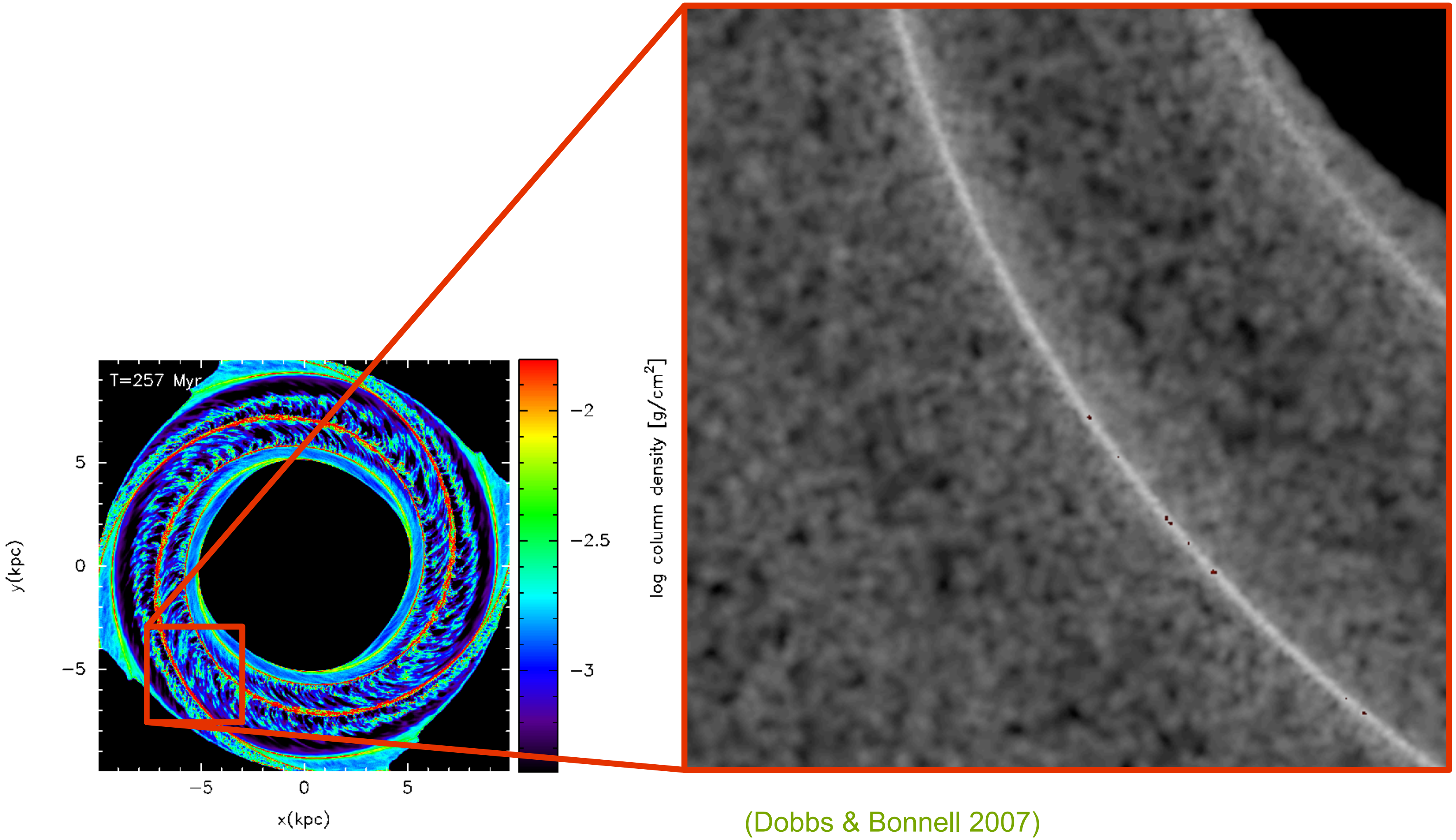


(Dobbs & Bonnell 2007)

# molecular cloud formation

molecular gas fraction as function of time

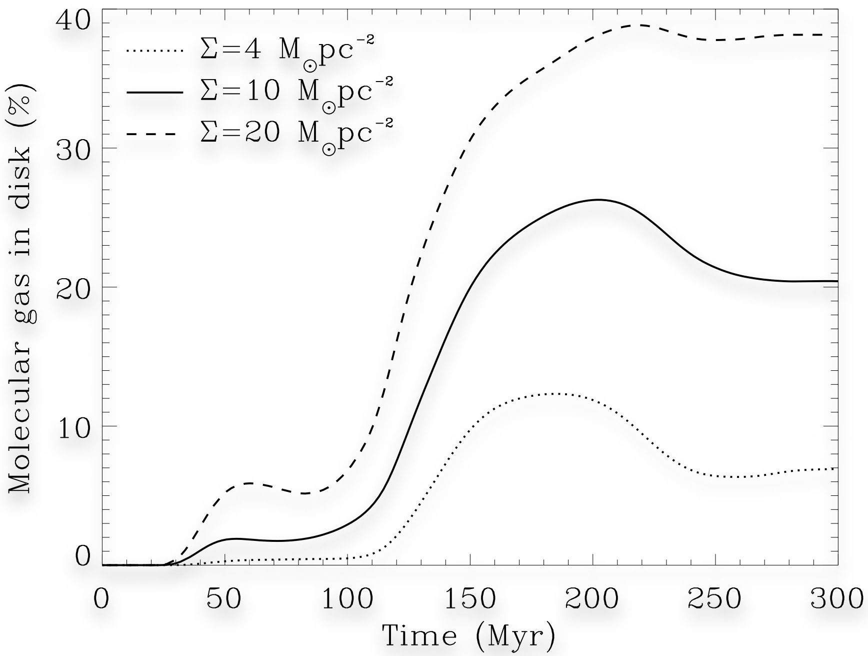


molecular gas fraction as function of density

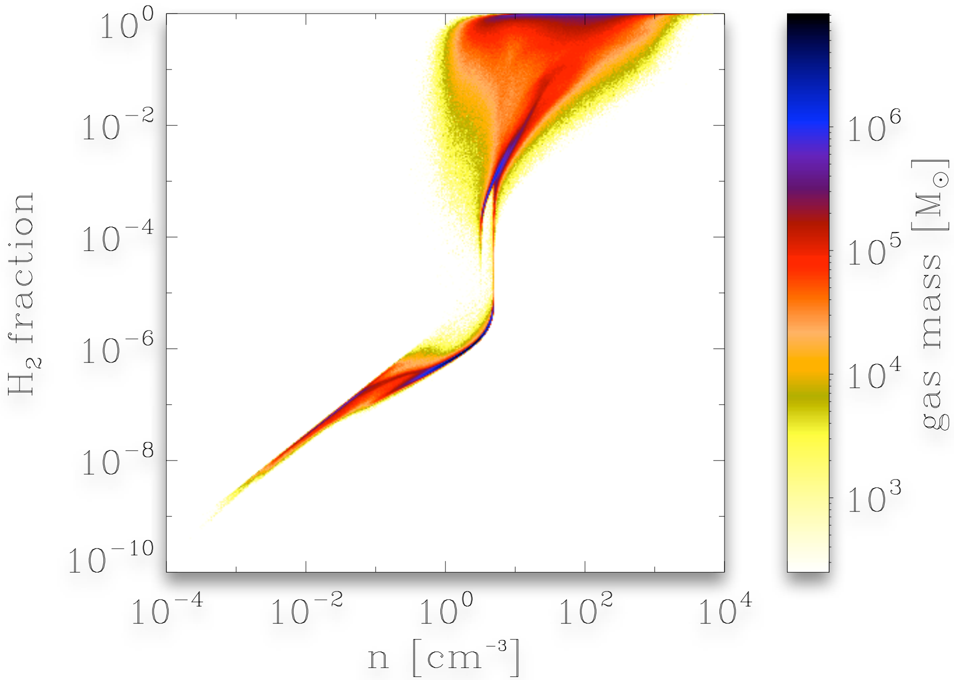


(Dobbs et al. 2008)

# molecular cloud formation

molecular gas fraction of fluid element as function of time

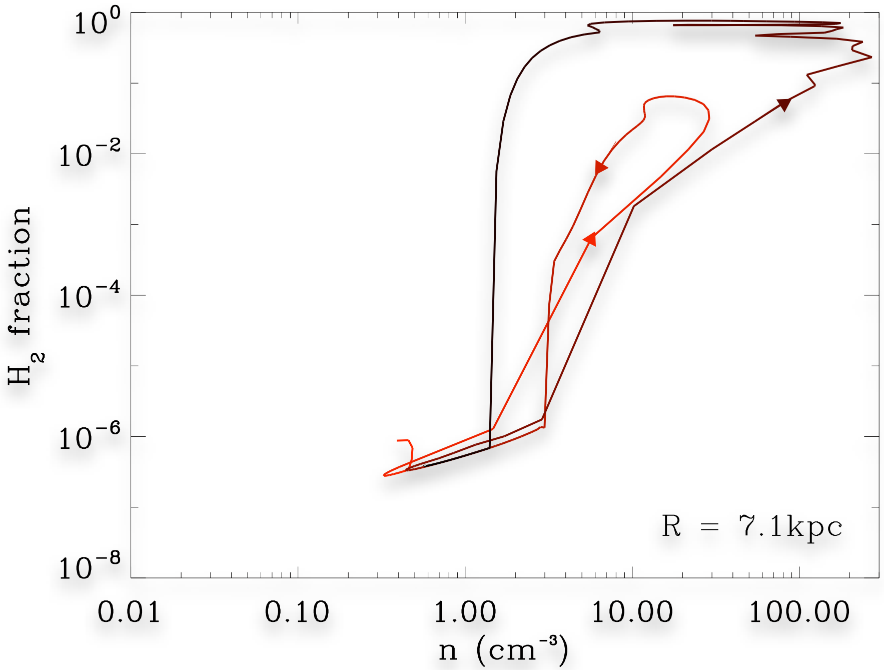


molecular gas fraction as function of density

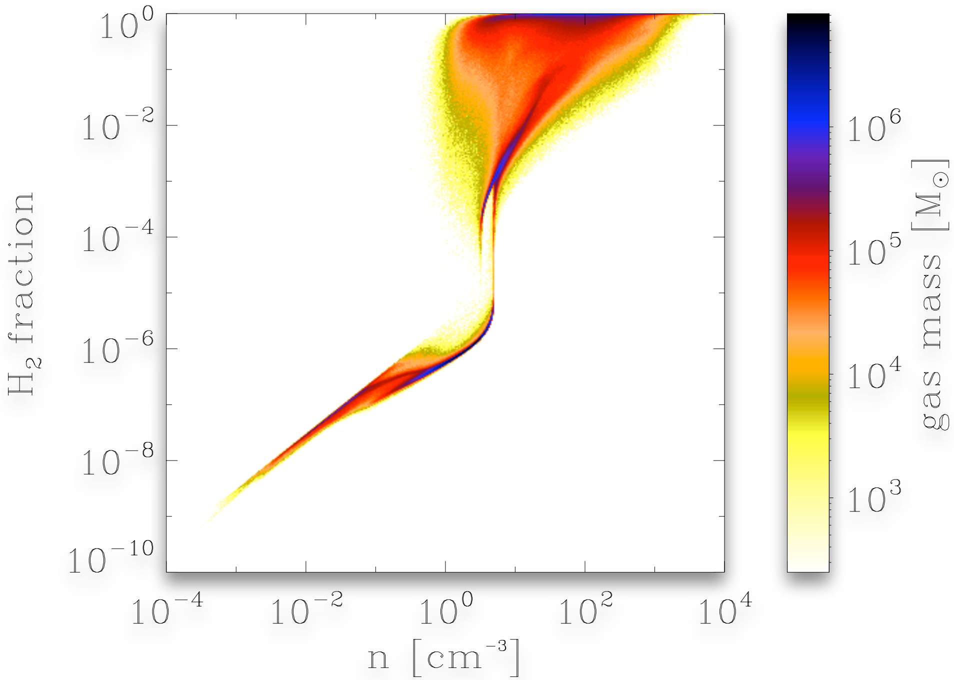


(Dobbs et al. 2008)

# observed timescales

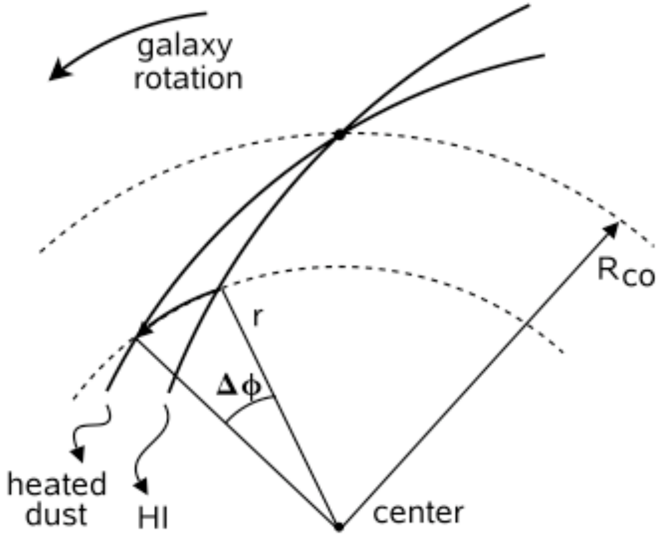


Tamburro et al. (2008)

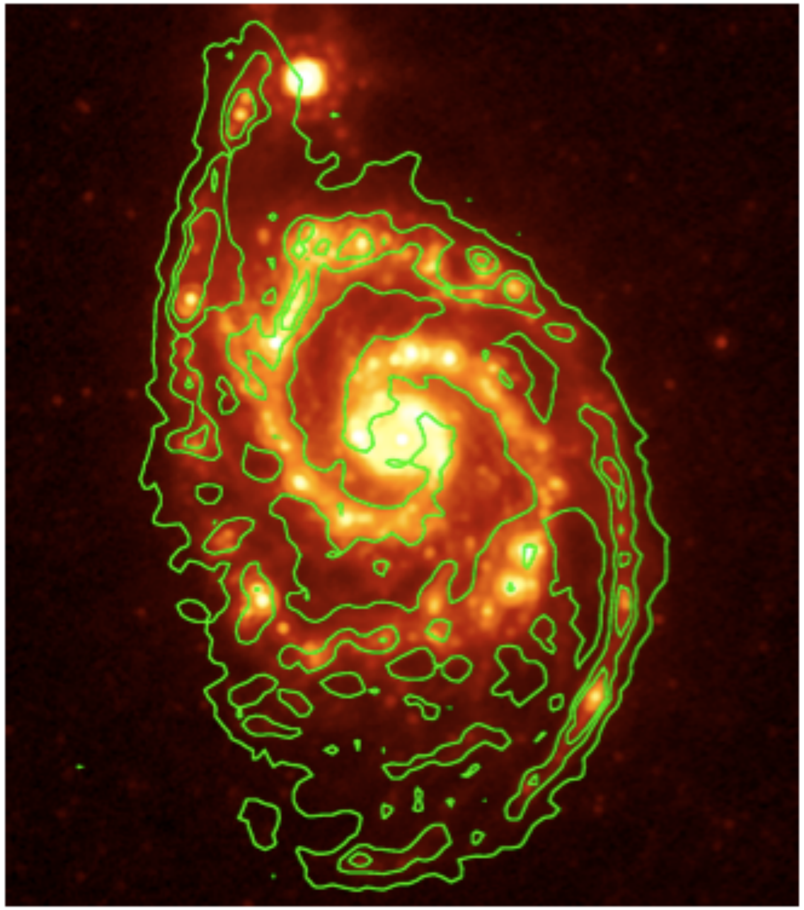

Fig. 1.— NGC 5194: the 24 $\mu$m band image is plotted in color scale; the H I emission map is overlayed with green contours.

# observed timescales

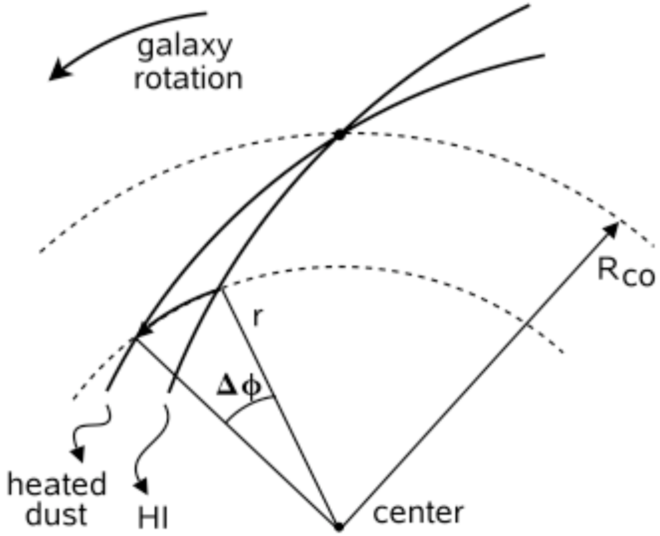


Tamburro et al. (2008)

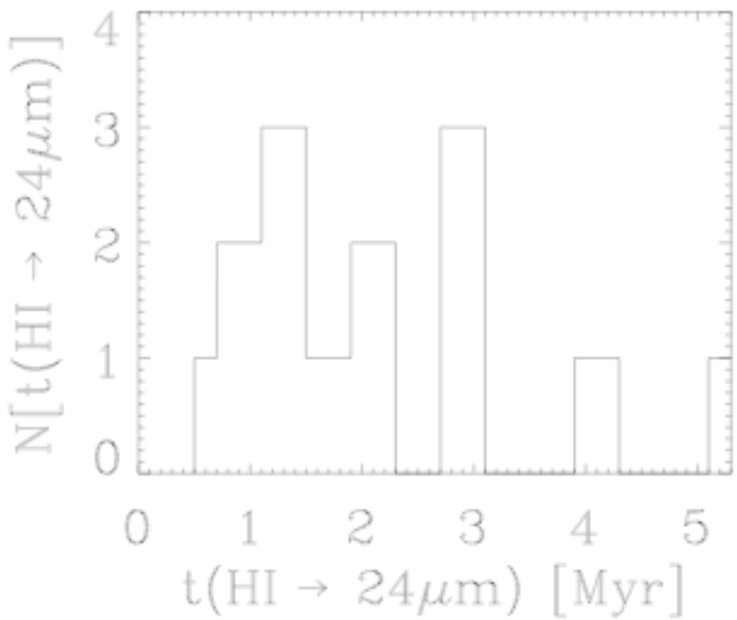


Fig. 5.— Histogram of the time scales $t_{\mathrm{HI}\mapsto 24\,\mu\mathrm{m}}$ derived from the fits in Figure 4 and listed in Table. 2 for the 14 sample galaxies listed in Table. 1. The timescales range between 1 and 4 Myr for almost all galaxies.

# calculated timescales

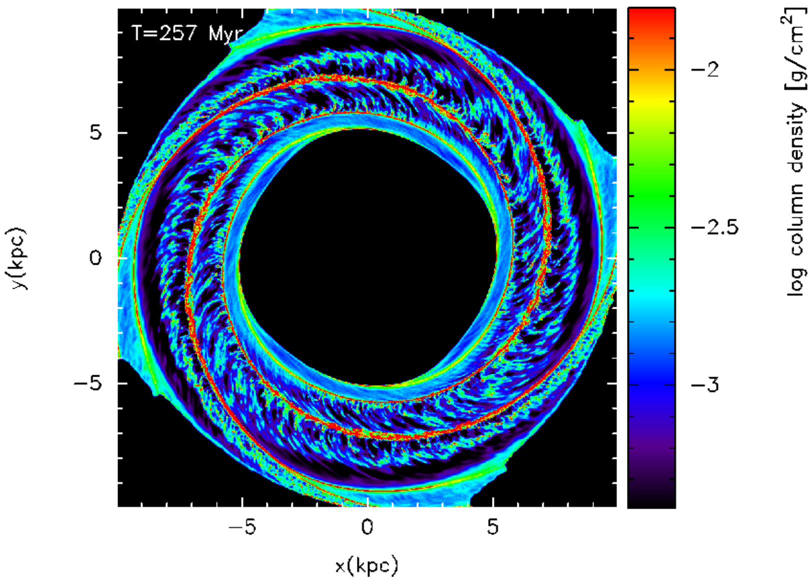


Dobbs et al. (2008)

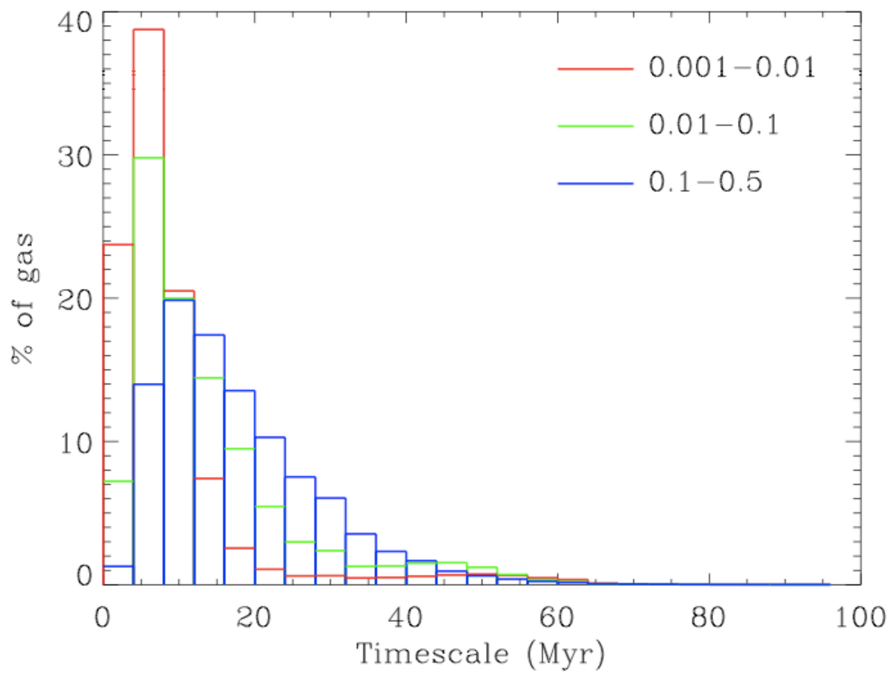


**Figure 16.** This histogram gives the distribution of timescales over which the gas reaches certain molecular gas fractions. The timescales denote the time for the $H_2$ fraction of a particle to increase from 0.001 to 0.01, 0.01 to 0.1 and 0.1 to 0.5, as indicated.

# molecular cloud formation

# zooming in ...

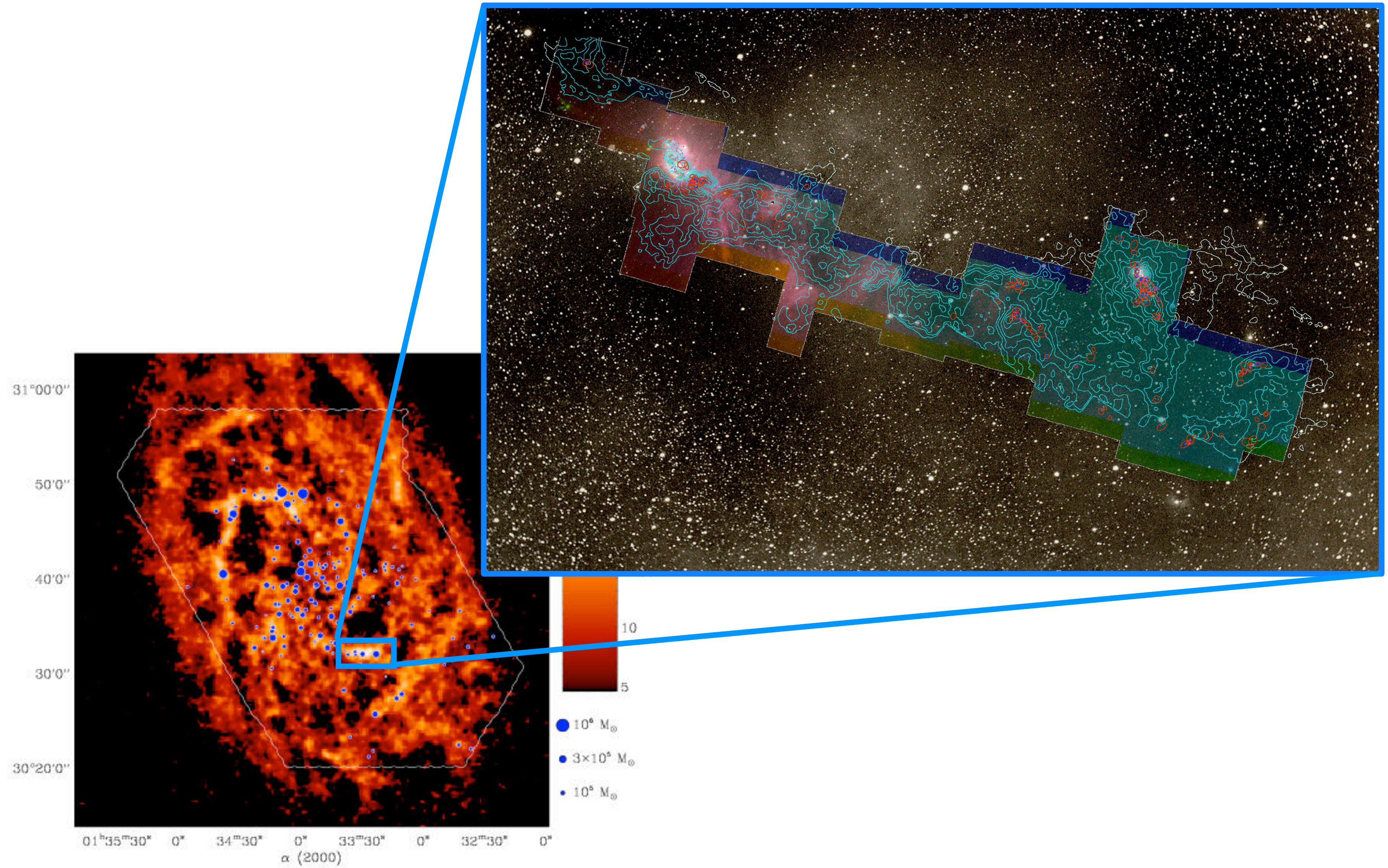

31°00'0''
50'0''
40'0''
30'0''
30°20'0''
01h35m30s
0s
34m30s
0s
33m30s
0s
32m30s
0s
α (2000)
10
5
10⁶ M⊙
3×10⁵ M⊙
10⁵ M⊙

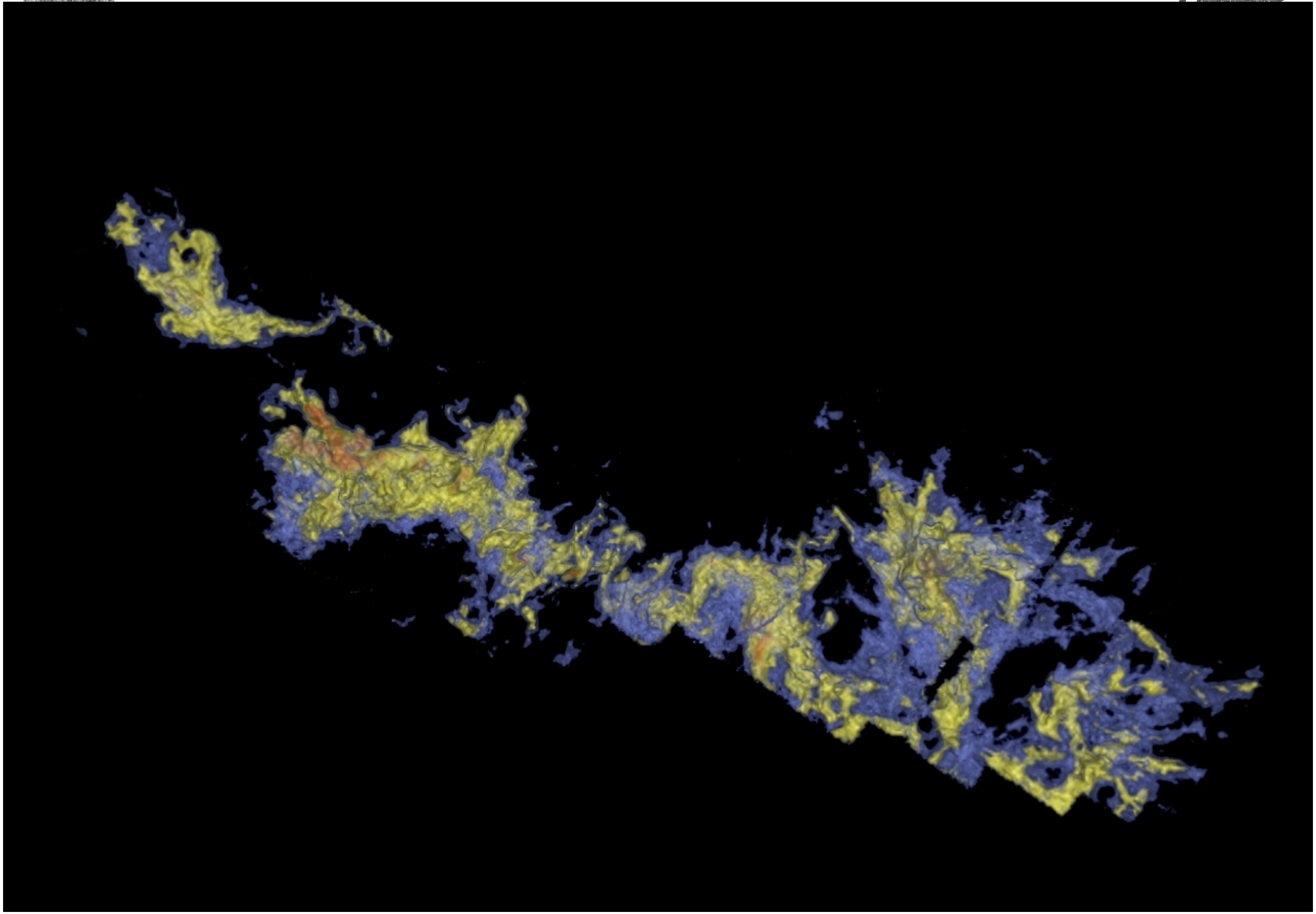

image from Alyssa Goodman: COMPLETE survey

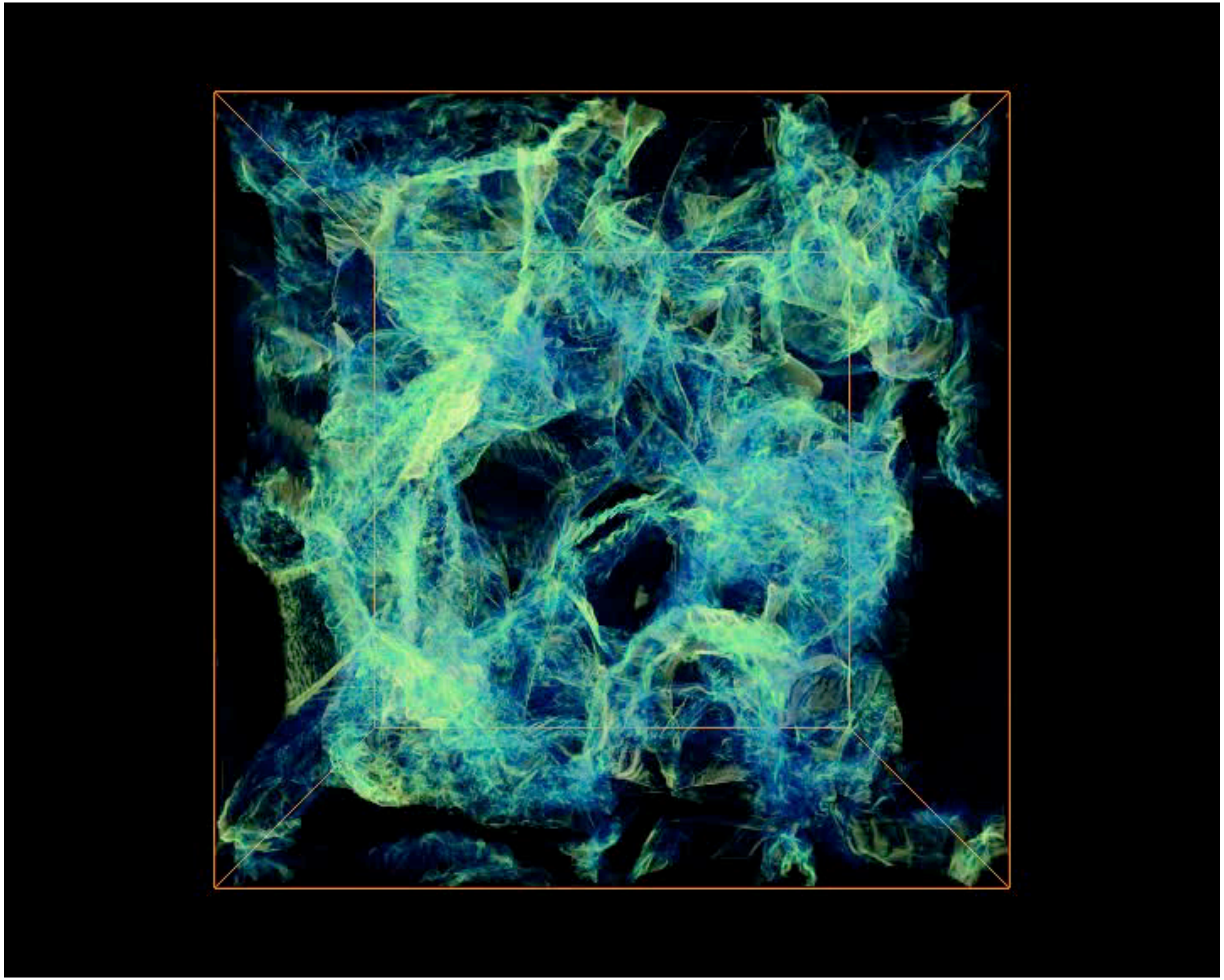

(movie from Christoph Federrath)

# Large-eddy simulations

- We use ***LES*** to model the large-scale dynamics
- Principal problem: only large scale flow properties
  - Reynolds number: Re = LV/ν ***($Re_{nature}$ >> $Re_{model}$)***
  - dynamic range much smaller than true physical one
  - need *subgrid model* (in our case simple: only dissipation)
  - but what to do for more complex when processes on subgrid scale determine large-scale dynamics
    (chemical reactions, nuclear burning, etc)
  - Turbulence is "space filling" --> difficulty for AMR (don't know what criterion to use for refinement)
- How *large* a Reynolds number do we need to catch basic dynamics right?

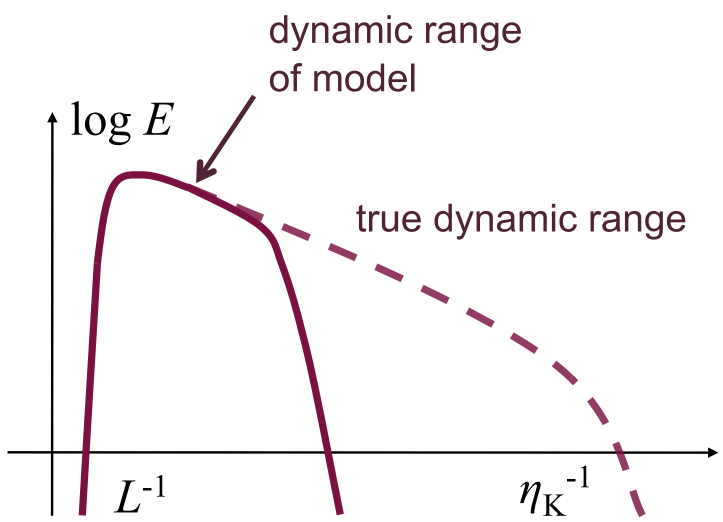

# experimental set-up

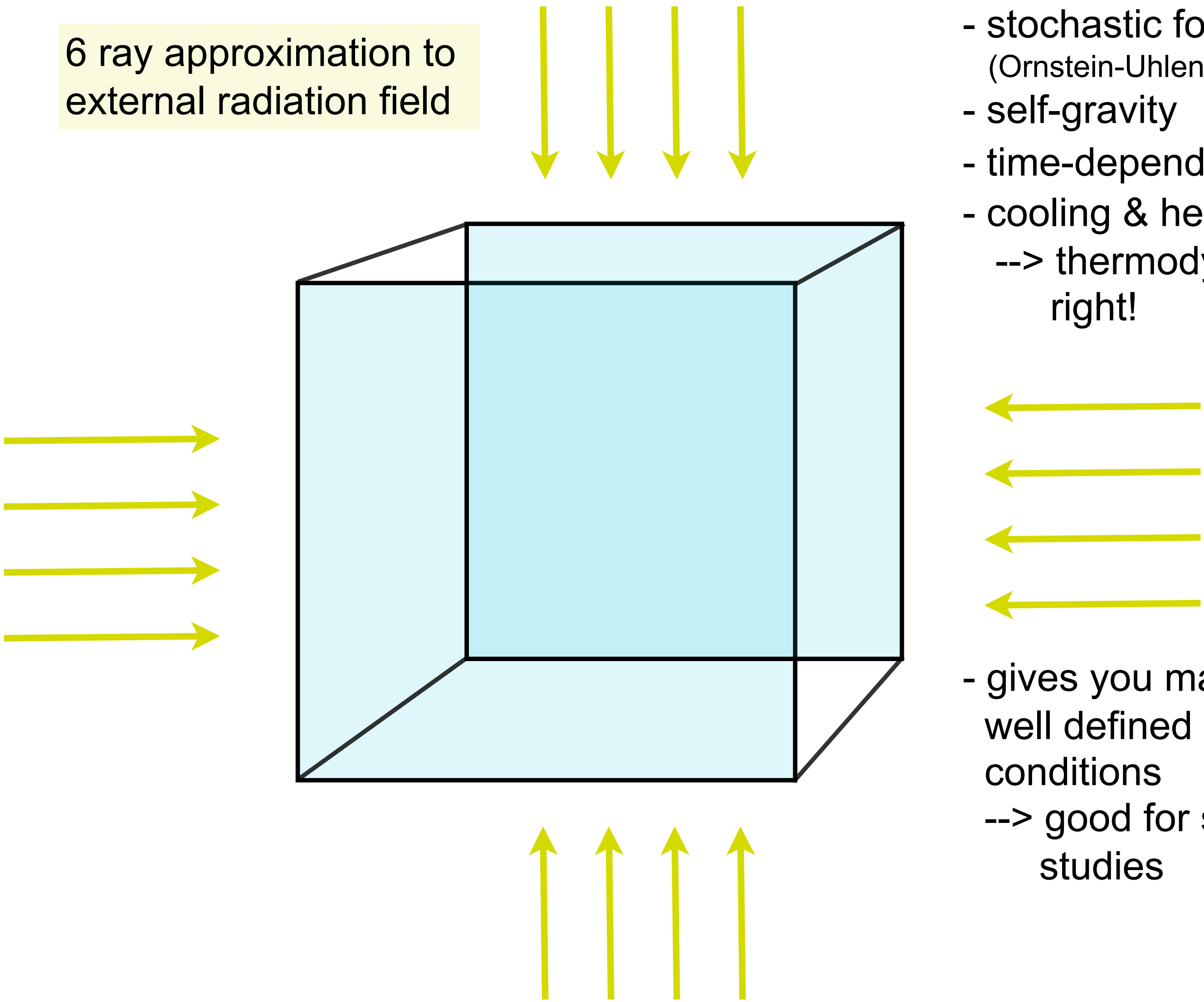


- AMR MHD (B = 2 muG)
- stochastic forcing
  (Ornstein-Uhlenbeck)
- self-gravity
- time-dependent chemistry
- cooling & heating processes
  --> thermodynamics done right!

- gives you mathematically well defined boundary conditions
  --> good for statistical studies

# chemical model 0

- 32 chemical species
  - 17 in instantaneous equilibrium:

$H^-$, $H_2^+$, $H_3^+$, $CH^+$, $CH_2^+$, $OH^+$, $H_2O^+$, $H_3O^+$, $CO^+$, $HOC^+$, $O^-$, $C^-$ and $O_2^+$

  - 19 full non-equilibrium evolution

$e^-$, $H^+$, H, $H_2$, He, $He^+$, C, $C^+$, O, $O^+$, OH, $H_2O$, CO,

$C_2$, $O_2$, $HCO^+$, CH, $CH_2$ and $CH_3^+$

- 218 reactions
- various heating and cooling processes

(Glover, Federrath, Mac Low, Klessen, 2010)

# chemical model 1

| Process | Reference(s) |
|---|---|
| **Cooling:** | |
| C fine structure lines | Atomic data – Silva & Viegas (2002) |
| | Collisional rates (H) – Abrahamsson, Krems & Dalgarno (2007) |
| | Collisional rates ($H_2$) – Schroder et al. (1991) |
| | Collisional rates ($e^-$) – Johnson et al. (1987) |
| | Collisional rates ($H^+$) – Roueff & Le Bourlot (1990) |
| $C^+$ fine structure lines | Atomic data – Silva & Viegas (2002) |
| | Collisional rates ($H_2$) – Flower & Launay (1977) |
| | Collisional rates (H, $T < 2000$ K) – Hollenbach & McKee (1989) |
| | Collisional rates (H, $T > 2000$ K) – Keenan et al. (1986) |
| | Collisional rates ($e^-$) – Wilson & Bell (2002) |
| O fine structure lines | Atomic data – Silva & Viegas (2002) |
| | Collisional rates (H) – Abrahamsson, Krems & Dalgarno (2007) |
| | Collisional rates ($H_2$) – see Glover & Jappsen (2007) |
| | Collisional rates ($e^-$) – Bell, Berrington & Thomas (1998) |
| | Collisional rates ($H^+$) – Pequignot (1990, 1996) |
| $H_2$ rovibrational lines | Le Bourlot, Pineau des Forêts & Flower (1999) |
| CO and $H_2O$ rovibrational lines | Neufeld & Kaufman (1993); Neufeld, Lepp & Melnick (1995) |
| OH rotational lines | Pavlovski et al. (2002) |
| Gas-grain energy transfer | Hollenbach & McKee (1989) |
| Recombination on grains | Wolfire et al. (2003) |
| Atomic resonance lines | Sutherland & Dopita (1993) |
| H collisional ionization | Abel et al. (1997) |
| $H_2$ collisional dissociation | See Table B1 |
| Compton cooling | Cen (1992) |
| **Heating:** | |
| Photoelectric effect | Bakes & Tielens (1994); Wolfire et al. (2003) |
| $H_2$ photodissociation | Black & Dalgarno (1977) |
| UV pumping of $H_2$ | Burton, Hollenbach & Tielens (1990) |
| $H_2$ formation on dust grains | Hollenbach & McKee (1989) |
| Cosmic ray ionization | Goldsmith & Langer (1978) |

(Glover, Federrath, Mac Low, Klessen, in prep)

# chemical model 2

Table B1. List of collisional gas-phase reactions included in our chemical model

| No. | Reaction | | | |
|---|---|---|---|---|
| 1 | $H + e^- \rightarrow H^- + \gamma$ | $k_1 = \mathrm{dex}[-17.845 + 0.762 \log T + 0.1523(\log T)^2$<br>$- 0.03274(\log T)^3]$<br>$= \mathrm{dex}[-16.420 + 0.1998(\log T)^2$<br>$- 5.447 \times 10^{-3}(\log T)^4$<br>$+ 4.0415 \times 10^{-5}(\log T)^6]$ | $T \leqslant 6000$ K<br><br><br><br>$T > 6000$ K | 1 |
| 2 | $H^- + H \rightarrow H_2 + e^-$ | $k_2 = 1.5 \times 10^{-9}$<br>$= 4.0 \times 10^{-9} T^{-0.17}$ | $T \leqslant 300$ K<br>$T > 300$ K | 2 |
| 3 | $H + H^+ \rightarrow H_2^+ + \gamma$ | $k_3 = \mathrm{dex}[-19.38 - 1.523 \log T$<br>$+ 1.118(\log T)^2 - 0.1269(\log T)^3]$ | | 3 |
| 4 | $H + H_2^+ \rightarrow H_2 + H^+$ | $k_4 = 6.4 \times 10^{-10}$ | | 4 |
| 5 | $H^- + H^+ \rightarrow H + H$ | $k_5 = 2.4 \times 10^{-6} T^{-1/2}(1.0 + T/20000)$ | | 5 |
| 6 | $H_2^+ + e^- \rightarrow H + H$ | $k_6 = 1.0 \times 10^{-8}$<br>$= 1.32 \times 10^{-6} T^{-0.76}$ | $T \leqslant 617$ K<br>$T > 617$ K | 6 |
| 7 | $H_2 + H^+ \rightarrow H_2^+ + H$ | $k_7 = [-3.3232183 \times 10^{-7}$<br>$+ 3.3735382 \times 10^{-7} \ln T$<br>$- 1.4491368 \times 10^{-7}(\ln T)^2$<br>$+ 3.4172805 \times 10^{-8}(\ln T)^3$<br>$- 4.7813720 \times 10^{-9}(\ln T)^4$<br>$+ 3.9731542 \times 10^{-10}(\ln T)^5$<br>$- 1.8171411 \times 10^{-11}(\ln T)^6$<br>$+ 3.5311932 \times 10^{-13}(\ln T)^7]$<br>$\times \exp\left(\frac{-21237.15}{T}\right)$ | | 7 |
| 8 | $H_2 + e^- \rightarrow H + H + e^-$ | $k_8 = 3.73 \times 10^{-9} T^{0.1121} \exp\left(\frac{-99430}{T}\right)$ | | 8 |
| 9 | $H_2 + H \rightarrow H + H + H$ | $k_{9,1} = 6.67 \times 10^{-12} T^{1/2} \exp\left[-(1 + \frac{63590}{T})\right]$ | | 9 |
| | | $k_{9,h} = 3.52 \times 10^{-9} \exp\left(-\frac{43900}{T}\right)$ | | 10 |
| | | $n_{cr,H} = \mathrm{dex}\left[3.0 - 0.416 \log\left(\frac{T}{10000}\right) - 0.327 \left\{\log\left(\frac{T}{10000}\right)\right\}^2\right]$ | | 10 |
| 10 | $H_2 + H_2 \rightarrow H_2 + H + H$ | $k_{10,1} = \frac{5.996 \times 10^{-30} T^{4.1881}}{(1.0 + 6.761 \times 10^{-6} T)^{5.6881}} \exp\left(-\frac{54657.4}{T}\right)$ | | 11 |
| | | $k_{10,h} = 1.3 \times 10^{-9} \exp\left(-\frac{53300}{T}\right)$ | | 12 |
| | | $n_{cr,H_2} = \mathrm{dex}\left[4.845 - 1.3 \log\left(\frac{T}{10000}\right) + 1.62 \left\{\log\left(\frac{T}{10000}\right)\right\}^2\right]$ | | 12 |
| 11 | $H + e^- \rightarrow H^+ + e^- + e^-$ | $k_{11} = \exp[-3.271396786 \times 10^1$<br>$+ 1.35365560 \times 10^1 \ln T_e$<br>$- 5.73932875 \times 10^0 (\ln T_e)^2$<br>$+ 1.56315498 \times 10^0 (\ln T_e)^3$<br>$- 2.87705600 \times 10^{-1} (\ln T_e)^4$<br>$+ 3.48255977 \times 10^{-2} (\ln T_e)^5$<br>$- 2.63197617 \times 10^{-3} (\ln T_e)^6$<br>$+ 1.11954395 \times 10^{-4} (\ln T_e)^7$<br>$- 2.03914985 \times 10^{-6} (\ln T_e)^8]$ | | 13 |
| 12 | $H^+ + e^- \rightarrow H + \gamma$ | $k_{12,A} = 1.269 \times 10^{-13} \left(\frac{315614}{T}\right)^{1.503}$<br>$\times [1.0 + \left(\frac{604625}{T}\right)^{0.470}]^{-1.923}$ | Case A | 14 |
| | | $k_{12,B} = 2.753 \times 10^{-14} \left(\frac{315614}{T}\right)^{1.500}$<br>$\times [1.0 + \left(\frac{115188}{T}\right)^{0.407}]^{-2.242}$ | Case B | 14 |
| 13 | $H^- + e^- \rightarrow H + e^- + e^-$ | $k_{13} = \exp[-1.801849334 \times 10^1$<br>$+ 2.36085220 \times 10^0 \ln T_e$<br>$- 2.82744300 \times 10^{-1} (\ln T_e)^2$<br>$+ 1.62331664 \times 10^{-2} (\ln T_e)^3$<br>$- 3.36501203 \times 10^{-2} (\ln T_e)^4$<br>$+ 1.17832978 \times 10^{-2} (\ln T_e)^5$<br>$- 1.65619470 \times 10^{-3} (\ln T_e)^6$<br>$+ 1.06827520 \times 10^{-4} (\ln T_e)^7$<br>$- 2.63128581 \times 10^{-6} (\ln T_e)^8]$ | | 13 |

(Glover, Federrath, Mac Low, Klessen, in prep)

# chemical model 2

Table B1. |

| No. | Rea |
|---|---|
| 1 | H + |
| 2 | $H^-$ |
| 3 | H + |
| 4 | H + |
| 5 | $H^-$ |
| 6 | $H_2^+$ |
| 7 | $H_2$ |
| 8 | $H_2$ |
| 9 | $H_2$ |
| 10 | $H_2$ |
| 11 | H + |
| 12 | $H^+$ |
| 13 | $H^-$ |

| | | | | |
|---|---|---|---|---|
| 14 | $H^- + H \rightarrow H + H + e^-$ | $k_{14} = 2.5634 \times 10^{-9} T_e^{1.78186}$ | $T_e \leqslant 0.1$ eV | 13 |
| | | $= \exp[-2.0372609 \times 10^1$ | | |
| | | $+ 1.13944933 \times 10^0 \ln T_e$ | | |
| | | $- 1.4210135 \times 10^{-1} (\ln T_e)^2$ | | |
| | | $+ 8.4644554 \times 10^{-3} (\ln T_e)^3$ | | |
| | | $- 1.4327641 \times 10^{-3} (\ln T_e)^4$ | | |
| | | $+ 2.0122503 \times 10^{-4} (\ln T_e)^5$ | | |
| | | $+ 8.6639632 \times 10^{-5} (\ln T_e)^6$ | | |
| | | $- 2.5850097 \times 10^{-5} (\ln T_e)^7$ | | |
| | | $+ 2.4555012 \times 10^{-6} (\ln T_e)^8$ | | |
| | | $- 8.0683825 \times 10^{-8} (\ln T_e)^9]$ | $T_e > 0.1$ eV | |
| 15 | $H^- + H^+ \rightarrow H_2^+ + e^-$ | $k_{15} = 6.9 \times 10^{-9} T^{-0.35}$ | $T \leqslant 8000$ K | 15 |
| | | $= 9.6 \times 10^{-7} T^{-0.90}$ | $T > 8000$ K | |
| 16 | $He + e^- \rightarrow He^+ + e^- + e^-$ | $k_{16} = \exp[-4.409864886 \times 10^1$ | | 13 |
| | | $+ 2.391596563 \times 10^1 \ln T_e$ | | |
| | | $- 1.07532302 \times 10^1 (\ln T_e)^2$ | | |
| | | $+ 3.05803875 \times 10^0 (\ln T_e)^3$ | | |
| | | $- 5.6851189 \times 10^{-1} (\ln T_e)^4$ | | |
| | | $+ 6.79539123 \times 10^{-2} (\ln T_e)^5$ | | |
| | | $- 5.0090561 \times 10^{-3} (\ln T_e)^6$ | | |
| | | $+ 2.06723616 \times 10^{-4} (\ln T_e)^7$ | | |
| | | $- 3.64916141 \times 10^{-6} (\ln T_e)^8]$ | | |
| 17 | $He^+ + e^- \rightarrow He + \gamma$ | $k_{17,rr,A} = 10^{-11} T^{-0.5} [12.72 - 1.615 \log T$ | Case A | 16 |
| | | $- 0.3162 (\log T)^2 + 0.0493 (\log T)^3]$ | | |
| | | $k_{17,rr,B} = 10^{-11} T^{-0.5} [11.19 - 1.676 \log T$ | Case B | 16 |
| | | $- 0.2852 (\log T)^2 + 0.04433 (\log T)^3]$ | | |
| | | $k_{17,di} = 1.9 \times 10^{-3} T^{-1.5} \exp\left(-\frac{473421}{T}\right)$ | | |
| | | $\times \left[1.0 + 0.3 \exp\left(-\frac{94684}{T}\right)\right]$ | | 17 |
| 18 | $He^+ + H \rightarrow He + H^+$ | $k_{18} = 1.25 \times 10^{-15} \left(\frac{T}{300}\right)^{0.25}$ | | 18 |
| 19 | $He + H^+ \rightarrow He^+ + H$ | $k_{19} = 1.26 \times 10^{-9} T^{-0.75} \exp\left(-\frac{127500}{T}\right)$ | $T \leqslant 10000$ K | 19 |
| | | $= 4.0 \times 10^{-37} T^{4.74}$ | $T > 10000$ K | |
| 20 | $C^+ + e^- \rightarrow C + \gamma$ | $k_{20} = 4.67 \times 10^{-12} \left(\frac{T}{300}\right)^{-0.6}$ | $T \leqslant 7950$ K | 20 |
| | | $= 1.23 \times 10^{-17} \left(\frac{T}{300}\right)^{2.49} \exp\left(\frac{21845.6}{T}\right)$ | $7950 \text{ K} < T \leqslant 21140$ K | |
| | | $= 9.62 \times 10^{-8} \left(\frac{T}{300}\right)^{-1.37} \exp\left(\frac{-115786.2}{T}\right)$ | $T > 21140$ K | |
| 21 | $O^+ + e^- \rightarrow O + \gamma$ | $k_{21} = 1.30 \times 10^{-10} T^{-0.64}$ | $T \leqslant 400$ K | 21 |
| | | $= 1.41 \times 10^{-10} T^{-0.66} + 7.4 \times 10^{-4} T^{-1.5}$ | | |
| | | $\times \exp\left(-\frac{175000}{T}\right) [1.0 + 0.062 \times \exp\left(-\frac{145000}{T}\right)]$ | $T > 400$ K | |
| 22 | $C + e^- \rightarrow C^+ + e^- + e^-$ | $k_{22} = 6.85 \times 10^{-8} (0.193 + u)^{-1} u^{0.25} e^{-u}$ | $u = 11.26/T_e$ | 22 |
| 23 | $O + e^- \rightarrow O^+ + e^- + e^-$ | $k_{23} = 3.59 \times 10^{-8} (0.073 + u)^{-1} u^{0.34} e^{-u}$ | $u = 13.6/T_e$ | 22 |
| 24 | $O^+ + H \rightarrow O + H^+$ | $k_{24} = 4.99 \times 10^{-11} T^{0.405} + 7.54 \times 10^{-10} T^{-0.458}$ | | 23 |
| 25 | $O + H^+ \rightarrow O^+ + H$ | $k_{25} = [1.08 \times 10^{-11} T^{0.517}$ | | 24 |
| | | $+ 4.00 \times 10^{-10} T^{0.00669}] \exp\left(-\frac{227}{T}\right)$ | | |
| 26 | $O + He^+ \rightarrow O^+ + He$ | $k_{26} = 4.991 \times 10^{-15} \left(\frac{T}{10000}\right)^{0.3794} \exp\left(-\frac{T}{1121000}\right)$ | | 25 |
| | | $+ 2.780 \times 10^{-15} \left(\frac{T}{10000}\right)^{-0.2163} \exp\left(\frac{T}{815800}\right)$ | | |
| 27 | $C + H^+ \rightarrow C^+ + H$ | $k_{27} = 3.9 \times 10^{-16} T^{0.213}$ | | 24 |
| 28 | $C^+ + H \rightarrow C + H^+$ | $k_{28} = 6.08 \times 10^{-14} \left(\frac{T}{10000}\right)^{1.96} \exp\left(-\frac{170000}{T}\right)$ | | 24 |
| 29 | $C + He^+ \rightarrow C^+ + He$ | $k_{29} = 8.58 \times 10^{-17} T^{0.757}$ | $T \leqslant 200$ K | 26 |
| | | $= 3.25 \times 10^{-17} T^{0.968}$ | $200 < T \leqslant 2000$ K | |
| | | $= 2.77 \times 10^{-19} T^{1.597}$ | $T > 2000$ K | |
| 30 | $H_2 + He \rightarrow H + H + He$ | $k_{30,l} = \text{dex}[-27.029 + 3.801 \log(T) - 29487/T]$ | | 27 |
| | | $k_{30,h} = \text{dex}[-2.729 - 1.75 \log(T) - 23474/T]$ | | |
| | | $n_{cr,He} = \text{dex}\left[5.0792 (1.0 - 1.23 \times 10^{-5} (T - 2000))\right]$ | | 27 |
| 31 | $OH + H \rightarrow O + H + H$ | $k_{31} = 6.0 \times 10^{-9} \exp\left(-\frac{50900}{T}\right)$ | | 28 |
| 32 | $HOC^+ + H_2 \rightarrow HCO^+ + H_2$ | $k_{32} = 3.8 \times 10^{-10}$ | | 29 |
| 33 | $HOC^+ + CO \rightarrow HCO^+ + CO$ | $k_{33} = 4.0 \times 10^{-10}$ | | 30 |
| 34 | $C + H_2 \rightarrow CH + H$ | $k_{34} = 6.64 \times 10^{-10} \exp\left(-\frac{11700}{T}\right)$ | | 31 |
| 35 | $CH + H \rightarrow C + H_2$ | $k_{35} = 1.31 \times 10^{-10} \exp\left(-\frac{80}{T}\right)$ | | 32 |

(Glover, Federrath, Mac Low, Klessen, in prep)

# chemical model 2

Table B1.

| | | | | |
|---|---|---|---|---|
| 14 | $H^- + H \rightarrow H + H + e^-$ | $k_{14} = 2.5634 \times 10^{-9} T_e^{1.78186}$ | $T_e \leqslant 0.1$ eV | 13 |

| | | | | |
|---|---|---|---|---|
| 36 | $CH + H_2 \rightarrow CH_2 + H$ | $k_{36} = 5.46 \times 10^{-10} \exp\left(-\frac{1943}{T}\right)$ | | 33 |
| 37 | $CH + C \rightarrow C_2 + H$ | $k_{37} = 6.59 \times 10^{-11}$ | | 34 |
| 38 | $CH +$ [illegible] $\rightarrow CO + H$ | $k_{38} = 6.6 \times 10^{-11}$ | $T \leqslant$ [illegible]000 K | [illegible]5 |
| | | $= 1.02 \times 10^{-10}$ exp [illegible] | $T >$ [illegible]000 K | [illegible]6 |
| 39 | [illegible] | [illegible] $\times 10^{-11}$ | | [illegible]7 |
| 40 | $CH_2 + O \rightarrow CO + H + H$ | $k_{40} = 1.33 \times 10^{-10}$ | | 38 |
| 41 | $CH_2 + O \rightarrow CO + H_2$ | $k_{41} = 8.0 \times 10^{-11}$ | | 39 |
| 42 | $C_2 + O \rightarrow CO + C$ | $k_{42} = 5.0 \times 10^{-11} \left(\frac{T}{300}\right)^{0.5}$ | $T \leqslant 300$ K | 40 |
| | | $= 5.0 \times 10^{-11} \left(\frac{T}{300}\right)^{0.757}$ | $T > 300$ K | 41 |
| 43 | $O + H_2 \rightarrow OH + H$ | $k_{43} = 3.14 \times 10^{-13} \left(\frac{T}{300}\right)^{2.7} \exp\left(-\frac{3150}{T}\right)$ | | 42 |
| 44 | $OH + H \rightarrow O + H_2$ | $k_{44} = 6.99 \times 10^{-14} \left(\frac{T}{300}\right)^{2.8} \exp\left(-\frac{1950}{T}\right)$ | | 43 |
| 45 | $OH + H_2 \rightarrow H_2O + H$ | $k_{45} = 2.05 \times 10^{-12} \left(\frac{T}{300}\right)^{1.52} \exp\left(-\frac{1736}{T}\right)$ | | 44 |
| 46 | $OH + C \rightarrow CO + H$ | $k_{46} = 1.0 \times 10^{-10}$ | | 34 |
| 47 | $OH + O \rightarrow O_2 + H$ | $k_{47} = 3.50 \times 10^{-11}$ | $T \leqslant 261$ K | 45 |
| | | $= 1.77 \times 10^{-11} \exp\left(\frac{178}{T}\right)$ | $T > 261$ K | 33 |
| 48 | $OH + OH \rightarrow H_2O + H$ | $k_{48} = 1.65 \times 10^{-12} \left(\frac{T}{300}\right)^{1.14} \exp\left(-\frac{50}{T}\right)$ | | 34 |
| 49 | $H_2O + H \rightarrow H_2 + OH$ | $k_{49} = 1.59 \times 10^{-11} \left(\frac{T}{300}\right)^{1.2} \exp\left(-\frac{9610}{T}\right)$ | | 46 |
| 50 | $O_2 + H \rightarrow OH + O$ | $k_{50} = 2.61 \times 10^{-10} \exp\left(-\frac{8156}{T}\right)$ | | 33 |
| 51 | $O_2 + H_2 \rightarrow OH + OH$ | $k_{51} = 3.16 \times 10^{-10} \exp\left(-\frac{21890}{T}\right)$ | | 47 |
| 52 | $O_2 + C \rightarrow CO + O$ | $k_{52} = 4.7 \times 10^{-11} \left(\frac{T}{300}\right)^{-0.34}$ | $T \leqslant 295$ K | 34 |
| | | $= 2.48 \times 10^{-12} \left(\frac{T}{300}\right)^{1.54} \exp\left(\frac{613}{T}\right)$ | $T > 295$ K | 33 |
| 53 | $CO + H \rightarrow C + OH$ | $k_{53} = 1.1 \times 10^{-10} \left(\frac{T}{300}\right)^{0.5} \exp\left(-\frac{77700}{T}\right)$ | | 28 |
| 54 | $H_2^+ + H_2 \rightarrow H_3^+ + H$ | $k_{54} = 2.24 \times 10^{-9} \left(\frac{T}{300}\right)^{0.042} \exp\left(-\frac{T}{46600}\right)$ | | 48 |
| 55 | $H_3^+ + H \rightarrow H_2^+ + H_2$ | $k_{55} = 7.7 \times 10^{-9} \exp\left(-\frac{17560}{T}\right)$ | | 49 |
| 56 | $C + H_2^+ \rightarrow CH^+ + H$ | $k_{56} = 2.4 \times 10^{-9}$ | | 28 |
| 57 | $C + H_3^+ \rightarrow CH^+ + H_2$ | $k_{57} = 2.0 \times 10^{-9}$ | | 28 |
| 58 | $C^+ + H_2 \rightarrow CH^+ + H$ | $k_{58} = 1.0 \times 10^{-10} \exp\left(-\frac{4640}{T}\right)$ | | 50 |
| 59 | $CH^+ + H \rightarrow C^+ + H_2$ | $k_{59} = 7.5 \times 10^{-10}$ | | 51 |
| 60 | $CH^+ + H_2 \rightarrow CH_2^+ + H$ | $k_{60} = 1.2 \times 10^{-9}$ | | 51 |
| 61 | $CH^+ + O \rightarrow CO^+ + H$ | $k_{61} = 3.5 \times 10^{-10}$ | | 52 |
| 62 | $CH_2 + H^+ \rightarrow CH^+ + H_2$ | $k_{62} = 1.4 \times 10^{-9}$ | | 28 |
| 63 | $CH_2^+ + H \rightarrow CH^+ + H_2$ | $k_{63} = 1.0 \times 10^{-9} \exp\left(-\frac{7080}{T}\right)$ | | 28 |
| 64 | $CH_2^+ + H_2 \rightarrow CH_3^+ + H$ | $k_{64} = 1.6 \times 10^{-9}$ | | 53 |
| 65 | $CH_2^+ + O \rightarrow HCO^+ + H$ | $k_{65} = 7.5 \times 10^{-10}$ | | 28 |
| 66 | $CH_3^+ + H \rightarrow CH_2^+ + H_2$ | $k_{66} = 7.0 \times 10^{-10} \exp\left(-\frac{10560}{T}\right)$ | | 28 |
| 67 | $CH_3^+ + O \rightarrow HCO^+ + H_2$ | $k_{67} = 4.0 \times 10^{-10}$ | | 54 |
| 68 | $C_2 + O^+ \rightarrow CO^+ + C$ | $k_{68} = 4.8 \times 10^{-10}$ | | 28 |
| 69 | $O^+ + H_2 \rightarrow OH^+ + H$ | $k_{69} = 1.7 \times 10^{-9}$ | | 55 |
| 70 | $O + H_2^+ \rightarrow OH^+ + H$ | $k_{70} = 1.5 \times 10^{-9}$ | | 28 |
| 71 | $O + H_3^+ \rightarrow OH^+ + H_2$ | $k_{71} = 8.4 \times 10^{-10}$ | | 56 |
| 72 | $OH + H_3^+ \rightarrow H_2O^+ + H_2$ | $k_{72} = 1.3 \times 10^{-9}$ | | 28 |
| 73 | $OH + C^+ \rightarrow CO^+ + H$ | $k_{73} = 7.7 \times 10^{-10}$ | | 28 |
| 74 | $OH^+ + H_2 \rightarrow H_2O^+ + H$ | $k_{74} = 1.01 \times 10^{-9}$ | | 57 |
| 75 | $H_2O^+ + H_2 \rightarrow H_3O^+ + H$ | $k_{75} = 6.4 \times 10^{-10}$ | | 58 |
| 76 | $H_2O + H_3^+ \rightarrow H_3O^+ + H_2$ | $k_{76} = 5.9 \times 10^{-9}$ | | 59 |
| 77 | $H_2O + C^+ \rightarrow HCO^+ + H$ | $k_{77} = 9.0 \times 10^{-10}$ | | 60 |
| 78 | $H_2O + C^+ \rightarrow HOC^+ + H$ | $k_{78} = 1.8 \times 10^{-9}$ | | 60 |
| 79 | $H_3O^+ + C \rightarrow HCO^+ + H_2$ | $k_{79} = 1.0 \times 10^{-11}$ | | 28 |
| 80 | $O_2 + C^+ \rightarrow CO^+ + O$ | $k_{80} = 3.8 \times 10^{-10}$ | | 53 |
| 81 | $O_2 + C^+ \rightarrow CO + O^+$ | $k_{81} = 6.2 \times 10^{-10}$ | | 53 |
| 82 | $O_2 + CH_2^+ \rightarrow HCO^+ + OH$ | $k_{82} = 9.1 \times 10^{-10}$ | | 53 |
| 83 | $O_2^+ + C \rightarrow CO^+ + O$ | $k_{83} = 5.2 \times 10^{-11}$ | | 28 |
| 84 | $CO + H_3^+ \rightarrow HOC^+ + H_2$ | $k_{84} = 2.7 \times 10^{-11}$ | | 61 |
| 85 | $CO + H_3^+ \rightarrow HCO^+ + H_2$ | $k_{85} = 1.7 \times 10^{-9}$ | | 61 |
| 86 | $HCO^+ + C \rightarrow CO + CH^+$ | $k_{86} = 1.1 \times 10^{-9}$ | | 28 |
| 87 | $HCO^+ + H_2O \rightarrow CO + H_3O^+$ | $k_{87} = 2.5 \times 10^{-9}$ | | 62 |

(Glover, Federrath, Mac Low, Klessen, in prep)

# chemical model 2

Table B1.

| | | | |
|---|---|---|---|
| 88 | $H_2 + He^+ \rightarrow He + H_2^+$ | $k_{88} = 7.2 \times 10^{-15}$ | 63 |
| 89 | $H_2 + He^+ \rightarrow He + H + H^+$ | $k_{89} = 3.7 \times 10^{-14} \exp\left(\frac{35}{T}\right)$ | 63 |
| 90 | $CH + H^+ \rightarrow CH^+ + H$ | $k_{90} = 1.9 \times 10^{-9}$ | 28 |
| 91 | $CH_2 + H^+ \rightarrow CH_2^+ + H$ | $k_{91} = 1.4 \times 10^{-9}$ | 28 |
| 92 | $CH_2 + He^+ \rightarrow C^+ + He + H_2$ | $k_{92} = 7.$[illegible]$ \times 10^{-10}$ | 28 |
| 93 | $C_2 + He^+ \rightarrow C^+ + C + He$ | $k_{93} = 1.6 \times 10^{-9}$ | 28 |
| 94 | $OH + H^+ \rightarrow OH^+ + H$ | $k_{94} = 2.1 \times 10^{-9}$ | 28 |
| 95 | $OH + He^+ \rightarrow O^+ + He + H$ | $k_{95} = 1.1 \times 10^{-9}$ | 28 |
| 96 | $H_2O + H^+ \rightarrow H_2O^+ + H$ | $k_{96} = 6.9 \times 10^{-9}$ | 64 |
| 97 | $H_2O + He^+ \rightarrow OH + He + H^+$ | $k_{97} = 2.04 \times 10^{-10}$ | 65 |
| 98 | $H_2O + He^+ \rightarrow OH^+ + He + H$ | $k_{98} = 2.86 \times 10^{-10}$ | 65 |
| 99 | $H_2O + He^+ \rightarrow H_2O^+ + He$ | $k_{99} = 6.05 \times 10^{-11}$ | 65 |
| 100 | $O_2 + H^+ \rightarrow O_2^+ + H$ | $k_{100} = 2.0 \times 10^{-9}$ | 64 |
| 101 | $O_2 + He^+ \rightarrow O_2^+ + He$ | $k_{101} = 3.3 \times 10^{-11}$ | 66 |
| 102 | $O_2 + He^+ \rightarrow O^+ + O + He$ | $k_{102} = 1.1 \times 10^{-9}$ | 66 |
| 103 | $O_2^+ + C \rightarrow O_2 + C^+$ | $k_{103} = 5.2 \times 10^{-11}$ | 28 |
| 104 | $CO + He^+ \rightarrow C^+ + O + He$ | $k_{104} = 1.4 \times 10^{-9} \left(\frac{T}{300}\right)^{-0.5}$ | 67 |
| 105 | $CO + He^+ \rightarrow C + O^+ + He$ | $k_{105} = 1.4 \times 10^{-16} \left(\frac{T}{300}\right)^{-0.5}$ | 67 |
| 106 | $CO^+ + H \rightarrow CO + H^+$ | $k_{106} = 7.5 \times 10^{-10}$ | 68 |
| 107 | $C^- + H^+ \rightarrow C + H$ | $k_{107} = 2.3 \times 10^{-7} \left(\frac{T}{300}\right)^{-0.5}$ | 28 |
| 108 | $O^- + H^+ \rightarrow O + H$ | $k_{108} = 2.3 \times 10^{-7} \left(\frac{T}{300}\right)^{-0.5}$ | 28 |
| 109 | $He^+ + H^- \rightarrow He + H$ | $k_{109} = 2.32 \times 10^{-7} \left(\frac{T}{300}\right)^{-0.52} \exp\left(\frac{T}{22400}\right)$ | 69 |
| 110 | $H_3^+ + e^- \rightarrow H_2 + H$ | $k_{110} = 2.34 \times 10^{-8} \left(\frac{T}{300}\right)^{-0.52}$ | 70 |
| 111 | $H_3^+ + e^- \rightarrow H + H + H$ | $k_{111} = 4.36 \times 10^{-8} \left(\frac{T}{300}\right)^{-0.52}$ | 70 |
| 112 | $CH^+ + e^- \rightarrow C + H$ | $k_{112} = 7.0 \times 10^{-8} \left(\frac{T}{300}\right)^{-0.5}$ | 71 |
| 113 | $CH_2^+ + e^- \rightarrow CH + H$ | $k_{113} = 1.6 \times 10^{-7} \left(\frac{T}{300}\right)^{-0.6}$ | 72 |
| 114 | $CH_2^+ + e^- \rightarrow C + H + H$ | $k_{114} = 4.03 \times 10^{-7} \left(\frac{T}{300}\right)^{-0.6}$ | 72 |
| 115 | $CH_2^+ + e^- \rightarrow C + H_2$ | $k_{115} = 7.68 \times 10^{-8} \left(\frac{T}{300}\right)^{-0.6}$ | 72 |
| 116 | $CH_3^+ + e^- \rightarrow CH_2 + H$ | $k_{116} = 7.75 \times 10^{-8} \left(\frac{T}{300}\right)^{-0.5}$ | 73 |
| 117 | $CH_3^+ + e^- \rightarrow CH + H_2$ | $k_{117} = 1.95 \times 10^{-7} \left(\frac{T}{300}\right)^{-0.5}$ | 73 |
| 118 | $CH_3^+ + e^- \rightarrow CH + H + H$ | $k_{118} = 2.0 \times 10^{-7} \left(\frac{T}{300}\right)^{-0.4}$ | 28 |
| 119 | $OH^+ + e^- \rightarrow O + H$ | $k_{119} = 6.3 \times 10^{-9} \left(\frac{T}{300}\right)^{-0.48}$ | 74 |
| 120 | $H_2O^+ + e^- \rightarrow O + H + H$ | $k_{120} = 3.05 \times 10^{-7} \left(\frac{T}{300}\right)^{-0.5}$ | 75 |
| 121 | $H_2O^+ + e^- \rightarrow O + H_2$ | $k_{121} = 3.9 \times 10^{-8} \left(\frac{T}{300}\right)^{-0.5}$ | 75 |
| 122 | $H_2O^+ + e^- \rightarrow OH + H$ | $k_{122} = 8.6 \times 10^{-8} \left(\frac{T}{300}\right)^{-0.5}$ | 75 |
| 123 | $H_3O^+ + e^- \rightarrow H + H_2O$ | $k_{123} = 1.08 \times 10^{-7} \left(\frac{T}{300}\right)^{-0.5}$ | 76 |
| 124 | $H_3O^+ + e^- \rightarrow OH + H_2$ | $k_{124} = 6.02 \times 10^{-8} \left(\frac{T}{300}\right)^{-0.5}$ | 76 |
| 125 | $H_3O^+ + e^- \rightarrow OH + H + H$ | $k_{125} = 2.58 \times 10^{-7} \left(\frac{T}{300}\right)^{-0.5}$ | 76 |
| 126 | $H_3O^+ + e^- \rightarrow O + H + H_2$ | $k_{126} = 5.6 \times 10^{-9} \left(\frac{T}{300}\right)^{-0.5}$ | 76 |
| 127 | $O_2^+ + e^- \rightarrow O + O$ | $k_{127} = 1.95 \times 10^{-7} \left(\frac{T}{300}\right)^{-0.7}$ | 77 |
| 128 | $CO^+ + e^- \rightarrow C + O$ | $k_{128} = 2.75 \times 10^{-7} \left(\frac{T}{300}\right)^{-0.55}$ | 78 |
| 129 | $HCO^+ + e^- \rightarrow CO + H$ | $k_{129} = 2.76 \times 10^{-7} \left(\frac{T}{300}\right)^{-0.64}$ | 79 |
| 130 | $HCO^+ + e^- \rightarrow OH + C$ | $k_{130} = 2.4 \times 10^{-8} \left(\frac{T}{300}\right)^{-0.64}$ | 79 |
| 131 | $HOC^+ + e^- \rightarrow CO + H$ | $k_{131} = 1.1 \times 10^{-7} \left(\frac{T}{300}\right)^{-1.0}$ | 28 |
| 132 | $H^- + C \rightarrow CH + e^-$ | $k_{132} = 1.0 \times 10^{-9}$ | 28 |
| 133 | $H^- + O \rightarrow OH + e^-$ | $k_{133} = 1.0 \times 10^{-9}$ | 28 |
| 134 | $H^- + OH \rightarrow H_2O + e^-$ | $k_{134} = 1.0 \times 10^{-10}$ | 28 |
| 135 | $C^- + H \rightarrow CH + e^-$ | $k_{135} = 5.0 \times 10^{-10}$ | 28 |
| 136 | $C^- + H_2 \rightarrow CH_2 + e^-$ | $k_{136} = 1.0 \times 10^{-13}$ | 28 |
| 137 | $C^- + O \rightarrow CO + e^-$ | $k_{137} = 5.0 \times 10^{-10}$ | 28 |
| 138 | $O^- + H \rightarrow OH + e^-$ | $k_{138} = 5.0 \times 10^{-10}$ | 28 |
| 139 | $O^- + H_2 \rightarrow H_2O + e^-$ | $k_{139} = 7.0 \times 10^{-10}$ | 28 |
| 140 | $O^- + C \rightarrow CO + e^-$ | $k_{140} = 5.0 \times 10^{-10}$ | 28 |

(Glover, Federrath, Mac Low, Klessen, in prep)

# chemical model 2

| | | | | |
|---|---|---|---|---|
| 88 | $H_2 + He^+ \rightarrow He + H_2^+$ | $k_{88} = 7.2 \times 10^{-15}$ | | 63 |
| 89 | $H_2 + He^+ \rightarrow He + H + H^+$ | $k_{89} = 3.7 \times 10^{-14} \exp\left(\frac{35}{T}\right)$ | | 63 |
| 90 | $CH + H^+ \rightarrow CH^+ + H$ | $k_{90} = 1.9 \times 10^{-9}$ | | 28 |
| 91 | $CH_2 + H^+ \rightarrow CH_2^+ + H$ | $k_{91} = 1.4 \times 10^{-9}$ | | 28 |
| 94 | $OH + H^+ \rightarrow OH^+ + H$ | $k_{94} = 2.1 \times 10^{-9}$ | | 28 |
| 95 | $OH + He^+ \rightarrow O^+ + He + H$ | $k_{95} = 1.1 \times 10^{-9}$ | | 28 |
| 96 | $H_2O + H^+ \rightarrow H_2O^+ + H$ | $k_{96} = 6.9 \times 10^{-9}$ | | 64 |
| 97 | $H_2O + He^+ \rightarrow OH + He + H^+$ | $k_{97} = 2.04 \times 10^{-10}$ | | 65 |

| | | | | |
|---|---|---|---|---|
| 142 | $C + e^- \rightarrow C^- + \gamma$ | $k_{142} = 2.25 \times 10^{-15}$ | | 81 |
| 143 | $C + H \rightarrow CH + \gamma$ | $k_{143} = 1.0 \times 10^{-17}$ | | 82 |
| 144 | $C + H_2 \rightarrow CH_2 + \gamma$ | $k_{144} = 1.0 \times 10^{-17}$ | | 82 |
| 145 | $C + C \rightarrow C_2 + \gamma$ | $k_{145} = 4.36 \times 10^{-18} \left(\frac{T}{300}\right)^{0.35} \exp\left(-\frac{161.3}{T}\right)$ | | 83 |
| 146 | $C + O \rightarrow CO + \gamma$ | $k_{146} = 2.1 \times 10^{-19}$ | $T \leqslant 300$ K | 84 |
| | | $= 3.09 \times 10^{-17} \left(\frac{T}{300}\right)^{0.33} \exp\left(-\frac{1629}{T}\right)$ | $T > 300$ K | 85 |
| 147 | $C^+ + H \rightarrow CH^+ + \gamma$ | $k_{147} = 4.46 \times 10^{-16} T^{-0.5} \exp\left(-\frac{4.93}{T^{2/3}}\right)$ | | 86 |
| 148 | $C^+ + H_2 \rightarrow CH_2^+ + \gamma$ | $k_{148} = 4.0 \times 10^{-16} \left(\frac{T}{300}\right)^{-0.2}$ | | 87 |
| 149 | $C^+ + O \rightarrow CO^+ + \gamma$ | $k_{149} = 2.5 \times 10^{-18}$ | $T \leqslant 300$ K | 84 |
| | | $= 3.14 \times 10^{-18} \left(\frac{T}{300}\right)^{-0.15} \exp\left(\frac{68}{T}\right)$ | $T > 300$ K | |
| 150 | $O + e^- \rightarrow O^- + \gamma$ | $k_{150} = 1.5 \times 10^{-15}$ | | 28 |
| 151 | $O + H \rightarrow OH + \gamma$ | $k_{151} = 9.9 \times 10^{-19} \left(\frac{T}{300}\right)^{-0.38}$ | | 28 |
| 152 | $O + O \rightarrow O_2 + \gamma$ | $k_{152} = 4.9 \times 10^{-20} \left(\frac{T}{300}\right)^{1.58}$ | | 82 |
| 153 | $OH + H \rightarrow H_2O + \gamma$ | $k_{153} = 5.26 \times 10^{-18} \left(\frac{T}{300}\right)^{-5.22} \exp\left(-\frac{90}{T}\right)$ | | 88 |
| 154 | $H + H + H \rightarrow H_2 + H$ | $k_{154} = 1.32 \times 10^{-32} \left(\frac{T}{300}\right)^{-0.38}$ | $T \leqslant 300$ K | 89 |
| | | $= 1.32 \times 10^{-32} \left(\frac{T}{300}\right)^{-1.0}$ | $T > 300$ K | 90 |
| 155 | $H + H + H_2 \rightarrow H_2 + H_2$ | $k_{155} = 2.8 \times 10^{-31} T^{-0.6}$ | | 91 |
| 156 | $H + H + He \rightarrow H_2 + He$ | $k_{156} = 6.9 \times 10^{-32} T^{-0.4}$ | | 92 |
| 157 | $C + C + M \rightarrow C_2 + M$ | $k_{157} = 5.99 \times 10^{-33} \left(\frac{T}{5000}\right)^{-1.6}$ | $T \leqslant 5000$ K | 93 |
| | | $= 5.99 \times 10^{-33} \left(\frac{T}{5000}\right)^{-0.64} \exp\left(\frac{5255}{T}\right)$ | $T > 5000$ K | 94 |
| 158 | $C + O + M \rightarrow CO + M$ | $k_{158} = 6.16 \times 10^{-29} \left(\frac{T}{300}\right)^{-3.08}$ | $T \leqslant 2000$ K | 35 |
| | | $= 2.14 \times 10^{-29} \left(\frac{T}{300}\right)^{-3.08} \exp\left(\frac{2114}{T}\right)$ | $T > 2000$ K | 67 |
| 159 | $C^+ + O + M \rightarrow CO^+ + M$ | $k_{159} = 100 \times k_{210}$ | | 67 |
| 160 | $C + O^+ + M \rightarrow CO^+ + M$ | $k_{160} = 100 \times k_{210}$ | | 67 |
| 161 | $O + H + M \rightarrow OH + M$ | $k_{161} = 4.33 \times 10^{-32} \left(\frac{T}{300}\right)^{-1.0}$ | | 43 |
| 162 | $OH + H + M \rightarrow H_2O + M$ | $k_{162} = 2.56 \times 10^{-31} \left(\frac{T}{300}\right)^{-2.0}$ | | 35 |
| 163 | $O + O + M \rightarrow O_2 + M$ | $k_{163} = 9.2 \times 10^{-34} \left(\frac{T}{300}\right)^{-1.0}$ | | 37 |
| 164 | $O + CH \rightarrow HCO^+ + e^-$ | $k_{164} = 2.0 \times 10^{-11} \left(\frac{T}{300}\right)^{0.44}$ | | 95 |
| 165 | $H + H(s) \rightarrow H_2$ | $k_{165} = 3.0 \times 10^{-18} T^{0.5} f_A [1.0 + 0.04(T + T_d)^{0.5} + 0.002\,T + 8 \times 10^{-6} T^2]^{-1}$ | $f_A = \left[1.0 + 10^4 \exp\left(-\frac{600}{T_d}\right)\right]^{-1}$ | 96 |

| | | | | |
|---|---|---|---|---|
| 129 | $HCO^+ + e^- \rightarrow CO + H$ | $k_{129} = 2.76 \times 10^{-7} \left(\frac{T}{300}\right)^{-0.64}$ | | 79 |
| 130 | $HCO^+ + e^- \rightarrow OH + C$ | $k_{130} = 2.4 \times 10^{-8} \left(\frac{T}{300}\right)^{-0.64}$ | | 79 |
| 131 | $HOC^+ + e^- \rightarrow CO + H$ | $k_{131} = 1.1 \times 10^{-7} \left(\frac{T}{300}\right)^{-1.0}$ | | 28 |
| 132 | $H^- + C \rightarrow CH + e^-$ | $k_{132} = 1.0 \times 10^{-9}$ | | 28 |
| 133 | $H^- + O \rightarrow OH + e^-$ | $k_{133} = 1.0 \times 10^{-9}$ | | 28 |
| 134 | $H^- + OH \rightarrow H_2O + e^-$ | $k_{134} = 1.0 \times 10^{-10}$ | | 28 |
| 135 | $C^- + H \rightarrow CH + e^-$ | $k_{135} = 5.0 \times 10^{-10}$ | | 28 |
| 136 | $C^- + H_2 \rightarrow CH_2 + e^-$ | $k_{136} = 1.0 \times 10^{-13}$ | | 28 |
| 137 | $C^- + O \rightarrow CO + e^-$ | $k_{137} = 5.0 \times 10^{-10}$ | | 28 |
| 138 | $O^- + H \rightarrow OH + e^-$ | $k_{138} = 5.0 \times 10^{-10}$ | | 28 |
| 139 | $O^- + H_2 \rightarrow H_2O + e^-$ | $k_{139} = 7.0 \times 10^{-10}$ | | 28 |
| 140 | $O^- + C \rightarrow CO + e^-$ | $k_{140} = 5.0 \times 10^{-10}$ | | 28 |

(Glover, Federrath, Mac Low, Klessen, in prep)

# chemical model 2

| | | | |
|---|---|---|---|
| 88 | $H_2 + He^+ \rightarrow He + H_2^+$ | $k_{88} = 7.2 \times 10^{-15}$ | 63 |
| 89 | $H_2 + He^+ \rightarrow He + H + H^+$ | $k_{89} = 3.7 \times 10^{-14} \exp\left(\frac{35}{T}\right)$ | 63 |
| 90 | $CH + H^+ \rightarrow CH^+ + H$ | $k_{90} = 1.9 \times 10^{-9}$ | 28 |
| 91 | $CH_2 + H^+ \rightarrow CH_2^+ + H$ | $k_{91} = 1.4 \times 10^{-9}$ | 28 |
| 95 | $OH + He^+ \rightarrow O^+ + He + H$ | $k_{95} = 1.1 \times 10^{-9}$ | 28 |
| 96 | $H_2O + H^+ \rightarrow H_2O^+ + H$ | $k_{96} = 6.9 \times 10^{-9}$ | 64 |
| 97 | $H_2O + He^+ \rightarrow OH + He + H^+$ | $k_{97} = 2.04 \times 10^{-10}$ | 65 |

**Table B2.** List of photochemical reactions included in our chemical model

| No. | Reaction | Optically thin rate ($s^{-1}$) | $\gamma$ | Ref. |
|---|---|---|---|---|
| 166 | $H^- + \gamma \rightarrow H + e^-$ | $R_{166} = 7.1 \times 10^{-7}$ | 0.5 | 1 |
| 167 | $H_2^+ + \gamma \rightarrow H + H^+$ | $R_{167} = 1.1 \times 10^{-9}$ | 1.9 | 2 |
| 168 | $H_2 + \gamma \rightarrow H + H$ | $R_{168} = 5.6 \times 10^{-11}$ | See §2.2 | 3 |
| 169 | $H_3^+ + \gamma \rightarrow H_2 + H^+$ | $R_{169} = 4.9 \times 10^{-13}$ | 1.8 | 4 |
| 170 | $H_3^+ + \gamma \rightarrow H_2^+ + H$ | $R_{170} = 4.9 \times 10^{-13}$ | 2.3 | 4 |
| 171 | $C + \gamma \rightarrow C^+ + e^-$ | $R_{171} = 3.1 \times 10^{-10}$ | 3.0 | 5 |
| 172 | $C^- + \gamma \rightarrow C + e^-$ | $R_{172} = 2.4 \times 10^{-7}$ | 0.9 | 6 |
| 173 | $CH + \gamma \rightarrow C + H$ | $R_{173} = 8.7 \times 10^{-10}$ | 1.2 | 7 |
| 174 | $CH + \gamma \rightarrow CH^+ + e^-$ | $R_{174} = 7.7 \times 10^{-10}$ | 2.8 | 8 |
| 175 | $CH^+ + \gamma \rightarrow C + H^+$ | $R_{175} = 2.6 \times 10^{-10}$ | 2.5 | 7 |
| 176 | $CH_2 + \gamma \rightarrow CH + H$ | $R_{176} = 7.1 \times 10^{-10}$ | 1.7 | 7 |
| 177 | $CH_2 + \gamma \rightarrow CH_2^+ + e^-$ | $R_{177} = 5.9 \times 10^{-10}$ | 2.3 | 6 |
| 178 | $CH_2^+ + \gamma \rightarrow CH^+ + H$ | $R_{178} = 4.6 \times 10^{-10}$ | 1.7 | 9 |
| 179 | $CH_3^+ + \gamma \rightarrow CH_2^+ + H$ | $R_{179} = 1.0 \times 10^{-9}$ | 1.7 | 6 |
| 180 | $CH_3^+ + \gamma \rightarrow CH^+ + H_2$ | $R_{180} = 1.0 \times 10^{-9}$ | 1.7 | 6 |
| 181 | $C_2 + \gamma \rightarrow C + C$ | $R_{181} = 1.5 \times 10^{-10}$ | 2.1 | 7 |
| 182 | $O^- + \gamma \rightarrow O + e^-$ | $R_{182} = 2.4 \times 10^{-7}$ | 0.5 | 6 |
| 183 | $OH + \gamma \rightarrow O + H$ | $R_{183} = 3.7 \times 10^{-10}$ | 1.7 | 10 |
| 184 | $OH + \gamma \rightarrow OH^+ + e^-$ | $R_{184} = 1.6 \times 10^{-12}$ | 3.1 | 6 |
| 185 | $OH^+ + \gamma \rightarrow O + H^+$ | $R_{185} = 1.0 \times 10^{-12}$ | 1.8 | 4 |
| 186 | $H_2O + \gamma \rightarrow OH + H$ | $R_{186} = 6.0 \times 10^{-10}$ | 1.7 | 11 |
| 187 | $H_2O + \gamma \rightarrow H_2O^+ + e^-$ | $R_{187} = 3.2 \times 10^{-11}$ | 3.9 | 8 |
| 188 | $H_2O^+ + \gamma \rightarrow H_2^+ + O$ | $R_{188} = 5.0 \times 10^{-11}$ | See §2.2 | 12 |
| 189 | $H_2O^+ + \gamma \rightarrow H^+ + OH$ | $R_{189} = 5.0 \times 10^{-11}$ | See §2.2 | 12 |
| 190 | $H_2O^+ + \gamma \rightarrow O^+ + H_2$ | $R_{190} = 5.0 \times 10^{-11}$ | See §2.2 | 12 |
| 191 | $H_2O^+ + \gamma \rightarrow OH^+ + H$ | $R_{191} = 1.5 \times 10^{-10}$ | See §2.2 | 12 |
| 192 | $H_3O^+ + \gamma \rightarrow H^+ + H_2O$ | $R_{192} = 2.5 \times 10^{-11}$ | See §2.2 | 12 |
| 193 | $H_3O^+ + \gamma \rightarrow H_2^+ + OH$ | $R_{193} = 2.5 \times 10^{-11}$ | See §2.2 | 12 |
| 194 | $H_3O^+ + \gamma \rightarrow H_2O^+ + H$ | $R_{194} = 7.5 \times 10^{-12}$ | See §2.2 | 12 |
| 195 | $H_3O^+ + \gamma \rightarrow OH^+ + H_2$ | $R_{195} = 2.5 \times 10^{-11}$ | See §2.2 | 12 |
| 196 | $O_2 + \gamma \rightarrow O_2^+ + e^-$ | $R_{196} = 5.6 \times 10^{-11}$ | 3.7 | 7 |
| 197 | $O_2 + \gamma \rightarrow O + O$ | $R_{197} = 7.0 \times 10^{-10}$ | 1.8 | 7 |
| 198 | $CO + \gamma \rightarrow C + O$ | $R_{198} = 2.0 \times 10^{-10}$ | See §2.2 | 13 |

(Glover, Federrath, Mac Low, Klessen, in prep)

# chemical model 2

**Table B2.** List of photochemical reactions included in our chemical model

| No. | Reaction | Optically thin rate ($s^{-1}$) | $\gamma$ | Ref. |
|---|---|---|---|---|
| 166 | $H^- + \gamma \rightarrow H + e^-$ | $R_{166} = 7.1 \times 10^{-7}$ | 0.5 | 1 |
| 167 | $H_2^+ + \gamma \rightarrow H + H^+$ | $R_{167} = 1.1 \times 10^{-9}$ | 1.9 | 2 |
| 168 | $H_2 + \gamma \rightarrow H + H$ | $R_{168} = 5.6 \times 10^{-11}$ | See §2.2 | 3 |
| 169 | $H_3^+ + \gamma \rightarrow H_2 + H^+$ | $R_{169} = 4.9 \times 10^{-13}$ | 1.8 | 4 |
| 170 | $H_3^+ + \gamma \rightarrow H_2^+ + H$ | $R_{170} = 4.9 \times 10^{-13}$ | 2.3 | 4 |
| 171 | $C + \gamma \rightarrow C^+ + e^-$ | $R_{171} = 3.1 \times 10^{-10}$ | 3.0 | 5 |
| 172 | $C^- + \gamma \rightarrow$ | | | |
| 173 | $CH + \gamma \rightarrow$ | | | |
| 174 | $CH + \gamma \rightarrow$ | | | |
| 175 | $CH^+ + \gamma$ | | | |
| 176 | $CH_2 + \gamma$ | | | |
| 177 | $CH_2 + \gamma$ | | | |
| 178 | $CH_2^+ + \gamma$ | | | |
| 179 | $CH_3^+ + \gamma$ | | | |
| 180 | $CH_3^+ + \gamma$ | | | |
| 181 | $C_2 + \gamma \rightarrow$ | | | |
| 182 | $O^- + \gamma \rightarrow$ | | | |
| 183 | $OH + \gamma \rightarrow$ | | | |
| 184 | $OH + \gamma \rightarrow$ | | | |
| 185 | $OH^+ + \gamma$ | | | |
| 186 | $H_2O + \gamma$ | | | |
| 187 | $H_2O + \gamma$ | | | |
| 188 | $H_2O^+ + \gamma$ | | | |
| 189 | $H_2O^+ + \gamma$ | | | |
| 190 | $H_2O^+ + \gamma$ | | | |
| 191 | $H_2O^+ + \gamma$ | | | |
| 192 | $H_3O^+ + \gamma$ | | | |
| 193 | $H_3O^+ + \gamma$ | | | |
| 194 | $H_3O^+ + \gamma$ | | | |
| 195 | $H_3O^+ + \gamma$ | | | |
| 196 | $O_2 + \gamma \rightarrow$ | | | |
| 197 | $O_2 + \gamma \rightarrow O + O$ | $R_{197} = 7.0 \times 10^{-10}$ | 1.8 | 7 |
| 198 | $CO + \gamma \rightarrow C + O$ | $R_{198} = 2.0 \times 10^{-10}$ | See §2.2 | 13 |

**Table B3.** List of reactions included in our chemical model that involve cosmic rays or cosmic-ray induced UV emission

| No. | Reaction | Rate ($s^{-1}\zeta_H^{-1}$) | Ref. |
|---|---|---|---|
| 199 | $H + c.r. \rightarrow H^+ + e^-$ | $R_{199} = 1.0$ | — |
| 200 | $He + c.r. \rightarrow He^+ + e^-$ | $R_{200} = 1.1$ | 1 |
| 201 | $H_2 + c.r. \rightarrow H^+ + H + e^-$ | $R_{201} = 0.037$ | 1 |
| 202 | $H_2 + c.r. \rightarrow H + H$ | $R_{202} = 0.22$ | 1 |
| 203 | $H_2 + c.r. \rightarrow H^+ + H^-$ | $R_{203} = 6.5 \times 10^{-4}$ | 1 |
| 204 | $H_2 + c.r. \rightarrow H_2^+ + e^-$ | $R_{204} = 2.0$ | 1 |
| 205 | $C + c.r. \rightarrow C^+ + e^-$ | $R_{205} = 3.8$ | 1 |
| 206 | $O + c.r. \rightarrow O^+ + e^-$ | $R_{206} = 5.7$ | 1 |
| 207 | $CO + c.r. \rightarrow CO^+ + e^-$ | $R_{207} = 6.5$ | 1 |
| 208 | $C + \gamma_{c.r.} \rightarrow C^+ + e^-$ | $R_{208} = 2800$ | 2 |
| 209 | $CH + \gamma_{c.r.} \rightarrow C + H$ | $R_{209} = 4000$ | 3 |
| 210 | $CH^+ + \gamma_{c.r.} \rightarrow C^+ + H$ | $R_{210} = 960$ | 3 |
| 211 | $CH_2 + \gamma_{c.r.} \rightarrow CH_2^+ + e^-$ | $R_{211} = 2700$ | 1 |
| 212 | $CH_2 + \gamma_{c.r.} \rightarrow CH + H$ | $R_{212} = 2700$ | 1 |
| 213 | $C_2 + \gamma_{c.r.} \rightarrow C + C$ | $R_{213} = 1300$ | 3 |
| 214 | $OH + \gamma_{c.r.} \rightarrow O + H$ | $R_{214} = 2800$ | 3 |
| 215 | $H_2O + \gamma_{c.r.} \rightarrow OH + H$ | $R_{215} = 5300$ | 3 |
| 216 | $O_2 + \gamma_{c.r.} \rightarrow O + O$ | $R_{216} = 4100$ | 3 |
| 217 | $O_2 + \gamma_{c.r.} \rightarrow O_2^+ + e^-$ | $R_{217} = 640$ | 3 |
| 218 | $CO + \gamma_{c.r.} \rightarrow C + O$ | $R_{218} = 0.21 T^{1/2} x_{H_2} x_{CO}^{-1/2}$ | 4 |

(Glover, Federrath, Mac Low, Klessen, 2010, MNRAS, 404, 2)

# HI to H2 conversion rate

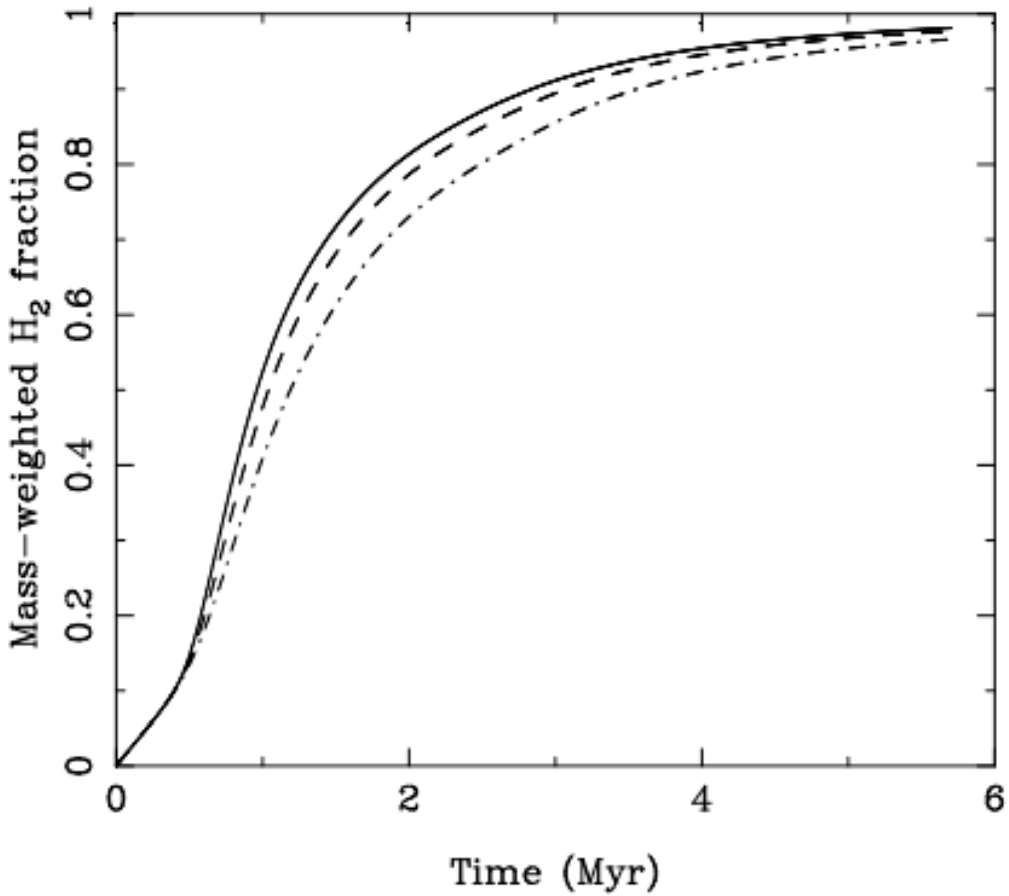


**Figure 4.** Time evolution of the mass-weighted $H_2$ abundance in simulations R1, R2 and R3, which have numerical resolutions of $64^3$ zones (dot-dashed), $128^3$ zones (dashed) and $256^3$ zones (solid), respectively.

(Glover, Federrath, Mac Low, Klessen, 2010)

# HI to H2 conversion rate

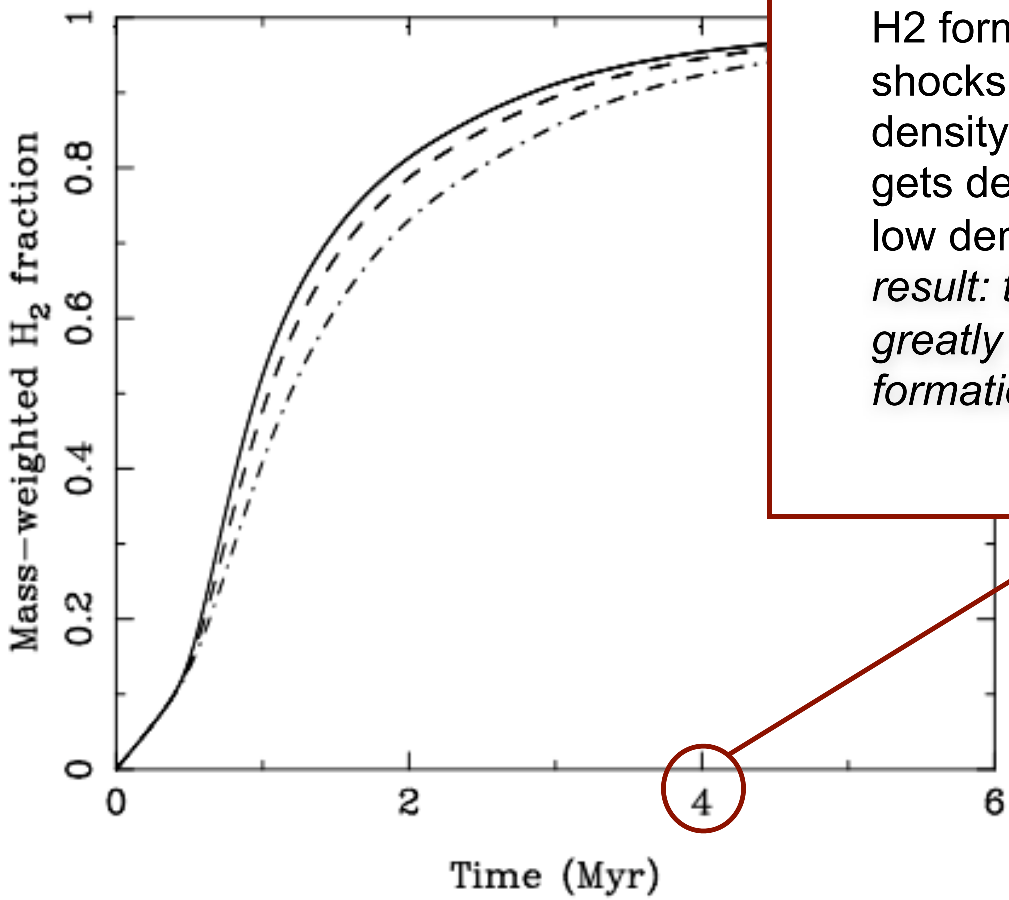


H2 forms rapidly in shocks / transient density fluctuations / H2 gets destroyed slowly in low density regions / *result: turbulence greatly enhances H2-formation rate*

**Figure 4.** Time evolution of the mass-weighted $H_2$ abundance in simulations R1, R2 and R3, which have numerical resolutions of $64^3$ zones (dot-dashed), $128^3$ zones (dashed) and $256^3$ zones (solid), respectively.

(Glover, Federrath, Mac Low, Klessen, 2010)

# HI to H2 conversion rate

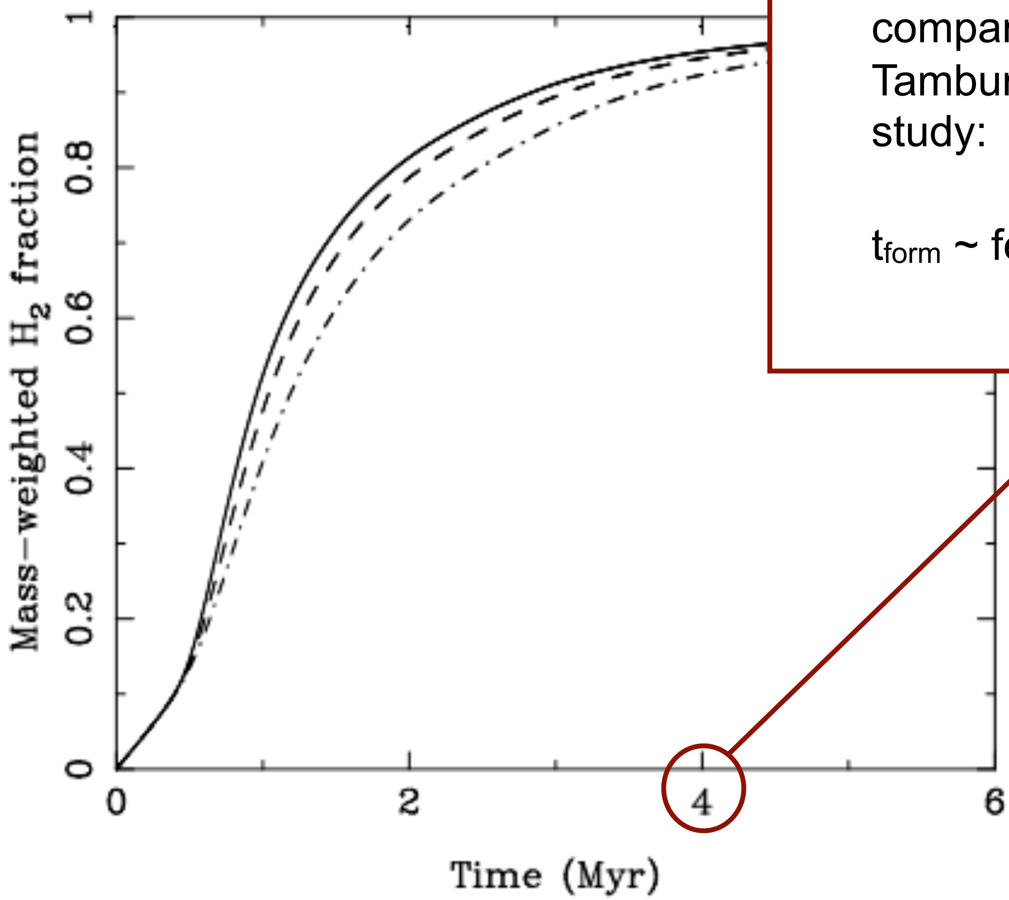


compare to data from Tamburro et al. (2008) study:

$t_{form}$ ~ few x $10^6$ years

**Figure 4.** Time evolution of the mass-weighted $H_2$ abundance in simulations R1, R2 and R3, which have numerical resolutions of $64^3$ zones (dot-dashed), $128^3$ zones (dashed) and $256^3$ zones (solid), respectively.

(Glover, Federrath, Mac Low, Klessen, 2010)

# CO, C$^+$ formation rates

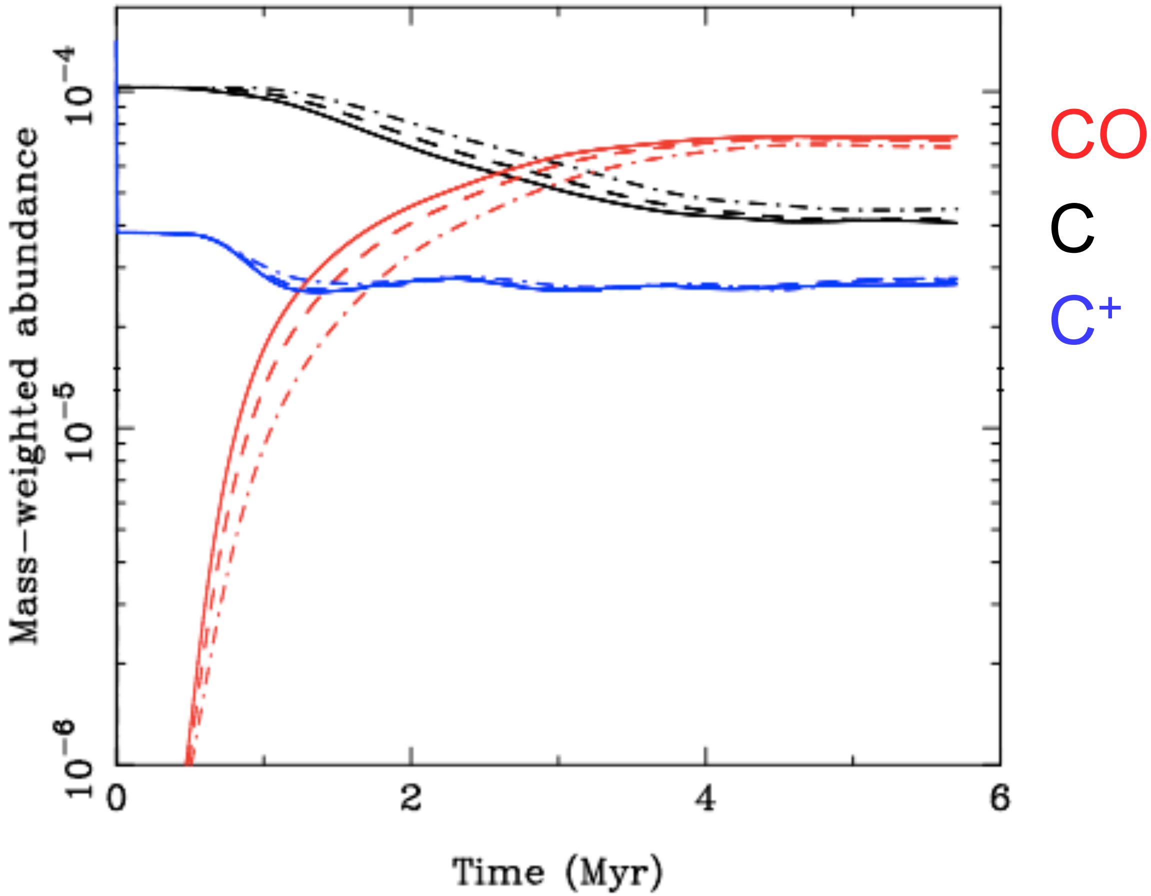


**Figure 5.** Time evolution of the mass-weighted abundances of atomic carbon (black lines), CO (red lines), and C$^+$ (blue lines) in simulations with numerical resolutions of $64^3$ zones (dot-dashed), $128^3$ zones (dashed) and $256^3$ zones (solid).

(Glover, Federrath, Mac Low, Klessen, 2010)

# effects of chemistry 1

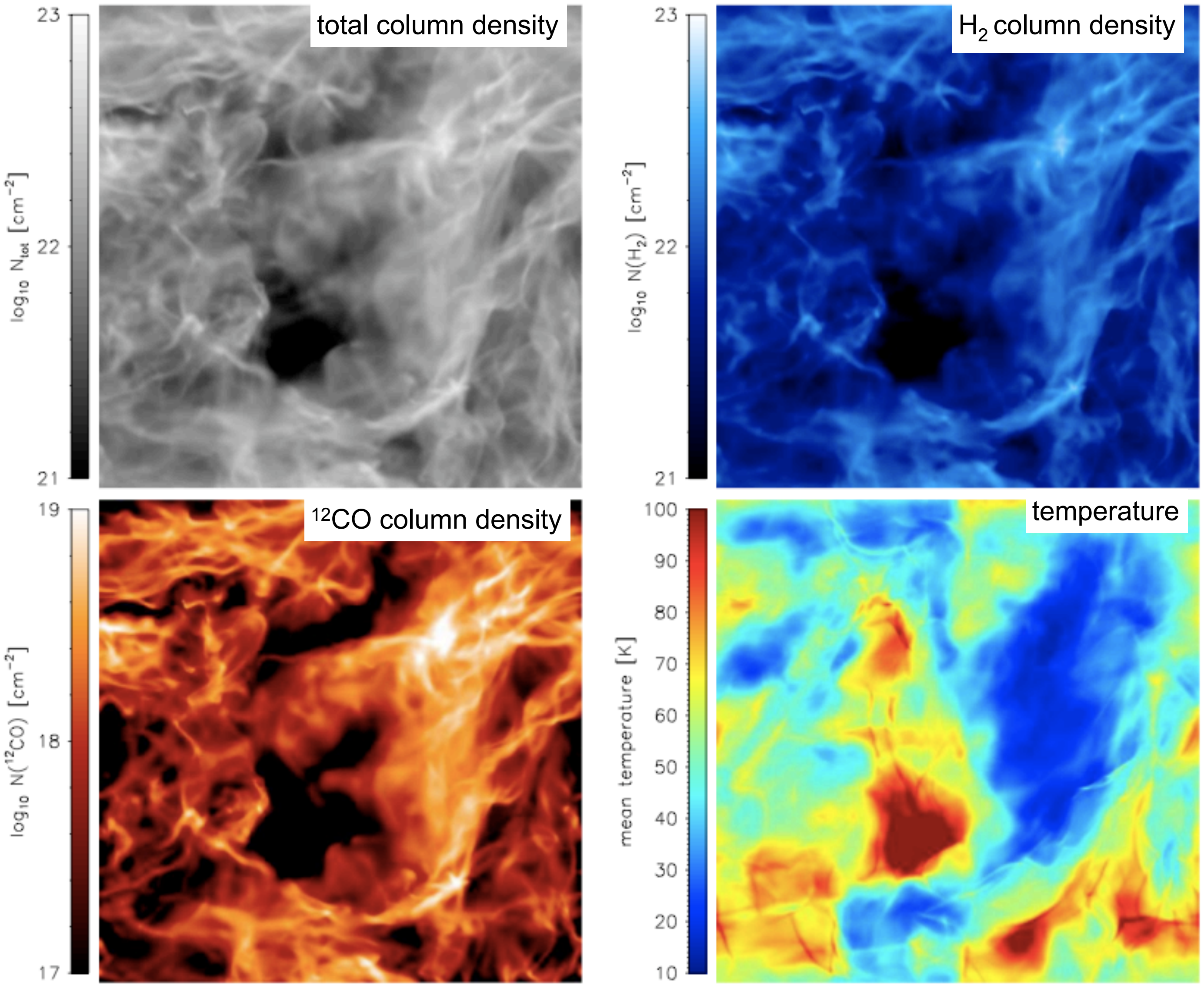


(Glover, Federrath, Mac Low, Klessen, 2010)

# effects of chemistry 2

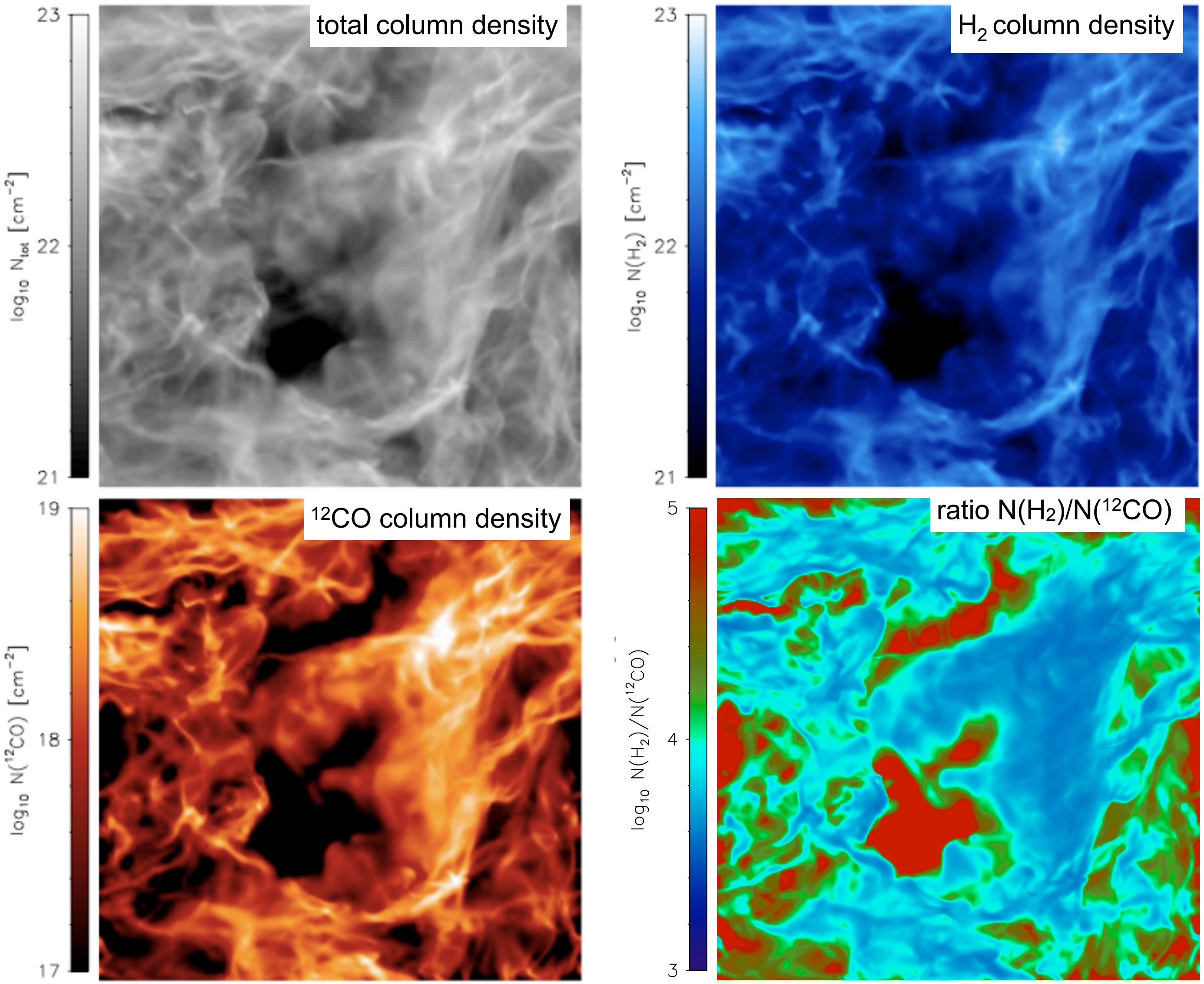


(Glover, Federrath, Mac Low, Klessen, 2010)

# effects of chemistry 4

- deliverables / predictions:
  - x-factor estimates (as function of environmental conditions)
  - synthetic line emission maps (in combination with line transfer)
  - pdf's of density, velocity, emissivity / structure functions (to directly connect to observational regime)
  - *COMMENT:* density pdf is *NOT* lognormal!
    --> implications for analytical IMF theories

# X-factor

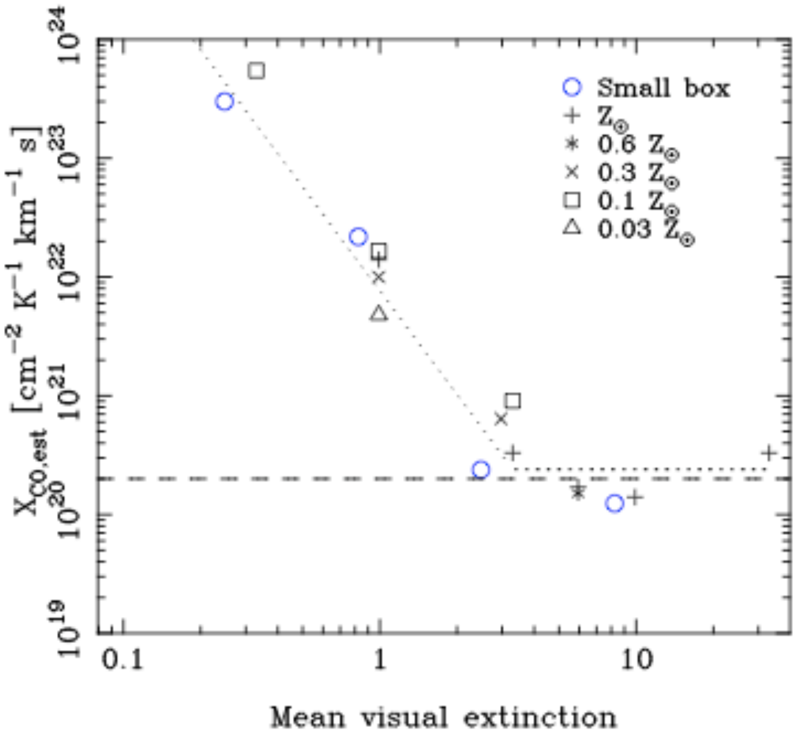


from Glover & Mac Low (2010, ApJ, submitted)

**Figure 8.** Estimate of the CO-to-$H_2$ conversion factor $X_{CO,est}$, plotted as a function of the mean visual extinction of the gas, $\langle A_V \rangle$. The simplifications made in our modelling mean that each value of $X_{CO,est}$ is uncertain by at least a factor of two. At $\langle A_V \rangle > 3$, the values we find are consistent with the value of $X_{CO} = 2 \times 10^{20} cm^{-2} K^{-1} km^{-1}$ s determined observationally for the Milky Way by Dame et al. (2001), indicated in the plot by the horizontal dashed line. At $\langle A_V \rangle < 3$, we find evidence for a strong dependence of $X_{CO,est}$ on $\langle A_V \rangle$. The empirical fit given by Equation 11 is indicated as the dotted line in the Figure, and demonstrates that at low $\langle A_V \rangle$, the CO-to-$H_2$ conversion factor increases roughly as $X_{CO,est} \propto A_V^{-2.8}$. It should also be noted that at any particular $\langle A_V \rangle$, the dependence of $X_{CO,est}$ on metallicity is relatively small. Previous claims of a strong metallicity dependence likely reflect the fact that there is a strong dependence on the mean extinction, which varies as $\langle A_V \rangle \propto Z$ given fixed mean cloud density and cloud size.

# from atomic gas to molecular clouds

- let's look at the details:
  - how does molecular cloud material form in convergent flows, e.g., as triggered by spiral density waves...
  - do sequence of idealized numerical experiments
- questions
  - are molecular clouds truly "multi-phase" media?
  - turbulence? dynamical & morphological properties?
  - what is relation to initial & environmental conditions?
  - magnetic field structure?

# convergent flows: set-up

numerical set-up

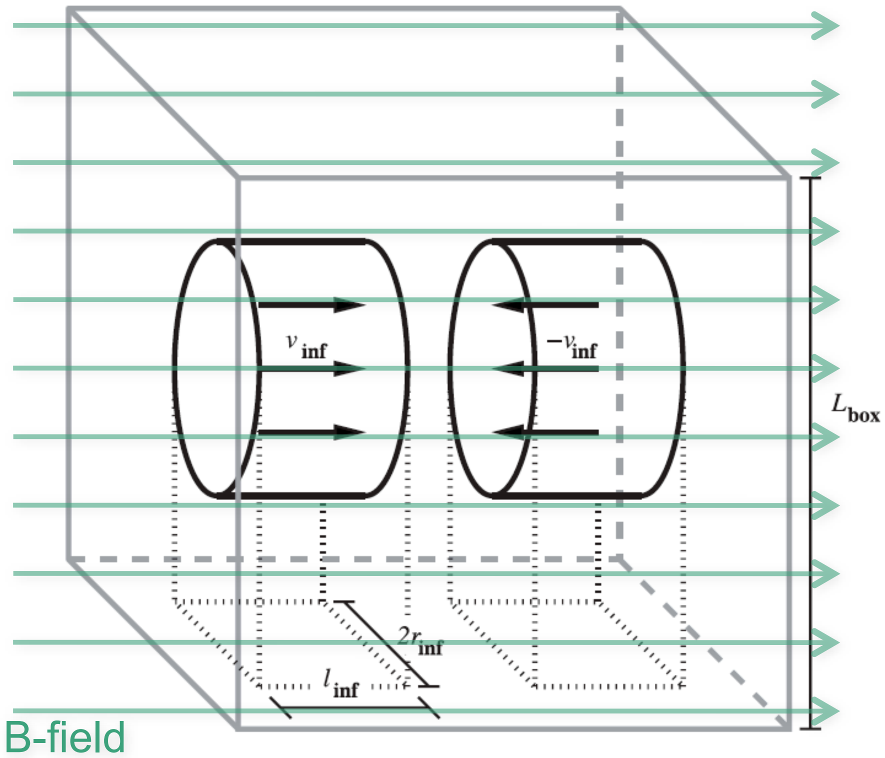


from Vazquez-Semadeni et al. (2007)

- convergent flow studies
  - atomic flows collide
  - cooling curve (soon chemistry)
  - gravity
  - magnetic fields
  - numerics: AMR, BGK, SPH

see studies by Banerjee et al., Heitsch et al., Hennebelle et al., Vazquez-Semadeni et al.

# convergent flows: set-up

adopted cooling curve

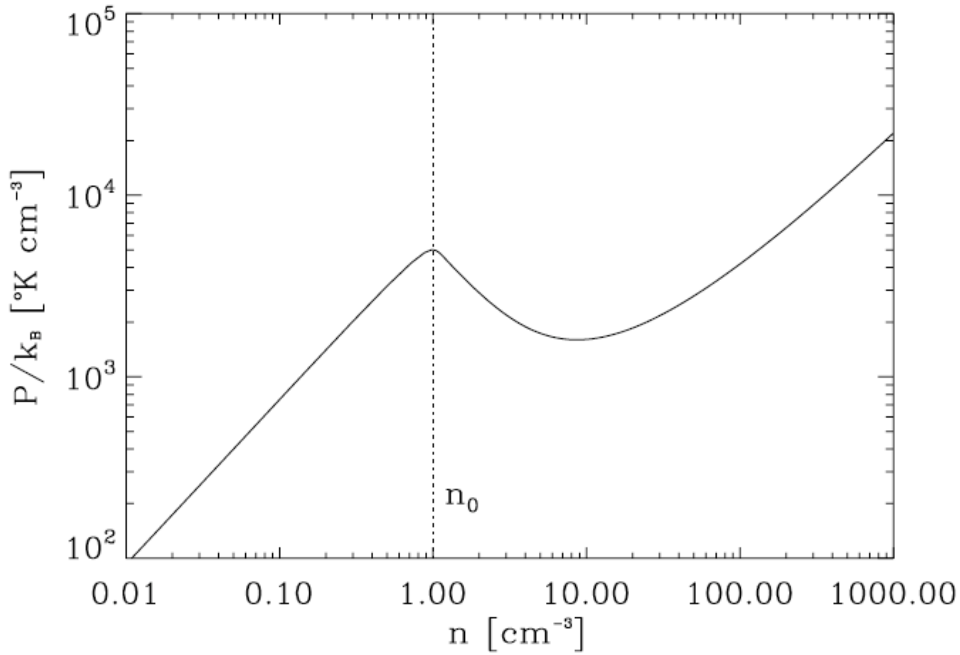


from Vazquez-Semadeni et al. (2007)

- convergent flow studies
  - atomic flows collide
  - cooling curve (soon chemistry)
  - gravity
  - magnetic fields
  - numerics: AMR, BGK, SPH

see studies by Banerjee et al., Heitsch et al., Hennebelle et al., Vazquez-Semadeni et al.

# MC formation in convergent flows

## the non-magnetic case

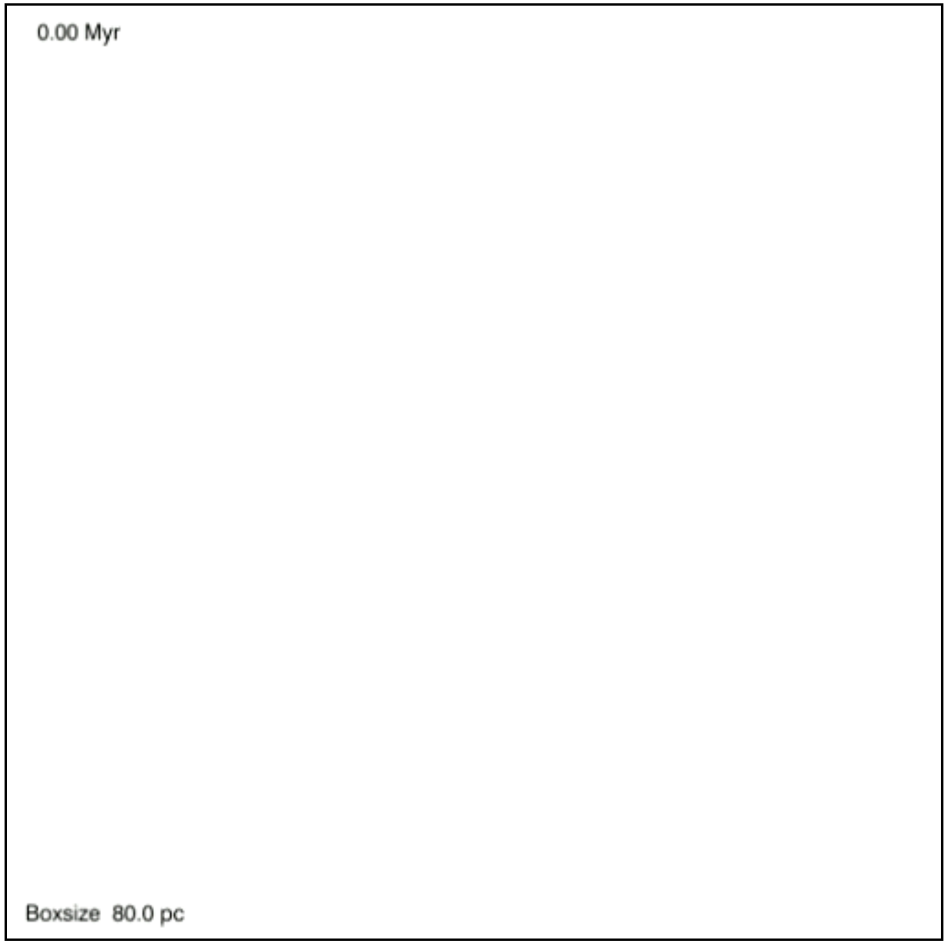


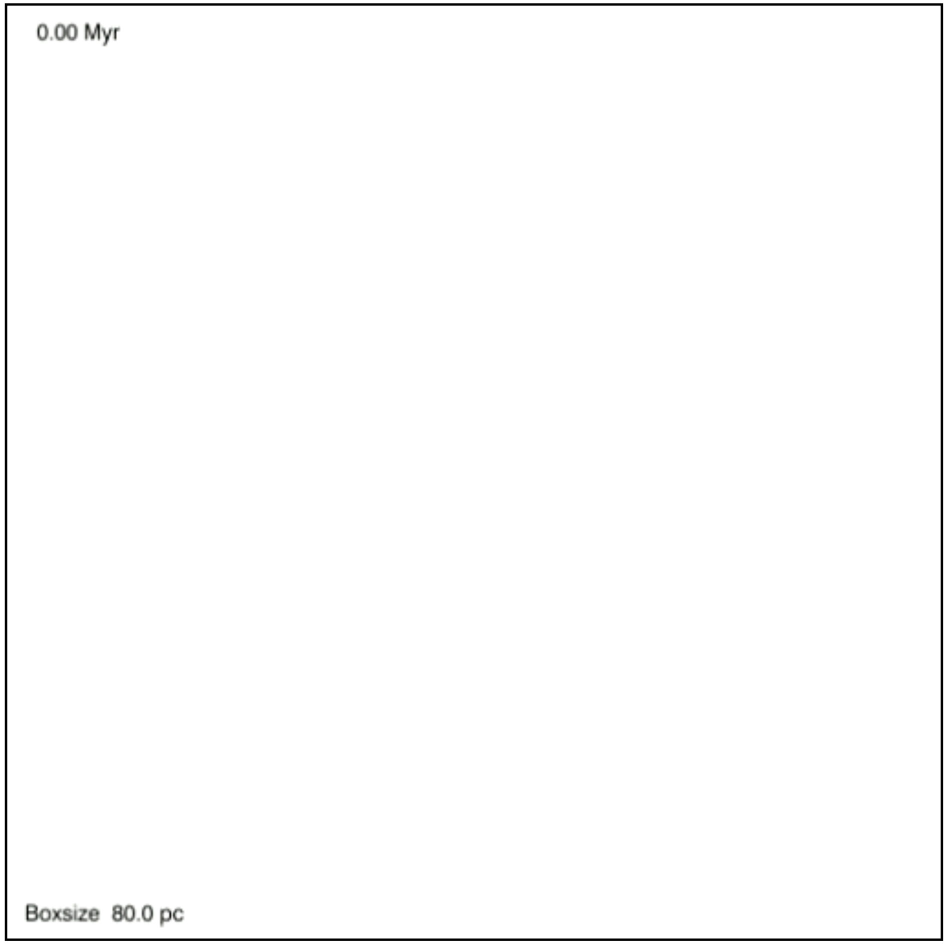


-edge-on view

-face-on view

thermal instability + gravity creates complex molecular cloud structure:

# MC formation in convergent flows

**this simple set-up reproduces (and explains!) some of the main properties of MCs:**

- highly patchy and clumpy
- high fraction of substructure
- cold dense molecular clumps coexist with warm atomic gas
- not a well bounded entity
- dynamical evolution (different star formation modes: from low mass to high mass SF?)

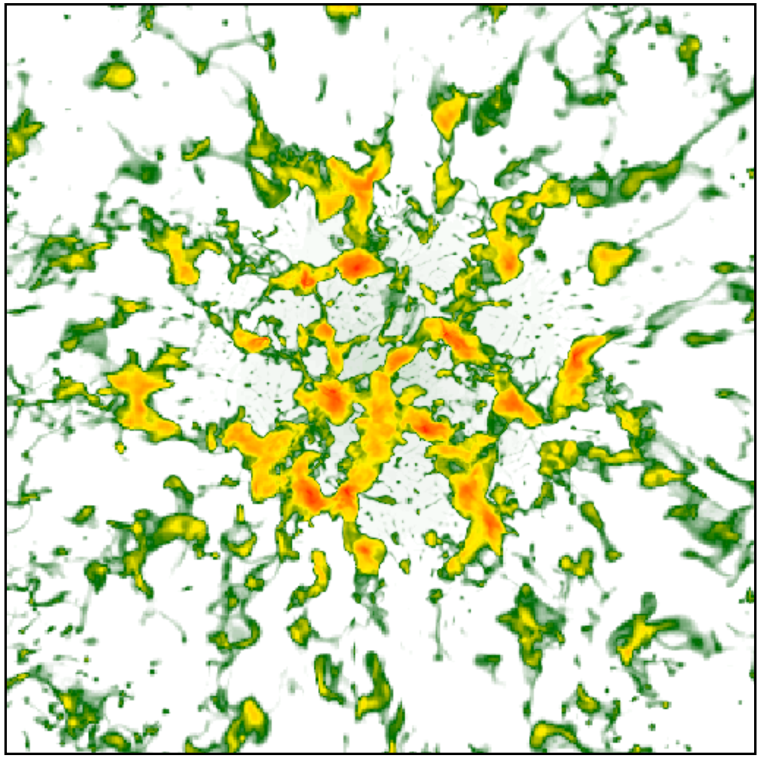

from Banerjee et al. (2008)
(see also studies by Hennebelle et al. and Vazquez-Semadeni et al. and Heitsch et al.)

# MC formation in convergent flows

the weakly magnetized ($B_x = 1\mu G$) case

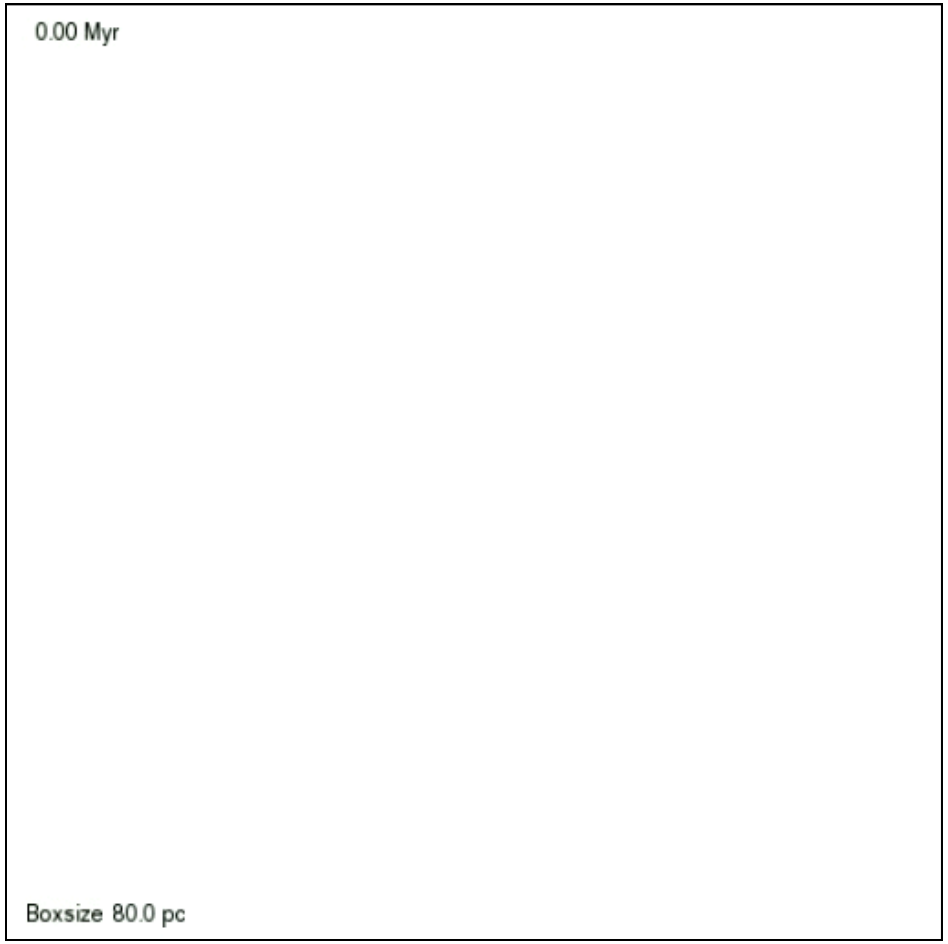


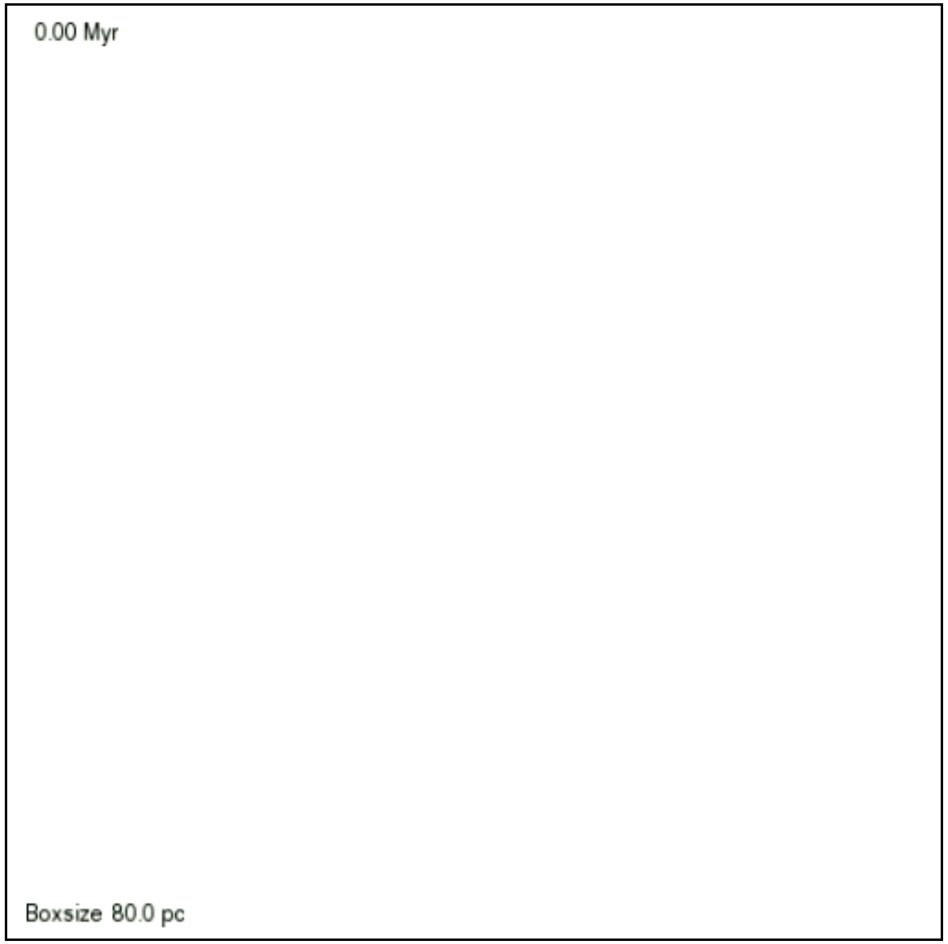


edge-on view

face-on view

from Banerjee et al. (2008)
(see also studies by Hennebelle et al. and Vazquez-Semadeni et al. and Heitsch et al.)

# MC formation in convergent flows

with random component: $B_x = 3\mu G + \delta b = 3\mu G$


Banerjee et al. in prep.

face-on view

# MC formation in convergent flows

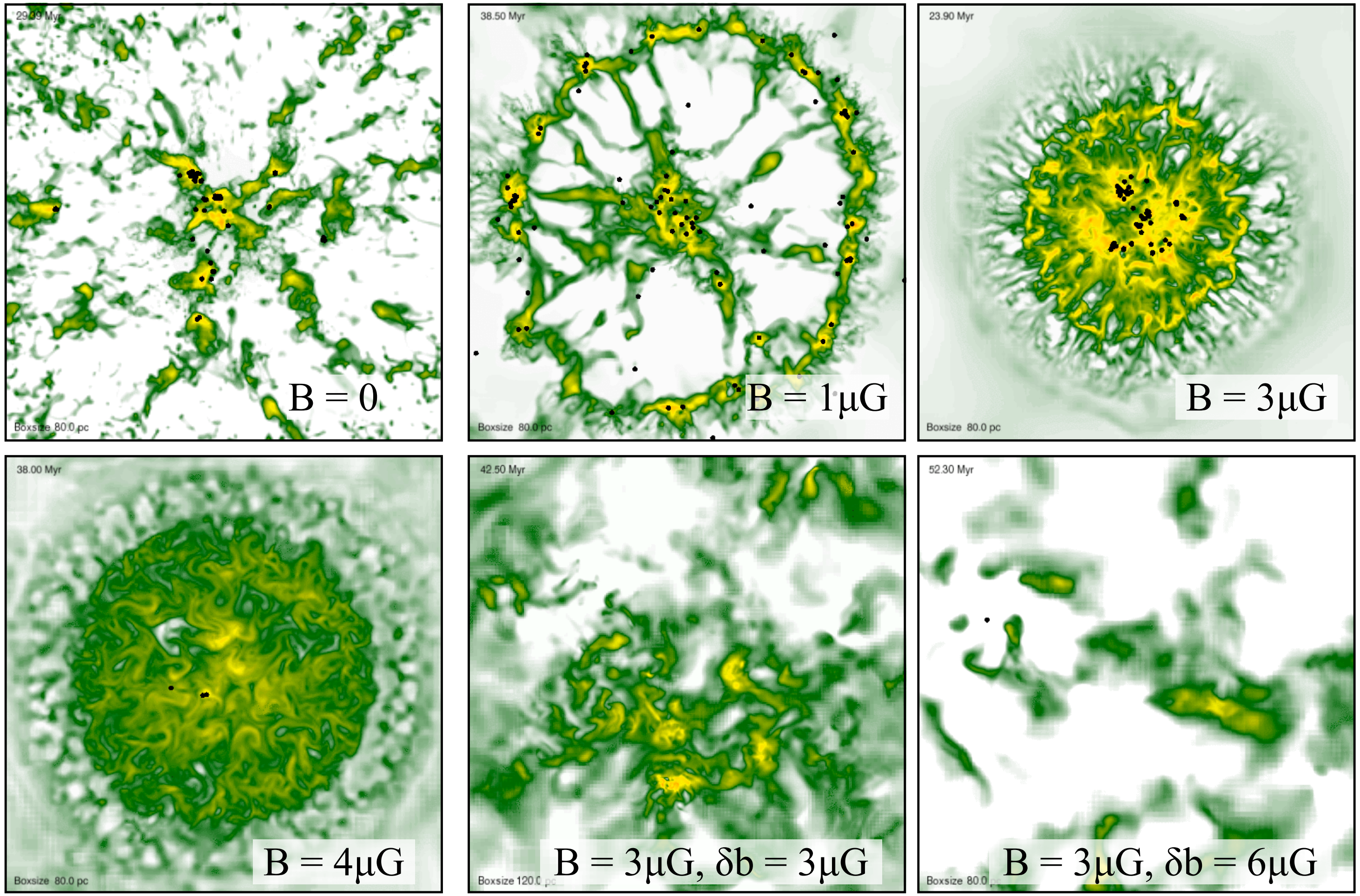


Morphology of the molecular cloud and star formation efficiency depends on the strength of the magnetic field

Banerjee et al. in prep.

# MC formation in convergent flows

Influence of Ambipolar Diffusion: $B_x = 3\mu G$ (super-critical)

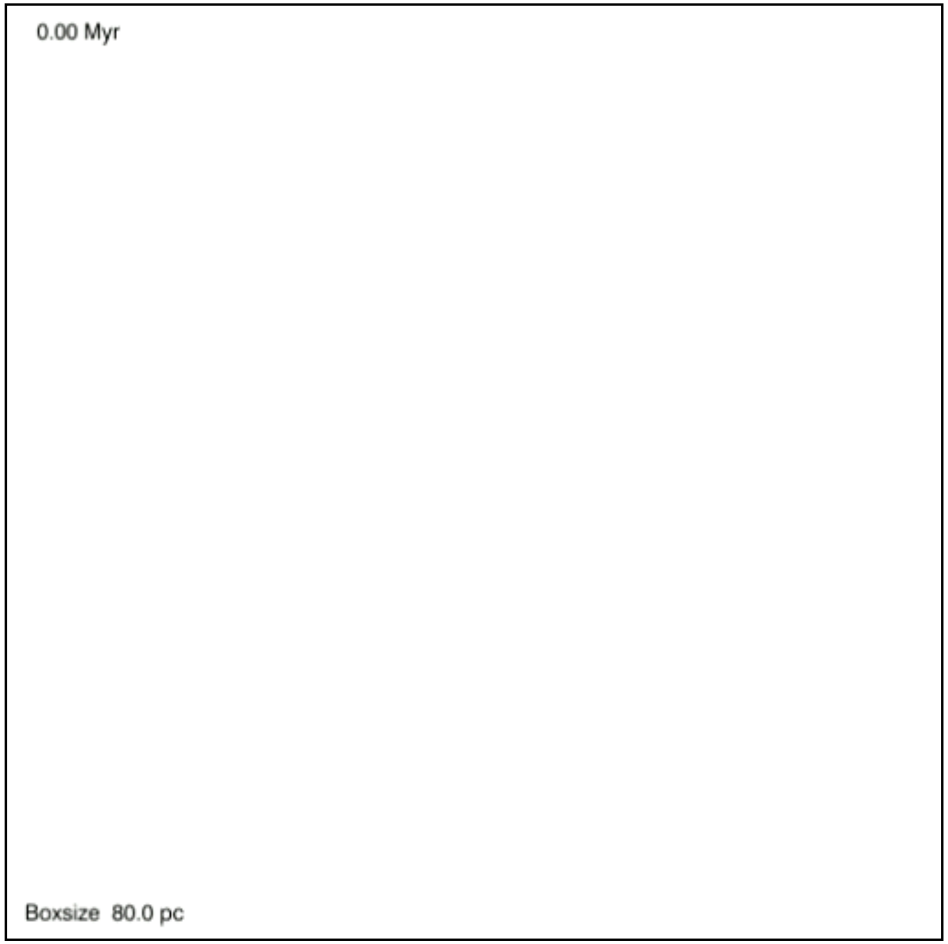


Ideal MHD

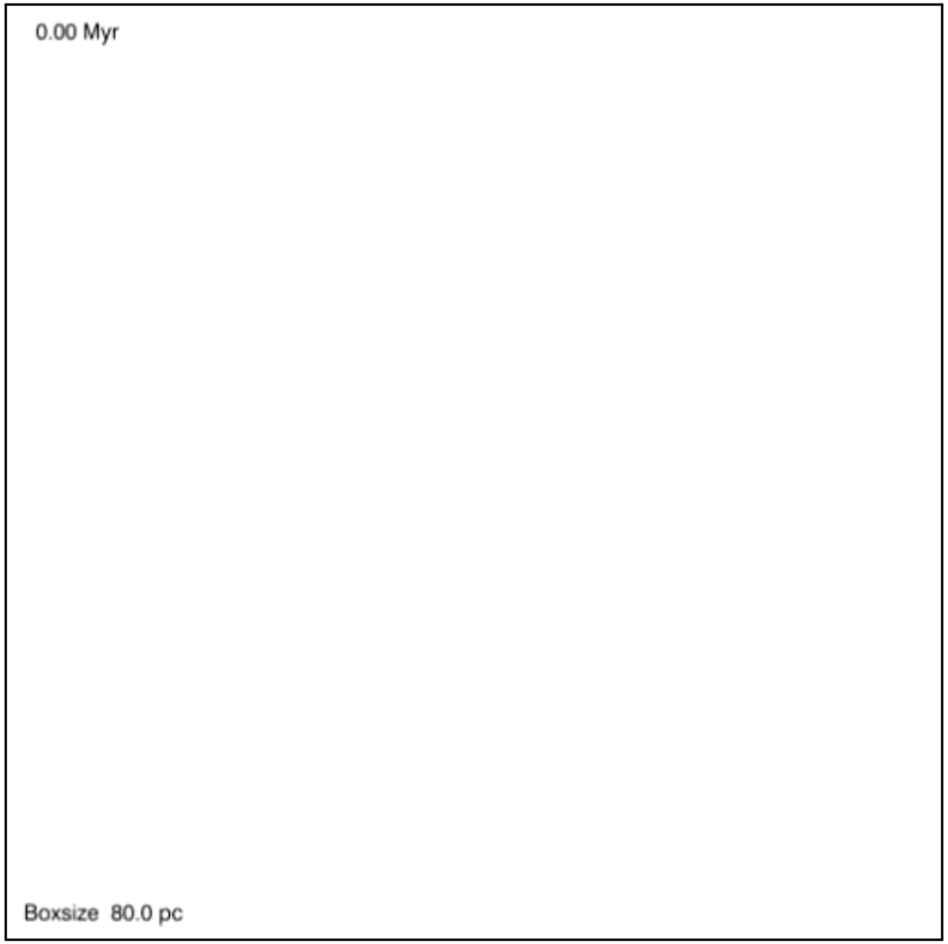


with AD

# MC formation in convergent flows

Influence of Ambipolar Diffusion: $B_x = 4\mu G$ (critical)

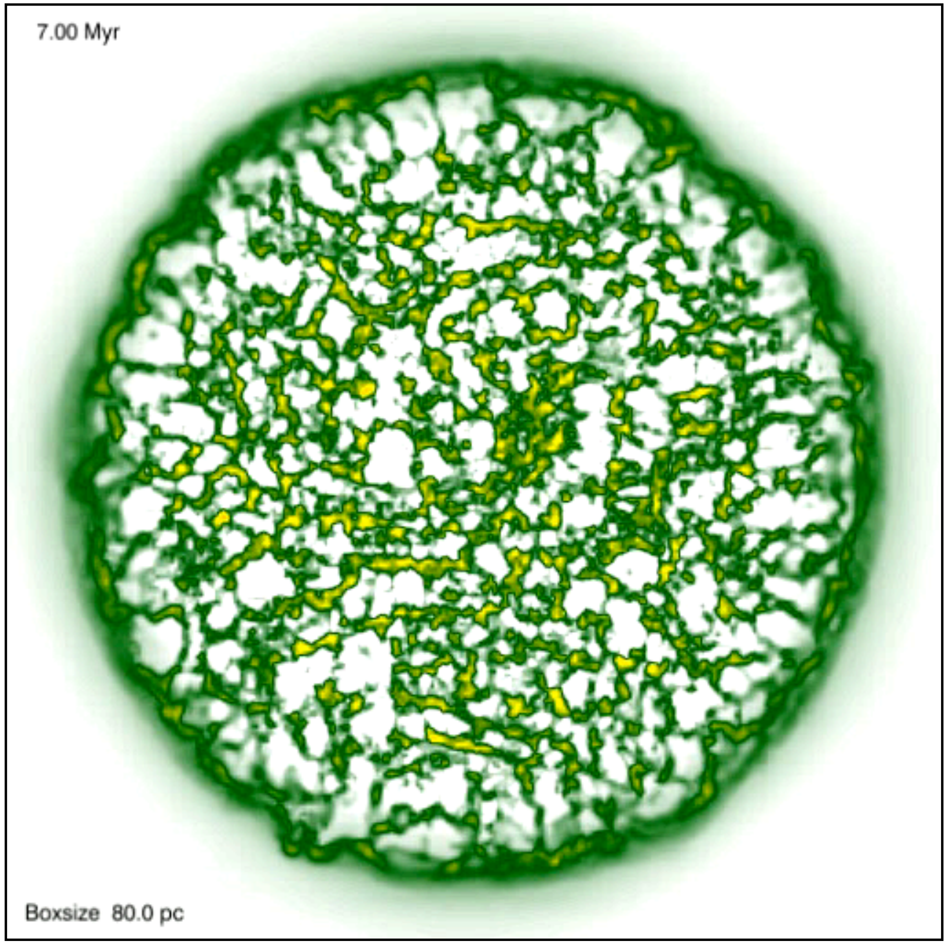


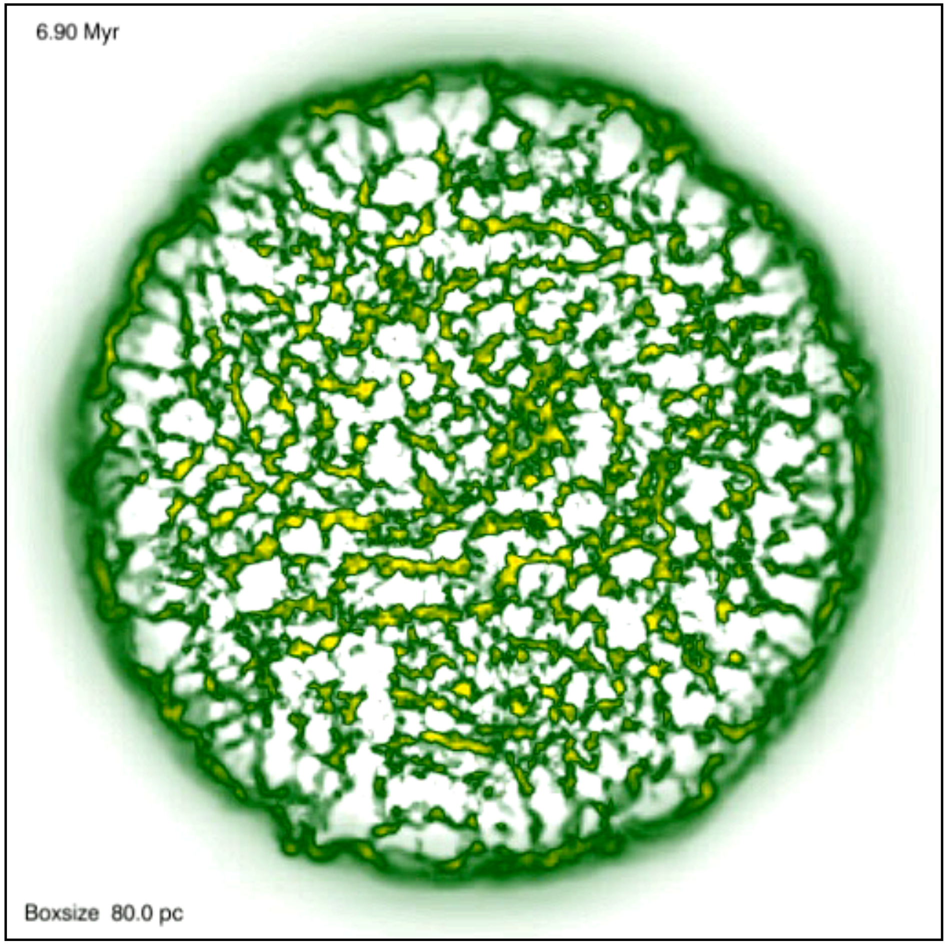


Ideal MHD

with AD

Banerjee et al. in prep.

# MC formation in convergent flows

## Influence of Ambipolar Diffusion

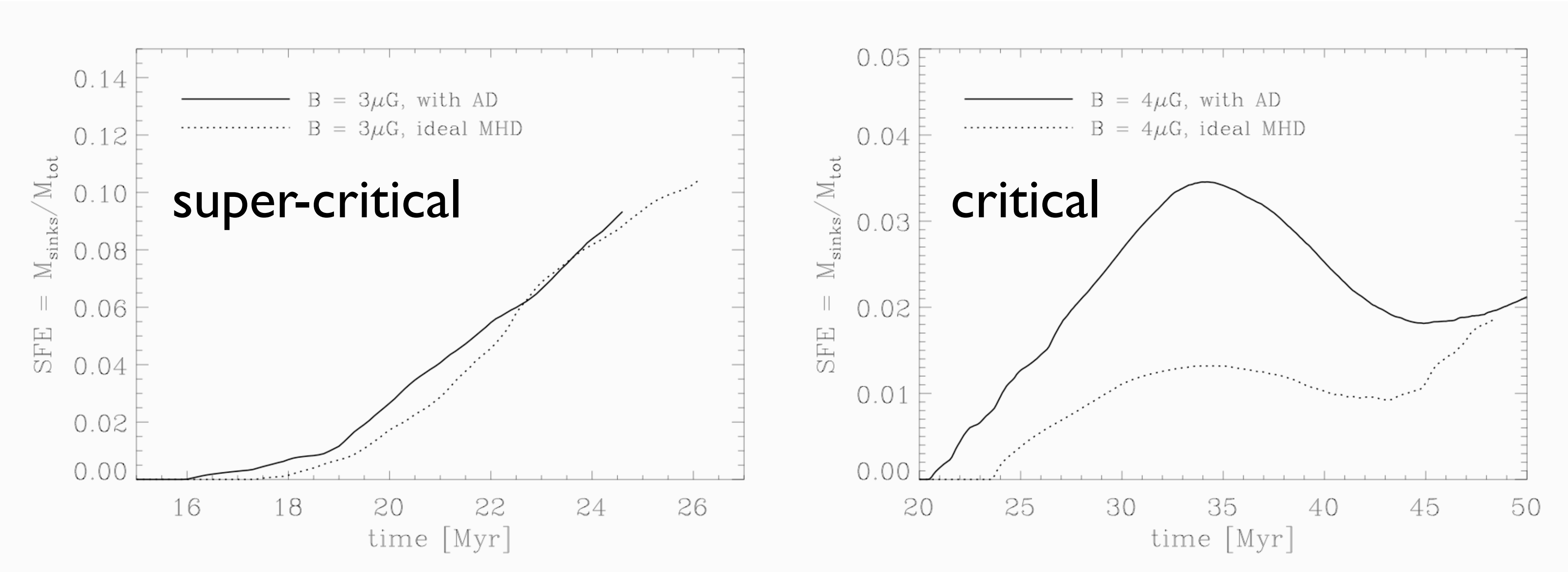


- Ambipolar diffusion is **not** a major player for star formation on molecular cloud scales
- this is different during protostellar collapse (Hennebelle et al.)

Banerjee et al. in prep.

# MC formation in convergent flows

**morphology and clump evolution**

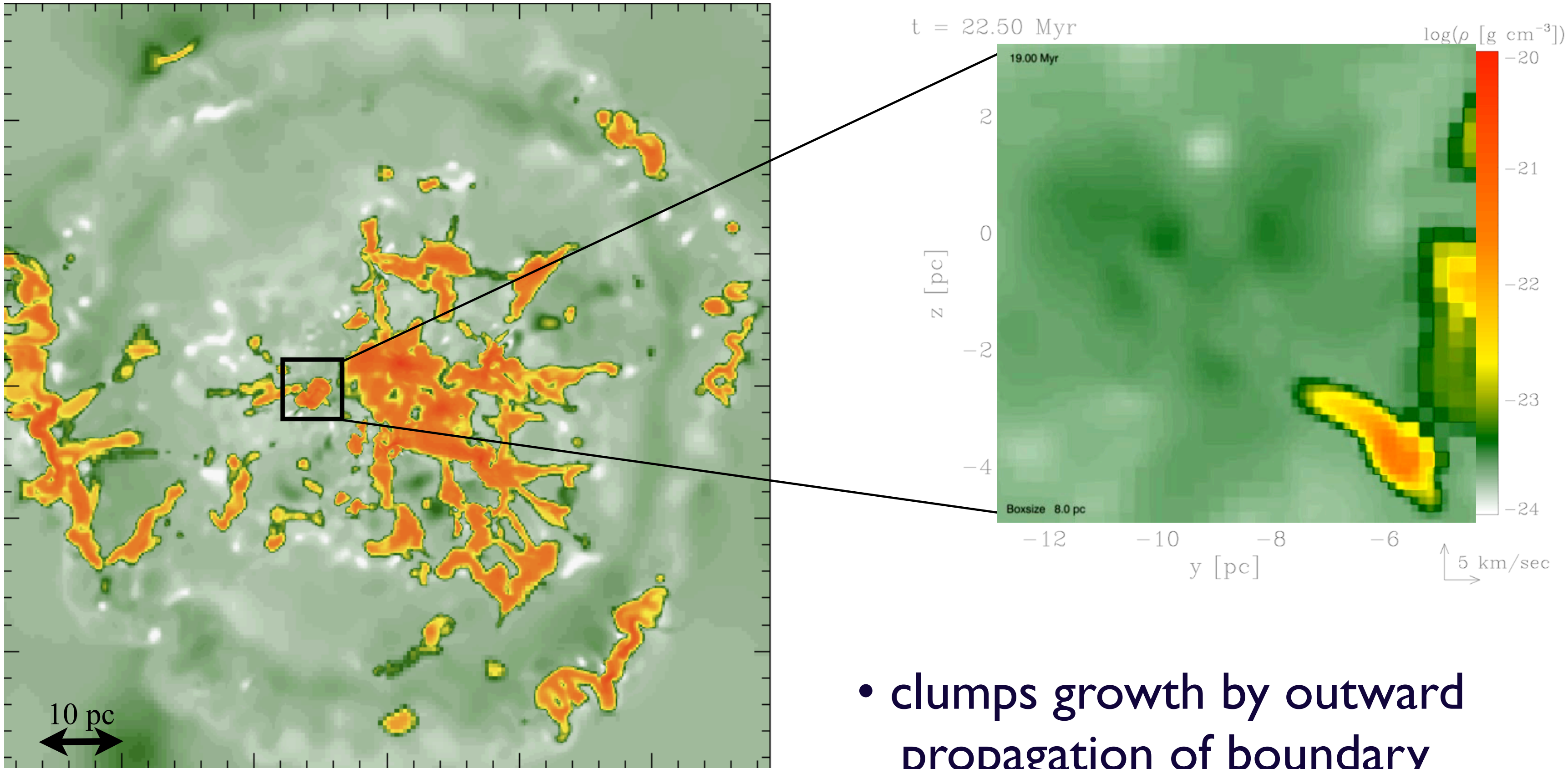


- MCs are inhomogeneous
- cold clumps embedded in warm atomic gas

- clumps growth by outward propagation of boundary layers and
- coalescence at later times

see studies by Banerjee et al., Heitsch et al., Hennebelle et al., Vazquez-Semadeni et al.

# some results: growth of cores

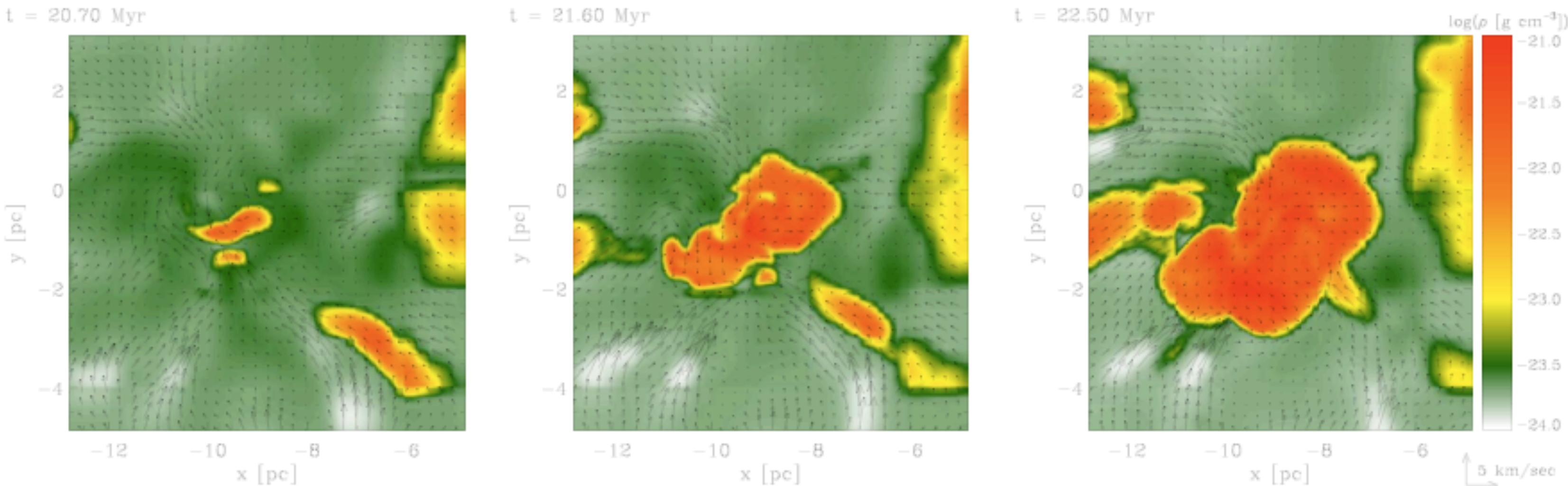


**Figure 2.** Shows the time evolution of a typical clump which initially develops out of the thermally unstable WNM in shock layers of turbulent flows. A small cold condensate grows by outward propagation of its boundary layer. Coalescence and merging with nearby clumps further increases the size and mass of these clumps. The global gravitational potential of the proto-cloud enhances the merging probability with time. The images show 2D slices of the density (logarithmic colour scale) and the gas velocity (indicated as arrows) in the plane perpendicular to the large scale flows.

*two phases of core growth:*
(1) by *outward propagation* of *boundary layer* → Jeans sub-critical phase
(2) *core mergers* → super-Jeans → gravitational collapse & star formation
example: *Pipe nebula* ???

from Banerjee et al. (2008)

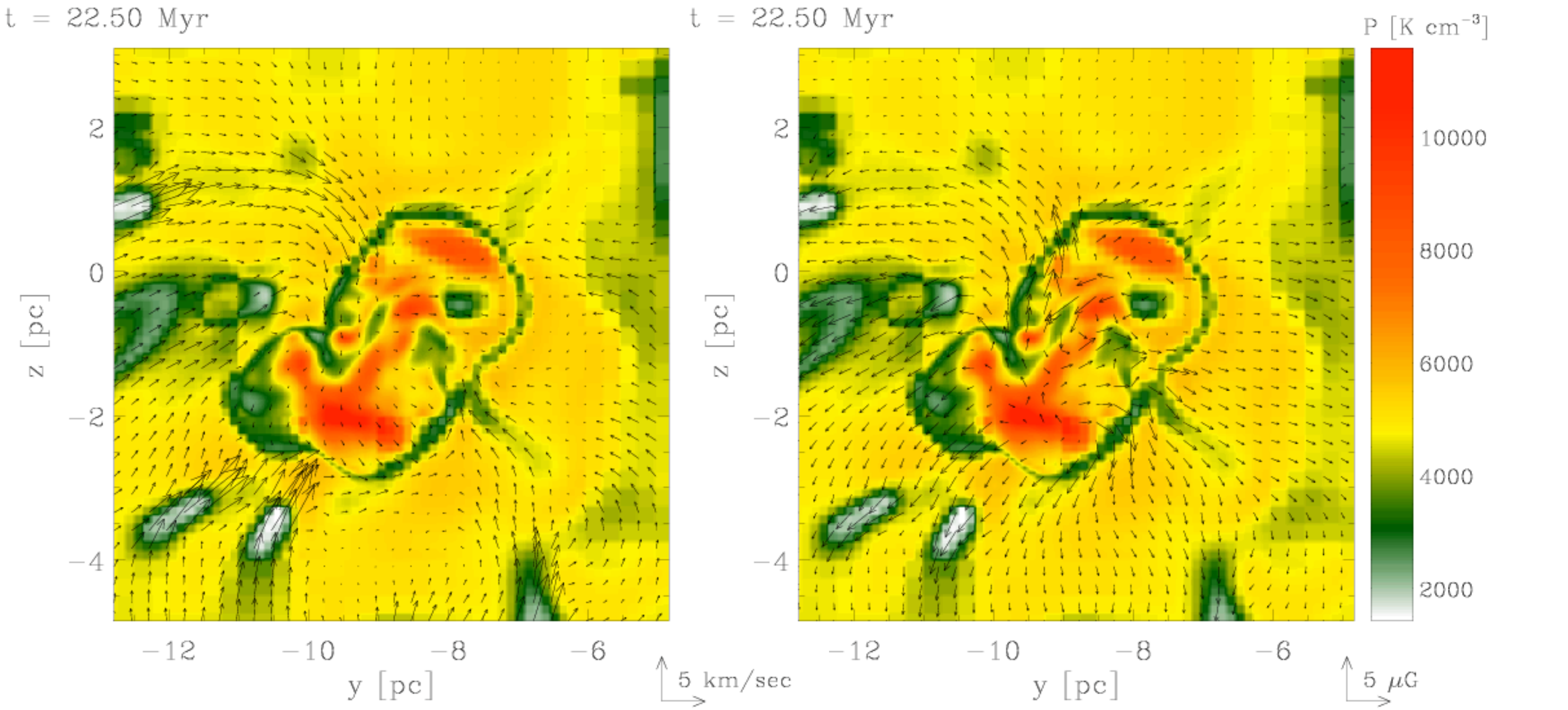


• cores roughly in pressure balance with surroudings
• relation between flow and magnetic field:
  mass flow mostly along field lines

from Banerjee et al. (2008)

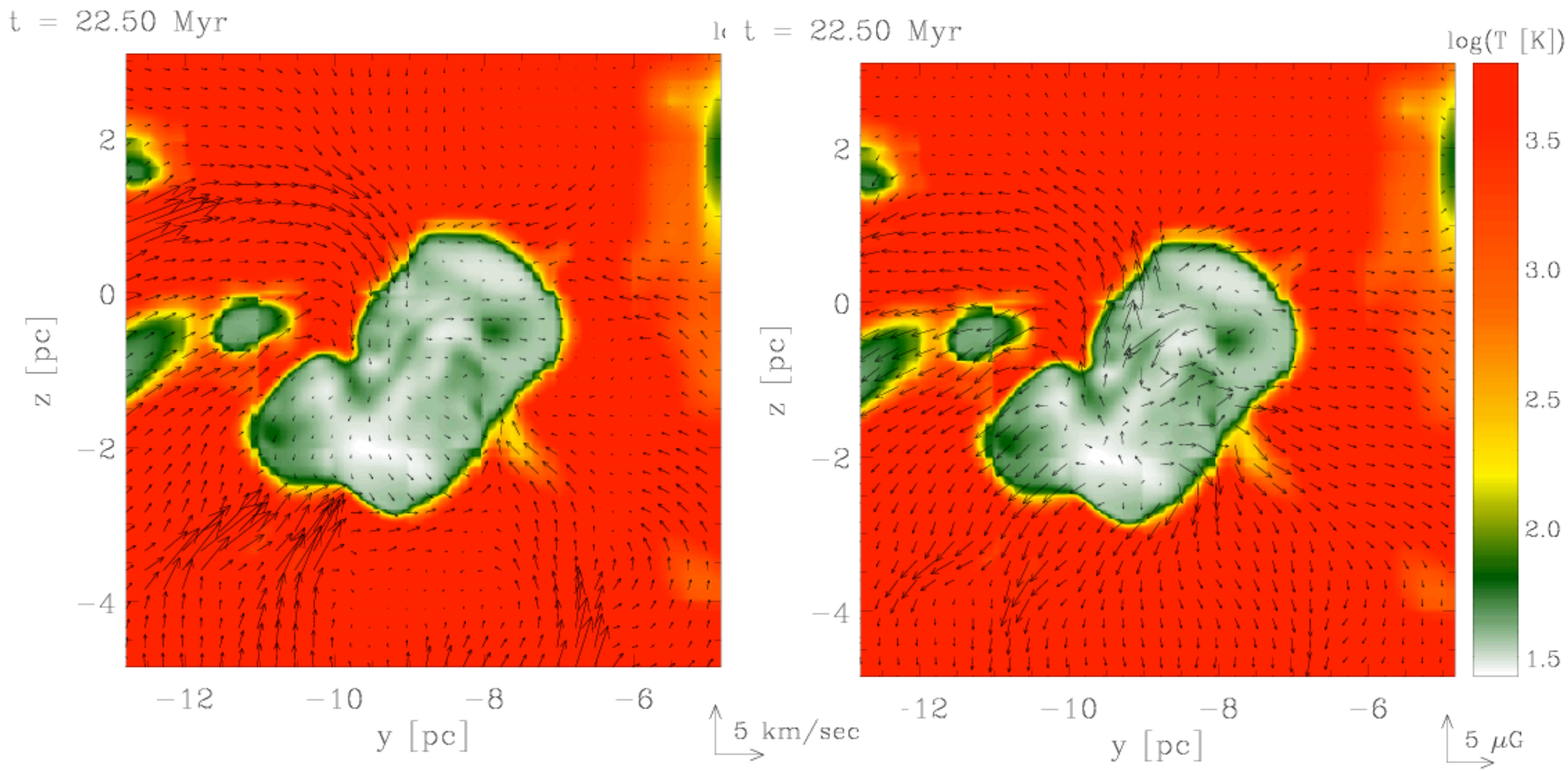


- typical core densities $n \sim 2 – 5 \times 10^3$ $cm^{-3}$
- typical core temperatures $T \sim 30 – 50$ $K$

from Banerjee et al. (2008)

# some results: statistical correlations

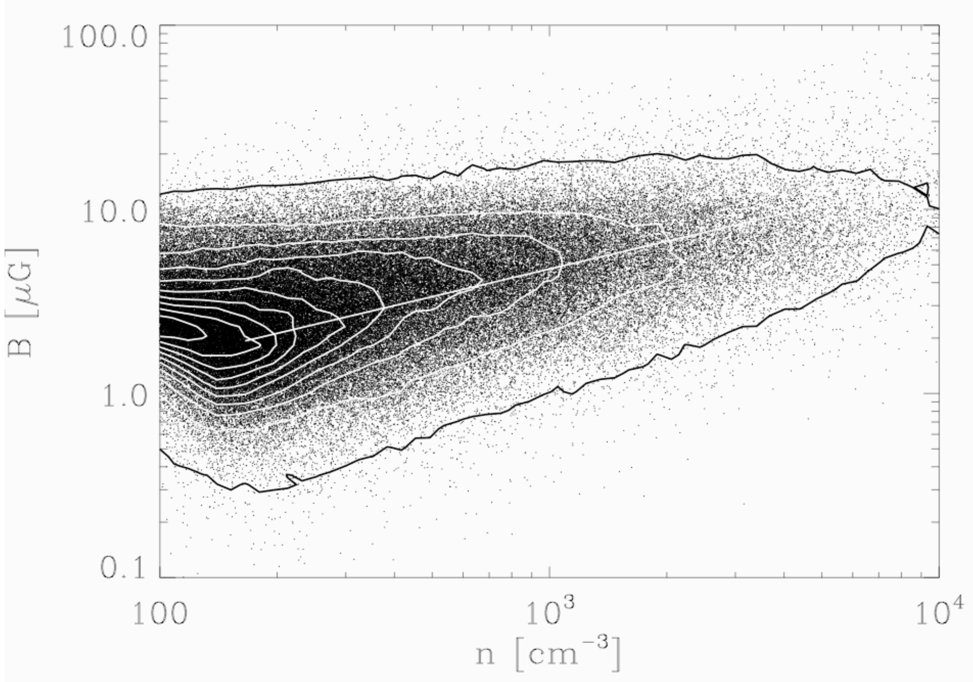


• strong correlation of gas streams and magnetic field lines

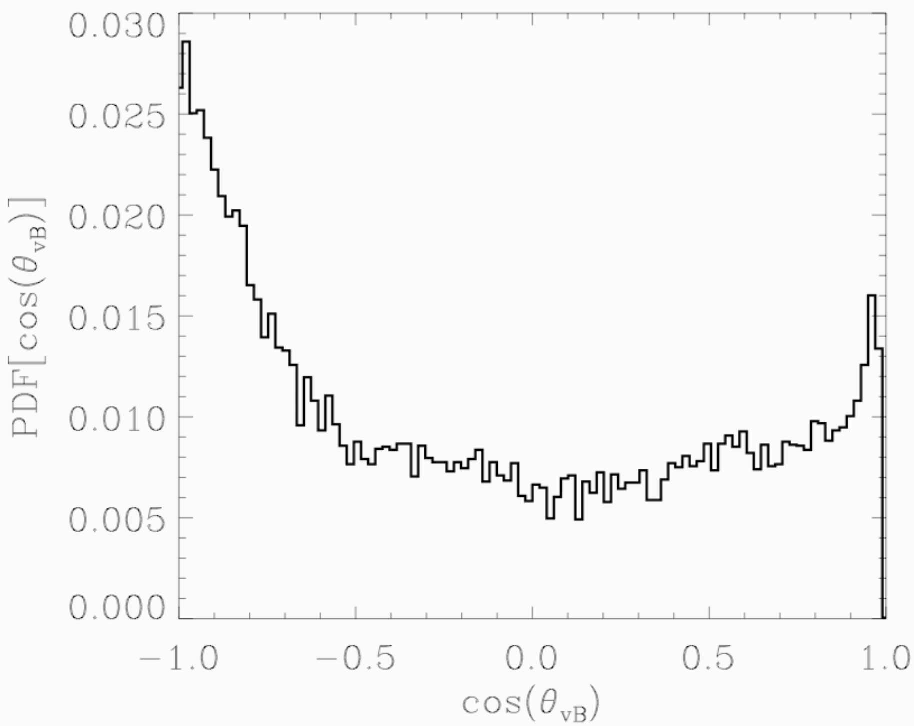


• large scatter of magnetic field strengths: sub- and super-critical cores exist

• median slope: $B \propto n^{0.5}$ (e.g. *Crutcher 1999*)

# some results: loci of high-mass stars

global contraction phase

center of the cloud
→ birthplace for
**massive stars**?
(eg. Zinnecker & Yorke 2007)

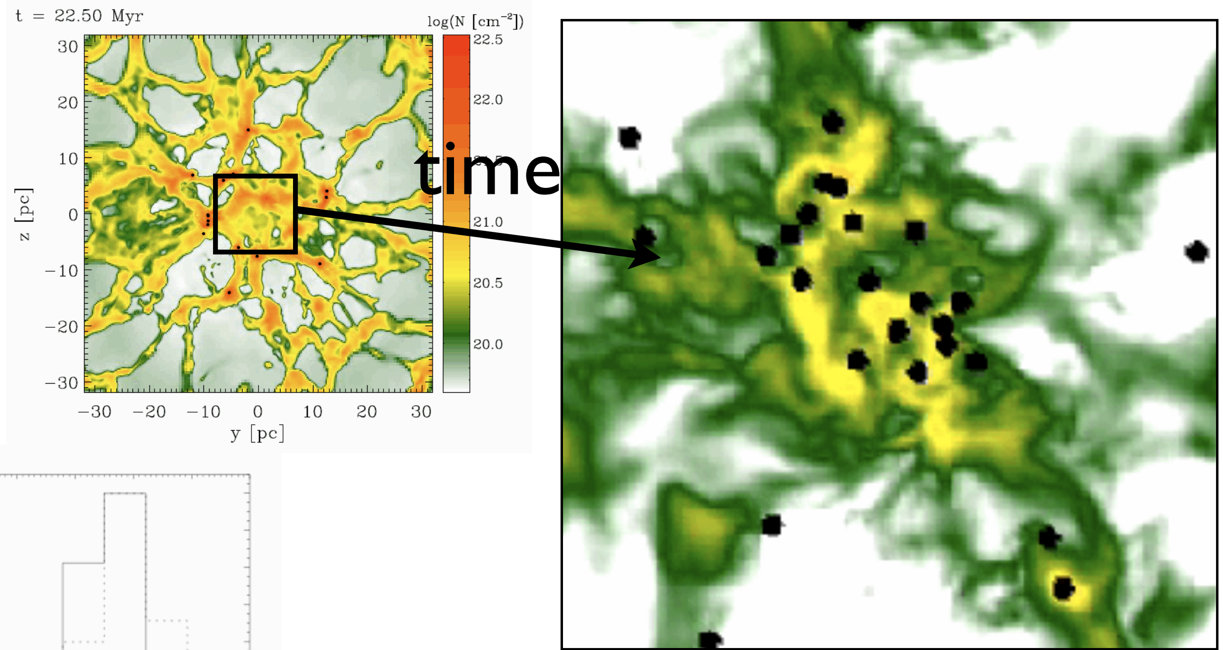


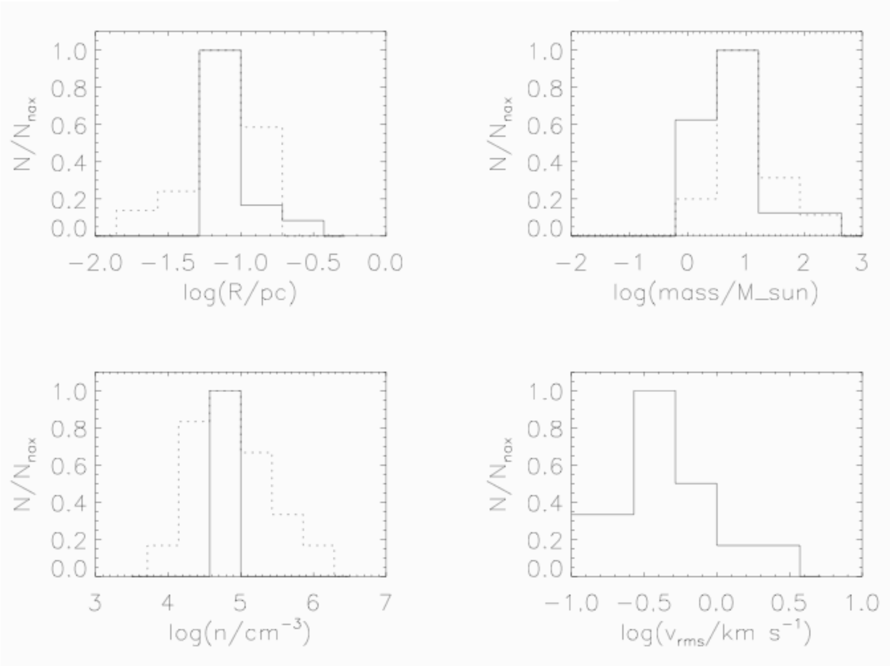


comparison of core properties with observation of Cygnus X by *Motte et al 2007*

*Vazquez-Semadeni et al. 2008*

# initial mass function

# initial mass function

- what is the relation between molecular cloud fragmentation and the distribution of stars?
- important quantity: *IMF*
- equally important CAVEAT:
  *"everyone" gets the right IMF*
  → better look for secondary indicators
  - *stellar multiplicity*
  - protostellar *spin* (including disk)
  - *spatial distribution* + *kinematics* in young clusters
  - *magnetic field strength* and *orientation*

# IMF

- distribution of stellar masses depends on
  - turbulent initial conditions
    --> mass spectrum of prestellar cloud cores
  - collapse and interaction of prestellar cores
    --> competitive accretion and *N*-body effects
  - thermodynamic properties of gas
    --> balance between heating and cooling
    --> EOS (determines which cores go into collapse)
  - (proto) stellar feedback terminates star formation
    ionizing radiation, bipolar outflows, winds, SN

(e.g. Larson 2003, Prog. Rep. Phys.; Mac Low & Klessen, 2004, Rev. Mod. Phys, 76, 125 - 194)

# IMF

- distribution of stellar masses depends on
  - turbulent initial conditions
    --> mass spectrum of prestellar cloud cores
  - collapse and interaction of prestellar cores
    --> competitive accretion and *N*-body effects
  - thermodynamic properties of gas
    --> balance between heating and cooling
    --> EOS (determines which cores go into collapse)
  - (proto) stellar feedback terminates star formation
    ionizing radiation, bipolar outflows, winds, SN

(e.g. Larson 2003, Prog. Rep. Phys.; Mac Low & Klessen, 2004, Rev. Mod. Phys, 76, 125 - 194)

# example: model of Orion cloud

„model“ of Orion cloud: 15.000.000 SPH particles, $10^4$ $M_{sun}$ in 10 pc, mass resolution 0,02 $M_{sun}$, forms ~2.500 „stars“ (sink particles)

isothermal EOS, top bound, bottom unbound

has clustered as well as distributed „star“ formation

efficiency varies from 1% to 20%

develops full IMF
(distribution of sink particle masses)

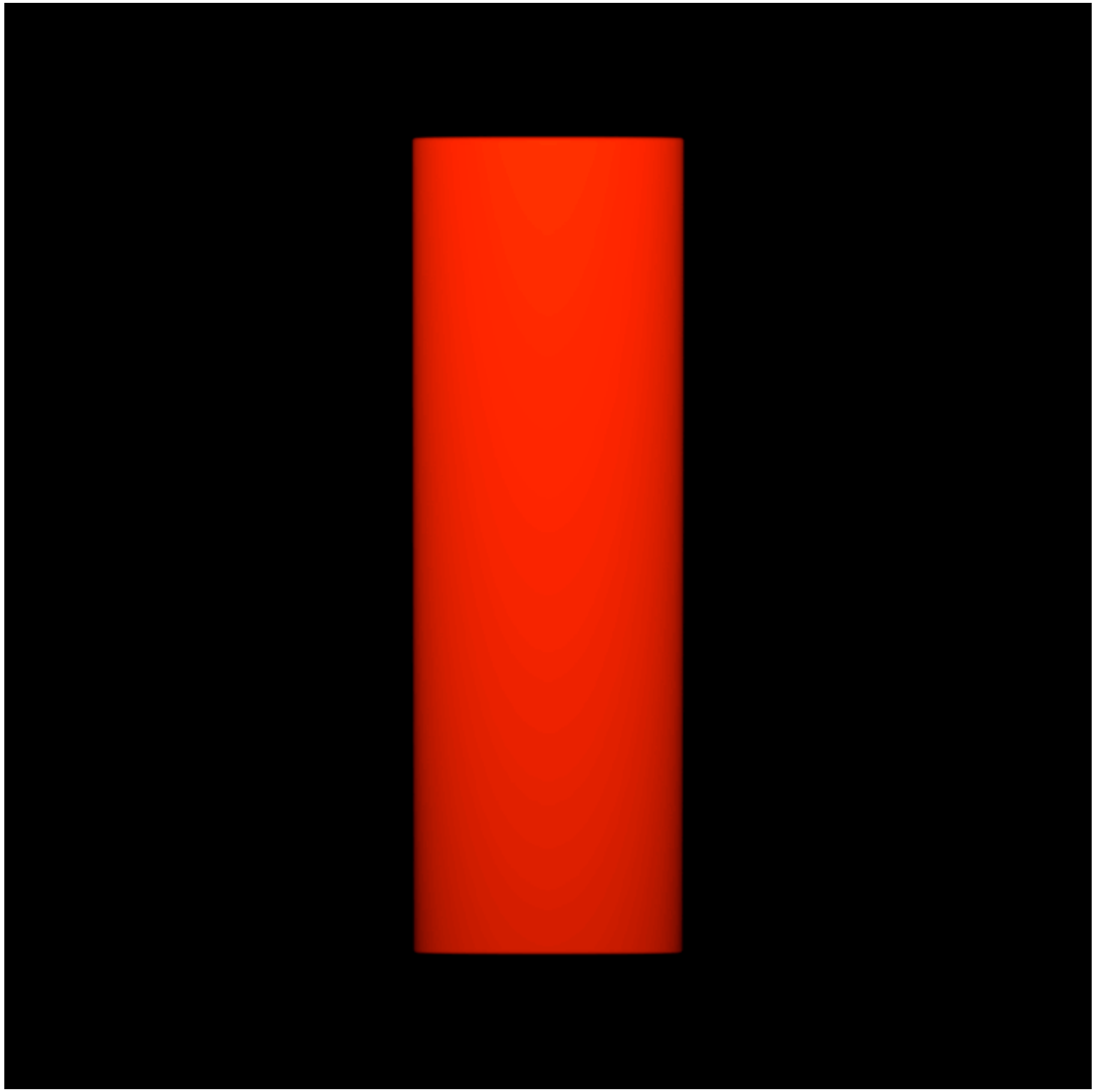

(Bonnell & Clark 2008)

# example: model of Orion cloud

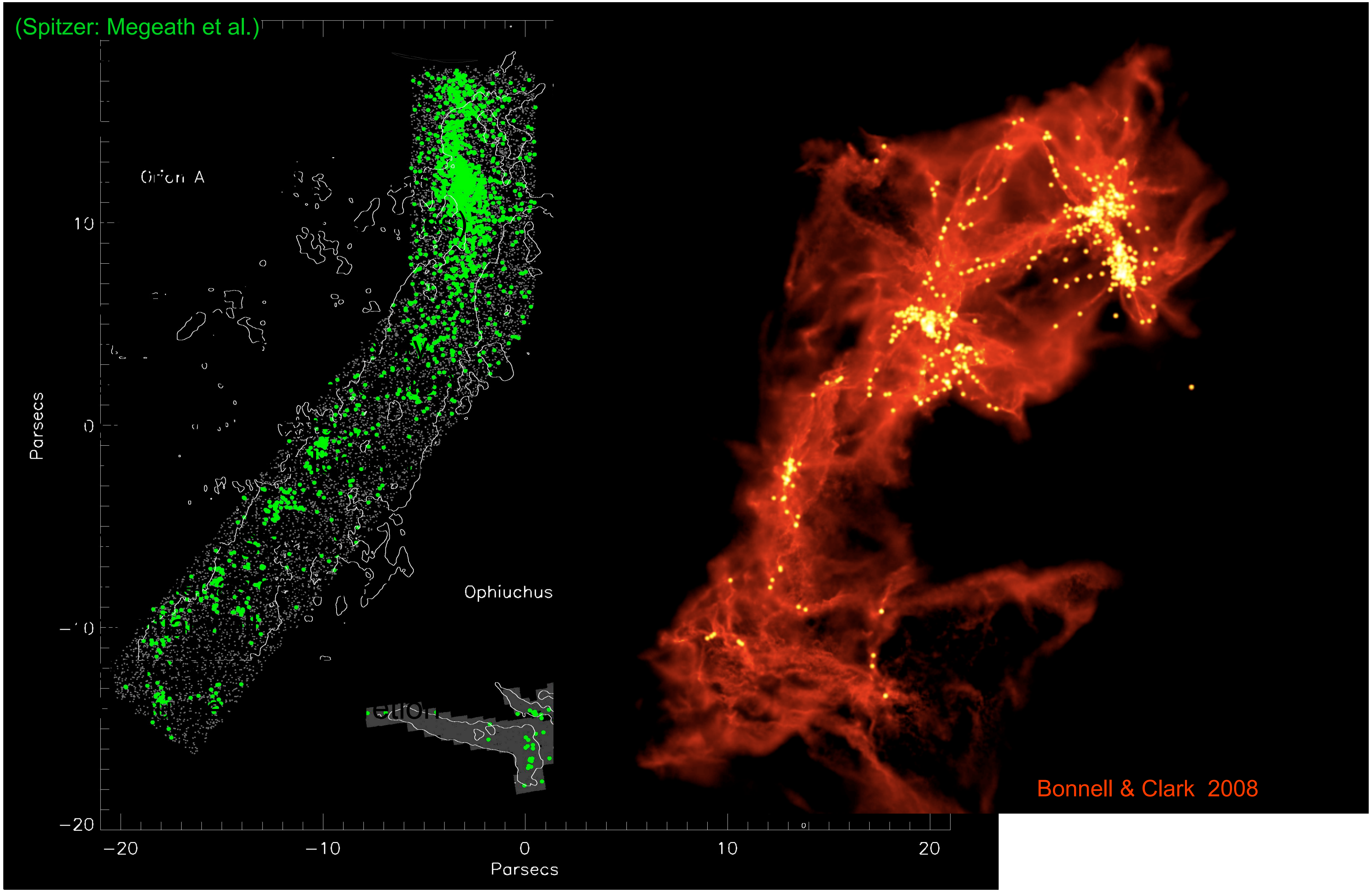

# dynamics of nascent star cluster

in dense clusters protostellar interaction may be come important!

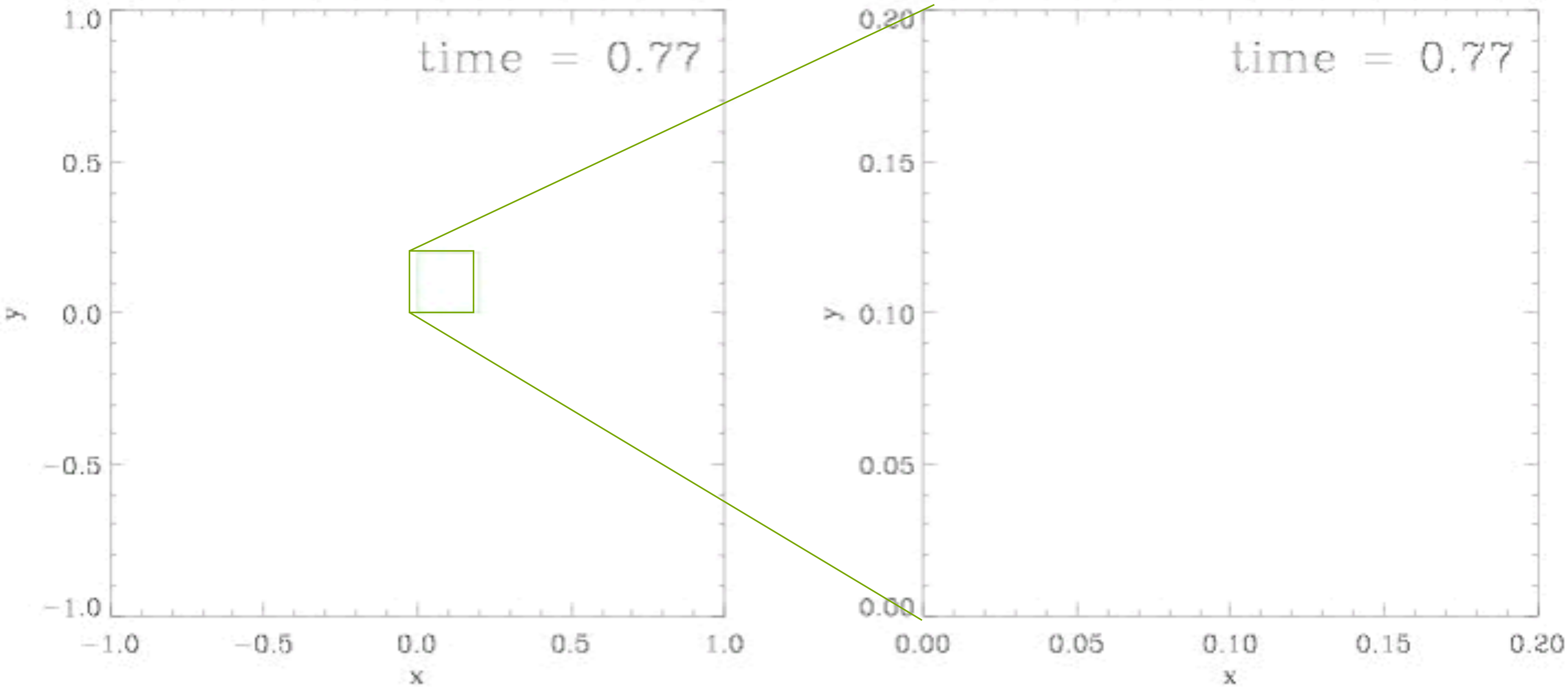


Trajectories of protostars in a nascent dense cluster created by gravoturbulent fragmentation
(from Klessen & Burkert 2000, ApJS, 128, 287)

# accretion rates in clust

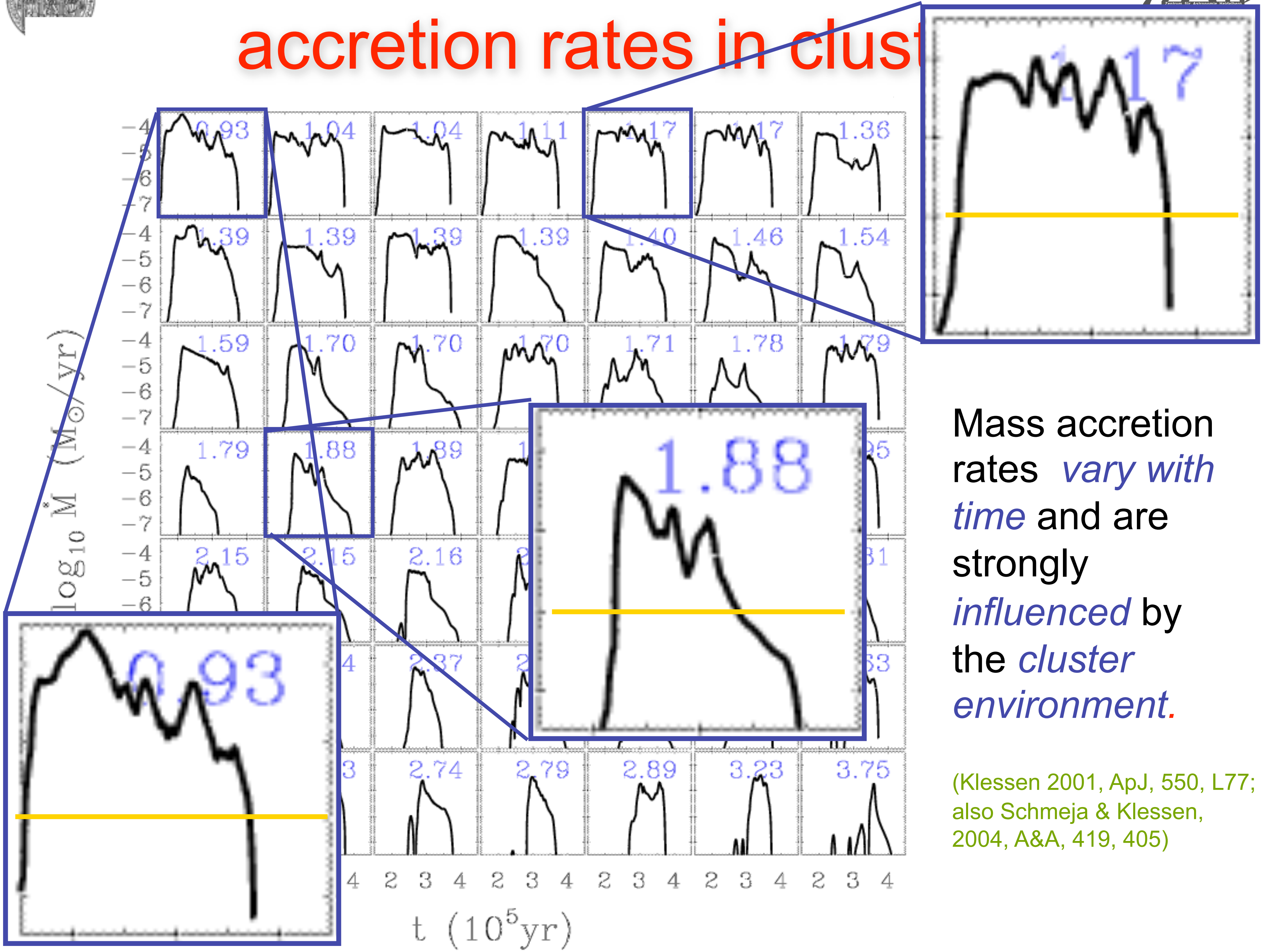


Mass accretion rates *vary with time* and are strongly *influenced* by the *cluster environment*.

(Klessen 2001, ApJ, 550, L77; also Schmeja & Klessen, 2004, A&A, 419, 405)

# IMF

- distribution of stellar masses depends on
  - turbulent initial conditions
    --> mass spectrum of prestellar cloud cores
  - collapse and interaction of prestellar cores
    --> competitive accretion and *N*-body effects
  - *thermodynamic properties of gas*
    *--> balance between heating and cooling*
    *--> EOS (determines which cores go into collapse)*
  - (proto) stellar feedback terminates star formation
    ionizing radiation, bipolar outflows, winds, SN

(e.g. Larson 2003, Prog. Rep. Phys.; Mac Low & Klessen, 2004, Rev. Mod. Phys, 76, 125 - 194)

# dependency on EOS

- degree of fragmentation depends on *EOS!*

- polytropic EOS: $\mathbf{p} \propto \rho^{\gamma}$
- $\gamma<1$: dense cluster of low-mass stars
- $\gamma>1$: isolated high-mass stars
- (see Li, Klessen, & Mac Low 2003, ApJ, 592, 975; also Kawachi & Hanawa 1998, Larson 2003)

# dependency on EOS

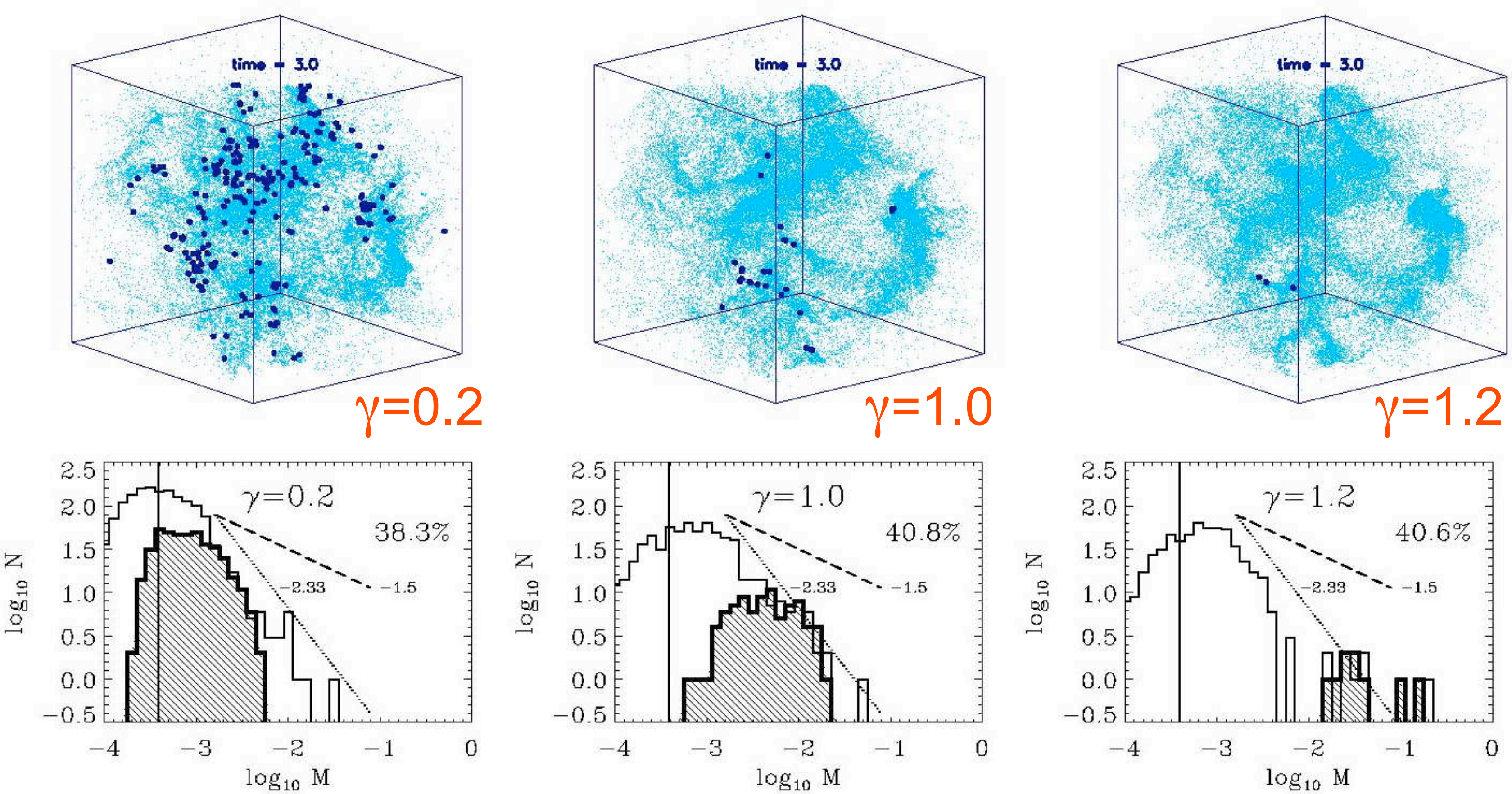


for $\gamma<1$ fragmentation is enhanced → *cluster of low-mass stars*

for $\gamma>1$ it is suppressed → formation of *isolated massive stars*

(from Li, Klessen, & Mac Low 2003, ApJ, 592, 975)

# how does that work?

(1) $\mathbf{p} \propto \rho^{\gamma} \quad \rightarrow \quad \rho \propto \mathbf{p}^{1/\gamma}$

(2) $\mathbf{M_{jeans}} \propto \gamma^{3/2}\, \rho^{(3\gamma-4)/2}$

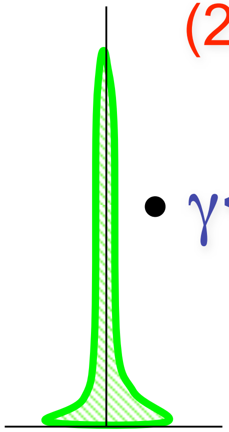

- $\gamma<1$: → *large* density excursion for given pressure
  - → $\langle M_{jeans} \rangle$ becomes small
  - → number of fluctuations with $M > M_{jeans}$ is large

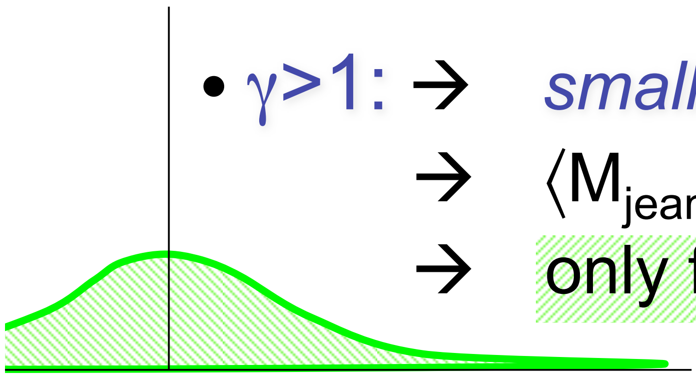

- $\gamma>1$: → *small* density excursion for given pressure
  - → $\langle M_{jeans} \rangle$ is large
  - → only few and massive clumps exceed $M_{jeans}$

# EOS in different environments

# EOS as function of metallicity

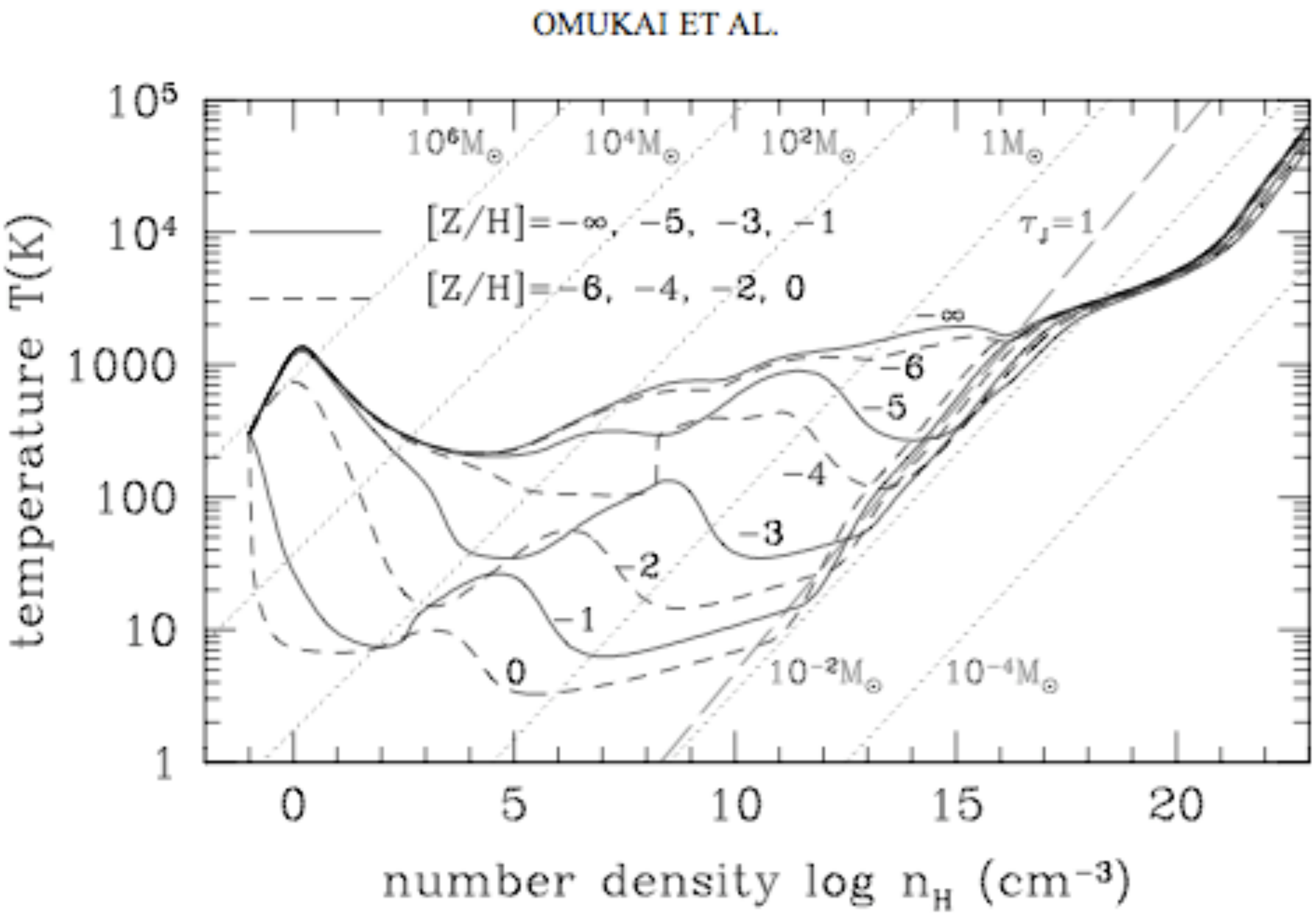


(Omukai et al. 2005)

# EOS as function of metallicity

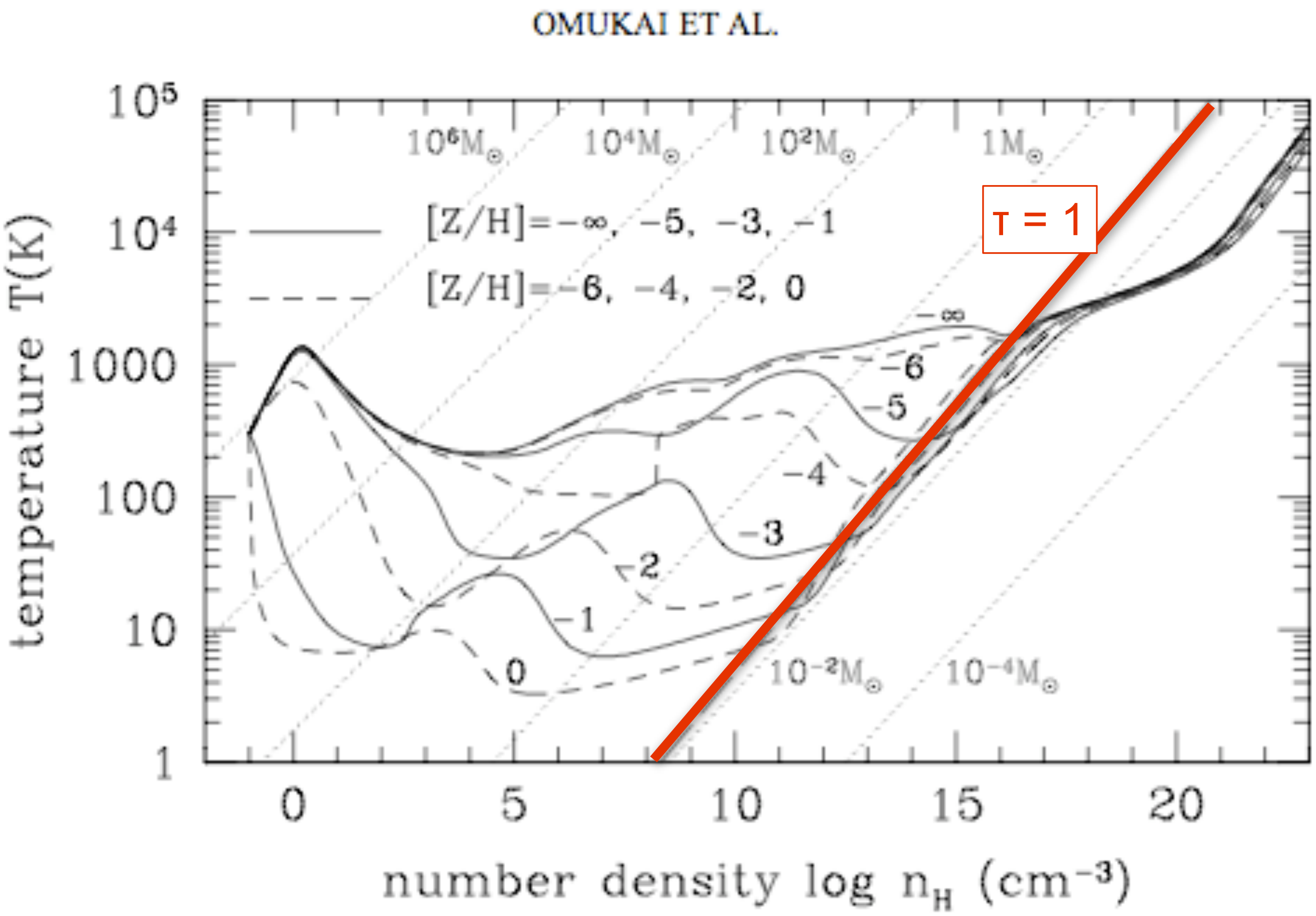


(Omukai et al. 2005)

# EOS as function of metallicity

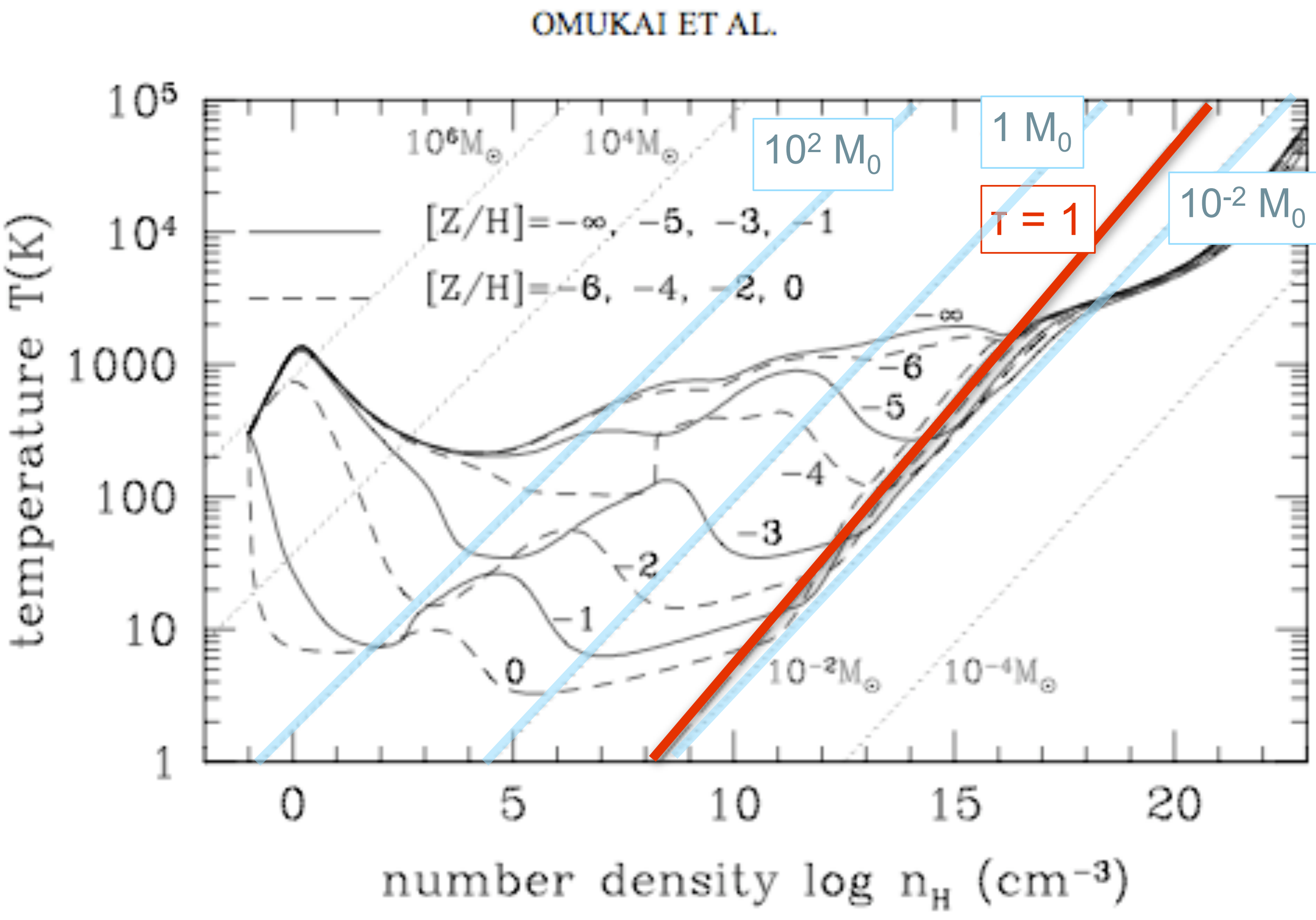


(Omukai et al. 2005)

# present-day star formation

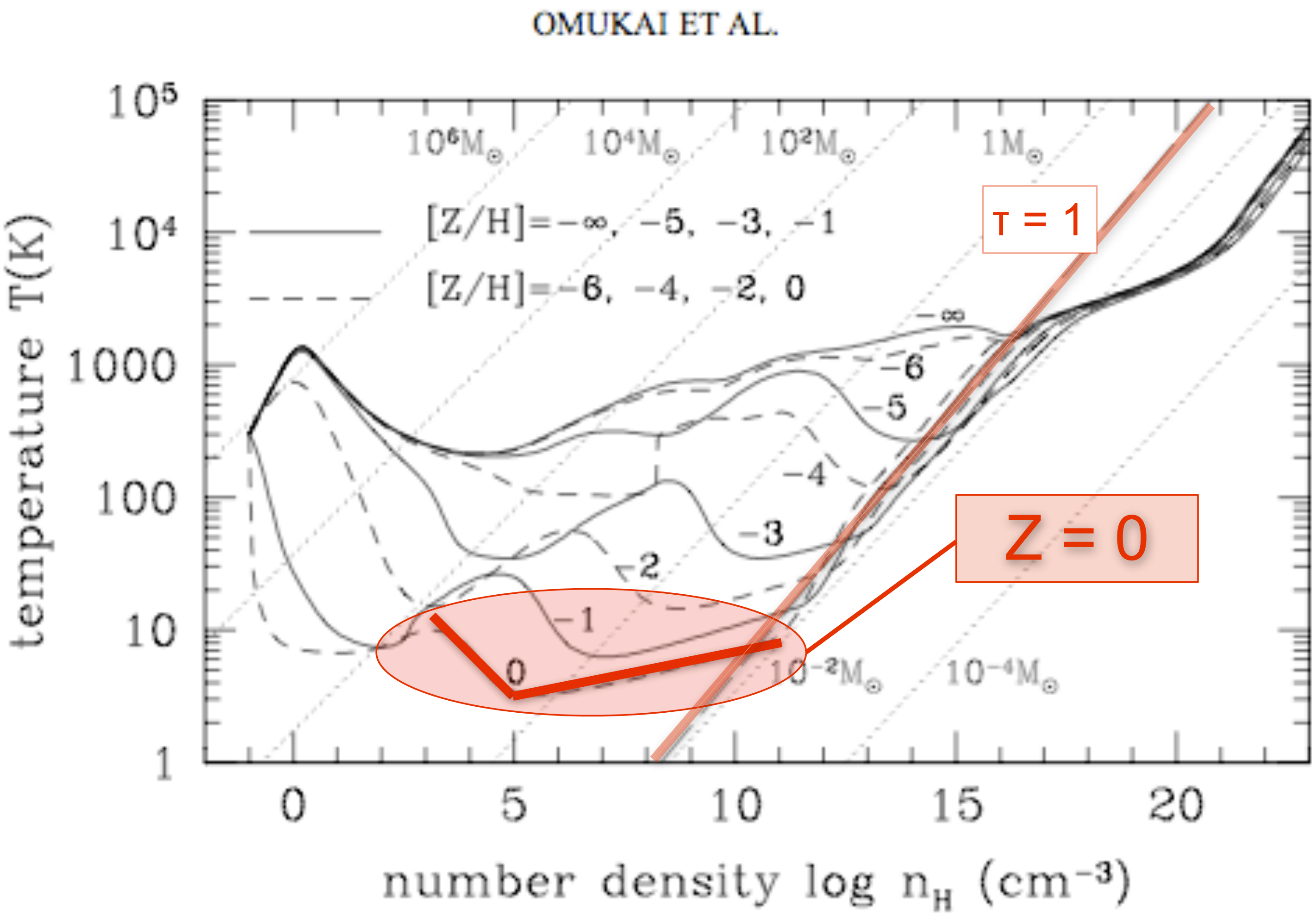


(Omukai et al. 2005, Jappsen et al. 2005, Larson 2005)

# present-day star formation

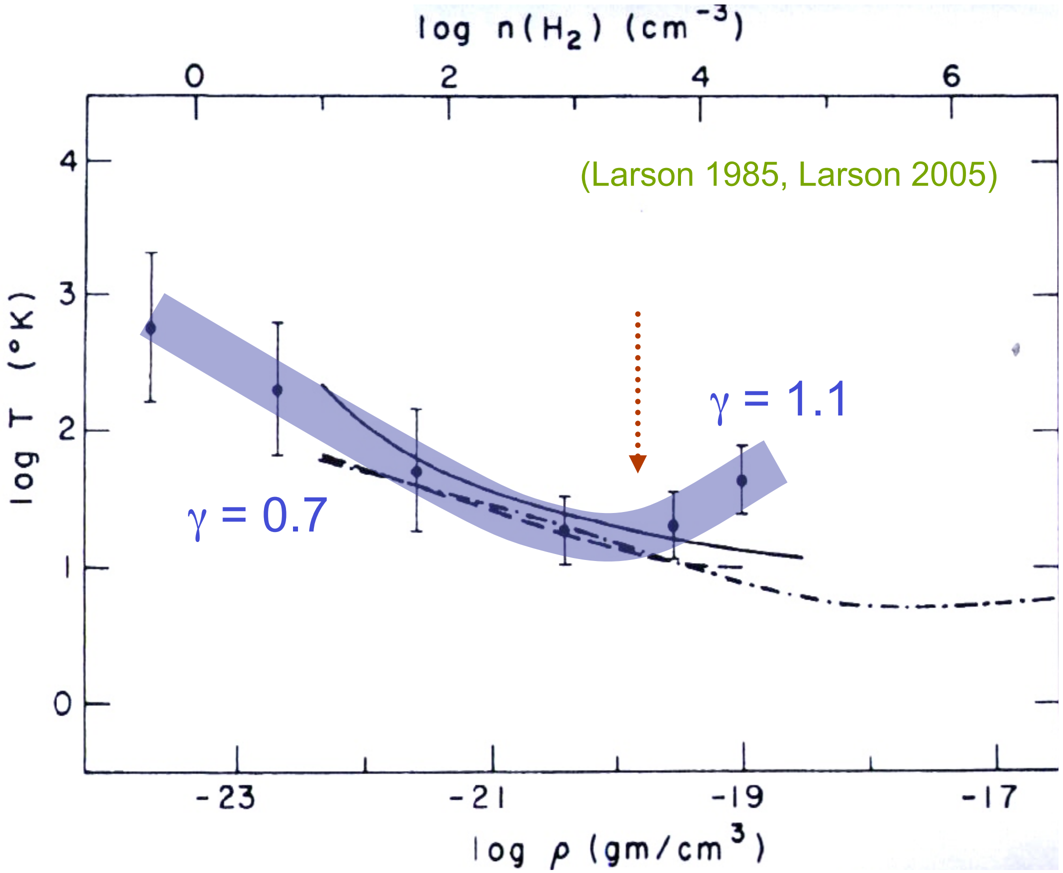

# present-day star formation

This kink in EOS is very insensitive to environmental conditions such as ambient radiation field
--> reason for universal for of the IMF? (Elmegreen et al. 2008)

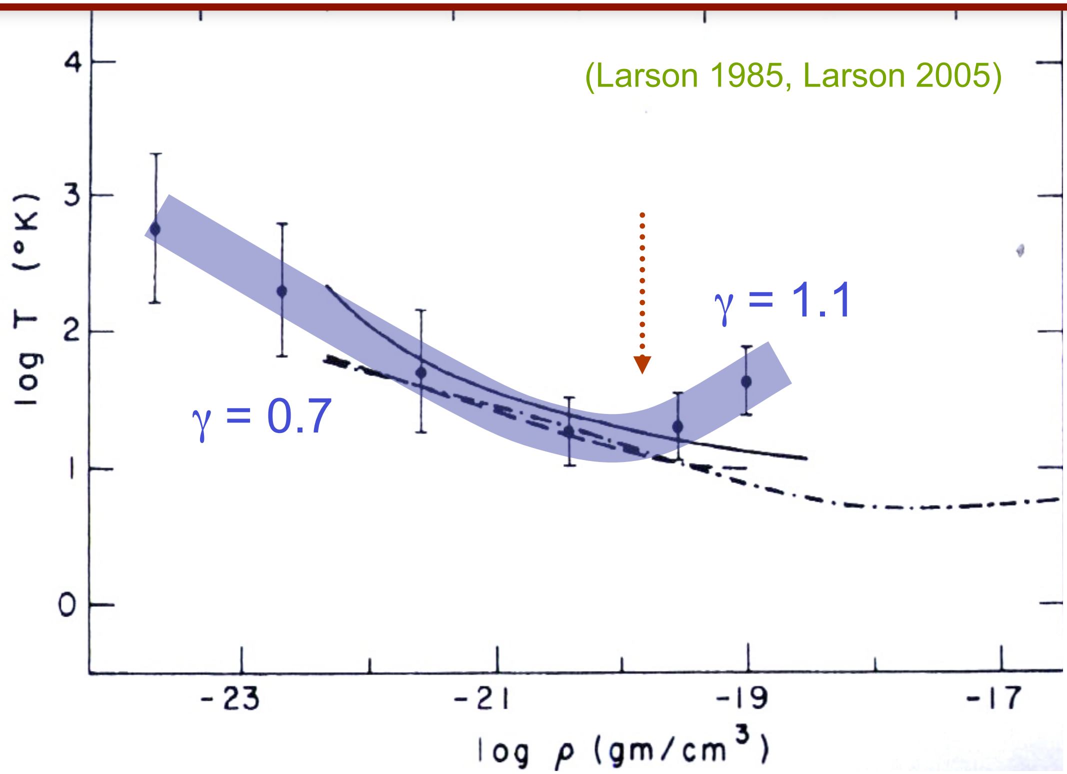

# IMF from simple piece-wise polytropic EOS

$\gamma_1 = 0.7$

$\gamma_2 = 1.1$

$$\boxed{T \sim \rho^{\gamma-1}}$$

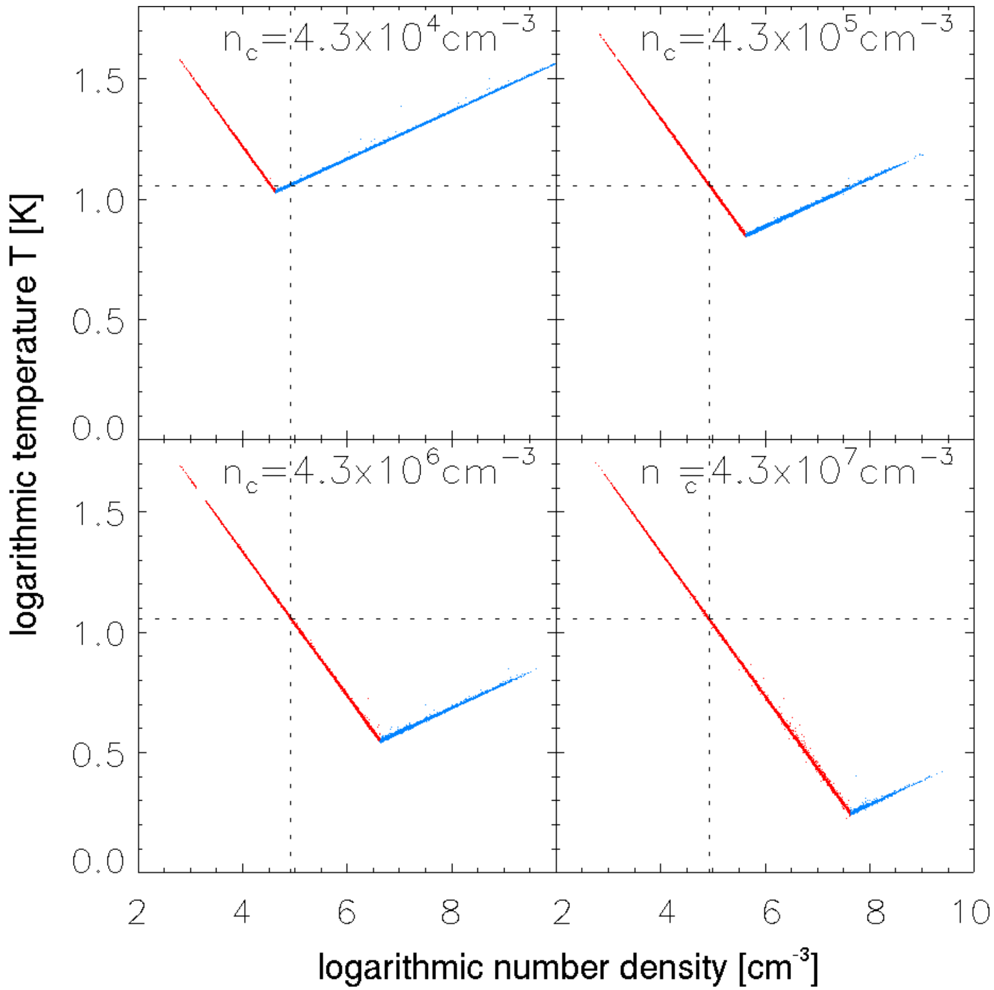


EOS and Jeans Mass:

$\mathbf{p} \propto \rho^{\gamma} \rightarrow \rho \propto \mathbf{p}^{1/\gamma}$

$\mathbf{M}_{\mathbf{jeans}} \propto \gamma^{3/2} \rho^{(3\gamma-4)/2}$

(Jappsen et al. 2005)

# IMF from simple piece-wise EOS

critical density ⬆ ⟹ median mass ⬇

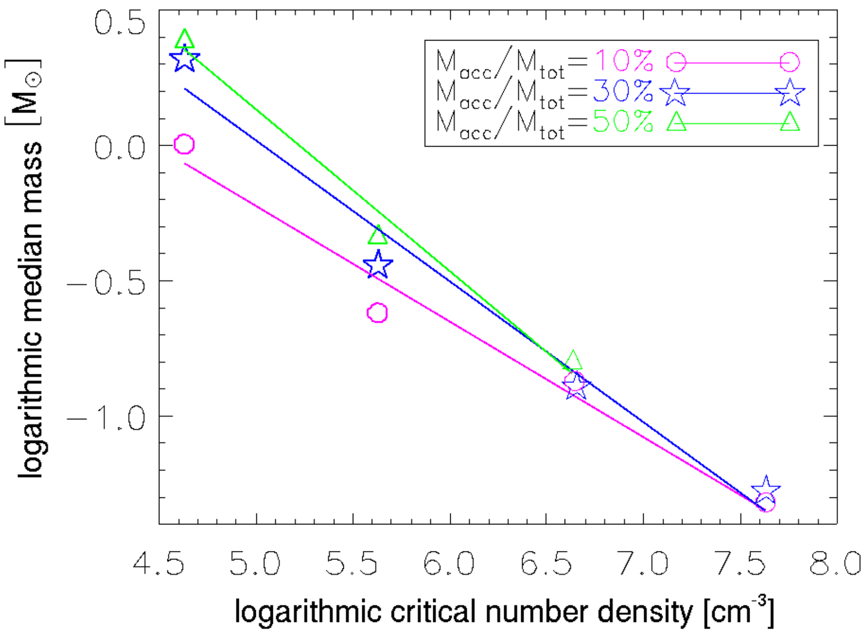


(Jappsen et al. 2005)

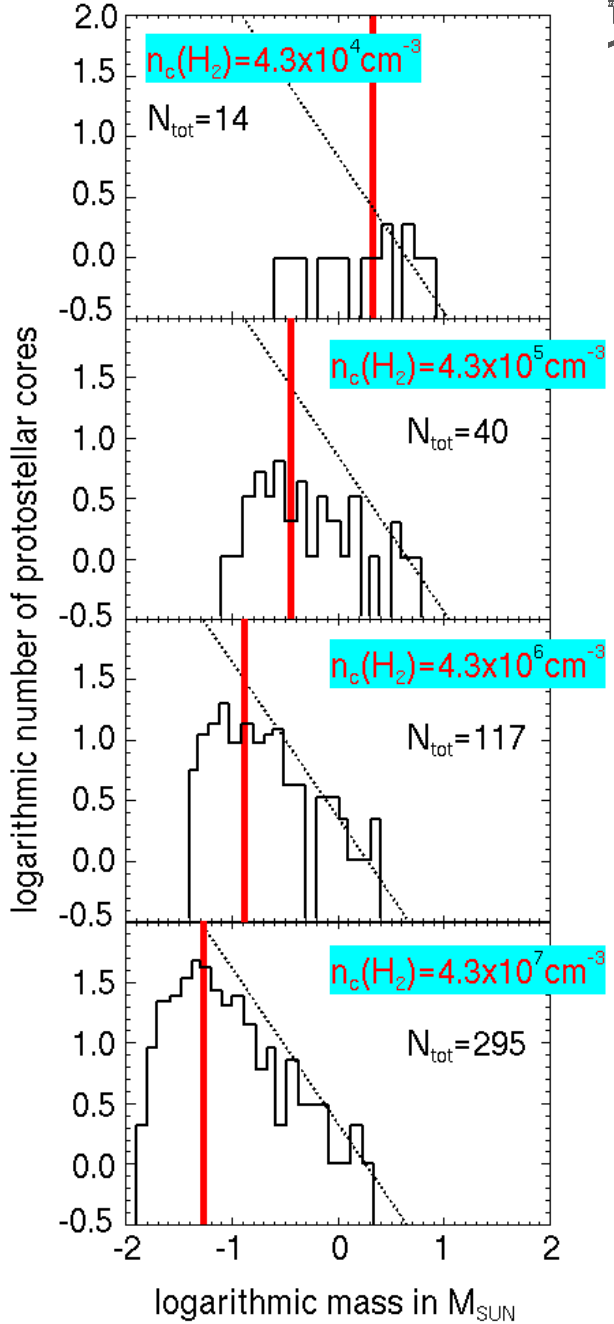

# IMF in nearby molecular clouds

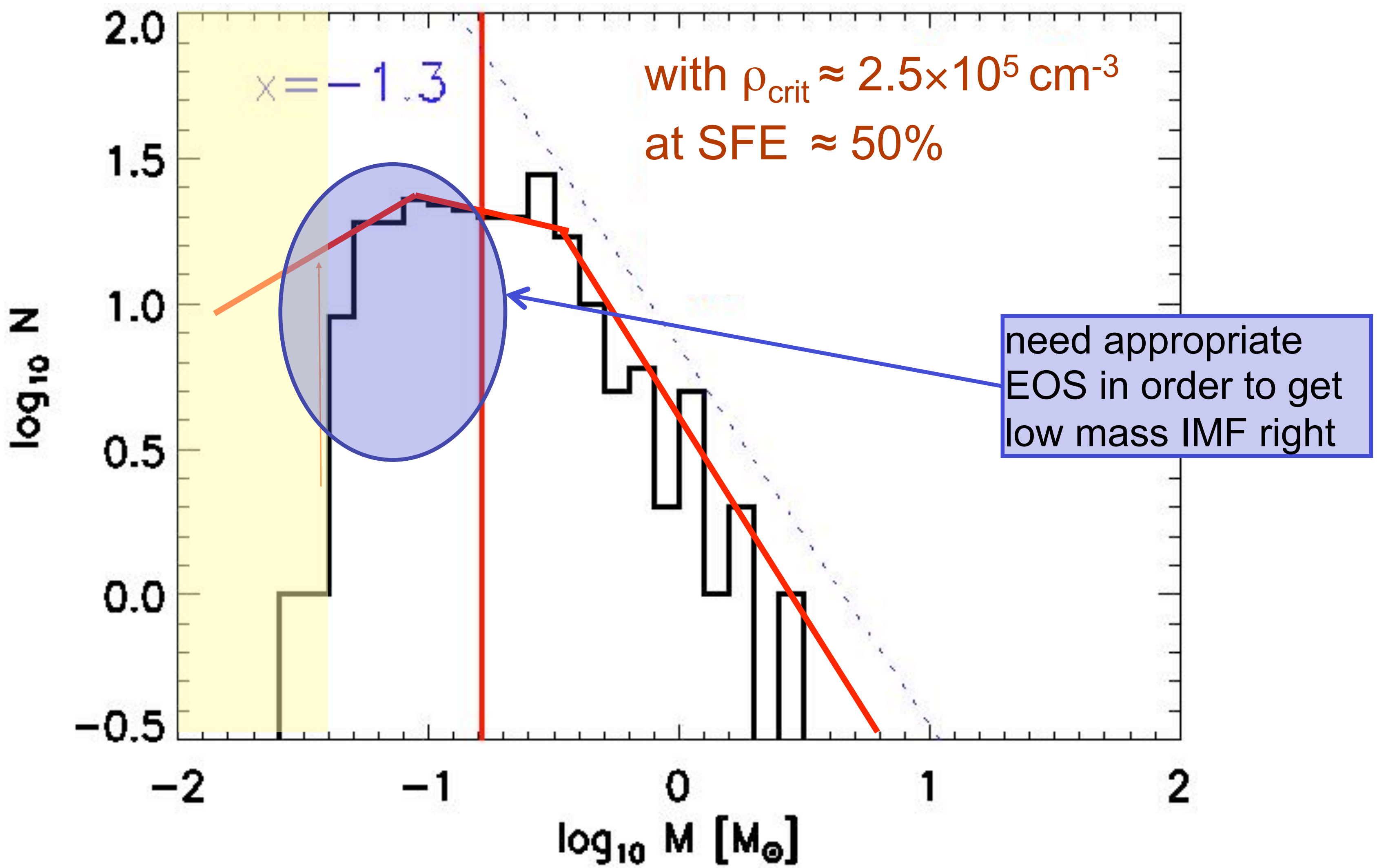


(Jappsen et al. 2005, A&A, 435, 611)c

# dependence on Z at low density

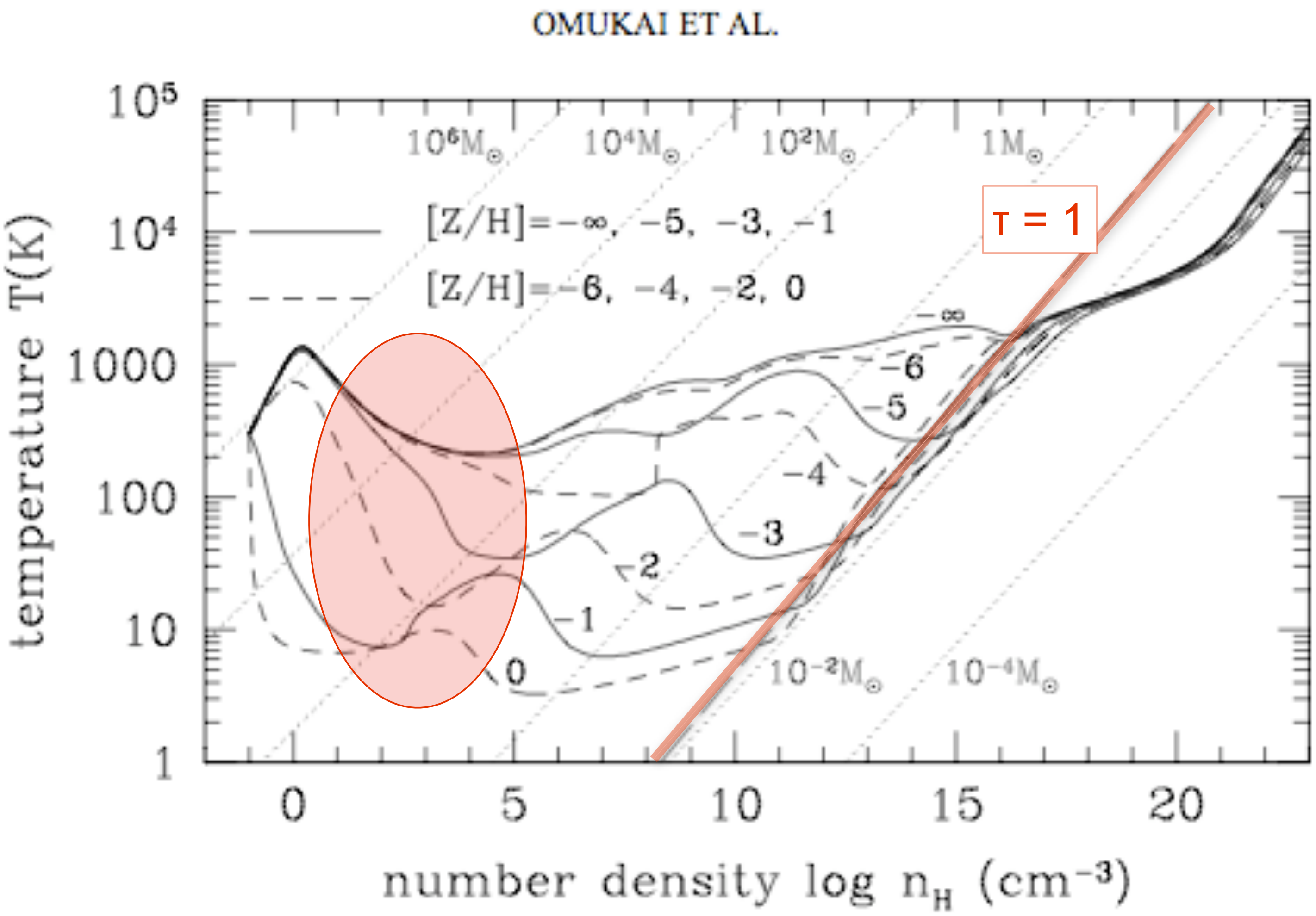


(Omukai et al. 2005)

# dependence on Z at low density

- at densities $n < 10^2$ cm$^{-3}$ and metallicities Z < $10^{-2}$ *$H_2$ cooling* dominates behavior.
  (Jappsen et al. 2007)
- fragmentation depends on *initial conditions*
  - example 1: *solid-body rotating top-hat* initial conditions with dark matter fluctuations (a la Bromm et al. 1999) fragment no matter what metallicity you take (in regime n ≤ $10^6$ cm$^{-3}$) → because *unstable disk* builds up
    (Jappsen et al. 2009a)
  - example 2: *centrally concentrated halo* does *not* fragment up to densities of n ≈ $10^6$ cm$^{-3}$ up to metallicities Z ≈ -1 (Jappsen et al. 2009b)

# implications for Pop III

- star formation will depend on *degree of turbulence* in protogalactic halo
- speculation: *differences in stellar mass function*?
- speculation:
  - low-mass halos → low level of turbulence → relatively massive stars
  - high-mass halos (atomic cooling halos) → high degree of turbulence → wider mass spectrum with peak at lower-masses?

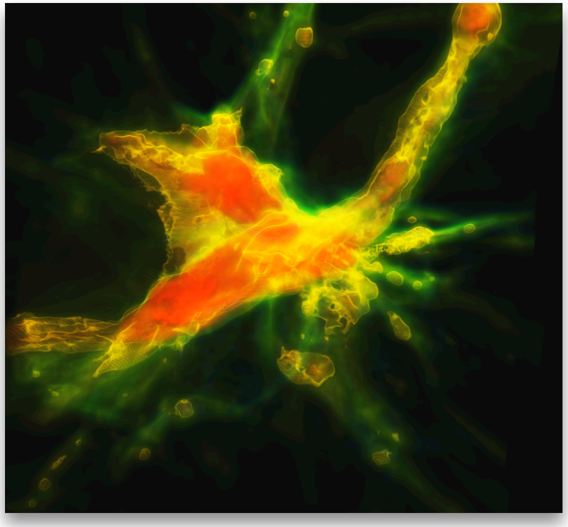

(Greif et al. 2008)

# turbulence developing in an atomic cooling halo

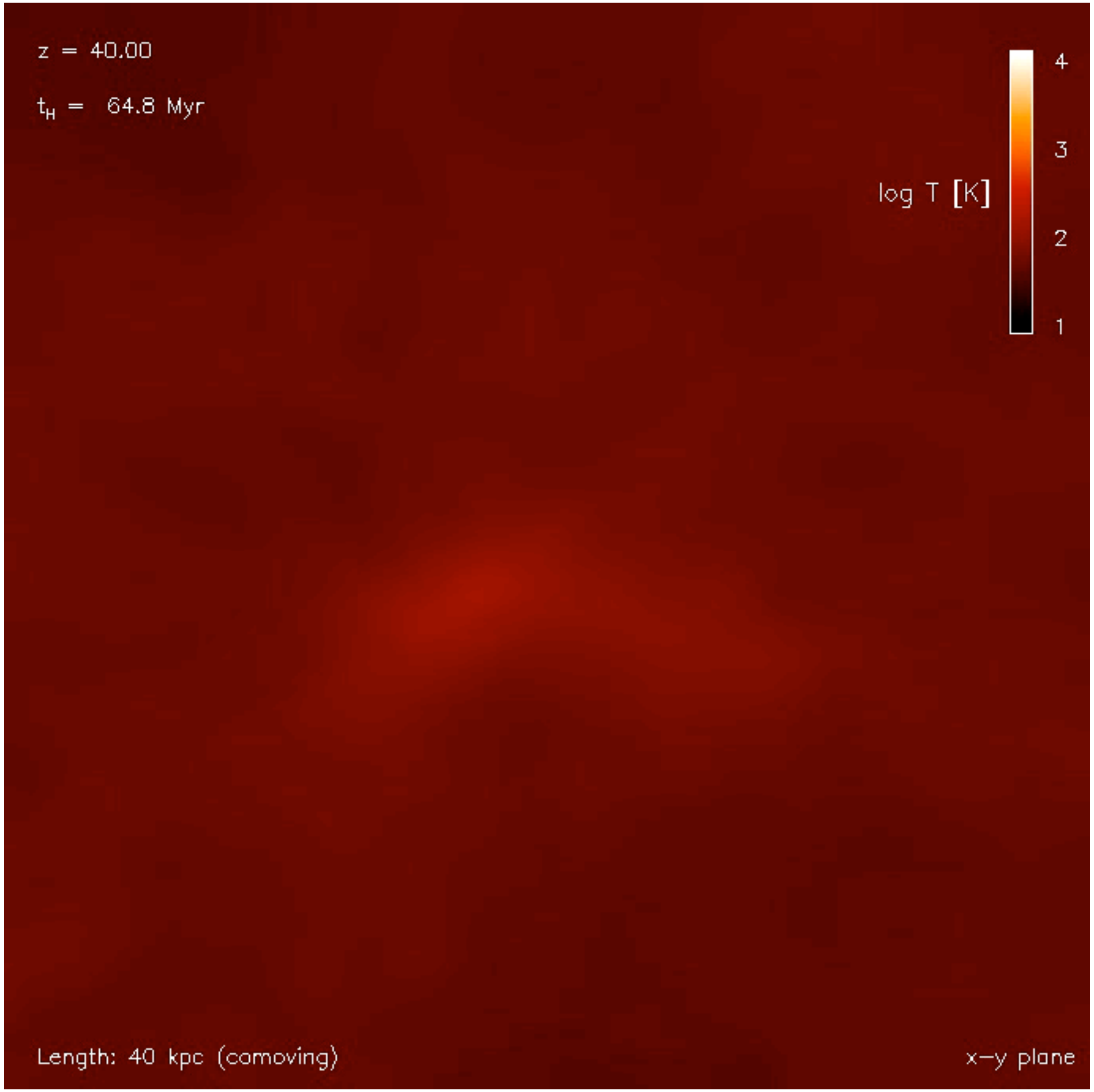


(Greif et al. 2008, see also Wise & Abel 2007)

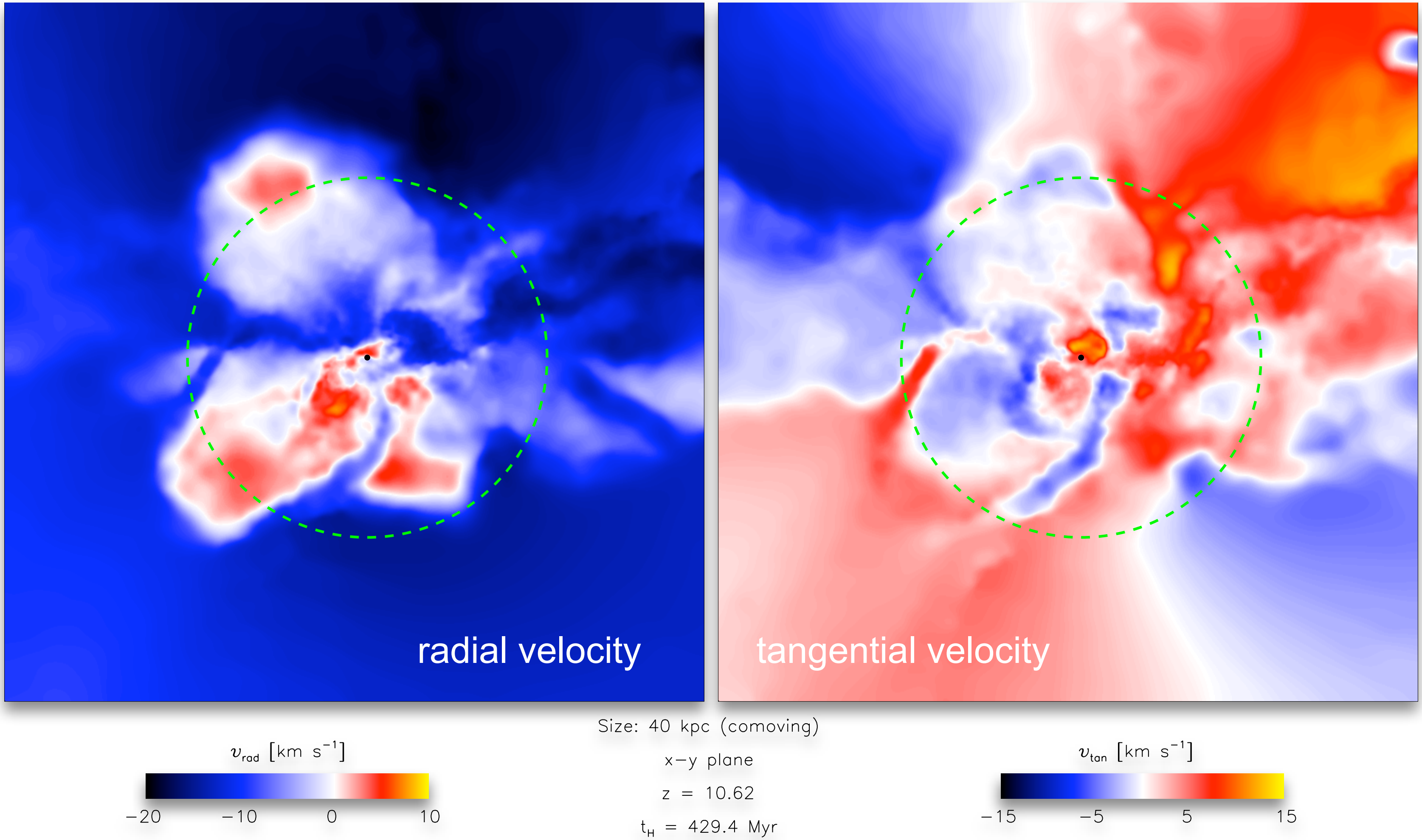


turbulence developing in an atomic cooling halo (Greif et al. 2008)

# Pop III.1

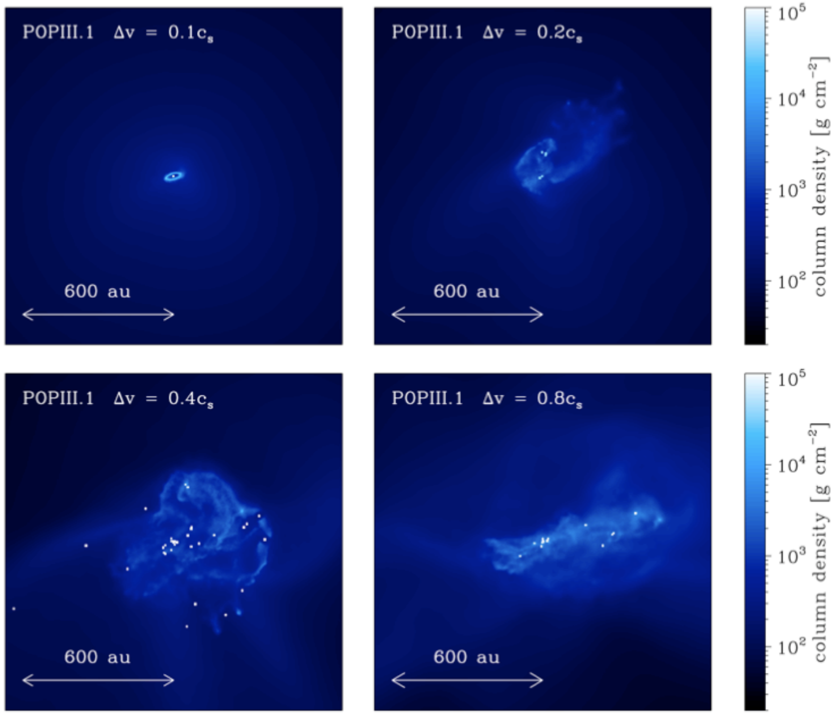


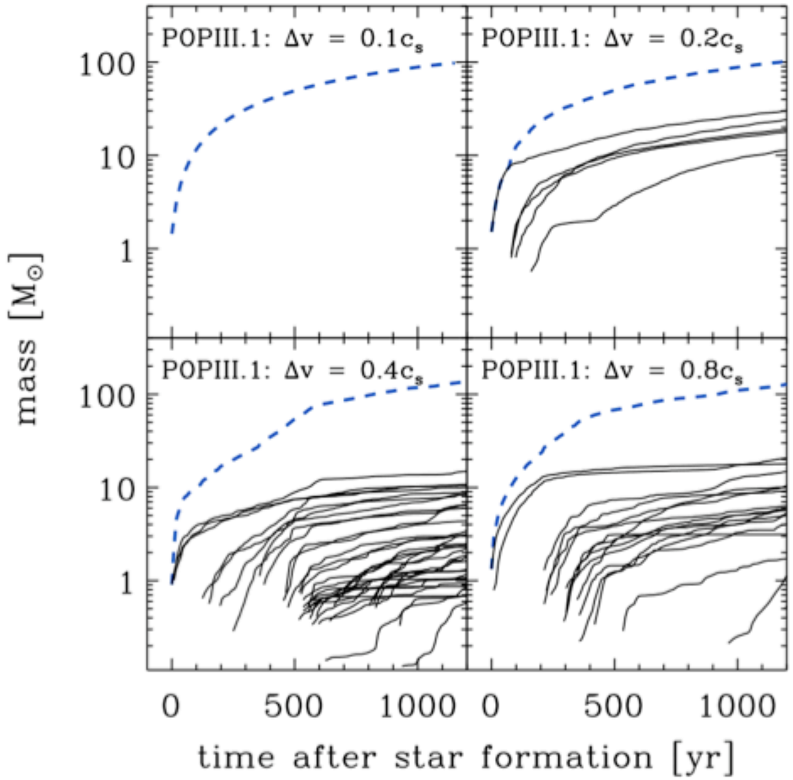


(Clark et al, in prep.)

# Pop III.2

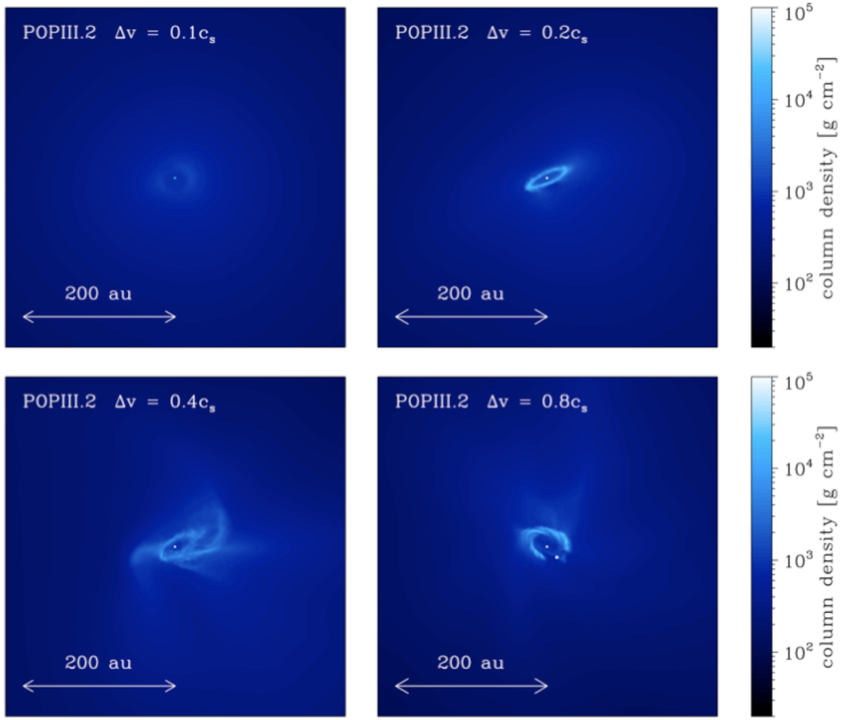


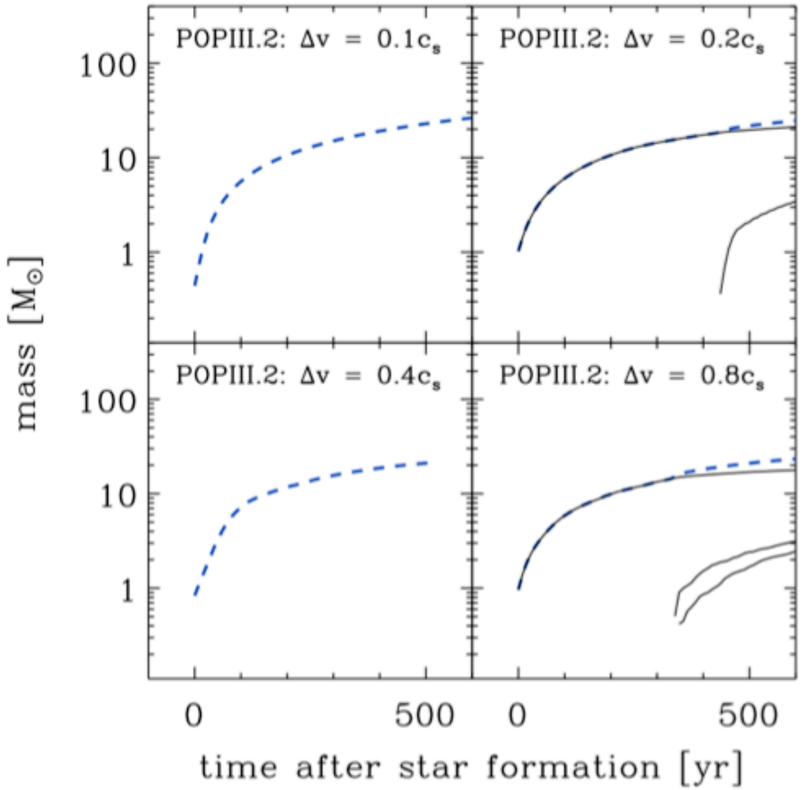


(Clark et al, in prep.)

# once again: thermodynamics

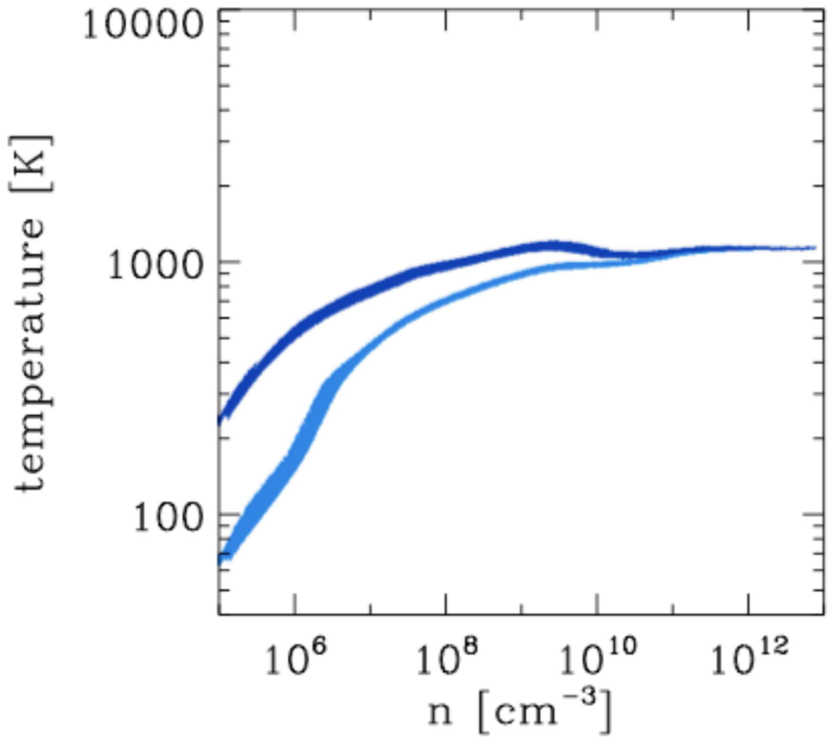


FIG. 6.— Temperature as a function of number density for the Pop. III.1 (dark blue) and Pop. III.2 (light blue) $\Delta v_{\rm turb} = 0.1\, c_{\rm s}$ simulations. In both cases, the curves denote the state of the cloud at the point just before the formation of the sink particle.

also Pop III.2 gas heats up above the CMB

--> weaker fragmentation!

# once again: thermodynamics

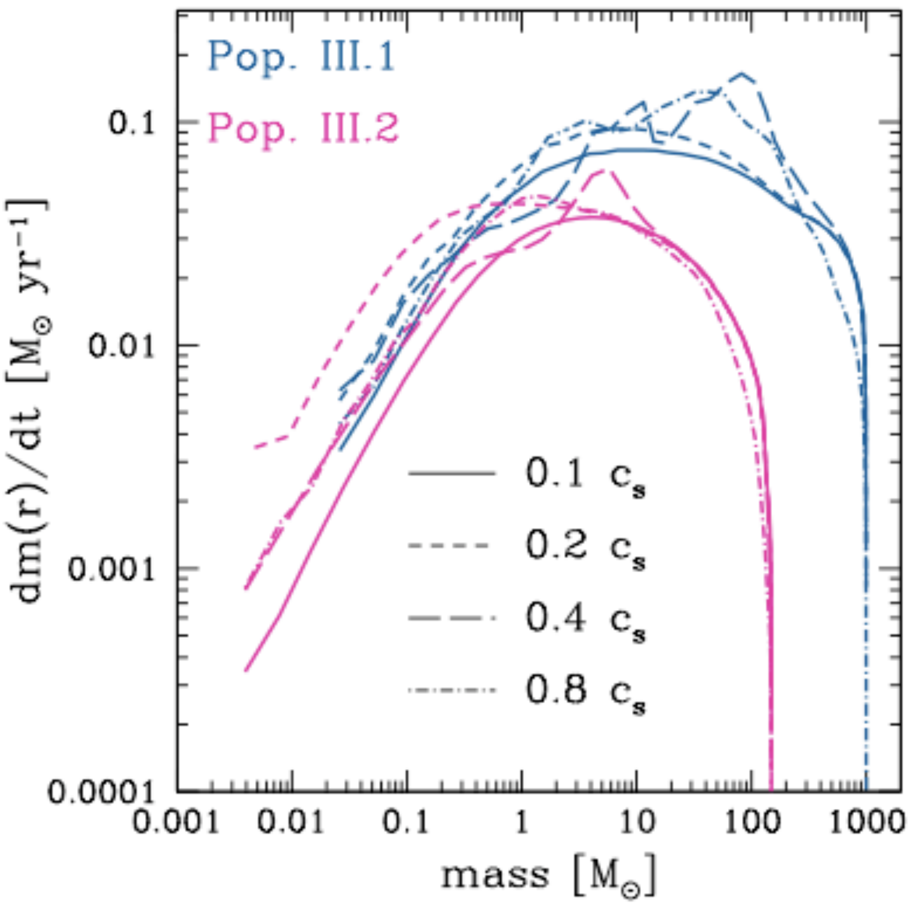


FIG. 8.— Accretion rates as a function of enclosed gas mass in the Pop. III.1 (upper lines; blue) and Pop. III.2 (lower lines; magenta) simulations, estimated as described in Section 4.1. Note that the sharp decline in the accretion rates for enclosed masses close to the initial cloud mass is an artifact of our problem setup; we would not expect to see this in a realistic Pop. III halo.

comparison of accretion rates...

# transition: Pop III to Pop II.5

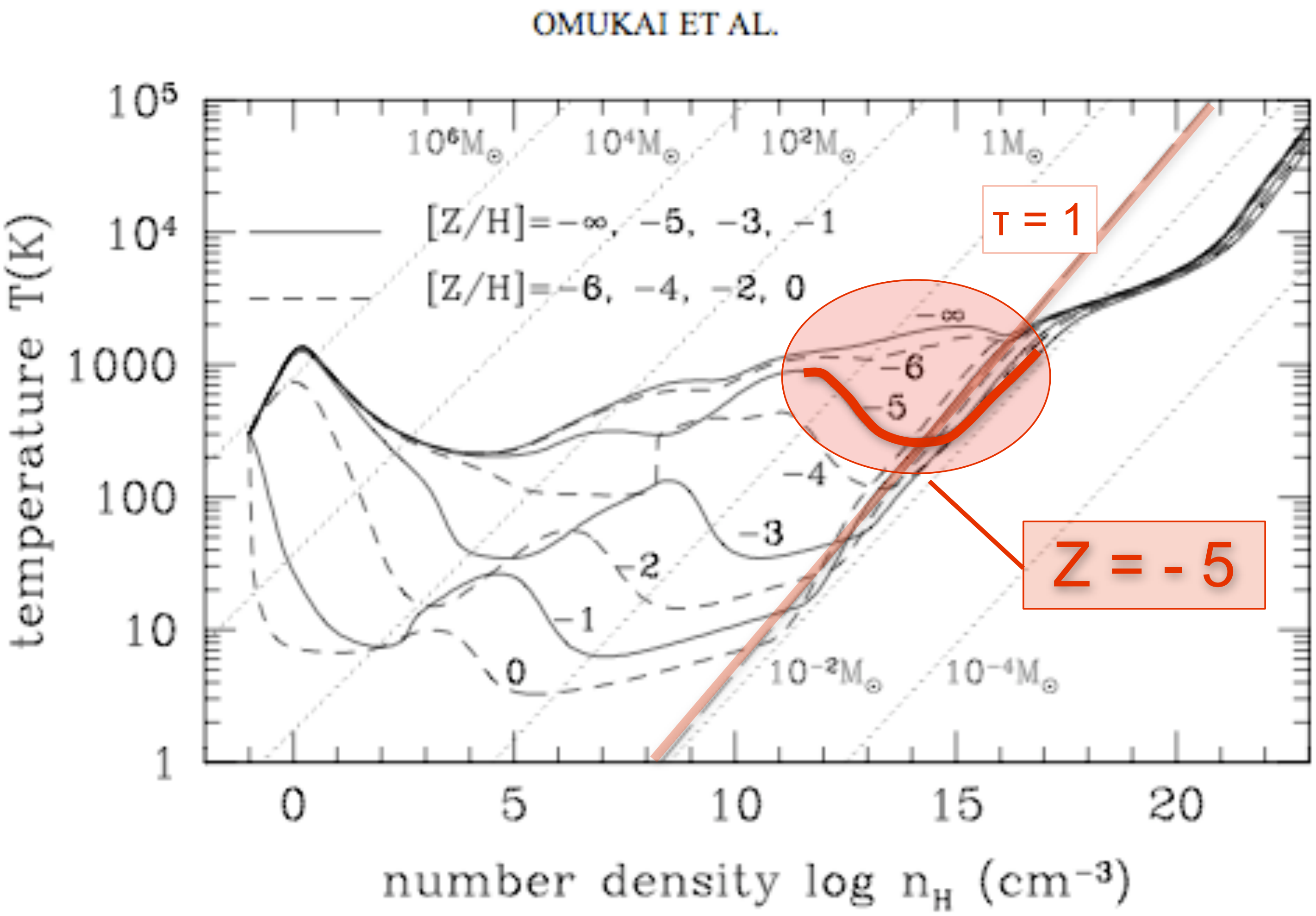


(Omukai et al. 2005)

# transition: Pop III to Pop II.5

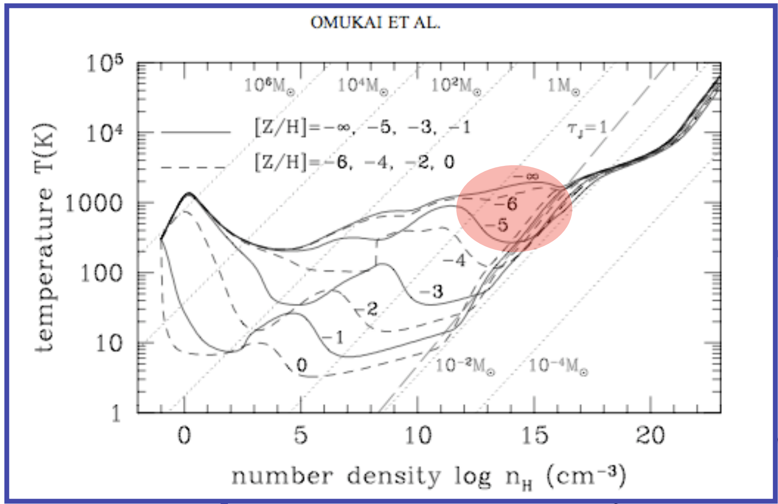


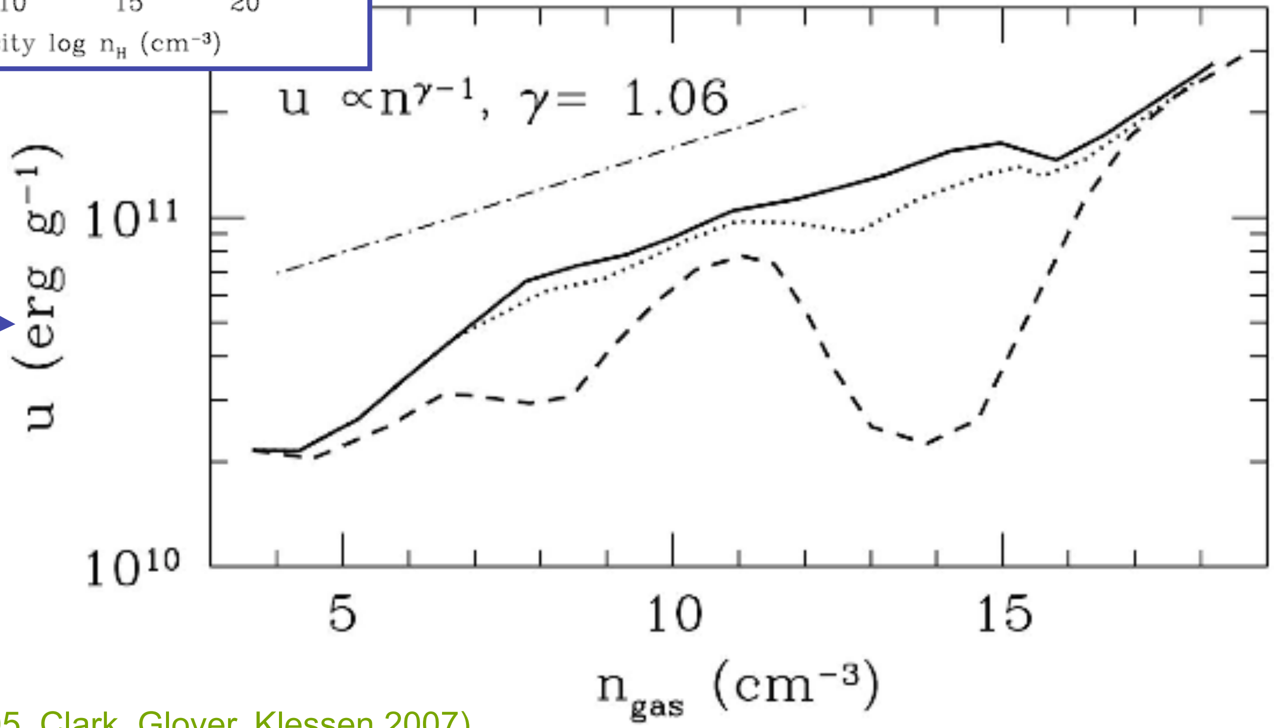


(Omukai et al. 2005, Clark, Glover, Klessen 2007)

# dust induced fragmentation at $Z=10^{-5}$

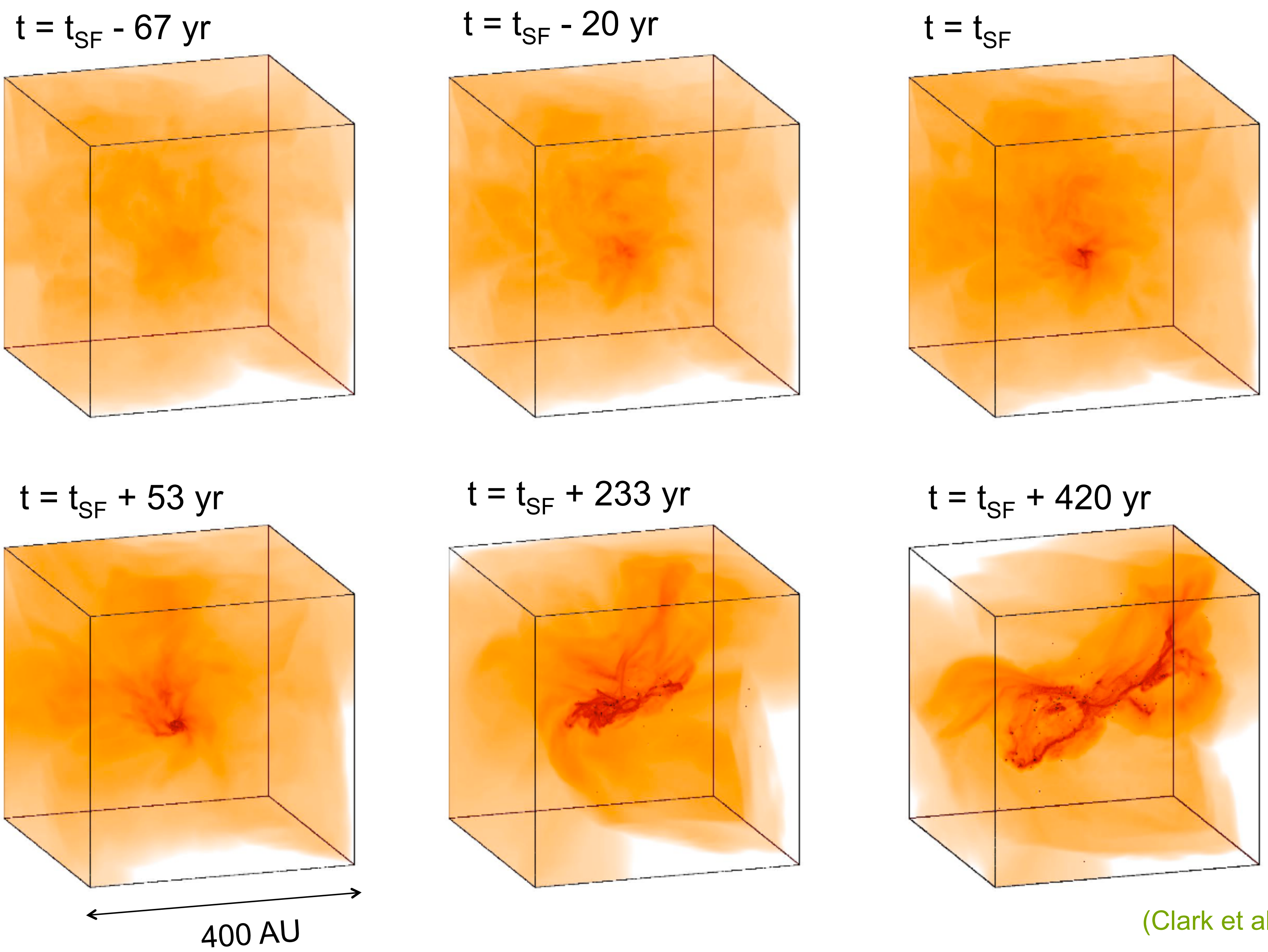


(Clark et al. 2007)

# dust induced fragmentation at $Z=10^{-5}$

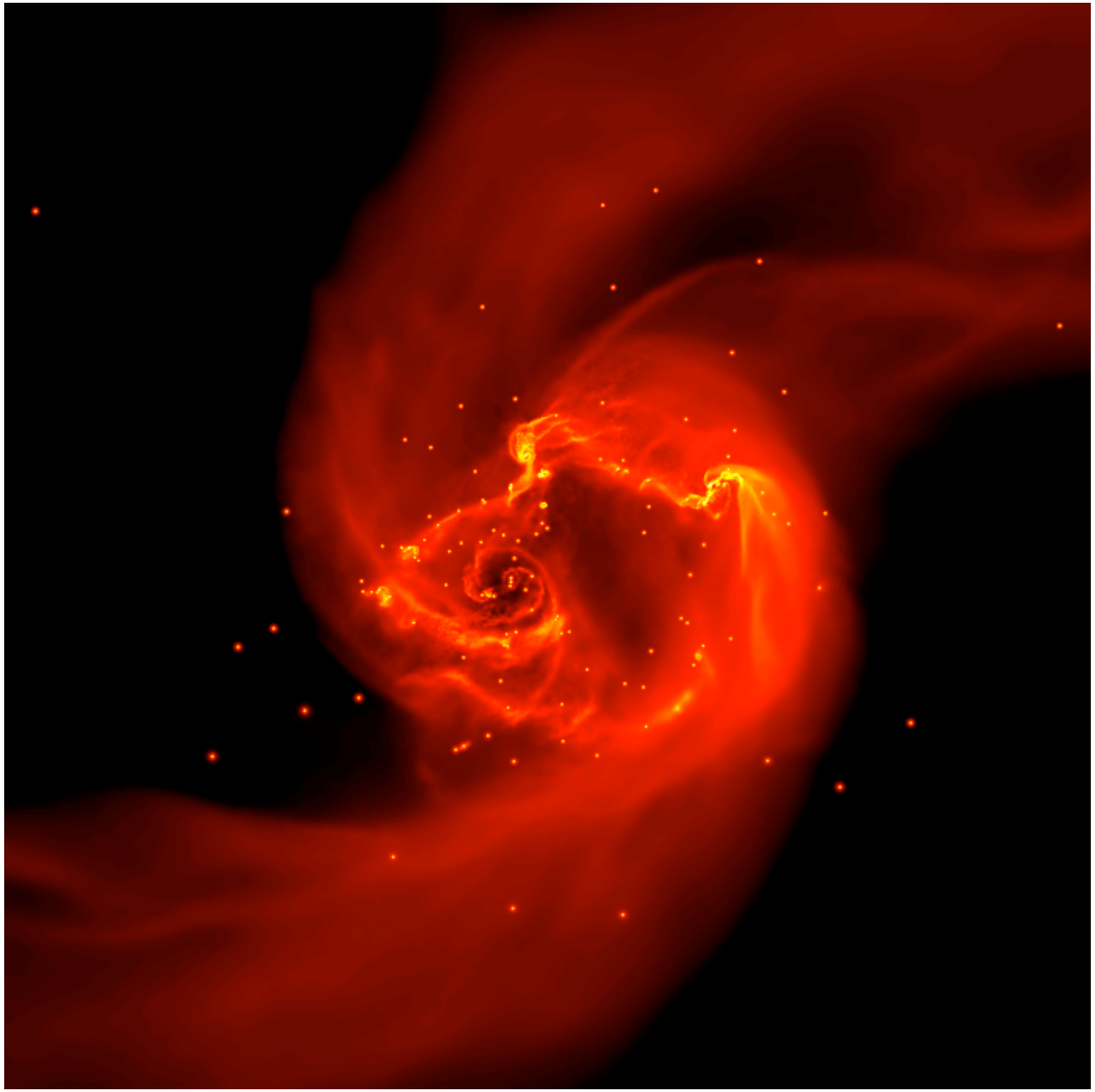

dense cluster of low-mass protostars builds up:

- mass spectrum peaks *below 1 $M_{sun}$*
- cluster VERY dense $n_{stars} = 2.5 \times 10^9\ pc^{-3}$
- fragmentation at density $n_{gas} = 10^{12} - 10^{13}\ cm^{-3}$

(Clark et al. 2008, ApJ 672, 757)

# dust induced fragmentation at $Z=10^{-5}$

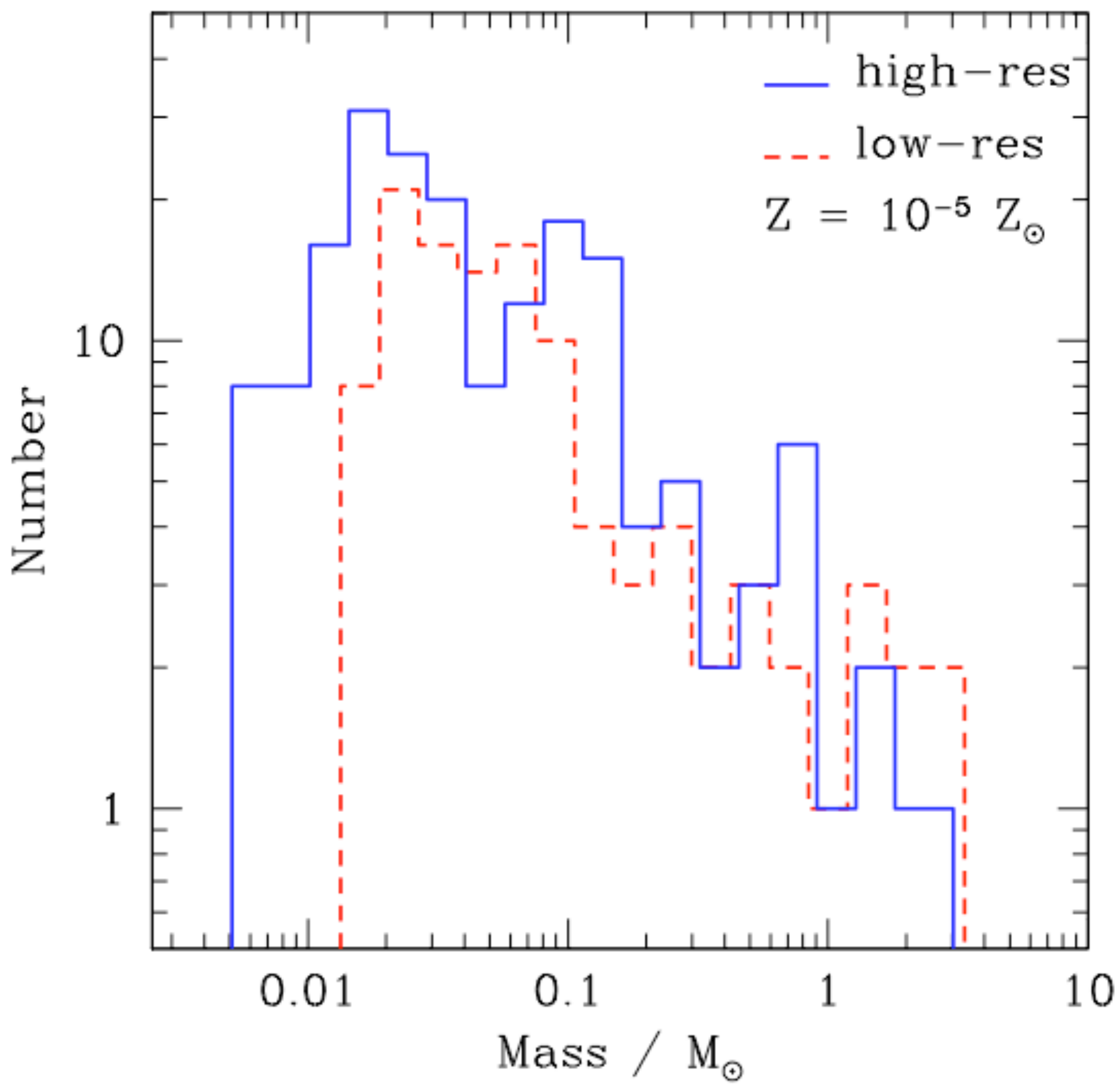


dense cluster of low-mass protostars builds up:

- mass spectrum peaks below 1 $M_{sun}$
- cluster VERY dense $n_{stars} = 2.5 \times 10^9\ pc^{-3}$

- *predictions:*
  * low-mass stars with [Fe/H] ~ $10^{-5}$
  * high binary fraction

(Clark et al. 2008)

# dust induced fragmentation at $Z=10^{-5}$

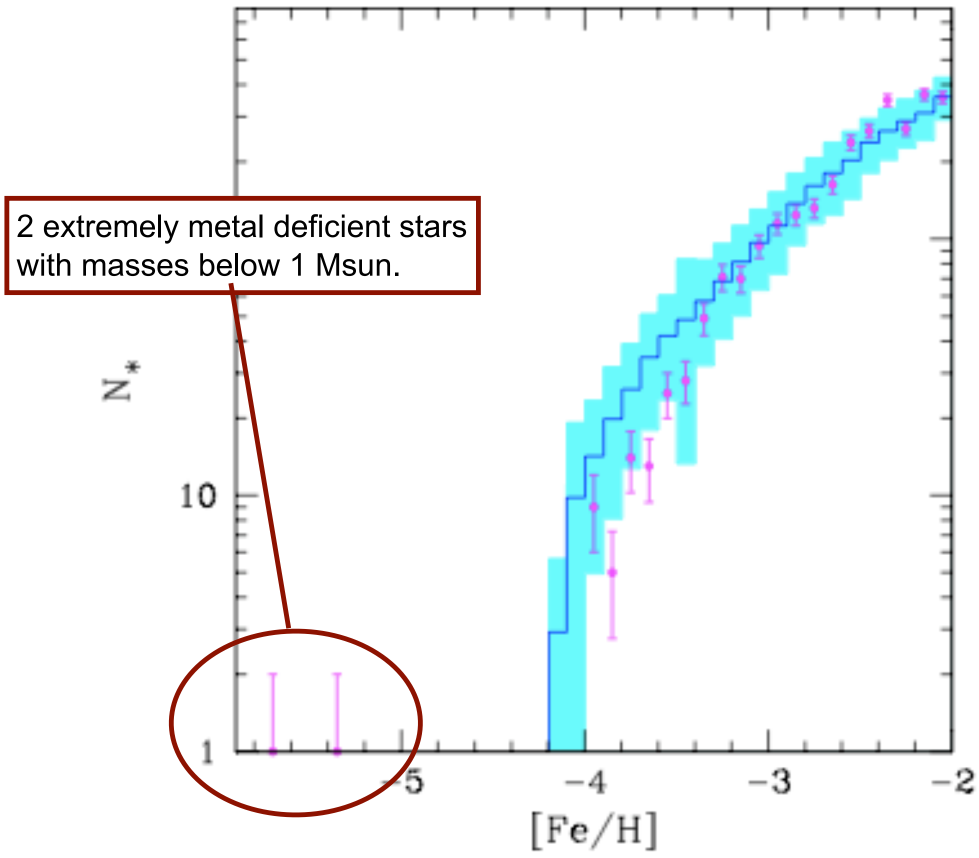


(plot from Salvadori et al. 2006, data from Frebel et al. 2005)

dense cluster of low-mass protostars builds up:

- mass spectrum peaks below 1 $M_{sun}$
- cluster VERY dense $n_{stars} = 2.5 \times 10^9 \, pc^{-3}$

- *predictions:*
  * low-mass stars with $[Fe/H] \sim 10^{-5}$
  * high binary fraction

(Clark et al. 2008)

# metal-free star formation

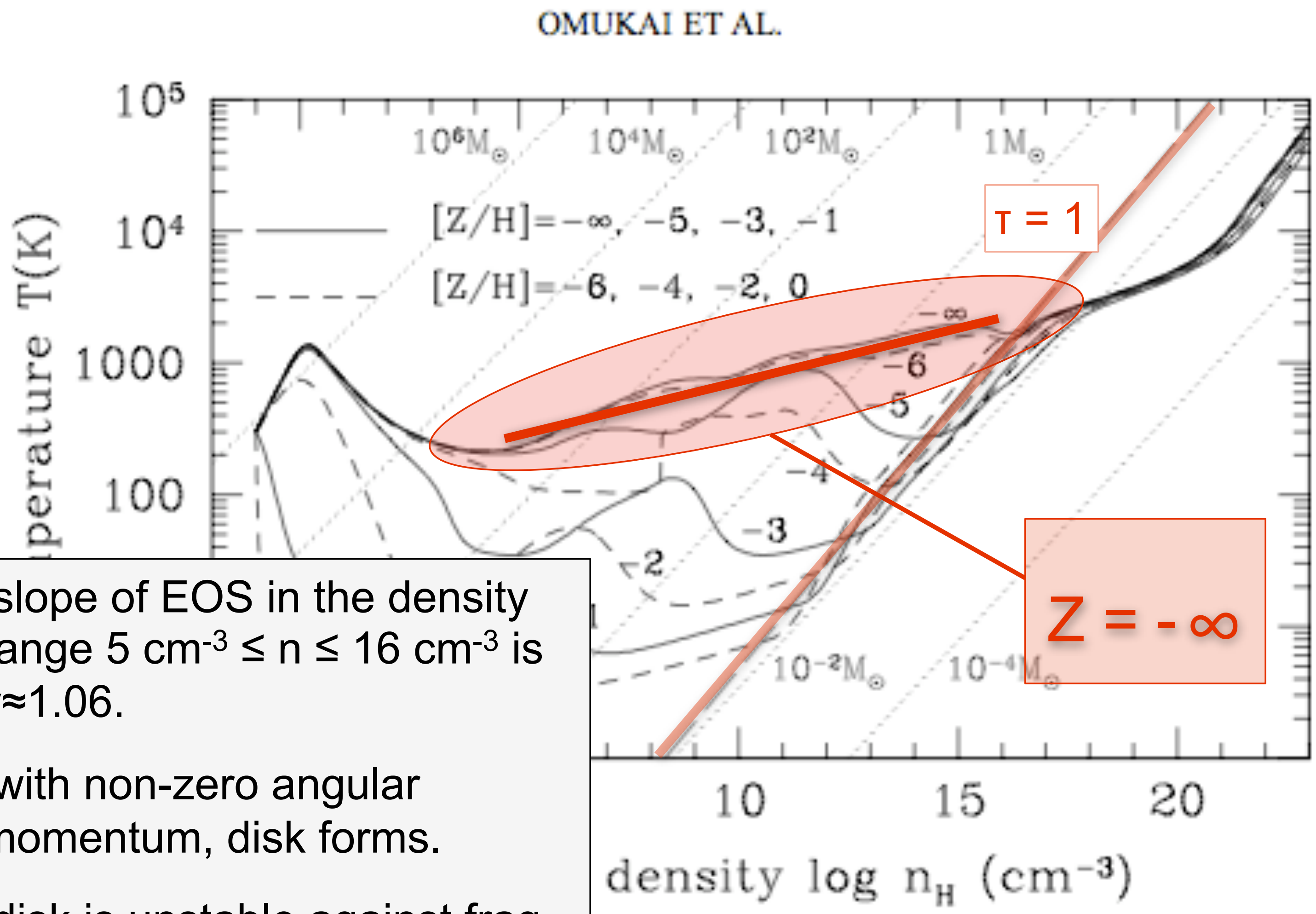


- slope of EOS in the density range 5 $cm^{-3}$ ≤ n ≤ 16 $cm^{-3}$ is γ≈1.06.
- with non-zero angular momentum, disk forms.
- disk is unstable against fragmentation at high density

# more on Z=0 star formation

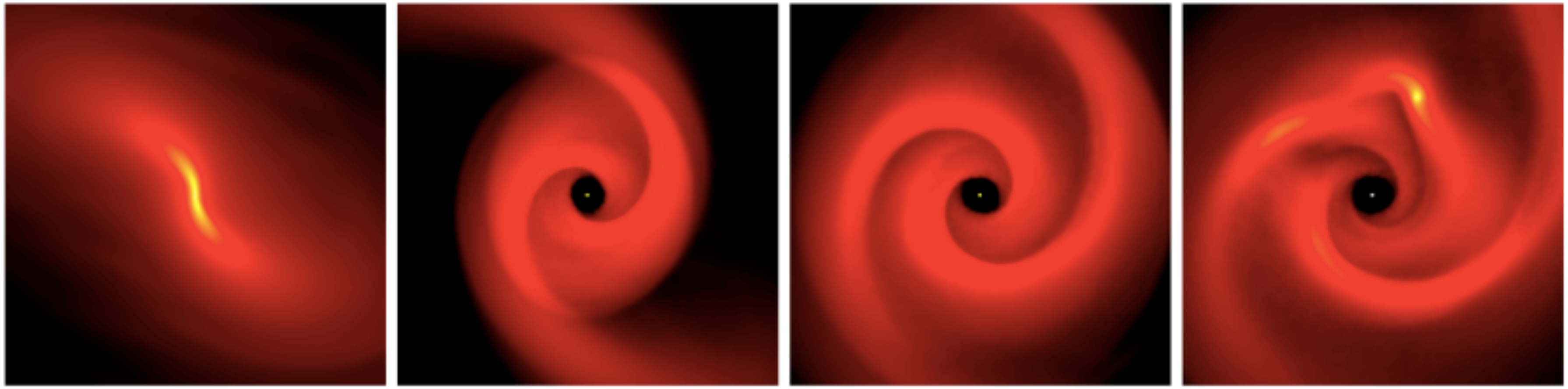

**FIGURE 1.** Column density images of the inner 66 au of the simulation, following the formation of the first protostar (sink particle) and the subsequent build-up of the protostellar disc and its eventual fragmentation. Starting from left-hand panel, which shows the gas at 1 yr before the protostar forms ($t_{SF}$ ), the next 3 panels show the evolution at times $t_{SF} + 76$ yr, $t_{SF} + 152$ yr and $t_{SF} + 228$ yr. The colour table is stretched from $10^3$ g cm$^{-2}$ to $10^6$ g cm$^{-2}$.

# more on Z=0 star formation

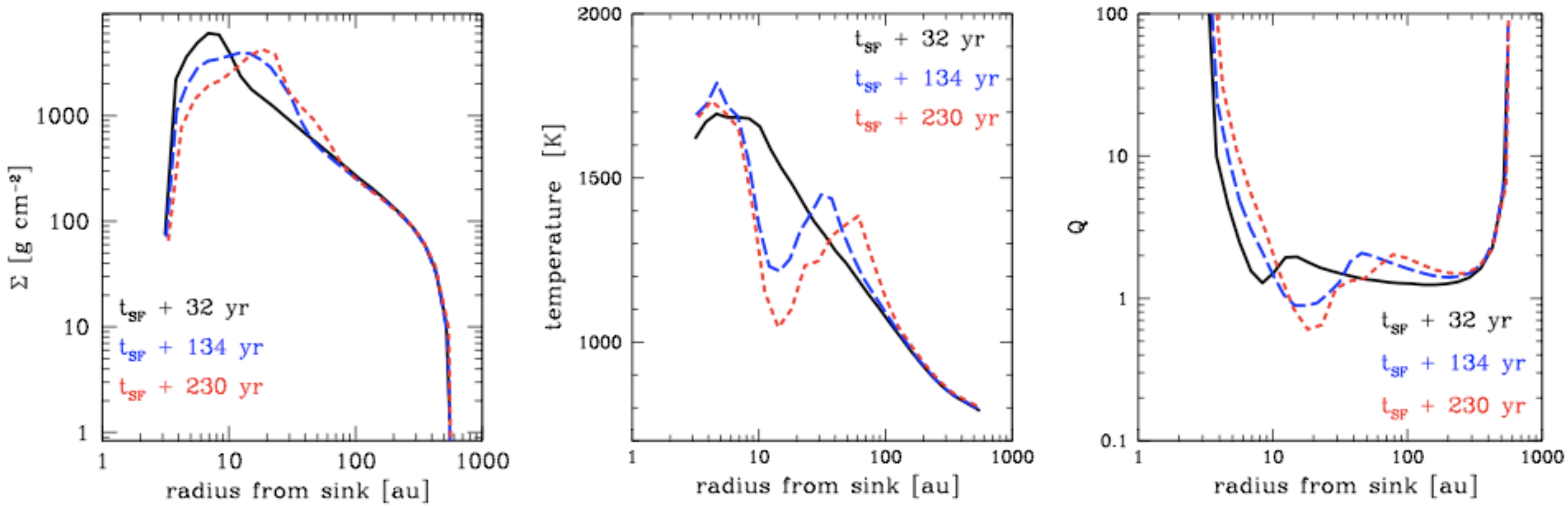


**FIGURE 2.** In the left-hand and central plots we show the radial profiles of the disc's surface density and gas temperature, centred on the first protostellar core to form in the simulation. The quantities are mass-weighted and taken from a slice through the midplane of the disc. In the right-hand plot we show the radial distribution of the corresponding Toomre parameter, $Q = c_s \kappa / \pi G \Sigma$, where $c_s$ is the sound speed and $\kappa$ is the epicyclic frequency. We adopt the standard simplification, and replace $\kappa$ with the orbital frequency.

# more on Z=0 star formation

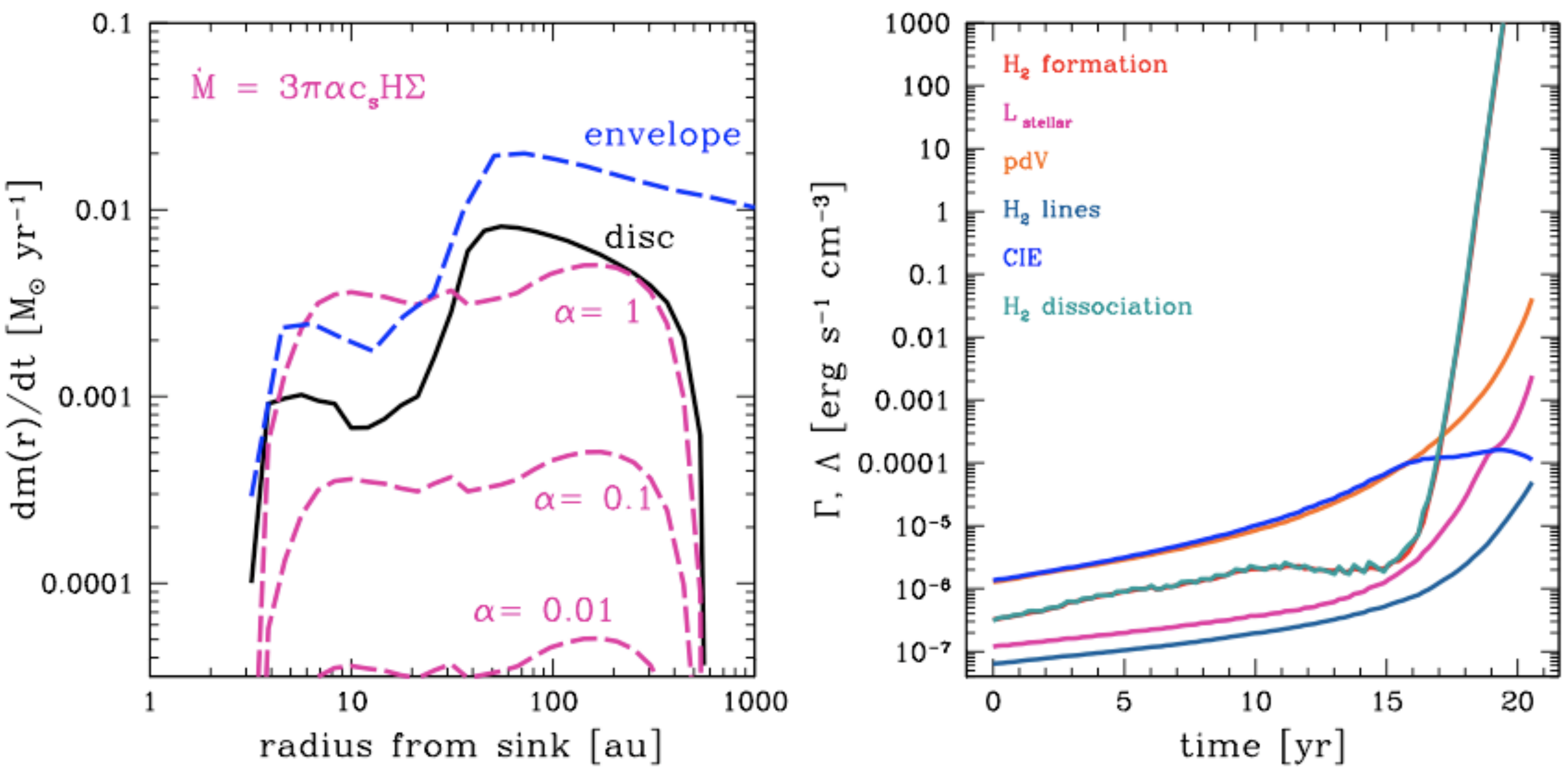


**FIGURE 3.** The left-hand plot shows the mass transfer through the disc. The solid black line shows the amount of mass moving inwards through each radial annulus in the disc per unit time. The dashed blue line shows the same quantity for the full spherical infalling envelope. The pink dashed lines show the accretion rates expected from an 'alpha' (thin) disc model, with three values of alpha. The right-hand plot shows the main heating and cooling processes that control the temperature evolution in the collapsing clump in the run-up to its eventual collapse.

summary

# Summary I

- interstellar gas is highly *inhomogeneous*
  - *thermal instability*
  - *gravitational instability*
  - *turbulent compression* (in shocks $\delta\rho/\rho \propto \mathcal{M}^2$; in atomic gas: $\mathcal{M} \approx 1...3$)

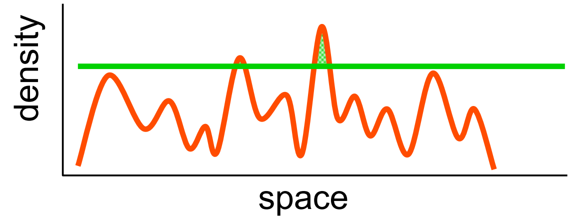


- cold *molecular clouds* can form rapidly in high-density regions at *stagnation points* of *convergent large-scale flows*
  - chemical *phase transition*: atomic → molecular
  - process is *modulated* by large-scale *dynamics* in the galaxy
- inside *cold clouds:* turbulence is highly supersonic ($\mathcal{M} \approx 1...20$)
  → *turbulence* creates density contrast, *gravity* selects for collapse

→ ***GRAVOTUBULENT FRAGMENTATION***

- *turbulent cascade:* local compression *within* a cloud provokes collapse → formation of individual *stars* and *star clusters*
- *star cluster:* gravity dominates in large region (--> competitive accretion)

(e.g. Mac Low & Klessen, 2004, Ballesteros-Paredes et al. 2006, McKee & Ostriker 2007)

# Summary II

- *thermodynamic response* (EOS) determines fragmentation behavior
  - characteristic stellar mass from fundamental atomic and molecular parameters
    --> explanation for quasi-universal IMF?


- *stellar feedback* is important
  - accretion heating may reduce degree of fragmentation
  - ionizing radiation will set efficiency of star formation
- *CAVEATS:*
  - star formation is *multi-scale, multi-physics* problem --> VERY difficult to model
  - in simulations: very small turbulent inertial range (Re < 1000)
  - can we use EOS to describe thermodynamics of gas, or do we need time-dependent chemical network and radiative transport?
  - stellar feedback requires (at least approximative) radiative transport, most numerical calculations so far have neglected that aspect

Thanks!